Fine scale ecohydrological processes in northern peatlands and their relevance for the carbon cycle

Jelmer J. Nijp

Fine scale ecohydrological processes in northern peatlands and their relevance for the carbon cycle

Jelmer J. Nijp

Thesis committee

Promotors

Prof. Dr F. Berendse
Professor of Nature Conservation and Plant Ecology
Wageningen University

Prof. Dr S.E.A.T.M. van der Zee
Personal Chair Ecohydrology
Wageningen University

Co-promotors

Dr J. Limpens
Assistant professor, Nature Conservation and Plant Ecology
Wageningen University

Dr K. Metselaar
Assistant professor, Soil Physics and Land Management
Wageningen University

Other members

Prof. Dr A.A.M. Holtslag, Wageningen University
Prof. Dr E.-S. Tuittila, University of Eastern Finland, Finland
Prof. Dr M.J. Wassen, Utrecht University
Prof. Dr L.P.M. Lamers, Radboud University Nijmegen

This research was conducted under the auspices of the Graduate School SENSE
(School for the Socio-Economic and Natural Sciences of the Environment)

Fine scale ecohydrological processes in northern peatlands and their relevance for the carbon cycle

---

Thesis

submitted in fulfilment of the requirements for the joint degree of doctor
at Wageningen University
by authority of the Rector Magnificus
Prof. Dr A.P.J. Mol
in the presence of the
Thesis Committee appointed by the Academic Boards
to be defended in public
on Tuesday 1 December 2015
at 4 p.m. in the Aula.

J.J. Nijp

Fine scale ecohydrological processes in northern peatlands and their relevance for the carbon cycle
208 pages

PhD thesis, Wageningen University, Wageningen, NL (2015)
With references, with summaries in English and Dutch

ISBN 978-94-6257-583-7


“I’m only happy when it rains”...!?
(Garbage, 1995)

Contents

1 General introduction

1.1 Northern peatlands

The high latitudes of our planet are characterized by extreme climatic conditions. Short growing seasons and freezing winters prevent many organisms to thrive in the boreal climate. Only few organisms survive in such harsh conditions, and if they do, they grow slowly. The boreal zone is vegetated by extensive coniferous forests, which cover about 70% of the boreal landscape (Hansen *et al.*, 2013). At some positions in the landscape, where water input by rain and lateral inflow exceed water losses through evapotranspiration and drainage, it is too wet for trees to survive. These are the sites where we encounter peatlands.

Peat & peatlands

Peat soils are soils formed by the accumulation of material that remains after the partial decay of organic matter. Due to the wet, cold, and anaerobic conditions, the plant material is not easily decomposed (Davidson & Janssens, 2006; Ise *et al.*, 2008; Knorr *et al.*, 2005). As a result, the dead plant material accumulates and forms a peat soil. Peatlands are ecosystems with a peat soil, generally defined as soils with an organic layer thickness larger than 30 cm and an organic matter content of at least 30% (Joosten & Clarke, 2002). Peatlands occur in various climatic conditions all around the world, ranging from the tropics to the arctic and cover around 4 million km2, representing 2.6% of the earth's total land surface (Fig. 1.1). The largest part (82%) of the total peatland area is found in temperate and boreal climates in the northern hemisphere. These peatlands, located at latitudes above 45°N, are referred to as northern peatlands (Fig. 1.2a).

Peat formation

The formation of northern peatlands started after the last glaciation (about 7,500 – 10,000 years ago) through infilling of lakes or paludification (peat accumulation on wet mineral soils) (Rydin & Jeglum, 2013). With the continuation of peat accumulation, the distance from the peat surface to mineral rich soil or water increases and the deeper peat material becomes more and more compacted, reducing the permeability to water flow (*hydraulic conductivity*) (Päivänen, 1973). As a result, the rooting zone becomes increasingly isolated from a mineral source, so that the influence of rainwater increases and the water quality becomes nutrient poor and acid (*ombrotrophic*). Due to the relatively high aeration and low degree of decomposition, most biogeochemical processes and water flow in northern peatlands takes place in the unsaturated zone (referred to as

acrotelm sensu Ingram (1978)), generally representing the top 8 – 70 cm of northern peatlands (Ivanov *et al.*, 1981).

Peatmoss

The dominant species that are successful to endure the waterlogged, nutrient poor and acid environment of northern peatlands are peatmosses, bryophytes of the genus *Sphagnum*, which constitute a major vegetation component of these ecosystems (Fig. 1.2b, Moore *et al.*, 2002). The litter of these mosses is very resistant to decomposition compared to vascular plants (Aerts *et al.*, 1999; van Breemen, 1995; Verhoeven & Toth, 1995), and its chemical composition is not conducive to microbial decomposition (Mellegård *et al.*, 2009; Rudolph & Samland, 1985). Therefore, the accumulated partially decomposed material in northern peatlands predominantly originates from peatmosses. While the apical part (top 1 – 5 cm; Fig. 1.2c), referred to as capitulum, is alive and grows, the degree of decomposition and compaction of the dead moss parts increases with depth.

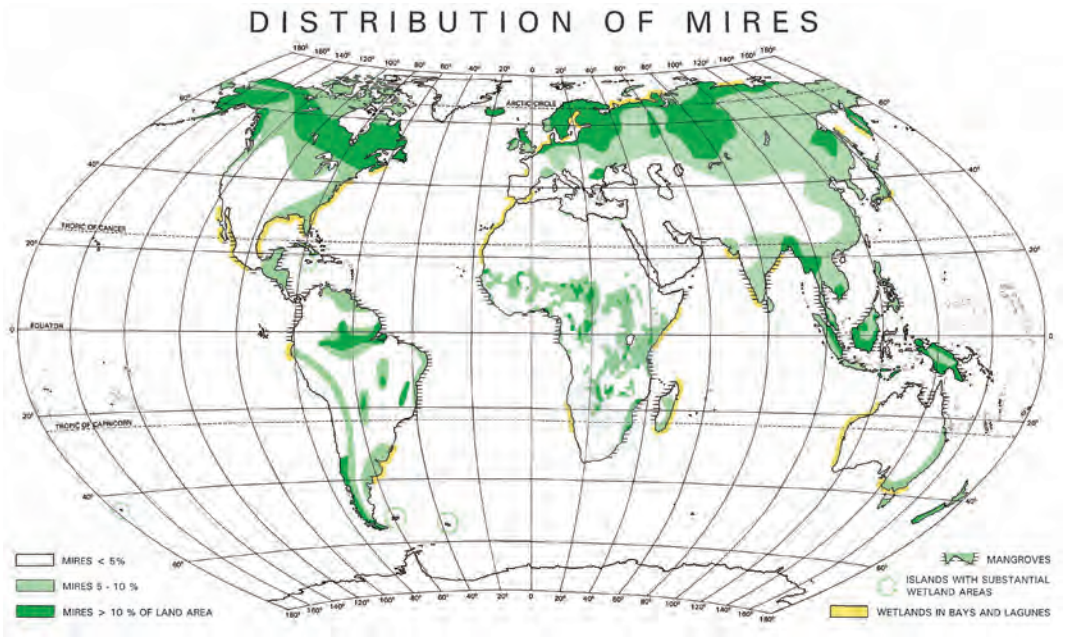

Figure 1.1. *Distribution of peatlands around the world (Lappalainen, 1996). Used with permission of the International Peatland Society.*

1.2 Northern peatlands and climate change

In regions with high peatland cover, peat has played an important role in human society for a long time. Peat has, for example, been used as fuel for at least 2000 years. Already in the first century (47 AD), the Roman naturalist and military officer Gaius Plinius Secundus described in his *Naturalis Historia* a Germanic marsh-dwelling society that *"burned earth as fuel to warm their food and so their own bodies, frozen by the north wind"*, which he encountered during a naval expedition along the northern coast of The Netherlands and Germany (Hoffmann, 2014; Rackham *et al.*, 1949). Since the 13th century, peat was excavated at progressively larger scales in areas where the stock of harvestable wood was depleted (de Zeeuw, 1978; Leenders, 1989). In the 20th century, about 95% of the total original peatland area was excavated for fuel supply in The Netherlands (de Zeeuw, 1978). Nowadays, still 5 – 7% of the primary energy consumption of Finland and Ireland is provided by peat (Gadonneix *et al.*, 2013).

More recently, peat has been used, due to its aeration, water retention, cation exchange capacity, and pH characteristics, as planting medium in horticulture, further reducing the peatland volume by about 30 – 40 million $m^3\ yr^{-1}$ (Joosten & Clarke, 2002; Rydin & Jeglum, 2013). Due to the extreme conditions in peatlands, peatland flora and fauna species are strongly specialized and restricted to peatlands (Holmes *et al.*, 1993; Spitzer & Danks, 2005; Weking *et al.*, 2013). Moreover, the inaccessibility of peatlands makes them an essential last refuge for fauna (Joosten & Clarke, 2002). Peatlands are therefore important from floristic and faunal perspective.

In addition to its economic value as fuel, planting medium and supporting floral and faunal diversity, northern peatlands provide an ecosystem service that – especially in the last decades – received considerable international attention from the perspective of global climate change (IPCC, 2013). Organic material consists for an important part of carbon. This implies that, by piling up dead, decaying, peatmoss over thousands of years, peatlands accumulated enormous amounts of carbon. Even though northern peatlands cover only 2.6% of the total land surface area (Joosten & Clarke, 2002), they represent an important component of the global climate as they store between 270 and 370 Tg of carbon, corresponding to about 20% of all terrestrial soil carbon worldwide or 50% of current total atmospheric carbon content (Gorham, 1991; Kleinen *et al.*, 2012; Turunen *et al.*, 2002; Yu, 2011). If all this carbon would end up as carbon dioxide (CO_2) in the atmosphere, the current atmospheric CO_2 concentration of around 400 ppm (micromoles CO_2 per mole air) would be doubled (NOAA, 2015). An increase in CO_2 concentration may have severe consequences for the global climate system and human society (IPCC, 2013). CO_2 is a greenhouse gas, absorbing energy and partially radiating

it back towards the earth surface, thereby increasing the temperature of the globe and its atmosphere. Besides storing CO_2, northern peatlands emit the greenhouse gas methane (CH_4) (Moore & Dalva, 1993; Roulet *et al.*, 1992) and contribute to 3 – 5% of CH_4 emissions worldwide (Frolking *et al.*, 2006).

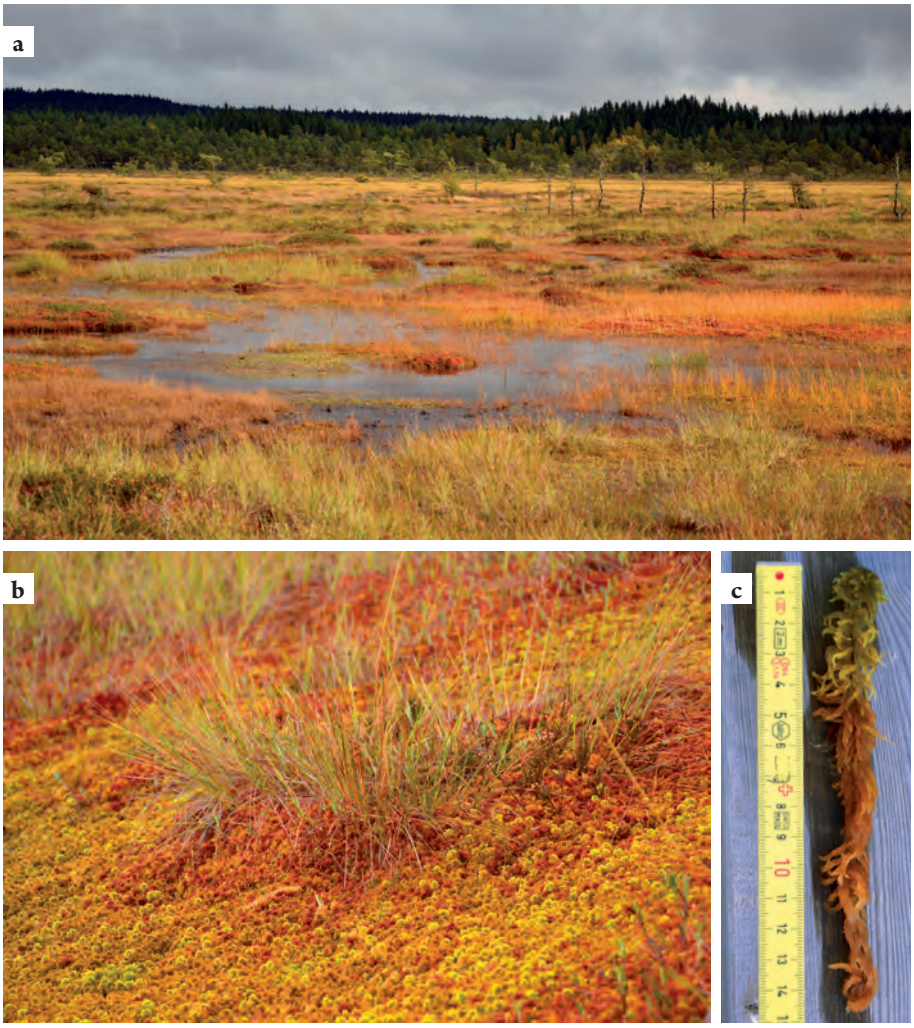

Figure 1.2. *(a) A Swedish example of an ombrotrophic northern peatland (Kulflyten, 59°N 15°E) with hummocky microtopography (b) A closer look at the peatland vegetation, dominated by various colourful peatmoss (Sphagnum) species. (c) Single Sphagnum shoot, with a green living capitulum (0 – 5 cm) and a larger degree of composition deeper in the peat profile; ruler units are in cm.*

1.2.1 Climate change

An increasing number of scientific studies shows that only a slight increase in averaged global temperature due to increased atmospheric CO_2 concentrations may have dramatic consequences for society and the environment we live in (IPCC, 2013). Historically, consequences of climate change were primarily associated with changes in temperature. Especially for the northern hemisphere at high latitudes, temperatures are expected to increase by about 2 – 6°C in the period from 1986 – 2005 to 2081 – 2100) (IPCC, 2013). However, changes in temperature also have consequences for the hydrological cycle. Water losses by evapotranspiration are expected to increase as a direct effect of increased temperature. Moreover, the hydrological cycle could be intensified and the probability of extreme events will increase (IPCC, 2013; O'Gorman & Schneider, 2009). In general, an intensification of the water balance is expected to result in dry areas becoming drier, while wet areas are likely to become wetter (IPCC, 2013). Peatlands are by definition distributed in wet areas, and based on the projections, climate change increases total rainfall in the boreal zone by 10 – 30%. However, rain is also projected to occur in less frequent, but more intense rain events (Allen & Ingram, 2002; O'Gorman & Schneider, 2009), so that the drought frequency may increase in a future climate.

1.2.2 Potential climate change impact on northern peatlands

Due to the projected future shift in the temporal distribution of rainfall, accompanied by increased evapotranspiration, it is possible that droughts become more common in peatlands. Droughts may have devastating effects on peatmoss growth and can substantially reduce atmospheric carbon sequestration by northern peatlands (Alm *et al.*, 1999; Bragazza, 2008; Fenner & Freeman, 2011). Measurements indicate that, in the present day climate, peatlands sequester carbon with rates of about 21 – 70 gC m^{-2} yr^{-1} (Dinsmore *et al.*, 2010; Koehler *et al.*, 2011; Nilsson *et al.*, 2008; Olefeldt *et al.*, 2012; Roulet *et al.*, 2007). As a consequence of shifts in climate, northern peatlands may switch from a carbon sink to a carbon source, and start emitting substantial amounts of CO_2. In this positive feedback, climate change increases the drought frequency, which in turn leads to deeper groundwater tables, resulting in lower water content in the living moss layer (Fig. 1.3). In turn, the decreased water content will reduce peatmoss photosynthesis and its carbon uptake, resulting in a net increased emission of carbon into the atmosphere. Due to the reduced carbon uptake, peatlands may become net carbon emitters, enhancing the greenhouse effect and thereby increasing the likelihood of (extreme) droughts. Whether or not this undesirable scenario will become a reality depends on how climate change affects positive and negative feedbacks controlling the balance between carbon sequestration and emissions rates in northern peatlands. As

indicated in Fig. 1.3, fine scale ecohydrological processes such as peat volume change and moss rain retention can alter the water content in the moss layer, hence net carbon uptake of northern peatlands. The functioning and relative importance of rain water retention and peat volume change for peatmoss water availability and carbon uptake are the main topics covered in this thesis.

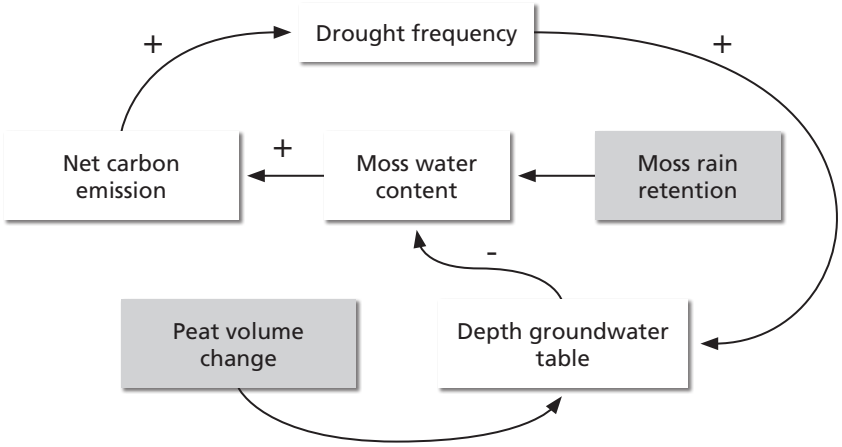

Figure 1.3. *Conceptual overview of positive (+) and negative (-) feedbacks between climate, peatmoss water balance and photosynthetic carbon uptake by peatmosses in northern peatlands due to a climate change induced increase in drought occurrence. The fine scale ecohydrological processes that can affect net peatland carbon emission through moss water content, and which are of main interest in this thesis, are indicated by grey boxes.*

1.3 Linking peatland ecology and -hydrology

For other ecosystems it has been shown that the temporal distribution of rainfall may be more important for ecosystem functioning and carbon cycling than rain quantity *per se* (Heisler & Weltzin, 2006; Knapp *et al.*, 2002; Vervoort & van der Zee, 2008; Xu *et al.*, 2013). It is unknown, however, how climate induced changes in temporal rainfall patterns affect peatmoss water supply and associated photosynthetic carbon uptake. Are peatmosses able to cope with a more intermittent rain water supply?

1.3.1 Water and peatmoss photosynthesis

In ombrotrophic (i.e. rainwater-dependent) peatlands, the fixation of atmospheric CO_2 is largely mediated by *Sphagnum* (Moore *et al.*, 2002). Just like any other plant, peatmosses

(*Sphagnum*) need an adequate water supply to grow. Unlike vascular plants, however, peatmosses lack roots, xylem vessels, and stomata (Proctor, 2000), and are therefore incapable of actively taking up water from their direct environment. As a consequence, the photosynthesis of these plants and associated carbon uptake is crucially dependent on the water present in the living layer (top 5 – 10 cm) of the moss carpet (Hájek & Beckett, 2008; Schipperges & Rydin, 1998), referred to as the capitulum layer.

Besides this direct effect of water content on peatmoss photosynthesis, the water content of this interface between soil and atmosphere regulates numerous other peatland – climate interactions. Examples of processes in which peatmoss water content plays an important role include plant species competition (Limpens *et al.*, 2014b), thermal regimes (Kujala *et al.*, 2008), partitioning of latent and sensible heat fluxes (Seneviratne *et al.*, 2010; Teuling *et al.*, 2009), litter decomposition (Belyea, 1996), and plant transpiration (Feddes *et al.*, 2001; Metselaar & de Jong van Lier, 2007).

Understanding the water balance of peatmosses and its role in the above processes is therefore crucial to predict whether northern peatlands will remain a persistent, long-term carbon sink in the future. This thesis focuses on consequences of climate change on peatmoss photosynthesis, and its feedback to the global climate. The water balance of the capitulum layer is mainly regulated by water inputs through rainfall and capillary rise, and water losses through moss evaporation and drainage to the groundwater table (Fig. 1.3).

1.3.1.1 Capillary rise and rainwater

Capillary rise is the process of water transport from the groundwater to the capitulum layer (Fig. 1.4) in the pore space between (partially decomposed) *Sphagnum* stems and branches. The efficiency of capillary transport may strongly depend on morphological traits of peatmosses, which differ per peatmoss species (Rydin & McDonald, 1985b). The various peatmoss species inhabiting northern peatlands are generally distributed along a microtopographical gradient (Figure 1.2a,b). Drier and elevated locations are represented by hummocks, and wet depressions by hollows, with lawns being in between. Hummocks *Sphagna* have a denser growth form and smaller capitula than hollow species (Rydin, 1995). As a result of the smaller pore spaces, hummock peatmosses possess a more efficient capillary water supply and larger capacity to retain rainwater (Hayward & Clymo, 1982). This provides hummock species with a competitive advantage in dry conditions and during droughts.

The capillary supply from groundwater to living moss layer depends on the depth of the groundwater table. While capillary water supply may be adequate for shallow water

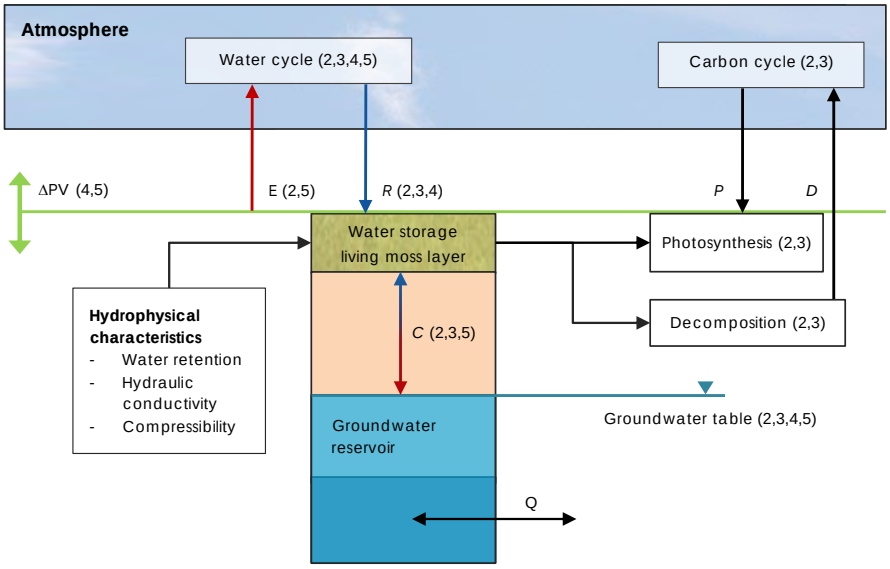

Figure 1.4. *Conceptual overview of most important peatmoss water balance components regulating water availability for peatmoss and carbon balance components in the living moss layer. R = rain, E = Moss evaporation, C = capillary flux, Q = lateral groundwater flow, ΔPV = peat volume change, P = photosynthesis, D = decomposition. Numbers between brackets represent chapters in which the subject is covered.*

tables, the capillary transport capacity decreases strongly and non-linearly with deeper water tables (McCarter & Price, 2014). In late summer, when water tables are deep, rainwater intercepted by the living moss layer may be an important water supply allowing *Sphagnum* to sustain photosynthesis and carbon uptake (Adkinson & Humphreys, 2011; Robroek *et al.*, 2009).

1.3.1.2 Peat volume change

In situations with a decreasing groundwater table, peat soils show an astonishing mechanism which may increase water availability for *Sphagnum*. Due to the open pore structure and compressible nature of the fibrous peat material (Price *et al.*, 2005; Waddington *et al.*, 2010), peat material expands in wet periods and compresses during dry spells (Almendinger *et al.*, 1986; Baden & Eggelsmann, 1964; Fritz *et al.*, 2008; Price, 2003; Price & Schlotzhauer, 1999; Roulet, 1991; Schothorst, 1977; Uhden, 1967; Whittington *et al.*, 2007). This process, referred to as peat volume change, may adjust water availability in the living moss layer and sustain photosynthesis during droughts. The contribution of peat volume change to maintain peatmoss photosynthesis during

droughts is, however, unknown. Moreover, it is unclear whether peat volume change varies among vegetation types, how spatially variable it is, and what its major controls are.

In natural peatlands, the driving factor of peat volume change is primary compression (Kennedy & Price, 2005). Primary consolidation of the peat matrix originates from changes in effective stress, which is largely modified by groundwater table fluctuations during the growing season (Kennedy & Price, 2004; Terzaghi, 1943). Upon drying, overlying weight of material above the surface of a peat cross-section exerts pressure on the contact points between the separate peat fibers in the peat matrix (skeleton). As a consequence the effective stress increases, causing the peat matrix to compress, and thereby stabilizing the distance between the groundwater table and peat surface. Peat volume change thus is a fundamental process by which peatmosses may maintain high water availability during dry spells so that atmospheric carbon uptake through photosynthesis is prolonged.

1.3.2 Simulating the peatmoss water balance

To predict how climate change may impact the overall functioning of northern peatlands, peatmoss water stress, and photosynthetic carbon uptake, dynamic simulation models are an indispensable tool. Based on such model simulations scientists can provide governmental institutions with information required to make informed decisions on policies regarding climate change. Many of such numerical models are available, varying in spatiotemporal scale, aim and processes included (Baird *et al.*, 2012; Frolking *et al.*, 2010; Granberg *et al.*, 1999; Heijmans *et al.*, 2008; Moore & Waddington, 2015; Price & Whittington, 2010; Schouwenaars & Gosen, 2007; St-Hilaire *et al.*, 2010; Stocker *et al.*, 2014; Wu & Blodau, 2013; Yurova *et al.*, 2007).

Frequently, models simulating peatland hydrology assume that the water content of the living moss layer is a direct function of the groundwater table (e.g. Granberg *et al.* (1999) and Yurova *et al.* (2007)). In these models, rainwater is assumed to bypass the living moss layer and to be directly transported to the groundwater. In reality, however, a single rainfall event may be fully retained in the living moss layer (Fig. 1.4; Strack & Price, 2009). Additionally, many models do not include peat volume change (but see Kennedy & Price (2004)), which as described in the previous section may reduce summer drought stress.

Including peatmoss rainfall retention and peat volume change in the model structure may modify peatmoss water balance dynamics in peatland models, but the relative effect of these processes on peatmoss water availability is unknown. To predict and quantify feedback strengths between northern peatlands and global climate, northern

peatlands and their dominant ecohydrological processes need to be part of larger scale climate models (Frolking *et al.*, 2013). The available calculation time in these so called regional or global circulation models to solve land-surface processes is highly restricted. It is therefore essential to test whether more hydrologically complex water balance models significantly improve model performance (i.e. reduces prediction error). Any additional process requires instrumental and labour costs for independent parameter measurements. These parameters do not necessarily represent 'effective' parameters for field conditions and may therefore increase prediction uncertainty, so that the addition of extra processes should be carefully considered (Beven, 2012; Oreskes *et al.*, 1994). At present, little research has been done to determine which degree of hydrological complexity is required to adequately predict how climate change may affect peatmoss water content and associated carbon uptake, and how such changes may feed back to the global climate.

1.4 Thesis aim and outline

The above shows that there are important interactions between water availability and peatmoss photosynthesis in northern peatlands. An analysis of these interactions could lead to a well-founded basis to understand how future climate change could affect the water balance of, and associated carbon sequestration, in peatlands.

Research aim

This thesis aims to improve the fundamental scientific understanding and simulation of fine scale ecohydrological processes in northern peatlands, and their effect on peatmoss photosynthesis. Although peatmosses are not the only vegetation in northern peatlands, they are the species group responsible for most of the net CO_2 uptake in ombrotrophic systems (Moore *et al.*, 2002; Street *et al.*, 2013) and generally form the major constituent of peat in northern peatlands (Dorrepaal *et al.*, 2005; Thormann *et al.*, 1999; Verhoeven & Toth, 1995). This thesis therefore focusses on peatmosses, and aims to answer the research questions listed in Table 1.1.

Outline

In **Chapter 2**, we explore the effect of the temporal variability of rainfall on peatmoss water availability, photosynthetic activity and carbon uptake. We hypothesize that rain is only of advantage if groundwater levels are deep, because only then peatmosses are dependent on rainwater supply for their photosynthesis. This hypothesis is tested with three contrasting peatmoss species under controlled conditions in a growth chamber

experiment. Although experiments under controlled conditions are essential to reveal important driving mechanisms, they only represent a simplified version of the real world and could therefore potentially give rise to biased results (Englund & Cooper, 2003; Limpens *et al.*, 2012). The results of Chapter 2 are therefore confronted with measurements under field conditions in **Chapter 3**. Using 11 years of half-hourly data on carbon exchange, water table, and meteorological variables of Degerö Stormyr, a northern peatland in the north of Sweden, the response of net carbon uptake to individual rain events was analysed. Also the effects of pre-rain groundwater table, drought length, and changes in other environmental factors such as light availability and vapour pressure deficit are tested.

Chapter 4 describes an explorative field study aiming to determine the spatial scale of peat volume change patterns and the major drivers that cause spatial variability of peat volume change. Digital terrain models are constructed applying digital photogrammetry to top-view digital images taken along a transect in a northern peatland at multiple points in time. Subtracting the digital terrain model from one point in time from another other provides a high-resolution (0.5 · 0.5 m) map of spatial peat volume change. Point measurements on vegetation composition, peat depth, saturated hydraulic conductivity and positional factors are included to relate spatial variation of peat volume change to potential drivers. The results of this study are key in understanding ecohydrological self-regulation of peatlands, and provide a basis for the spatial representativeness of peatland models including, and point measurements of, peat volume change.

Chapter 5 shows the results of a modelling study, aimed to 1) determine the relative importance of peat volume change and rain water retention and 2) test the consequences of increasing hydrological complexity on peatmoss drought stress predictions by simulations models. A reference reservoir model assuming a direct relation between groundwater table and moss water content is combined with a module describing (1) moss water storage (i.e. rainwater retention by the living peatmoss layer), (2) peat volume change, and (3) the combination of both processes. Field data are collected, and are used as model input and to validate the predictive quality of the different models. Future climate scenarios are employed to determine how adding ecohydrological processes affects peatmoss drought stress predictions.

This thesis concludes with a synthesis of the results in **Chapter 6**. On the basis of the findings described in Chapter 2 – 5, recommendations are provided for future ecohydrological field- and modelling studies in northern peatlands.

Table 1.1. *Overview of research questions, associated hypotheses, and chapters.*

Research question	Hypothesis	Chapter
How does temporal variability in rainfall affect photosynthesis and carbon uptake of peatmoss?	At shallow water tables the water content in the living moss layer is high enough to maintain photosynthesis. At deep water tables, more frequent rain will result in higher photosynthetic carbon uptake.	2
How do rain events and their characteristics affect net carbon uptake in northern peatlands?	In addition to the hypothesis for the previous question, it was expected that longer pre-rain droughts result in larger release of CO_2 after rain in field conditions.	2,3
How spatially variable is peat volume change, and which processes are related to this spatial variability?	Spatial variations in peat volume change are mainly driven by spatial variability in groundwater dynamics and vegetation composition.	4
Does including peat volume change and/or moss water storage dynamics in simulation models affect peatmoss drought projections in a future climate?	Compared to a model excluding peat volume change or moss water storage dynamics, peatmoss water stress is significantly lower in models including at least one of these hydrological processes.	5

2 Can frequent precipitation moderate the impact of drought on peatmoss carbon uptake in northern peatlands?

Jelmer J. Nijp, Juul Limpens, Klaas Metselaar, Sjoerd E.A.T.M. van der Zee, Frank Berendse, Bjorn J.M. Robroek

Published in *New Phytologist*, **1**, 70-80 (2014)

Abstract

Northern peatlands represent a large global carbon store that potentially can be destabilised by summer water table drawdown. Precipitation can moderate negative impacts of water table drawdown by rewetting peatmoss (*Sphagnum spp.*), the ecosystems' key species. Yet, the frequency for such rewetting to be effective remains unknown. We experimentally assessed the importance of precipitation frequency for *Sphagnum* water supply and carbon uptake during a stepwise decrease in water tables in a growth chamber.

CO_2 exchange and the water balance were measured for intact cores of three peatmoss species (*Sphagnum majus*, *S. balticum* and *S. fuscum*) representative of three hydrologically distinct peatland microhabitats (hollow, lawn, hummock) and expected to differ in their water table-precipitation relationships.

Precipitation contributed significantly to peatmoss water supply at deep water tables, demonstrating the importance of precipitation during drought. The ability to exploit transient resources was species-specific; *S. fuscum* carbon uptake increased linearly with precipitation frequency at deep water tables, whereas carbon uptake by *S. balticum* and *S. majus* was depressed at intermediate precipitation frequencies.

Our results highlight an important role for precipitation on carbon uptake by peatmosses. Yet, the potential to moderate drought impact is species-specific and dependents on the temporal distribution of precipitation.

Keywords: Climate change, desiccation tolerance, photosynthesis, rain variability, mires, moisture stress, *Sphagnum* physiology, water balance

2.1 Introduction

Although northern peatlands cover only about 3% of the earth's land surface, they accumulated an equivalent of 20% of total terrestrial soil carbon throughout the Holocene (Kleinen *et al.*, 2012; Turunen *et al.*, 2002; Yu, 2011), acting as a significant sink for atmospheric CO_2 (Jobbágy & Jackson, 2000; Nilsson *et al.*, 2008; Roulet *et al.*, 2007). Whether these ecosystems will continue to function as carbon sink in a warmer future climate is currently uncertain, calling for a mechanistic understanding of feedbacks between atmosphere and ecosystems. Climate projections for the northern hemisphere indicate a shift towards higher temperatures (IPCC, 2007), and less frequent, but more intense precipitation events (Allen & Ingram, 2002; O'Gorman & Schneider, 2009), that will likely lead to deeper water tables and drier surface conditions in peatlands. How these deeper water tables will affect carbon exchange and how this will interact with the changes in temporal distribution of precipitation remains to be explored (Fenner & Freeman, 2011; Heijmans *et al.*, 2013; Robroek *et al.*, 2009).

Changes in the temporal distribution of precipitation are of crucial importance for carbon cycling and may even have more impact on ecosystem functioning than precipitation quantity *per se* (Heisler & Weltzin, 2006; Knapp *et al.*, 2002; Vervoort & van der Zee, 2008; Xu *et al.*, 2013). The above may be particularly important for northern peatlands, where a significant part of ecosystem carbon uptake takes place by peatmosses (genus *Sphagnum*) (Frolking *et al.*, 2002; Kuiper *et al.*, 2013; Riutta *et al.*, 2007; Street *et al.*, 2013). Peatmosses lack stomata, water conducting tissue and roots, making their photosynthesis and associated carbon uptake highly dependent on the water present in the living layer (top 5 – 10 cm) of the moss carpet (Robroek *et al.*, 2009; Schipperges & Rydin, 1998). In case of shallow water tables, water supply to the living moss layer is dominated by capillary rise (i.e. water transport from the water table to the peat surface) (Ketcheson & Price, 2013), and carbon uptake is not limited by water deficiency. At deeper water tables, however, capillary rise strongly decreases (McCarter & Price, 2014), resulting in lower water availability and associated reduced carbon uptake by the mosses (e.g. Alm *et al.*, 1999; Aurela *et al.*, 2007; Ciais *et al.*, 2005). In conditions with a deep water table, precipitation water intercepted by the living moss layer can be used for *Sphagnum* photosynthesis (Adkinson & Humphreys, 2011; Robroek *et al.*, 2009). However, as water retention of *Sphagnum* plants is limited (Ketcheson & Price, 2013), the effect of precipitation may be strongly modified by the frequency of precipitation and the speed at which mosses can use this transient resource for photosynthesis (Campbell & Grime, 1989). Yet, these frequency dependent effects have received limited attention in northern peatlands, with previous studies focussing on total precipitation amount,

rather than on the temporal distribution of precipitation (Adkinson & Humphreys, 2011; Keuper *et al.*, 2012; Robroek *et al.*, 2009; Sonesson *et al.*, 2002).

We experimentally assessed the importance of the temporal distribution of precipitation for water content, photosynthesis and carbon uptake of peatmoss during a stepwise decrease in water tables, using three species representative of northern peatlands. We hypothesized that (1) carbon uptake would decrease with deeper water tables, but that precipitation moderates this effect. More specifically, we expected (2) carbon uptake to be larger for small but frequent events than for large infrequent events. We further (3) expected the effect of precipitation frequency on carbon uptake to be species-specific.

2.2 Material and Methods

2.2.1 Plant material

We selected three species representative for the three most common microhabitats (hollow, lawn, hummock) in peatlands (Table 2.1). *Sphagnum majus* is characteristic for (semi)continuously inundated microhabitats (hollows), *S. fuscum* for elevated microhabitats further from the water table (hummocks), while *S. balticum* occupies intermediate positions (lawn).

Moss cores were collected in September 2011 at Kulflyten, a 1 km2 ombrotrophic mire in southern Sweden (59°54'N 15°50'E; 130 m a.s.l.; see (Sjörs, 1948) for a detailed site description). We collected 25 cores per species from monospecific patches (> 95% cover; < 2% vascular plant cover) spread over five different locations in the mire. The cores were obtained by gently pressing PVC cylinders (inner diameter 15 cm, height 10 cm) into the moss carpet while cutting around them with a finely serrated knife to prevent sample compression along the cylinder wall. Vascular plant shoots, if present, were removed by clipping.

After transport to The Netherlands, cores were allowed to acclimate for a 84-day period, after which treatments were randomly assigned to the cores (from now on referred to as mesocosms). The acclimation period consisted of 44 days outside under a roof (60% shading, temperature of 12.2 ± 3.4 [SD] °C) and 40 days in the growth chamber at experimental climate settings (18.5 °C on average, see section growth chamber climate settings) and at a water table of 4 cm below the moss surface.

2.2.2 Growth chamber experiment

We assessed the importance of precipitation frequency for water supply and carbon

uptake of peatmoss in a growth chamber experiment with two factors: water table (four treatment levels) and precipitation frequency (five treatment levels) for three *Sphagnum* species, with five replicates for each precipitation frequency – water table treatment combination.

Table 2.1. *Water table treatment levels and water contents per species.*

	Wet Wet field conditions	**Moist** Optimal field conditions	**Dry** Drought, no capillary rise	**Rewetted** Wet field conditions
Water table below moss surface (cm)				
S. fuscum	25	34	54	25
S. balticum	9.4	15	31	11.1
S. majus	2.5	6.5	15	2.5
Duration (days)	15	14	17	17
Volumetric water content (m^3 m^{-3})				
S. fuscum	0.40[a]	0.35[b]	0.27[c]	0.35[b]
S. balticum	0.76[a]	0.65[b]	0.44[c]	0.65[b]
S. majus	0.95[a]	0.93[a]	0.73[b]	0.94[a]

The duration of each water table treatment is given in the row 'duration'. Volumetric water contents (m^3 H_2O per m^3 Sphagnum) per water table treatment are averaged over time and precipitation frequency treatments. Small letters indicate, per row, which water table treatments have statistically similar water contents.

2.2.2.1 Water tables

Water tables were lowered in three steps through time (*wet, moist, dry*), simulating the seasonal drop in water tables during summer (Table 2.1; Fig. 2.1). At the end of the experiment, water tables were raised back from *dry* conditions to wet pre-drought levels (*rewetted*), enabling assessment of the recovery of carbon uptake after summer drought (Fig. 2.1). The three consecutive water tables reflect natural conditions for each species during wet field conditions (*wet*), optimal field conditions (*moist*) and summer-drought (*dry*) conditions (Table 2.1). The exact water table treatment settings were species-specific and were based on the vertical zonation of the three peatmosses along the water table under field conditions as reported in literature (Andrus *et al.*, 1983; Lafleur *et al.*, 2005; Nilsson *et al.*, 2008; Rydin, 1986).

The water table treatments were imposed by changing suction at a given time. To this end the mesocosms were placed in water retention cylinders (Fig. 2.2), an adaptation of the generally accepted sandbox method (e.g. Klute, 1986). Water tables were kept constant using a Mariotte bottle to correct for evaporation, and an overflow level to drain percolated precipitation (Fig. 2.2, for more details see Appendix 2.1). Accordingly,

precipitation did not result in a rise of the groundwater level.

Our physical approach allows direct translation of the relation between water content in the living moss layer and water table to field conditions, provided atmospheric conditions are similar. Potential differences in suction and water content of the top moss layer may arise from differences in capillary rise between a natural field column and the moss-sand column we used. Within the suction range applied, the sand was well able to sustain water transport to the moss columns, as evidenced by the saturated conditions of the fine sand layer. (For more information and soil physical detail see Appendix 2.1). Furthermore, as the sand remained saturated throughout the experiment, precipitation only reduced the upward capillary flux and increased drainage in the *Sphagnum* mesocosms.

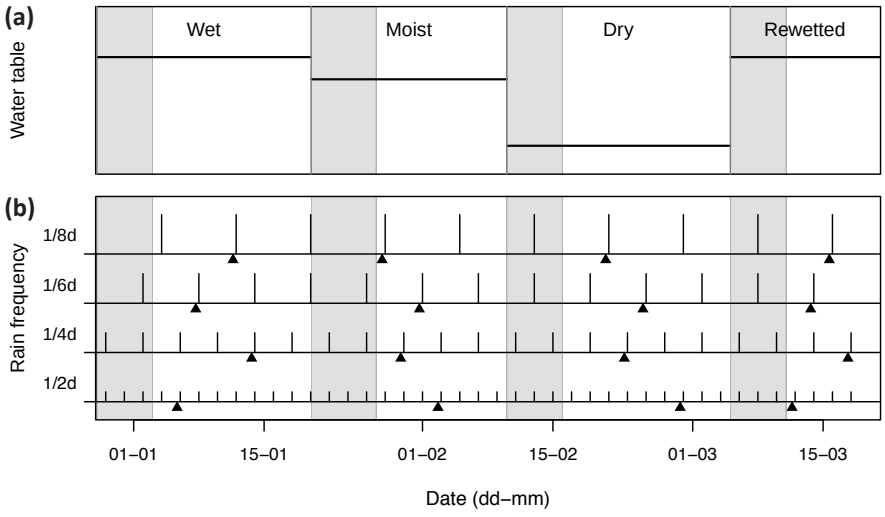

Figure 2.1. *Water table treatment (a) and precipitation frequency treatment (b) application through time. The shaded grey areas represent the stabilization periods throughout which water table and water content were allowed to equilibrate. In the bottom panel, the vertical lines indicate dates of precipitation application, the length of the lines represent the precipitation amount. The black triangles indicate the timing of NEE measurements, 5 – 30 minutes before rain application.*

Water tables were maintained for a measurement period of about 15 days (see Table 2.1 for details) with 6-7 days of equilibration between consecutive water tables (Fig. 2.1). This approach allowed the pore water pressure and associated mesocosm water content to equilibrate with the altered water table and evaporation. No substantial changes in water content were observed after these equilibration periods, indicating that equilibrium between water content and water table was reached.

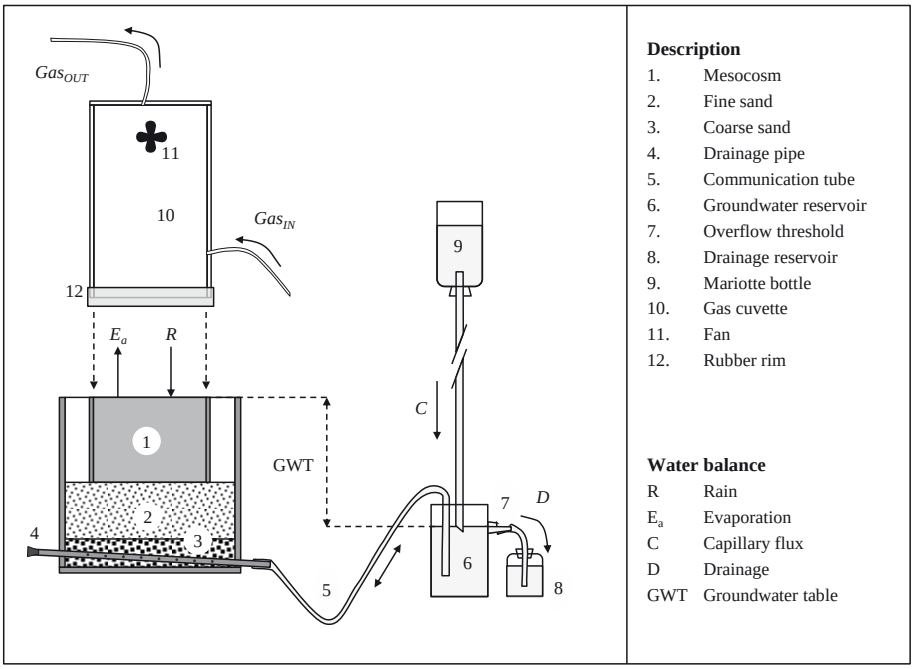

Figure 2.2. *Overview of the experimental setup. Numbers represent components of the water retention cylinders and letters are water balance components. Mesocosms were placed in water retention cylinders on fine sand. A drainage pipe in the coarse sand communicates via tube (5) with the groundwater reservoir (6). By lowering the position of this reservoir the depth of the water table increases. Evaporation from the moss surface is compensated for by the Mariotte bottle (8). Gas exchange was measured by placing the cuvette tightly on the mesocosm. Internal mixing of air was established with a fan (10). Interaction with the outer atmosphere was prevented with the rubber rim (12).*

2.2.2.2 Precipitation frequency

Precipitation frequency treatments (1/2 d, 1/4 d, 1/6 d, 1/8 d, no precipitation; Table 2.2) remained constant throughout the whole experimental period (Fig. 2.1). For each precipitation frequency treatment the total precipitation amount and precipitation intensity were kept constant while precipitation duration was varied. This was done to avoid effects of total precipitation amount and intensity on carbon uptake. Duration and intensity of the precipitation events were representative of natural conditions and were calculated from intensity-duration-frequency diagrams (Dahlström (2006), Appendix 2.1). The average precipitation amount was set to compensate daily potential evaporative water losses in the growth chamber (2 mm d^{-1}). Precipitation was applied using a peristaltic pumping system (Masterflex Console Drive 7520-47, Cole Parmer,

Schiedam, The Netherlands) with 24 drip points. The pump was calibrated before precipitation application, to allow regulating the precipitation intensity with high precision (1.18 ± 0.01 (SE) mm min^{-1}). Natural precipitation water quality was simulated using a commonly used diluted seawater solution (Garrels & Christ, 1965).

2.2.3 Growth chamber climate settings

The day/night temperature in the growth chamber was 20/17.5 °C (10/14 h) and corresponds to average 1961 1990 July conditions at the collection site (Kulflyten). Day temperature reflects the average temperature at noon, whereas the night temperature corresponds to the average temperature between 18:00 and 6:00 (local time, Västerås meteorological station, 59°60'N 16°46'E, Swedish Meteorological and Hydrological Institute (SMHI)). The relative humidity was 70% RH and the CO_2 concentration 400 ppm CO_2. At the moss surface, the photosynthetic photon flux density (PPFD) was 246 ± 20 (SD) μmol m^{-2} s^{-1}, net radiation at daytime was 101 ± 4 (SD) W m^{-2} and the wind speed was ≤ 0.1 m s^{-1}.

2.2.4 Measurements

2.2.4.1 Water balance

To determine the importance of precipitation as water source for moss evaporation, the water balance of all mesocosms was quantified over all water table treatments (Eq. 2.1).

$$R + C - D + \Delta S = E_a + \varepsilon \qquad (2.1)$$

For each precipitation treatment, the amount of precipitation (R) added during the measurement period was known. The capillary supply (C) and drainage (D) were obtained by weighing the capillary- and drainage reservoir at the start and end of a 7 day period (Fig. 2.2). The change in water content in the mesocosms (ΔS) was quantified as the change in volumetric water content (m^3 m^{-3}) over the measurement period measured with moisture sensors, multiplied by the mesocosm volume. Changes in volumetric water content in the top 1 – 5 cm of the moss layer were assessed with EC5-H_2O moisture sensors (Decagon Devices, Pullman, USA) installed at 3 cm depth in one randomly selected mesocosm per species – precipitation treatment combination (n = 15). The moisture sensors measured the dielectric constant (Hillel, 2004) with a five-minute frequency. Dielectric constants were converted to volumetric water contents using species-specific calibration functions (Appendix 2.2).

As the evaporative loss from the moss surface (E_a) is the only unknown in Eq. 2.1, it can be derived from the water balance, together with water balance errors ε as E_a and ε cannot be distinguished. Negative values for evaporation and capillary fluxes (3%

Table 2.2. *Precipitation characteristics for all precipitation frequency treatment levels.*

Precipitation frequency treatment	Precipitation amount (mm)	Precipitation duration (minutes)	Dry spell length (d)
1/(2 d)	4.1	3.47	2
1/(4 d)	8.2	6.92	4
1/(6 d)	12.3	10.38	6
1/(8 d)	16.6	13.83	8
No precipitation	None	-	-

All precipitation frequency treatments have the same precipitation intensity (1.18 mm min^{-1}) and average daily water supply. Dry spell length is the inverse of precipitation frequency.

of data) were excluded prior to statistical analysis to reduce error variation: treatment patterns remained unaffected. Technical problems in the first week prevented assessment of the water balance for the wet treatment. The water balance components in Eq. 2.1 were used to obtain a measure for the fraction of evaporation originating from retained precipitation (f_p; Eq. 2.2), which we used as a measure for precipitation dependence of *Sphagnum*.

$$f_p = 1 - \frac{C}{E_a} \qquad (2.2)$$

An f_p ratio of one represents 100% dependence on precipitation as source of water (C = 0 mm d^{-1}), whereas a value of zero represents 100% dependence on capillary water supply.

2.2.4.2 Gas flux measurements

Carbon uptake was assessed by measuring the net CO_2 flux per mesocosm (net ecosystem exchange; NEE) from each species at each precipitation treatment and each water table depth. We expressed carbon uptake relative to the atmosphere, with negative values indicating net carbon sequestration by the mesocosms, and positive values net emission of carbon from the mesocosms (c.f. Chapin III *et al.*, 2006). To assess the potential effects of precipitation frequency on NEE, we measured NEE in driest conditions, i.e. just before application of precipitation. For the *rewetted* water table treatment, we measured NEE 7 – 11 days after rewetting. Closed flux chambers (diameter 15 cm, height 24.3 cm, fitted with a circulating fan at 20 cm from the moss surface) were placed tightly over the mesocosms to measure CO_2 fluxes using a photoacoustic multi gas analyzer (Bruel and Kjær, type Innova 1302, Denmark), connected to a multipoint sampler (CBISS MK2, 4-channel, CBISS Ltd. England).

Tubes were flushed at 15 mL s^{-1} to enable independent sampling and chamber measurements comprised three successive sampling points with a 2 minute interval. Accuracy of gas exchange measurements was further increased by compensating for water vapour interference. Partial pressures of CO_2 and H_2O entering the cuvettes were set to ambient CO_2 by adding CO_2 free air, and to ambient H_2O by dehumidifying air to a pre-set dew point. NEE was calculated from the linear change in CO_2 concentration in the chamber headspace with time.

2.2.4.3 Chlorophyll fluorescence

To directly explore the photosynthetic response of moss as a function of water content, the efficiency of photosystem II (PSII) was estimated by measuring chlorophyll fluorescence with a portable chlorophyll fluorometer (Mini-PAM, WALZ, Effeltrich, Germany). Chlorophyll fluorescence was measured at least once per water table treatment, on the mesocosms with moisture sensors and under steady state conditions (i.e. before, or more than 1d after precipitation application).

First the dark-adapted minimal fluorescence yield (F_0) was determined by illumination with a far-red light. To this end, a PVC lid with 11 covered holes was placed on the samples for a 15-minute period of dark adaptation. One by one the cover of each hole was removed, after which the fibre-optic probe was immediately inserted approximately level at 0.5 – 2 cm above the moss surface. The maximum chlorophyll fluorescence (F_M) was then obtained by emitting an 800 ms, high intensity saturation pulse. This procedure was repeated at the different water table treatments to obtain a broad range of water contents. To be able to compare measurements at different points in time, the lid was positioned at the same location every time. The maximum quantum yield of PSII photochemistry, F_V/F_M, can be calculated as $(F_M - F_0)/F_M$ and is a measure for the efficiency of PSII (Maxwell & Johnson, 2000).

To determine if water content affects the efficiency of PSII, a generalized logistic function (Eq. 2.3) was fitted using an adaptive non-linear least squares algorithm (*nls* package, R v2.13.0, R Core team) for each species.

$$F_V/F_M = F_{MAX} + \frac{F_{MAX} - F_{MIN}}{1 + e^{-\beta(VWC - VWC_{PSII50})}} \qquad (2.3)$$

Here, parameter VWC_{PSII50} represents the volumetric water content (VWC; m^3 H_2O per m^3 *Sphagnum*) at which PSII efficiency is 50% and switches from active to inactive, while the parameter β represents the steepness of this switch.

2.2.4.4 Chlorophyll a + b content

To determine if treatment effects on carbon uptake could be attributed to damaged chloroplasts and decreased photosynthetic capacity, the chlorophyll content was analysed destructively at the end of the experiment. From each mesocosm, the capitulum (top 1 cm) of five random *Sphagnum* shoots were collected, snap-frozen in liquid nitrogen, and stored at 70 °C. Next, the samples were freeze-dried and ground, after which chlorophyll a and b were extracted with a 96% ethanol solvent and their contents determined spectrophotometrically using specific absorption coefficients and equations as described by Lichtenthaler (1987).

2.2.5 Data analysis

All data were tested for normality (Shapiro-Wilk) and equality of variances (Levene's test). As water table treatment levels were species-specific, treatment effects were tested for each species separately. Treatment effects on precipitation dependence (f_p) and NEE were tested with full factorial linear mixed models with precipitation frequency as fixed factor, water table treatment as within-subjects factor and mesocosm as random effect using SPSS (v19.0.0.1; SPSS/IBM Inc., Somers, NY). Likelihood ratio tests were performed to select the most parsimonious covariance structure from a set of covariance structures that account for correlation and heterogeneous variances. If significant interactions ($P < 0.05$) between precipitation frequency and water table were present, the effect of precipitation frequency on f_p and NEE was tested with separate one-way ANOVA's for each water table treatment. Multiple comparisons were carried out per species and water table treatment to determine which precipitation frequency treatments differed significantly from each other. *P*-values were corrected for multiple comparisons using the Benjamini-Hochberg method (Waite & Campbell, 2006). In the analysis of both f_p and NEE, the first order autoregressive covariance structure was the most parsimonious for all species and was adopted in all linear mixed models accordingly.

Recovery of NEE after drought was quantified by comparing NEE at the *wet* and *rewetted* water table treatment (Table 2.1). To test if more frequent precipitation enhanced recovery of NEE, repeated-measures ANOVA was set up per species. Precipitation was included as between-subjects factor, water table treatment (*wet* versus *rewetted*) as within-subjects factor and NEE as dependent variable. Separate paired sample t tests were performed per precipitation frequency to check if the effect of water table on NEE interacted with precipitation frequency.

To also check if water availability affected NEE and to determine how this response was reflected in PSII efficiency, regression analyses were performed with NEE or PSII as dependent variable and water content as independent variable. *Sphagnum* carbon

uptake is known to decrease with reduced water availability, but also decreases in the near saturation range due to the diffusional limitation of water to CO_2 transport (Schipperges & Rydin, 1998; Williams & Flanagan, 1996). Hence, the response of carbon uptake to water availability was expected to be unimodal but not necessarily symmetric. Accordingly, first to third order polynomials were fitted and the most parsimonious variant was selected with likelihood ratio tests. Differences in mean total capitulum chlorophyll content between precipitation frequency treatments at the end of the experiment were determined with a one way ANOVA for each species.

2.3 Results

2.3.1 Precipitation dependence

The water table treatments successfully imposed differences in water contents of the living moss layer representative for field conditions (Table 2.1) for all species. Precipitation tended to increase water contents in the top layer, particularly at deep water tables (data not shown). This effect could not be further quantified, however, due to the limited number of moisture sensors (one per precipitation treatment per species). Precipitation dependence (f_p) increased significantly with increased water table depth, irrespective of species (Fig. 2.3, Table 2.3). Precipitation dependence was significantly higher in *dry* conditions (deep water table treatment; Table 2.1) than in *moist* conditions (intermediate water table treatment) for all species (Benjamini-Hochberg (BH) corrected multiple comparisons, $P < 0.05$). Overall, rainwater dependence for all species increased by 37% between *moist* and *dry* conditions. During *moist* conditions 8 – 34% of evaporation originated from precipitation, whereas under *dry* conditions this shifted to 53 – 67%, with *S. majus* showing the lowest precipitation dependence and *S. balticum* the highest precipitation dependence. For *S. fuscum*, the imposed water tables resulted in intermediate values (23% under *moist* conditions and 53% under *dry* conditions). Precipitation frequency had a limited influence on precipitation dependence. Only for *S. balticum*, precipitation dependence was significantly higher at intermediate precipitation frequencies (BH multiple comparison, $P < 0.05$).

2.3.2 Carbon uptake

Net ecosystem exchange (NEE) was significantly affected by both water table and precipitation frequency for all species (Table 2.4, Fig. 2.4). In general, precipitation compensated adverse effects of deep water tables (*dry* conditions) on carbon uptake and interacted with precipitation frequency (Fig. 2.4). For all species, frequent precipitation seemed to moderate drought impact on carbon uptake. However, the exact effect of

Table 2.3. *Significance of precipitation frequency (FREQ) and water table (WT) effects on precipitation dependence (f_p) per species.*

Effect	*S. fuscum*			*S. balticum*			*S. majus*		
	F	df	P	F	df	P	F	df	P
Intercept	317	1, 13.5	**<0.001**	95.5	1, 15.9	**<0.001**	309	1, 12.8	**<0.001**
FREQ	2.72	3, 13.4	0.086	33.6	3, 15.5	**0.037**	2.13	3, 12.6	0.148
WT	62.7	1, 16.2	**<0.001**	24.2	1, 15.6	**<0.001**	5.83	1, 13.9	**0.030**
FREQ * WT	1.26	3, 16.6	0.320	0.40	3, 15.0	0.752	0.74	3, 13.7	0.545

The f_p indicates whether groundwater ($f_p < 0.5$) or precipitation ($f_p > 0.5$) dominates water supply. WT is treated as within-subject effect. Bold values indicate significant effects ($P < 0.05$). See Fig. 2.3 for interaction effects and significant subgroups (Benjamini-Hochberg corrected multiple comparisons) of precipitation frequency per water table treatment level.

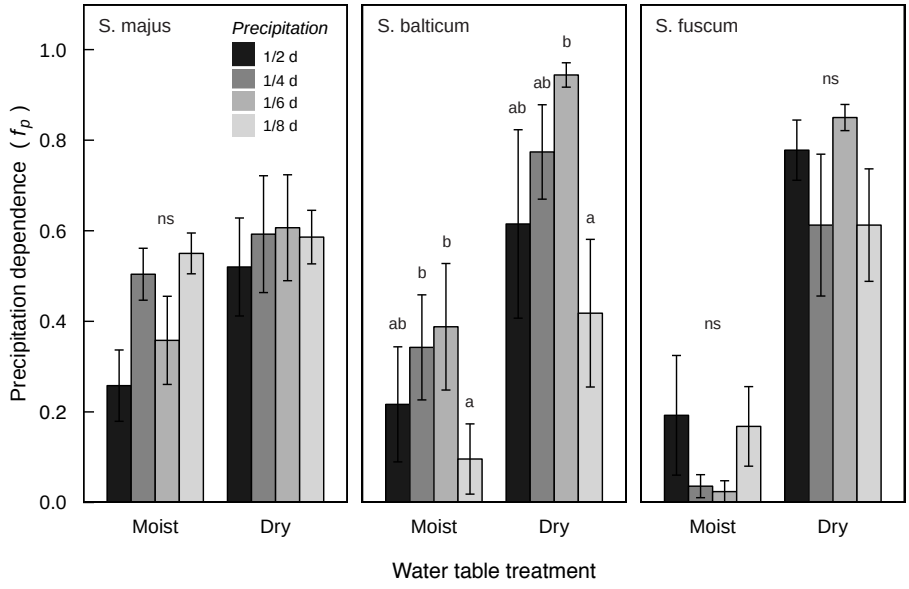

Figure 2.3. *Interactive effect of water table and precipitation frequency treatments (greyscale) on precipitation dependence (fraction of evaporation from retained precipitation water; f_p) of three Sphagnum species. f_p values indicate whether groundwater ($f_p \leq 0.5$) or precipitation ($f_p > 0.5$) dominates water supply. Letters represent homogeneous subgroups of precipitation frequency treatments per water table (Benjamini-Hochberg corrected multiple comparisons). Error bars represent one standard error. See Table 2.3 for significance of main and interaction effects.*

precipitation frequency on carbon uptake was species specific and depended on water table. For *S. fuscum*, precipitation frequency did not affect carbon uptake under *wet*

conditions (One way ANOVA, $F_{4,19} = 0.80$, $P = 0.54$; BH multiple comparisons $P > 0.05$), but significantly increased carbon uptake under *dry* conditions (One-way ANOVA, $F_{4,20} = 4.41$, $P = 0.01$; BH multiple comparisons $P < 0.05$). Similar to *S. fuscum*, the carbon uptake of *S. balticum* and *S. majus* remained unaffected by precipitation frequency in wet conditions (One-way ANOVA, $F_{4,18} \leq 0.709$, $P \geq 0.596$). In *dry* conditions, however, carbon uptake of these species responded non-linearly to precipitation frequency. For *S. balticum* for example, carbon uptake was significantly lower at the 1/4d than the 1/2d precipitation frequency treatment, indicating that carbon uptake was depressed at this intermediate precipitation frequency (Fig. 2.4; BH multiple comparison, $P < 0.05$).

2.3.3 Water, carbon uptake and photosystem efficiency

To explore the existence of critical moisture thresholds, we expressed carbon uptake and efficiency of photosystem II (PSII) as a function of volumetric water content (VWC) of the living moss layer, combining all water table and precipitation treatments. In a stepwise polynomial regression with VWC as explanatory variable, 28% of the variation in carbon uptake for *S. balticum* could be explained with volumetric water content. Despite the limited explained variation, fitted parameters were significant ($P < 0.05$) and *Sphagnum balticum* switched from carbon uptake to carbon emission at a water content of 0.48 $m^3\ m^{-3} \pm 0.04$ (SE) (polynomial regression; see Fig. 2.5a). The water content at which the switch between carbon uptake and emission occurred, corresponded with the water content at which PSII efficiency reduced sharply ($0.49\ m^3\ m^{-3} \pm 0.02$ (SE), regression of Eq. 2.3, $P < 0.001$; Fig. 2.5b), illustrating photosynthesis dominated the NEE response of the mesocosms. The water content threshold at which photosynthesis practically stopped, corresponded to a water table of about 30 cm (Table 2.1). Analysis suggests that the range in water contents imposed by the treatments was not large enough to reliably derive PSII efficiency response curves for *S. fuscum* and *S. majus*. Nonetheless, also these species showed comparable trends in PSII efficiency as function of water content. With decreasing water content, first the PSII efficiency of S. majus approached the inactive state, followed by *S. balticum* and then by *S. fuscum*.

2.3.4 Recovery after drought

Eleven days after the water table was raised back to wet conditions (*rewetted* water table treatment), carbon uptake (almost) fully recovered to initial conditions for *S. fuscum* ($P = 0.081$, paired samples t-test). For *S. majus* and *S. balticum*, carbon uptake was still significantly lower, suggesting lag-effects of drought on carbon uptake (Fig. 2.6, Table 2.5).

Recovery of *S. balticum* increased with precipitation frequency, illustrating the importance of frequent precipitation for longer term carbon uptake of this species. For *S. fuscum* and

S. majus, however, recovery remained unaffected by precipitation frequency (Table 2.5). For all species recovery was unrelated to NEE at the *dry* treatment ($R^2 \leq 0.07$, $P > 0.19$) and was not significantly related to chlorophyll content. Average chlorophyll contents

Table 2.4. *Effects of precipitation frequency (FREQ) and water table (WT) on net ecosystem exchange (NEE).*

Effect	*S. fuscum*			*S. balticum*			*S. majus*		
	F	df	P	F	df	P	F	df	P
Intercept	233	1, 20.2	**<0.001**	94.6	1, 20.5	**<0.001**	580	1, 19.5	**<0.001**
FREQ	3.19	4, 20.1	**0.035**	2.69	4, 20.4	0.060	2.63	4, 19.5	0.066
WT	22.0	2, 38.9	**<0.001**	166	2, 32.8	**<0.001**	157	2, 36.7	**<0.001**
FREQ * WT	2.20	8, 38.8	**0.049**	2.65	8, 32.7	**0.023**	3.12	8, 36.7	**0.009**

Bold values indicate significant effects ($P < 0.05$) and WT is treated as within-subject effect. See Fig. 2.4 for interaction effects and significant subgroups (BH corrected multiple comparison) of precipitation frequency per water table treatment level.

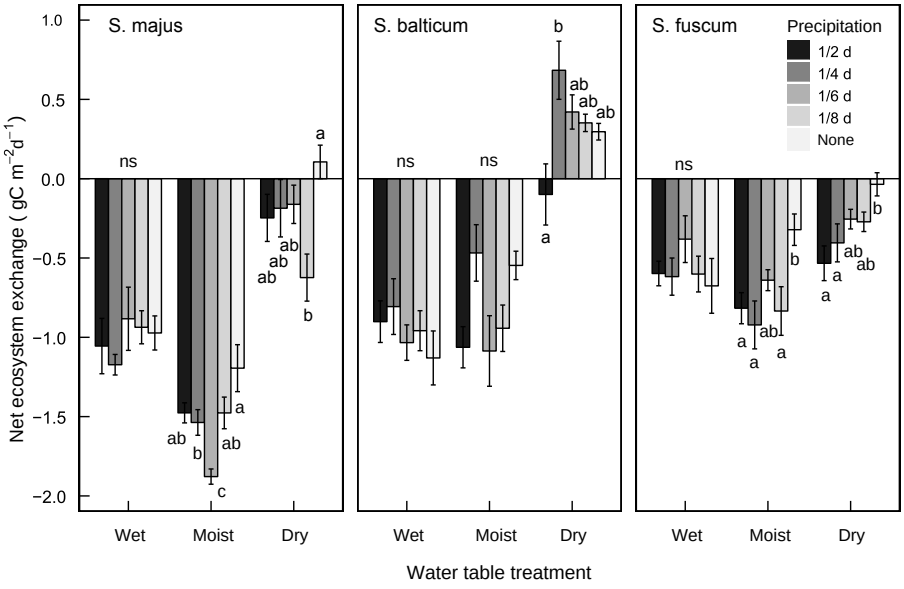

Figure 2.4. *Mean net ecosystem exchange (NEE) per treatment per precipitation frequency for three Sphagnum species. NEE values are expressed relative to the atmosphere, with negative values indicating net carbon sequestration by the mesocosms, and positive values net emission of carbon from the mesocosms (c.f. Chapin III et al., 2006). Error bars are one standard error and letters indicate significant differences between precipitation frequency treatments within each water table treatment (Benjamini-Hochberg corrected multiple comparisons). See Table 2.4 for statistics on main and interaction effects.*

for each precipitation frequency (*S. fuscum* 1.26 ± 0.09 (SE), *S. balticum* 0.81 ± 0.06, *S. majus* 1.63 ± 0.13 mg chlorophyll a + b per gram dried *Sphagnum*) were well within the range of field conditions for *Sphagnum* (Granath *et al.*, 2009; Marschall & Proctor, 2004).

2.4 Discussion

2.4.1 Precipitation frequency is important at deep water tables

We show that precipitation becomes an important source of water for *Sphagnum* plants and carbon uptake at deep water tables, supplementing capillary water supply. In summer-drought conditions, we found that the relative importance of precipitation as water source for peatmoss was on average 37% higher than for optimal field conditions (Fig. 2.3, Table 2.3), irrespective of precipitation frequency. Despite its negligible effect on *Sphagnum* water supply, however, precipitation frequency did affect carbon uptake at deep water tables, with frequent precipitation (once per two days) partly offsetting the negative effects of deep water tables for all species considered in this study. The imposed drought conditions in this study are characteristic of average July conditions in southern Sweden and hence represent a relatively mild drought. Consequently, our results provide a conservative estimate on the importance of precipitation for moderating drought impact on carbon uptake of peatmoss in northern peatlands.

In ecosystem models, water table is often implemented as the only representation for water availability in the living moss layer and (in)directly linked to *Sphagnum* carbon (Heijmans *et al.*, 2008; Turetsky *et al.*, 2012; Yurova *et al.*, 2007). Our results suggest that the predictive power of such models is reduced when deep water tables prevail, as precipitation becomes the dominant source of water and capillary supply by groundwater is only of secondary importance.

Table 2.5. *Effects of rewetting after drought and precipitation frequency (FREQ) on recovery of net carbon exchange (NEE).*

Effect	*S. fuscum*			*S. balticum*			*S. majus*		
	F	df	P	F	df	P	F	df	P
Intercept	107	1, 19	**<0.001**	162	1, 18	**<0.001**	321	1, 20	**<0.001**
FREQ	1.35	4, 19	0.289	1.30	4, 18	0.308	2.98	4, 20	**0.044**
WT	3.40	1, 19	0.081	61.7	1, 18	**<0.001**	30.2	1, 20	**<0.001**
FREQ * WT	0.65	4, 19	0.631	4.32	4, 18	**0.013**	1.28	4, 20	0.310

Recovery was quantified by comparing the wet water table (WT) treatment with the rewetted water table treatment for each precipitation frequency in a repeated measures ANOVA. Bold values indicate significant effects at the 0.05 level and WT was included as within subjects factor.

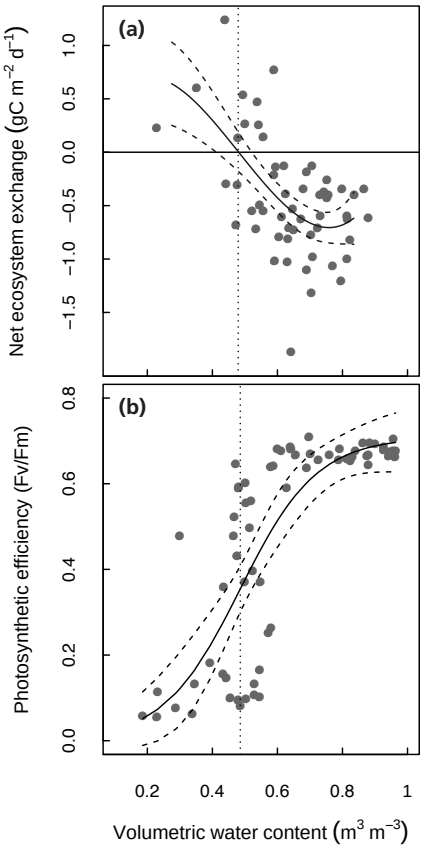

Figure 2.5. *(a) Relationship between net ecosystem exchange (NEE) and volumetric water content (VWC) for Sphagnum balticum. Negative NEE represents Sphagnum carbon uptake. The solid line represents a third order polynomial without intercept ($F_{3,52}$ = 23.9, R^2_{adj} = 0.28, P < 0.001, NEE = 7.6 VWC - 23.8 VWC^2 + 16.5 VWC^3), the dashed lines represent 95% confidence intervals and the vertical dotted line the water content at which carbon uptake switches to emission. (b) Photosystem II efficiency (PSII) as function of volumetric water content for S. balticum. A generalized logistic function (Eq. 2.3;* $F_V/F_M = \frac{0.68}{1 + e^{-22.6(VWC - 0.16)}}$*) was fitted (solid line). The F_{MIN} parameter was not significant and therefore excluded from the model but all other parameters were highly significant (P < 0.001, R^2_{adj} = 0.55). The dashed and dotted lines represent the 95% confidence bounds and the water content at which steepest decline in PSII efficiency takes place, respectively.*

2.4.2 Response of carbon uptake to precipitation frequency is species-specific

The relationship between precipitation frequency and carbon uptake differed between species. During drought, carbon uptake of *S. fuscum* was linearly promoted with higher precipitation frequency (Fig. 2.4) whereas *S. balticum* and *S. majus* responded non-linearly, showing decreased carbon uptake, or even release, at intermediate frequency. The mechanisms underlying these species-specific responses are unclear and may be related to (i) short-term heterotrophic respiration responses after rewetting or (ii) to species-specific strategies to deal with transient water supply. Short-term heterotrophic respiration responses after rewetting, also known as resaturation respiration, are generally restricted to 2 – 24 (72) hours after a rewetting event (Lee *et al.*, 2004; Smith & Molesworth, 1973; Unger *et al.*, 2010). As there were at least 48 hours between precipitation events and carbon uptake (NEE) measurements, the contribution of heterotrophic respiration response seems limited.

An alternative explanation is that the species-specific response of carbon-uptake to precipitation frequency is related to differences in strategies to deal with transient water supply and the time needed to re-activate photosynthesis after rewetting. Rewetting for an insufficient period of time could lead to incomplete recovery, no time for significant growth to maintain a positive carbon balance and flushing away of valuable metabolic compounds released after membrane rupture (Dilks & Proctor, 1976; Gerdol *et al.*, 1996; Gupta, 1977; Proctor *et al.*, 2007a). As a consequence, infrequent precipitation during summer droughts could potentially intensify the negative effect of drought on carbon uptake of species with a slow response to rewetting, such as lawn and hollow species. This counterintuitive response is in line with work by Proctor & Tuba (2002). These authors linked species water use strategy to habitat and indicate that species that respond quickly to rewetting generally dominate exposed habitats with erratic water supply at fine time scales ('low-inertia' species), while species that respond slowly to rewetting occupy habitats with a more predictable water availability on coarser time scales ('high-inertia'

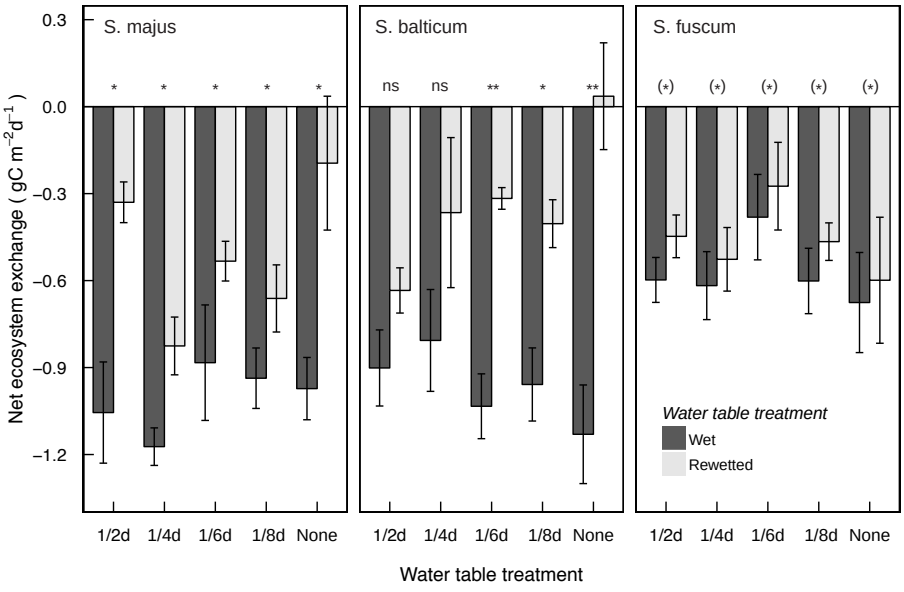

Figure 2.6. *Net ecosystem exchange before (wet water table treatment) and after rewetting (rewetted water table treatment) per Sphagnum species to identify recovery of carbon uptake after drought. Negative net ecosystem exchange values denote Sphagnum carbon uptake. Error bars represent one standard error and symbols the significance of the difference in carbon uptake between the two water table treatments per precipitation frequency as determined with paired sample t tests (**, P < 0.01; *, P < 0.05; (*), P < 0.10; ns, not significant). See Table 2.5 for significance of main- and interaction effects.*

species). Applying this concept to northern peatlands, we find that the species with a quick response time (*S. fuscum*) indeed occupies the most exposed (hummock) habitat whereas species responding slowly to rewetting (*S. balticum*, *S. majus*) occupy less exposed lawn and hollow habitats (Fig. 2.4). A higher drought tolerance for hummock peatmoss species than lawn or hollow species has also been observed by Hájek & Beckett (2008). If we consider recovery of carbon uptake at longer time scales, we again see a contrasting behaviour between hummock (*S. fuscum*) and lawn/hollow (*S. balticum*, *S. majus*) species. Eleven days after raising the water table to pre-drought wet conditions (Table 2.1), carbon uptake almost fully recovered for *S. fuscum* only. This suggests that species that are able to quickly switch from a photosynthetically inactive to an active state after rewetting (i.e. hummock species) may have a competitive advantage over species that take longer to recover (lawn, hollow species) when precipitation becomes less frequent but more intense.

Although it seems reasonable to assume that the reduced carbon uptake after drought observed for hollow and lawn species was a long-term, desiccation induced, damage to the photosynthetic apparatus, chlorophyll contents at the end of the experiment were within the range observed for optimal field conditions (Granath *et al.*, 2009; Marschall & Proctor, 2004), indicating that either denaturation of chlorophyll did not occur or that chlorophyll was resynthesized in the post drought period (11 days). Precipitation frequency did not affect the rate of recovery, except for *S. balticum*, where recovery of carbon uptake increased with precipitation frequency.

The observed effects of water table and precipitation frequency on carbon uptake were based on CO_2 flux measurements at one point in time, just before precipitation application. Hence, it cannot be excluded that time integrated, frequent measurements on carbon uptake throughout a drying-wetting cycle would yield different patterns. Nonetheless, a limited number of carbon exchange measurements (data not shown) with higher frequency throughout a few rewetting cycles suggest that a precipitation event was generally followed by a small respiration burst, followed by a stabilization of carbon exchange within six hours after rewetting. This quick stabilisation suggests that the patterns we found at longer time-scales will likely remain unaffected by more frequent measuring. However, we encourage other workers to test how carbon uptake responds to precipitation frequency at an even finer temporal resolution, and to upscale such findings over longer timescales and larger spatial scales.

2.4.3 Relating photosynthesis to water availability

For one species (*S. balticum*) we were able to identify a critical moisture threshold for photosynthetic efficiency that coincided with the point at which net ecosystem exchange of *S. balticum* shifted from carbon uptake to emission (Fig. 2.5b). Although photosynthetic efficiency around this break-even point varied, this illustrates that moss photosynthesis and carbon exchange of the living peatmoss layer of peatlands are closely connected. Identifying such species-specific moisture thresholds is of crucial importance in predicting climate change impact on carbon uptake in northern peatlands (le Roux *et al.*, 2013; Strack *et al.*, 2009).

In this study we show that precipitation can moderate the impact of drought on peatmoss carbon uptake, but that the temporal distribution of precipitation, species identity and water table depth modify this response. These results imply that processes emerging at small spatiotemporal scales at the peat atmosphere interface are crucial in understanding how carbon uptake of peatmosses and, ultimately, peatlands, will respond to altered precipitation regimes.

2.5 Acknowledgements

This study was made possible by the Schure-Beijerinck-Popping fund (KNAW) and the Dutch Foundation for the Conservation of Irish Bogs. BJMR was supported through the Division for Earth and Life Sciences (ALW) with financial aid from the Netherlands Organization for Scientific Research (NWO; Research Innovation Scheme 863.10.014). We are indebted to Fia Bengtsson, and Håkan Rydin for sharing their knowledge on *Sphagnum* species identification. We thank Bingxi Li, Dirk-Jan Pasma, Frans Möller, Gilian van Duijvendijk, Hennie Gertsen, Harm Gooren, Huib van Veen, Jan van Walsem, Jasper Wubs, Stijn Schreven, Stijn van Gils and Suzanne Okken for their help during different stages of the experiment.

Appendix 2.1 Establishing precipitation- and water table treatments

Precipitation frequency

The average daily precipitation amount was set to compensate for daily water loss by evaporation from the peat moss surface. Based on the Penman-Monteith model (Monteith, 1965; Penman, 1948), meteorological conditions in the growth chamber and a crop coefficient (a factor to translate evapotranspiration from a reference crop to evapotranspiration from a *Sphagnum* surface) of 0.77 (Kellner, 2001), the potential evaporation (E_p) in the growth chamber was estimated at 2 mm d^{-1}. Equal potential evaporation rates were assumed for the three *Sphagnum* species. To simulate natural precipitation, a realistic precipitation intensity and duration were derived from a thermodynamically based relationship between precipitation intensity, duration and frequency following Dahlström (2006)

$$R = 200\,\tau^{1/3}\ln(\Delta t)/\Delta t \qquad \text{(A2.1)}$$

where R is precipitation intensity (L s^{-1} ha^{-1}), τ is the return period (months) and Δt is the precipitation duration (min). A return period of 5 years was selected. For each precipitation frequency treatment, R and Δt in Eq. A2.1 were chosen such that $R \cdot \Delta t$ corresponded with the precipitation amount for the given precipitation treatment (Table 2.1). The treatment averaged precipitation intensity was then used for all precipitation frequency treatment levels to calculate a new precipitation duration given the required amount of precipitation to cover expected cumulative evaporative losses.

Water table treatments

Water retention cylinders were developed to be able to impose deep water tables. The functioning of the water retention cylinders (WRC's) is analogous to the principle of the sandbox, a standard procedure in soil hydrology to obtain the water retention characteristic (e.g. Klute, 1986). The WRC consisted of a PVC cylinder (ID 20 cm, height 20 cm) filled with two layers of sand separated by a filter cloth. The upper layer consisted of 6 cm fine sand (D_{50} 130 μm) and the bottom layer consisted of 4 cm very coarse sand (D_{50} 1045 μm). With the particle size of the fine sand a water table of 60 cm could be simulated by applying a suction of 60 cm. Both sands were low in iron- and magnesium oxides (Fe_2O_3 < 0.21%; MgO < 0.10%) and have a low acid buffering capacity (1.06 mmol H^+ per kg dry soil is required to raise the H^+ concentration with 1 mmol H^+; see for protocol in Scheffer & Schachtschabel (1989). The sand is therefore assumed to not alter water quality or affect moss performance significantly.

A drainage tube installed in the coarse sand is connected to the groundwater reservoir which is used to control the groundwater level. Lowering this reservoir results in drainage of water from the mesocosm in the WRC into the groundwater reservoir. If the water level exceeds the overflow threshold, water is transported to a drainage reservoir (Fig. 2.2). Evaporation from the moss surface will result in a decrease of water level in the groundwater reservoir. The decrease in water level of the groundwater reservoir activates the Mariotte bottle which replenishes the groundwater reservoir. To prevent evaporation from the free sand surface surrounding the mesocosm in the water retention cylinder, reflective isolation material was placed in the space between the mesocosm and the WRC. This guarantees that the suction pressure established in the WRCs is not affected by this evaporation and that no additional loss term needs to be included in the water balance.

Connection between water table treatments and field conditions

From soil physical perspective, the fine sand in WRCs can differ from peat in i) the water retention function and ii) the (unsaturated) hydraulic conductivity function. As a consequence of these differences, experimental conditions could conceivably not be translated to field conditions. In this section we aim to demonstrate that treatment conditions established in the growth chamber experiment can be translated to field conditions.

Water retention

The fine sand in the setup was used, together with adjusting the position of the groundwater reservoir, to apply suction to the *Sphagnum* mesocosms in the WRCs. The suction pressure is an applied physical quantity, affects water retention of the living moss layer, and is identical for experimental and field conditions. Suction pressure is controlled by atmospheric conditions and water table. With similar atmospheric conditions in the growth chamber and in the field, suctions (i.e. water tables) applied with WRCs result in the same moisture contents in both situations.

Hydraulic conductivity

Throughout the experiment the WRCs remained saturated. Given that the saturated hydraulic conductivity of the fine sand is much larger (1 – 10 m d^{-1}) than a representative evaporative demand of about 0.002 m d^{-1}, the hydraulic conductivity of the sand in the WRC will not limit water transport from the WRC towards the living moss layer. At a suction of 25 cm, the unsaturated hydraulic conductivity of the living moss layer is 0.0035 m d^{-1} (Price & Whittington, 2010). Consequently, the hydrophysical characteristics of the unsaturated living moss layer control water transport from the

groundwater reservoir to the moss surface and not the underlying fine sand.

Altogether, differences in hydrophysical characteristics between the WRC sand and *Sphagnum* peat material under field conditions are unlikely to affect water content and -transport in the living moss layer. The water table treatments established with the WRCs are therefore representative for field conditions.

Appendix 2.2 Moisture sensor calibration

The moisture sensors (EC5-H_2O, Decagon Devices, Pullman, USA), which were used to obtain time series of volumetric water content (VWC), provided a voltage output (mV), which had to be converted into VWC. Although calibration functions are available for *Sphagnum* (Yoshikawa *et al.*, 2004) the dielectric properties of is likely to differ among *Sphagnum* species. Moreover it is recommended to perform site specific calibrations for *Sphagnum* moss (Yoshikawa *et al.*, 2004). To increase the accuracy of the VWC measurements we therefore conducted a calibration experiment in which saturated peat cores were subjected to drying.

Sphagnum cores (inner diameter 15 cm, height 10 cm) of each species (*S. fuscum* [n = 3], *S. balticum* [n = 2], *S. majus* [n = 3]) were taken as described in the Methods section (main text). To prevent air entrapment, the cores were saturated from below for 24 hours. Here, saturation was defined as a groundwater level (in the *Sphagnum* core) approximating the peat moss surface as near as possible. After saturation, each core was placed on a balance and an EC5-H_2O moisture sensor (Decagon Devices, Pullman, USA) was installed horizontally at a depth of 3 cm below the peat moss surface with tines flat, representing the average water content of the upper 1-5 cm. In this set up the weight and moisture sensor voltage output during drying of each core were logged every 15 minutes with a CR1000 datalogger (Campbell Scientific, Logan, USA). Accordingly, for each point in time, the gravimetric water content (GMC) and sensor voltage output were known.

At the end of the calibration experiment, samples were oven dried for 48 hours at 70 °C to obtain the bulk density (ρ_b) , which was used to transform gravimetric water contents at time i to volumetric water contents (Eq. A2.2). We assumed that the error in VWC caused by shrinkage of the *Sphagnum* matrix was of minor importance.

$$VWC_i = \frac{GWC_i}{\rho_b} \qquad \text{(A2.2)}$$

At the start of the experiment some samples were oversaturated, as a thin layer of standing water was present due to the irregular moss surface. As a consequence VWC values larger than the saturated water content were calculated. For each sample, these water contents were removed. The saturated water content (θ_s) was defined as the total porosity (ϕ_t) and was calculated with Eq. A2.3, where ρ_p is the particle density of peat.

$$\theta_s = \phi_t = 1 - \frac{\rho_b}{\rho_p} \qquad \text{(A2.3)}$$

The particle density was estimated at 1.6 g cm^{-3} for low humified *Sphagnum* peat (Cannavo & Michel, 2013; Heiskanen, 1995). Although the particle density might vary

among species and with the commercially used *Sphagnum* peat, a 50% change in particle density resulted only in a 2% change of the total porosity.

For each species, several functions relating EC5-H_2O sensor output to VWC were fitted with non-linear regression using a Gauss-Newton algorithm (*nls* package, R v2.13.0, R Core team). Based on RMSE and visual inspection the Weibull function (Eq. A2.4) fitted the data best and all parameters were significantly different from 0.

$$VWC = 1 - e^{-\left(\frac{EC_5 - \alpha}{\beta}\right)^{\gamma}} \quad \text{(A2.4)}$$

However, fitted water contents near saturation were structurally about 10 – 15% lower than the calculated total porosities and values for saturated water content of undecomposed *Sphagnum* (Cagampan & Waddington, 2008; Schlotzhauer & Price, 1999). To force the fit through more realistic saturated water contents, extra weight (half of the total number of observations) was added to the calculated saturated water contents. The weighted Weibull calibration functions fitted the data well, especially for *S. balticum*, where the mean difference between observed and modelled VWC was only 0.022 $cm^3\ cm^{-3}$ (Table A2.1).

Table A2.1. *Parameter values for the Weibull calibration functions for relating EC5-H_2O sensor output (mV) to volumetric water content (m^3 H_2O per m^3 Sphagnum). All parameters were significant ($P < 0.001$). The goodness of fit of the calibration functions is given by the root mean square error (RMSE). Average saturated water contents estimated with Eq. A2.3 are presented in the column $\theta_s \pm SE$. Additionally the average bulk density $\rho_b \pm SE$ of the top 0 – 5 cm is given per species.*

Species	ρ_b	θ_s	RMSE	Parameter values (± 1 standard error)		
	($g\ cm^{-3}$)	($m^3\ m^{-3}$)	($m^3\ m^{-3}$)	α	β	γ
S. fuscum	0.057 ± 0.001	0.982 ± 0.003	0.086	-660.3 ± 50.6	1269.7 ± 50.9	7.389 ± 0.301
S. balticum	0.054 ± 0.001	0.981 ± 0.001	0.022	244.5 ± 1.54	296.1 ± 1.61	1.930 ± 0.010
S. majus	0.064 ± 0.001	0.983 ± 0.001	0.064	-530.5 ± 40.7	1153.6 ± 40.9	7.486 ± 0.267

3 Rain events decrease boreal peatland net CO_2 uptake through reduced light availability

Jelmer J. Nijp, Juul Limpens, Klaas Metselaar, Matthias Peichl, Mats B. Nilsson, Sjoerd E.A.T.M. van der Zee, Frank Berendse

Published in *Global Change Biology*, **21**, 2309 – 2320 (2015)

Abstract

Boreal peatlands store large amounts of carbon, reflecting their important role in the global carbon cycle. The short-term exchange and the long-term storage of atmospheric carbon dioxide (CO_2) in these ecosystems are closely associated with the permanently wet surface conditions. Especially the single most important peat forming plant genus, *Sphagnum*, depends heavily on surface wetness for its primary production. Changes in rainfall patterns are expected to affect surface wetness, but how this transient rewetting affects net ecosystem exchange of CO_2 (NEE) remains unknown.

This study explores how the timing and characteristics of rain events during photosynthetic active periods, i.e. daytime, affect peatland NEE and whether rain event associated changes in environmental conditions modify this response (e.g. water table, radiation, vapour pressure deficit, temperature). We analysed an 11 year time series of half-hourly eddy-covariance and meteorological measurements from Degerö Stormyr, a boreal peatland in northern Sweden.

Our results show that daytime rain events systematically decreased the sink strength of peatlands for atmospheric CO_2. The decrease was best explained by rain associated reduction in light, rather than by rain characteristics. An average daytime growing season rain event reduced net ecosystem CO_2 uptake by 0.23 – 0.54 gC m^{-2}. On an annual basis this reduction of net CO_2 uptake corresponds to 24% of the annual net CO_2 uptake (NEE) of the study site, equivalent to a 4.4% reduction of gross primary production (GPP) during the growing season.

We conclude that reduced light availability associated with rain events is more important in explaining the NEE response to rain events than rain characteristics and changes in water availability. This suggests that peatland CO_2 uptake is highly sensitive to changes in cloud cover formation and to altered rainfall regimes, a process hitherto largely ignored.

Keywords: Climate change, ecosystem productivity, precipitation, drought, cloud cover, eddy-covariance, mires, *Sphagnum*

3.1 Introduction

Boreal peatlands are a vital component of the global carbon cycle, accumulating an equivalent of about 50% of the current total atmospheric carbon throughout the Holocene (Kleinen *et al.*, 2012; Turunen *et al.*, 2002; Yu, 2011). In the present day climate, peatlands sequester carbon with rates of about 21 – 70 gC m^{-2} yr^{-1} (Dinsmore *et al.*, 2010; Koehler *et al.*, 2011; Nilsson *et al.*, 2008; Olefeldt *et al.*, 2012; Roulet *et al.*, 2007). How these rates will change in a future climate remains largely unknown. Annual rainfall is generally projected to increase at high latitudes (> 40°N) (IPCC, 2013), but the consequences of changes in rainfall regimes for the carbon balance of ecosystems are still hotly debated (e.g. Fenner & Freeman, 2011; Hovenden *et al.*, 2014).

The net effect of rain on the carbon balance is a result of both its effect on CO_2 gains and CO_2 losses. For peatlands it is generally expected that more rain will lower heterotrophic respiration by raising the groundwater table (Fenner & Freeman, 2011; Ise *et al.*, 2008; Scanlon & Moore, 2000). More rain also leads to wetter surface conditions, which has been shown to stimulate photosynthesis of peatmoss (*Sphagnum spp.*) (Nijp *et al.*, 2014; Robroek *et al.*, 2009; Schipperges & Rydin, 1998; Strack & Price, 2009), the keystone genus of most boreal peatlands (Rydin & Jeglum, 2013). Consequently, it seems reasonable to assume that rain would increase net CO_2 uptake of peatlands. However, recent experimental work suggests that peatmoss photosynthesis does not respond linearly to rain frequency (Nijp *et al.*, 2014). These authors showed in a growth chamber experiment that rewetting by rain may be too brief for peatmoss to offset the autotrophic respiration cost associated with restarting their photosynthetic machinery. From other ecosystems it is known that rain frequency, intensity and duration may have a larger impact on key carbon cycling processes than the total rain amount, indicating that rain characteristics are important controls on the carbon balance (Knapp *et al.*, 2002; Shi *et al.*, 2014; Xu *et al.*, 2013). Small rain events may for example trigger short-term bursts of heterotrophic respiration in semi-arid ecosystems due to increased water and substrate availability, whereas larger rain events may also stimulate photosynthesis (Lee *et al.*, 2004; Schwinning & Sala, 2004; Unger *et al.*, 2010). If these processes also operate in boreal peatlands remains unknown, despite the importance of these ecosystems for the global carbon cycle and their susceptibility to drought (Alm *et al.*, 1999; Fenner & Freeman, 2011; Heijmans *et al.*, 2013; Lund *et al.*, 2012).

In this study, we investigated the response of net ecosystem CO_2 exchange (NEE) to rain events using eleven years of meteorological and eddy-covariance measurements from the peatland Degerö Stormyr in northern Sweden. Our main objectives were to (1) identify the effect of rain event characteristics on the magnitude of NEE and (2) estimate the

impact of rain events on the annual CO_2 budget of peatlands. We hypothesized that larger rain amount, shorter drought length and shallower water table before rain events would increase ecosystem net CO_2 uptake (Knapp *et al.*, 2008; Lund *et al.*, 2012; Nijp *et al.*, 2014; Porporato *et al.*, 2004). As rain also alters environmental conditions that may directly or indirectly affect NEE, we analysed the effect of rain characteristics together with changes in environmental conditions associated with rain such as light availability, temperature, vapour pressure deficit, water table and air pressure (Chapman, 1916; Letts *et al.*, 2005; Tokida *et al.*, 2007).

3.2 Material and methods

3.2.1 Study site

This study was conducted at Degerö Stormyr (64°11'N, 19°33'E), a 6.5 km^2 minerogenic, ombrotrophic mixed peatland complex in northern Sweden, approximately 70 km inland from the Gulf of Botnia. The eddy-covariance footprint is located in the centre of the peatland complex, where peat depth generally ranges between 3 – 4 m, while depths up to 8 m have been observed at some locations in the peatland complex. The deepest peat layers correspond to a basal age of about 8000 years. The vegetation in the footprint area is fairly homogeneous and consists of both *Sphagnum* mosses and a vascular plant cover. Vegetation relevés in the footprint area indicate that the moss layer is dominated by the peatmoss species *Sphagnum balticum*, *S. majus* and *S. lindbergii* in a lawn-hollow mosaic, while the vascular plant cover consists of *Eriophorum vaginatum*, *Vaccinium oxycoccos*, *Trichophorum cespitosum*, *Carex limosa*, *Scheuchzeria palustris*, and *Andromeda polifolia*. The total green leaf biomass in the footprint is estimated at about 125 g m^{-2}, where the relative contribution of peatmoss and vascular plants is 48% and 52% (Laine *et al.*, 2011). Nilsson *et al.* (2008) and Peichl *et al.* (2013) provide a detailed site description.

At the regional scale, peatland vegetation composition varies with gradients in precipitation and temperature (Daniels & Eddy, 1985; Gignac *et al.*, 1991; Wieder *et al.*, 2006). The synoptic climate during the 2001 – 2011 study period at the study site was classified with the Köppen-Geiger system as a cold climate without a dry season and with cold summers (Dfc) (Peel *et al.*, 2007). The 30-year (1961 – 1990) mean annual rainfall and air temperature are 523 mm and +1.2 °C. January and July have the coldest (-12.4 °C) and warmest (+14.7 °C) mean monthly temperatures (Alexandersson *et al.*, 1991). The growing season rainfall, potential evapotranspiration and temperature during the measurement period closely reflected the 30-year climatic means measured (Table 3.1) at the meteorological station at Norsjö (Swedish Meteorological and

Hydrological Institute), 85 km north of Degerö Stormyr. The potential growing season rainfall deficit is estimated at 35 mm while it may reach up to 60 mm in June (Table 3.1). The growing season water table in a lawn plant community during the measurement period varied between -23.6 cm (10% percentile) and -6.2 cm (90% percentile), with a median of -14.2 cm.

Table 3.1. *Rain, potential evapotranspiration (PET) and temperature (T_{air}) during the measurement period (2001 – 2011) at Degerö Stormyr and for the 30-year climate (1983 – 2012). Potential evapotranspiration is calculated on a monthly basis following Hargreaves & Samani (1985). The 30-year climate is derived from synoptic climate station Norsjö (SMHI, 2014), 81 km north of the study site. Rain and PET values represent mean monthly amounts (mm) ± standard deviation, T_{air} is mean air temperature. In this study, growing season is defined as the period from 15 May until 15 October.*

Period	Norsjö (1983 – 2012)			Degerö Stormyr (2001 – 2011)		
	Rain (mm)	PET (mm)	T_{air} (°C)	Rain (mm)	PET (mm)	T_{air} (°C)
May	44 ± 19	95 ± 16	7.0 ± 1.5	43 ± 21	100 ± 10	7.4 ± 1.4
June	61 ± 30	119 ± 18	12 ± 1.5	60 ± 23	120 ± 18	12 ± 1.8
July	101 ± 44	115 ± 12	15 ± 1.4	99 ± 50	116 ± 11	15 ± 1.3
August	82 ± 38	85 ± 12	12 ± 1.7	105 ± 55	88 ± 9.7	13 ± 1.6
September	65 ± 34	43 ± 5.6	7.2 ± 1.4	79 ± 47	43 ± 4.5	8.0 ± 1.3
October	56 ± 32	16 ± 1.8	1.3 ± 2.1	51 ± 32	16 ± 2.3	1.7 ± 2.0
Growing season	366 ± 89	427 ± 25	10 ± 0.9	397 ± 83	432 ± 30	9.9 ± 1.6

3.2.2 Measurements of CO_2 fluxes and abiotic variables

The net exchange of CO_2 between peatland and atmosphere was measured using the eddy-covariance technique consisting of a three-dimensional sonic anemometer (1012R3 Solent, Gill Instruments, UK) and a closed-path infrared gas analyser (IRGA model 6262, LI-COR, Lincoln, Nebraska, US) mounted at 1.8 m height on a flux tower. The high frequency 20 Hz data were processed and fluxes were calculated with the EcoFlux software (In Situ Flux AB, Ockelbo, Sweden) following the EUROFLUX methodology (Aubinet *et al.*, 2000) and averaged to 30 min mean values. Only non-gapfilled data were used in this study because gap filling procedures require additional assumptions that may bias the NEE response to rain events. See Peichl *et al.* (2014) and Sagerfors *et al.* (2008) for more details on the eddy-covariance measurements.

Rainfall was measured during April – October with a tipping-bucket rain gauge (ARG 100, Campbell, Scientific, Logan, Utah, US, 0.2 mm resolution) at 10-min frequency, 4 m away from the eddy-covariance tower. Water table (WT) depth was measured

with a float- and counterweight system attached to a potentiometer (Roulet, 1991) in a lawn microhabitat 100 m away from the flux tower. Rain measurements were corrected for a 10% systematic underestimation of tipping bucket measurements following (Eriksson, 1983). Air temperature (T_{air}; °C) and relative humidity (RH; %) were measured 1.8 m above the peat surface with an MP100 moisture sensor (Rotronic AG, Bassersdorf, Switzerland) inside a self-ventilated radiation shield. Vapour pressure deficit (VPD; hPa), the difference between saturated and actual vapour pressure, was calculated following FAO standards (Allen *et al.*, 1998). Photosynthetic photon flux density (PPFD; µmol photons m^{-2} s^{-1}) was measured with a Quantum sensor (SKP 215, Skye Instruments Ltd, Powys, UK). All environmental variables were averaged to 30- minute average values. See Sagerfors *et al.* (2008) for more details on environmental measurements.

3.2.3 Data analysis

3.2.3.1 Defining and separation of rain events

Independent rain events were obtained by disaggregating the rainfall time series in individual rain events on the basis of the minimum inter event time (MIT; Dunkerley, 2008). The MIT is a fixed minimum time interval without rainfall between two rain measurements. If the inter-event time between two consecutive rain measurements is smaller than the MIT, the rain measurements are aggregated into one event (Fig. 3.1a). The MIT was determined as the minimum time elapsed until rainfall measurements were independent from each other, i.e. the separation time between rain measurements at which the temporal autocorrelation was minimal (less than 5%; See Appendix 3.1). The analysis revealed that this threshold was reached at both 1.5 hrs and at 10 hrs. These values were used as MIT criteria in all subsequent analyses.

3.2.3.2 Calculating the NEE response to rain events

Net ecosystem exchange (NEE) of carbon dioxide uptake is defined as the imbalance between photosynthetic CO_2 uptake (gross primary production; GPP) and ecosystem respiration (R_e). In R_e we can distinguish microbial decomposition (heterotrophic respiration; R_h) and a plant component (autotrophic respiration; R_a). The difference between GPP and R_e is referred to as net ecosystem exchange (NEE) of atmospheric CO_2 (Eq. 3.1).

$$NEE = GPP - R_e = GPP - R_h - R_a \qquad (3.1)$$

We explored the effect of rain events on NEE (gC m^{-2} d^{-1}) by standardizing NEE after the start of a rain event (NEE response; NEE_{RES}) with NEE prior to this event (NEE

reference; NEE_{REF}). Thus, the effect of rain on NEE, ΔNEE ($gC\ m^{-2}$), was defined as the difference between NEE_{RES} and NEE_{REF} (Eq. 3.2).

$$\Delta NEE = \Delta t_{RES}\left(\frac{1}{n}\sum_{i=1}^{n} NEE_{RES,i} - \frac{1}{m}\sum_{j=1}^{m} NEE_{REF,j}\right) \quad (3.2)$$

Here, Δt_{RES} is the duration of the response timeframe (d), n is the number of NEE observations during the response timeframe and m is the number of NEE observations during the reference timeframe (Δt_{REF}). Generally m equals n, but may differ in case of missing values. Carbon fluxes were expressed relative to the atmosphere following Chapin III *et al.* (2006), with negative values indicating net CO_2 uptake by the peatland and positive values net emission of CO_2 from the peatland into the atmosphere. Hence, positive values of ΔNEE indicate more positive (or less negative) NEE after a rain event than prior to this event, i.e. decreased uptake or increased release of CO_2. However, since ΔNEE represents the effect of rain events on NEE, the cause of this effect cannot be attributed specifically to GPP or R_e in this analysis.

To determine how long rain events could influence NEE, NEE_{RES} was calculated over multiple timeframes (*response timeframe*, Δt_{RES}). The duration of Δt_{RES} ranged between 3 – 72 hrs, starting from the onset of a rain event (Fig. 3.1b). NEE_{REF} was calculated over a period (*reference timeframe*, Δt_{REF}) equal in length and diurnal characteristics as Δt_{RES} (Fig. 3.1b). For response timeframes up to 24 hours, Δt_{REF} equalled Δt_{RES} shifted 24 hours back in time. For response timeframes larger than 24 hours, we used a sequence of multiple copies of the same 24 hours reference timeframe to calculate NEE_{REF}. For example, for NEE_{RES} = 30 hrs, we created a sequence of two identical 24 hour reference timeframes. Of the first copy, the full 24 hour period was used, while for the second only the first 6 hours were used. Consequently, both length and time of day of the timeframes over which NEE_{RES} and NEE_{REF} were averaged remained identical, thus preventing overlap between the reference and response timeframes.

3.2.3.3 Rain event selection

After aggregating rain measurements into rain events using the MIT, we applied a number of selection criteria (Table 3.2) to (1) control for the timing of the event within the year and day (2) for potential measurement errors in rain measurements and (3) for the influence of one rain event on the other. The final number of suitable rain events depended on both MIT and the length of the response timeframe (Fig. 3.1b), yielding a smaller number of suitable events for MIT = 1.5 hrs and a larger number for MIT = 10 hrs. With longer response timeframes, fewer events were suitable due to rainfall occurrence during the response timeframe.

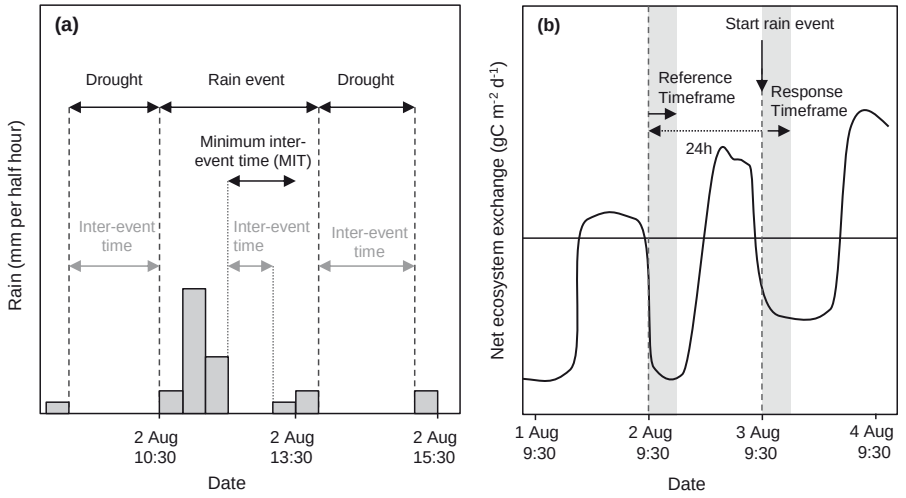

Figure 3.1. *(a) Example illustrating definitions of rain event, the minimum inter-event time (MIT), and drought length before and after a rain event. (b) Definition of reference and response timeframes over which NEE was averaged to calculate the effect of rain on ecosystem net CO_2 uptake (ΔNEE; $(NEE_{RES} - NEE_{REF}) \cdot \Delta t_{REF}$), illustrated for a response timeframe (Δt_{REF}) of 6 hours. NEE_{RES} and NEE_{REF} were calculated as the mean NEE flux over the timeframe concerned (Eq. 3.2). Shaded areas indicate the duration of timeframes.*

3.2.3.4 Explanatory variables

Besides rain event characteristics, also environmental changes related to rain events may affect the NEE response to rain events. We therefore distinguished two types of variables that could explain the NEE response to rain: I) variables describing the rain event (amount, duration, intensity, pre-rain drought length), and II) variables describing the changes in the environmental variables associated with rain events (i.e. light availability, vapour pressure deficit, temperature, water table depth, air pressure). Furthermore the timeframe of NEE_{RES} was included as explanatory variable to determine the response time of the rain effect on NEE. The changes in the environment were calculated using the same response- and reference timeframes as those used for ΔNEE. The selection of the tested explanatory variables was based on their reported effect on NEE and examination of the used dataset.

3.2.3.5 Statistical analysis

We analysed the relationships between the response variable (ΔNEE) and explanatory variables using both bivariate correlations (Spearman rank-correlation) and generalized additive regression models (GAM). The GAM regression represents a non-linear and

Table 3.2. *Rain event selection criteria settings and their impact on rain event selection* [a].

Selection criterion	Settings	% of total events	Remaining # events
Growing season only	15 May – 15 October	100	565 [b]
Minimum number of daytime measurements	At least 5 half-hour NEE measurements between sunrise and sunset should be included (corresponding to a minimum of 83% of NEE data values per event during daytime, in case of the smallest timeframe of 3 hours i.e. 6 half hourly observations). In this way we allow for instantaneous NEE changes after a rain event due to increased GPP, which cannot occur during the night due to light limitation [c].	98	538
Rain amount per event	Minimum of 0.6 mm to assure accurate estimates of the rain amount. Assuming uniform rainfall during half an hour, at least 0.6 mm of rain needs to fall in three consecutive 10-minute tipping bucket measurement intervals.	63	346
Minimum pre-rain drought length	2 days, to limit influence of preceding rain event on the reference NEE	51	279
Post-rain drought length	No rain during NEE response timeframe. Rain events were selected if *rain event duration + post-rain drought duration ≥ timeframe (c.f. Fig. 3.1a)*.	16	89

[a] Example for an NEE response timeframe length of one day and a MIT of 10 hours. The column with % of total events shows the percentage of events that remains after applying the selection criterion. The remaining number of events after application of the selection criterion is presented in the last column.

[b] This number represents the total number of rain events during growing season where rain characteristics, NEE response and mean environmental conditions (See Table 3.3) could be calculated.

[c] Sunset and sunrise were calculated as a function of day of year, declination angle of the earth and sunset hour-angle for latitude 64.11°N following Brock (1981).

non-parametric alternative to linear regression. With GAM we estimated which fraction of the total variation in ΔNEE could minimally and maximally (hereafter referred to as bottom and top marginal contribution (c.f. Janssen, 1994), be explained by each of the explanatory variables. ΔNEE was modelled as a linear combination of cubic regression splines fitted to the explanatory variable – NEE relationship using the *gam* utility in the *mgcv* package in R (R Core Team, 2014). The optimal number of cubic splines included in the smoother functions of explanatory variables was determined with penalized maximum likelihood estimation, in which both goodness of fit and model parsimony were maximized (Wood, 2004).

For each explanatory variable, the top marginal contribution was derived from the

R^2 obtained when the target variable was added first to a full model (R^2 with a Type I sum of squares approach), while the bottom marginal contribution was derived from the R^2 when the target variable was added last to a full model (R^2 with a Type III sum of squares approach). If both the top and bottom marginal contributions are high, the explanatory variable has a large contribution to the variation in ΔNEE. A high top marginal contribution combined with a small bottom marginal contribution indicates high collinearity with other explanatory variables. See Metselaar (1999) and Janssen (1994) for more details. With this approach, difficulties intrinsic to stepwise regression techniques, such as selecting a single model from a set of models with equally good performance, biased regression parameter estimates, and collinearity among explanatory variables, are circumvented (Mac Nally, 2000; Smith *et al.*, 2009; Whittingham *et al.*, 2006). The above analysis was performed using both MIT settings (10 hrs and 1.5 hrs). As only for MIT = 10 hrs the sample size was sufficient for adequate statistical analysis, we only present the results of MIT = 10 hrs. Nonetheless, general patterns were very similar for both MITs (data for MIT = 1.5 hrs not shown).

3.3 Results

3.3.1 Rain event effect on environmental conditions

A total number of 89 independent rain events fulfilling the selection criteria given in Table 3.2 were extracted from the 2001 – 2011 dataset, using a minimum inter-event time (MIT) of 10 hours. These selected rain events had a median rain amount of 5.6 mm, lasted for 0.5 days and were preceded by a drought length of 3.3 days (Appendix 3.2). All following statistical analyses were performed using these 89 rain events.

Rain events were accompanied by a decrease of vapour pressure deficit (VPD), light availability (PPFD), air temperature (T_{air}) and air pressure (P_{air}), but an increase of the water table (WT) (Table 3.3). Although the change in P_{air} was negligibly small, all median changes in environmental conditions were significant (Wilcoxon signed-rank test, $W > 64$, $P < 0.001$). As indicated by the standardized effects, rain events most strongly altered vapour pressure deficit and light availability (Table 3.3). The effect of rain on environmental conditions decreased with time after rain.

3.3.2 Impact of NEE response to rain on the annual CO_2 budget

Net ecosystem exchange (NEE) was consistently more positive after, than before rain events, suggesting that the selected daytime rain events reduced the ecosystem net CO_2 uptake during the growing season (Fig. 3.2). The rain effect on NEE (ΔNEE) increased

with the timeframe over which NEE was calculated up until 1 – 1.5 days after rain. From that point onwards ΔNEE stabilized into a slightly oscillating pattern. These oscillations are the result from random variation in the NEE data and not related to systematic effects of the calculation method (tested on a synthetic dataset, not shown). Moreover, because of the large standard error around ΔNEE for all timeframes, these oscillations are of minor importance only. The overall ΔNEE response could be well described with an asymptotic negative exponential curve, with 95% of the fitted asymptotic ΔNEE value being reached at 1.3 days (Fig. 3.2). The asymptotic value of the ΔNEE response represents the maximum effect of rain on NEE, and can thus be estimated as 0.54 ± 0.01 gC m^{-2} (mean ± SE) per rain event. With an average number of 62 daytime rain events per growing season, this would mean rain could potentially reduce ecosystem net CO_2 -C uptake over the growing season with 33.5 gC m^{-2} yr^{-1}. This is considerable, as the growing season GPP and annual NEE at the study site are estimated at 325 ± 95 gC m^{-2} yr^{-1} (mean ± SD) and 58 ± 21 gC m^{-2} yr^{-1} during 2001 – 2012 (Peichl *et al.*, 2014).

Table 3.3. *Effect of selected rain events on environmental variables for two response timeframes (0.5 and 1 days) and MIT = 10 hours.*

Variable	Unit	Timeframe = 0.5 day					Timeframe = 1 day		
		Median pre-rain value	P_{25} [a]	P_{75} [a]	Median change [b] ± 95% CI	Std effect [c] (%)	Median pre-rain value	Median change [b] ± 95% CI	Std effect [c] (%)
PPFD	μmol m^{-2} s^{-1}	381	158	539	-176 ± 34	-46	320	-163 ± 38	-51
VPD	kPa	0.44	0.15	0.75	-0.28 ± 0.04	-65	0.47	-0.36 ± 0.05	-79
WT	cm	-16.7	-25.1	-8.5	0.64 ± 0.38	-3.8	-16.7	0.49 ± 0.31	-2.9
T_{air}	°C	11.6	3.3	17.9	-1.63 ± 0.44	-14	11.3	-1.04 ± -0.61	-9.2
P_{air}	hPa	979	916	987	-3.82 ± 1.07	-0.3	979	-4.04 ± 1.12	-0.4

[a] The 25% and 75% percentile of pre-rain values are presented in columns P_{25} and P_{75}.

[b] The change of an environmental variable due to rain events was calculated as its time-averaged value during the response timeframe minus its time-averaged value during the reference timeframe (i.e. similar to Eq. 2.2).

[c] The rain effect on environmental variables is presented with the median change and its 95% confidence interval (CI). The standardized effect (Std effect), estimated as the median change divided by the pre-rain value (expressed as percentage), shows which variable changed most after rain.

The analysis above represents the potential effect of independent isolated rain events on NEE for the events fulfilling the selection criteria (Table 3.2). To determine the sensitivity of the results for the selection criteria we repeated the analysis above excluding all rain

event selection criteria with the exception of the daytime only criterion (Table 3.2). In that case, the reduction in net CO_2 uptake per daytime rain event is estimated at 0.23 ± 0.01 gC m^{-2}, and is comparable to 4.4% of growing season GPP and 24% of annual NEE at the study site.

3.3.3 Variables explaining magnitude of NEE response to rain events

The NEE response to rain (ΔNEE) correlated most with the changes in photon flux density (ΔPPFD) and water vapour deficit (ΔVPD) associated with the rain events (Table 3.4). Furthermore, an increased rain amount per event and increased duration of the rain event were positively correlated with ΔNEE (Table 3.4; Fig. 3.3). Rain slightly raised the water table (with respect to peat surface; positive ΔWT), which in turn was weakly positively correlated with ΔNEE. The drought length prior to the rain event and the water table depth prior to the rain event were not correlated with ΔNEE (Table 3.4; Fig. 3.3d).

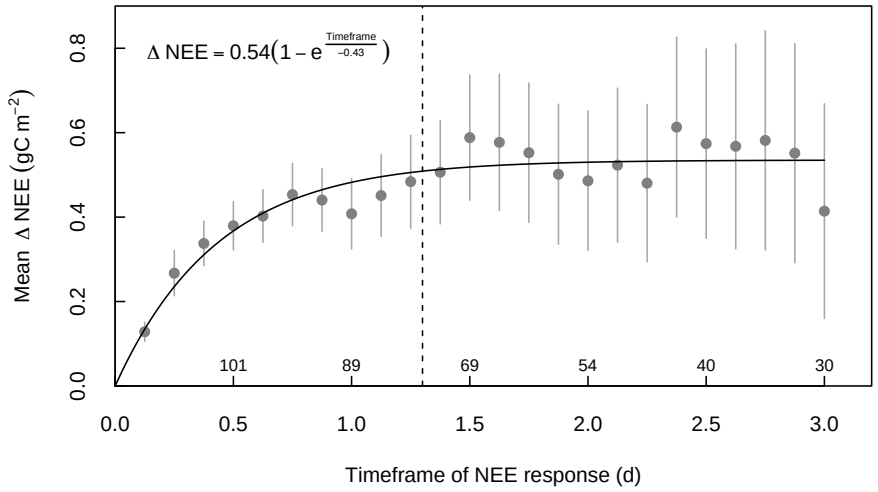

Figure 3.2. *Rain effect on ecosystem net CO_2 uptake (ΔNEE) as a function of the response timeframe over which NEE was averaged. Positive ΔNEE values indicate a net atmosphere CO_2 uptake, which corresponds with a net decrease in ecosystem CO_2 uptake. Only rain events fulfilling selection criteria in Table 3.2 were selected; the number of events fulfilling the criteria for the corresponding timeframe is shown in the figure for a minimum inter-event time (MIT) of 10 hours. Error bars denote one standard error from the mean. The solid line represents the fit of the presented equation ($R^2 = 0.97$; RMSE = 0.05 gC m^{-2}; both fitting parameters were significant at the 0.05 level). The vertical dashed line shows the timeframe at which 95% of the asymptotic value of ΔNEE was reached.*

The high collinearity between changes in photon flux density and vapour pressure deficit and between total rain amount and rain duration makes it difficult to separate the effects further. The moderately strong negative correlation between change in light availability and rain duration indicates that longer rain events were generally associated with larger light reductions. The results described above (Table 3.4) were further supported by the regression analyses (Fig. 3.3; Fig. 3.4), illustrating that ΔNEE was mainly explained by reductions in light or vapour pressure deficit and total amount of rain events (or duration). The contribution of all other explanatory variables to variation in ΔNEE was minor. Due to the high collinearity among variables (Table 3.4) it was

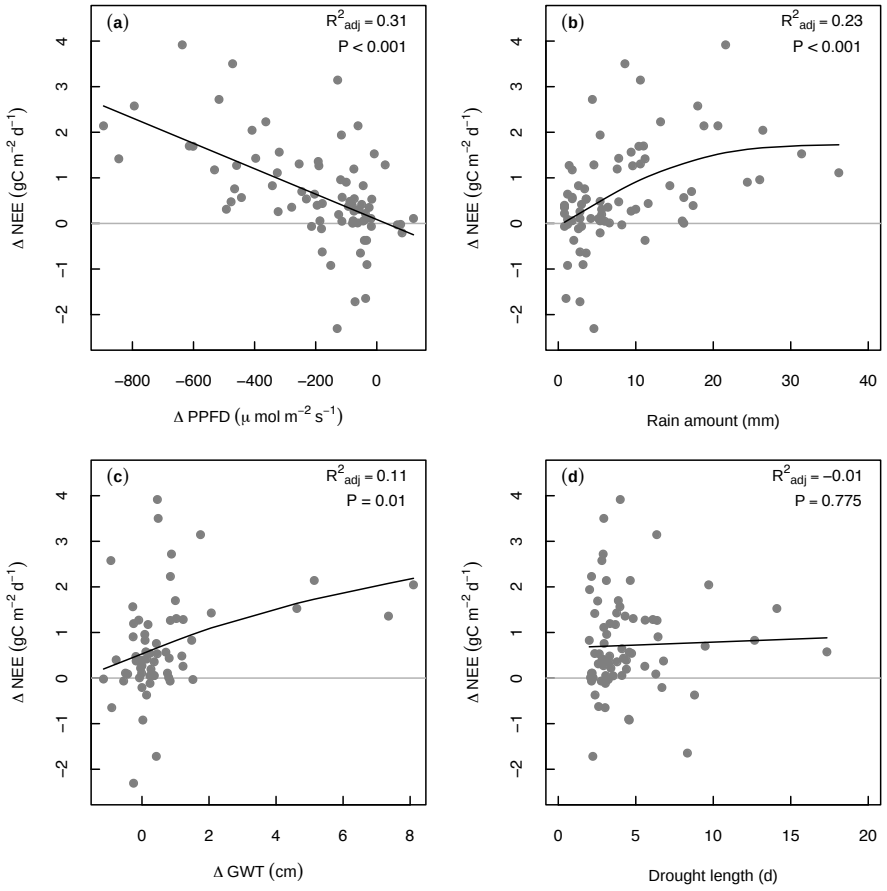

Figure 3.3 *Univariate GAM models presenting the effect of change in light availability (a), rain amount (b), change in water table (c) and drought length (d) on NEE response to rain events (ΔNEE) for MIT = 10 hours and response timeframe duration = 24 hours. The goodness of fit is presented with R^2_{adj} and the level of significance with the P value.*

not possible to establish the relative contribution of each variable to variation in ΔNEE. Highly correlated explanatory variables were therefore removed in the regression analysis to avoid small bottom marginal contributions. The goodness of fit (R^2_{adj}) of the overall multivariate generalized additive model including all additive main effects of the presented variables was 0.50 and the additive model components were significant for all variables ($P < 0.05$) (Fig. 3.4).

To explore if the minor contributions of water table or drought length could be related to wet conditions dominating the ΔNEE response, we repeated our analyses on data subsets. Experimental work suggests that rain may only moderate drought impact on peatmoss photosynthesis at deep water levels (Nijp *et al.*, 2014; Robroek *et al.*, 2009). To test if such interactive effects between drought length and water table were present, we grouped the data in categories with shallow (≥ 12 cm) and deep (≤ 18 cm) water tables, and short (0 – 1 day) and long (≥ 3 day) pre-rain drought lengths. This analysis however yielded the same result: pre-rain water table depth and pre-rain drought length did not explain the response of NEE to rain (data not shown).

3.4 Discussion

3.4.1 Controls on the NEE response to rain events

Our results show that daytime rain events significantly affected net ecosystem CO_2 exchange (NEE) up until 1.3 days after a rain event, with larger rain amounts and longer rain event durations having a stronger effect. Daytime rain events systematically decreased the sink strength of peatlands for atmospheric CO_2. This response was contradictory to our hypothesis, as we expected that rewetting by rain would increase net ecosystem CO_2 uptake by enhancing peatmoss photosynthesis (Schipperges & Rydin, 1998; Strack & Price, 2009), and that rising water tables would reduce heterotrophic respiration (e.g. Fenner & Freeman, 2011; Ise *et al.*, 2008). Several processes may be responsible for the reduced net CO_2 uptake after rain, of which the likelihood is discussed below.

First, peatmoss photosynthesis during the selected rain events may simply have not been limited by water. In that case wetter surface conditions after rain could only have had a neutral-negative effect on photosynthesis and net CO_2 uptake, as high water content may inhibit CO_2 diffusion and limit photosynthetic carbon uptake of *Sphagnum* (Williams & Flanagan, 1996). Optimal water tables for photosynthesis of the lawn peatmoss species dominating the footprint (*S. majus*, *S. lindbergii* and *S. balticum*) range between 5 – 15 cm below moss surface, depending on species (Andrus *et al.*, 1983; Nijp *et al.*, 2014; Rydin & McDonald, 1985b). Since the median water table was 17 cm (Table 3.3), it

seems reasonable to assume that moss photosynthesis was (co-) limited by water stress during the studied rain events. Still, it may have been possible that rain temporarily increased peatmoss water content beyond the optimum for photosynthesis (Williams & Flanagan, 1996). Nevertheless, since undecomposed *Sphagnum* peat has a high hydraulic conductivity at high water contents (McCarter & Price, 2014; Price *et al.*, 2008), rain water likely infiltrates too rapidly for this effect to be present up to 1.3 days after rain.

Second, the magnitude of the NEE response to rain events may be controlled by rain event characteristics. Both rain amount and duration are moderately associated with the NEE response to rain events (Table 3.4). Due to the high collinearity between amount and duration we were unable to conclusively determine the strongest control on the NEE response to rain events. More importantly, however, rain events with larger rain amounts and longer duration reduced net CO_2 uptake rather than enhancing it. A process that could potentially explain this positive correlation is the physical displacement of CO_2 in the peat matrix by rain water (Chen *et al.*, 2005a; Unger *et al.*, 2010). However, the potential CO_2 displacement for an average daytime rain event corresponds to 20% of the mean rain induced decreased net CO_2 uptake of 0.54 ± 0.01 gC m^{-2} (See Appendix 3.3 for calculation details). It thus seems very unlikely that physical displacement of CO_2 is the dominant process responsible for the decreased net CO_2 uptake after rain.

Third, vapour pressure deficit shows a strong positive correlation with the NEE (Table 3.4), but the relation is opposite to what is expected for both photosynthetic CO_2 uptake by peatmoss (Skre *et al.*, 1983) and vascular plants (e.g. Bunce, 1998). Therefore, it is most unlikely that vapour pressure deficit is an important control on the NEE response to rain events.

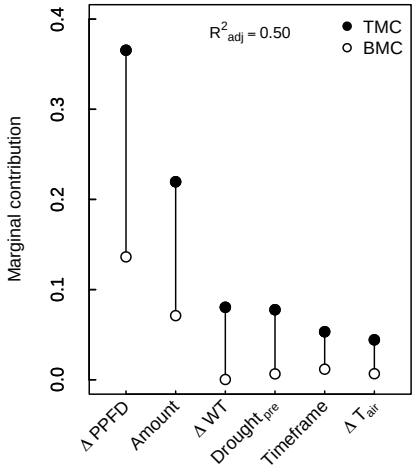

Figure 3.4. *Bottom (○) and top (●) marginal contribution of a selected subset of explanatory variables to variation in ΔNEE, the rain effect on short-term ecosystem net CO_2 uptake, as acquired with generalized additive regression models for MIT = 10 hours. The goodness of fit is presented by R^2_{adj}. The top marginal contribution represents the R^2 obtained when the target variable was added first to a full model, while the bottom marginal contribution was derived from the R^2 when the target variable was added last to a full model.*

Table 3.4. *Correlation matrix showing collinearity among rain characteristics, rain induced changes in environmental variables and the rain effect on ΔNEE (gC m^{-2}). Positive ΔNEE values indicate reduced net CO_2 uptake by the peatland ecosystem* [a].

Variables[b]	ΔPPFD	ΔVPD	Amount	Duration	ΔP_{air}	ΔWT	Time frame	ΔT_{air}	Drought	Intensity	WT
ΔNEE	**-.60**	**-.54**	**.40**	**.36**	**-.29**	**.26**	**-.23**	**-.14**	**.06**	**.05**	-.01
ΔPPFD		**.73**	**-.39**	**-.33**	**.32**	**-.30**	**.35**	**.29**	**.07**	**-.08**	.00
ΔVPD			**-.45**	**-.42**	**.23**	**-.41**	**.27**	**.57**	**-.11**	**-.06**	**.19**
Amount				**.77**	**-.17**	**.62**	.04	**-.25**	**.10**	**.33**	**-.12**
Duration					**-.19**	**.50**	**.07**	**-.14**	**.05**	**-.31**	**-.16**
ΔP_{air}						**-.21**	**.17**	**-.11**	**.11**	.01	**-.05**
ΔWT							.04	**-.20**	**.15**	**.23**	**-.43**
Time frame								**-.08**	**.07**	-.04	-.05
ΔT_{air}									**-.19**	**-.20**	**.19**
Drought										**.06**	**-.15**
Intensity											**.09**

a Spearman rank correlation coefficients. Explanatory variables are sorted by their absolute correlation with ΔNEE; significant correlations ($P \leq 0.05$) are in bold.

b All variables preceded with Δ represent a change in conditions (i.e. after – before rain). PPFD = Light availability (μmol m^{-2} s^{-1}); VPD = Vapour pressure deficit (kPa); Amount = Total rain amount in event (mm); Duration = Rain event duration (hours); P_{air} = air pressure (hPa); WT = Water table prior to rain (cm below peat surface, positive changes indicates rise in WT); Timeframe = Duration of response timeframe (hours); T_{air} = Air temperature (°C); Drought = pre-rain drought length (days); Intensity = Mean rain event intensity (mm h^{-1}); WT = mean water table depth during the reference timeframe (cm below peat surface).

Fourth, the reduced net CO_2 uptake after rain may originate from the short-term heterotrophic respiration response to rewetting (resaturation respiration) (e.g. Fenner & Freeman, 2011). However, resaturation respiration is strongly coupled to antecedent moisture conditions (Cable *et al.*, 2013; Potts *et al.*, 2006). Since our results show that both water table depth and drought length before rain events had negligible effect on the NEE response to rain events (Table 3.4), it is unlikely that resaturation respiration can explain the NEE response. To disentangle the response of NEE to rain, future studies where the distinct responses of GPP, R_a and R_h are measured at fine temporal scales are essential.

Fifth, the reduced light availability accompanying rain events may have depressed photosynthesis (Letts *et al.*, 2005), resulting in a net reduction of CO_2 uptake after rain events, as seems to be indicated by their strong negative correlation (Table 3.4). On average, rain events reduced light availability with 163 μmol m^{-2} s^{-1} (Table 3.3). To determine the potential contribution of such a light reduction on GPP, a light response curve was constructed following Barr *et al.* (2004). By comparing mean GPP at pre-rain

light levels with GPP at post-rain light levels, we estimated that reduced light availability associated with rain events could decrease GPP by at least 31% (See Appendix 3.4 for calculation details). This would amount to a reduction of the net CO_2 uptake by 1.1 ± 0.02 gC m^{-2} for an individual cloud event, which is even more than the estimated 0.54 ± 0.01 gC m^{-2} for a rain event. The latter suggests that reduced light availability rather than an altered moisture regime is most likely the explanation for the reduction in ecosystem net CO_2 uptake associated with rain events. This corresponds with results of Loisel *et al.* (2012), who showed that integrated growing season light availability is a better predictor for annual *Sphagnum* growth than effective moisture availability. Accordingly, NEE at the ecosystem scale may be well predicted from light availability, and including water availability as predictor for NEE is likely of minor importance at this spatial scale. Water availability remains a crucial factor for e.g. hydrological niche differentiation (Rydin, 1986), and an important predictor for moss photosynthesis at constant light availability (e.g. Nijp *et al.*, 2014; Schipperges & Rydin, 1998). In the boreal and (sub)arctic zone, however, light availability is often below light saturation levels of most plant species during autumn, thus reducing the potential CO_2 fixation rate. This suggests that in these periods NEE is sensitive to changes in light, stressing the importance of adequate parameterization of light response curves in ecosystem models.

Peatmoss and vascular plants both contribute importantly to green biomass in many boreal peatlands (Laine *et al.*, 2011), implying that our results reflect a combined response of both these plant groups. As peatmoss photosynthesis is light-saturated at lower PPFD (325 – 620 μmol m^{-2} s^{-1}; Titus & Wagner (1984)) than vascular plants (> 1500 μmol m^{-2} s^{-1}; Peichl *et al.* (2014)), it may be that the observed NEE response to rain events is dominated by vascular plants rather than by peatmoss. The latter is supported by the fraction of the total number of growing season days for which mean midday (10:00 – 14:00) light availability drops below the light saturation value of vascular plants (84%) and peatmosses (22%).

3.4.2 Implications of reduced net CO_2 uptake by rain for the annual CO_2 balance

Peatland formation and peat accumulation are strongly defined by the magnitude and seasonality of the rainfall surplus (Ivanov *et al.*, 1981). Increased rainfall is generally assumed to promote peat accumulation (Belyea & Baird, 2006) and thus increase carbon sequestration. However, our study clearly reveals the delicate role of daytime rain events through maintaining a positive water balance, but at the same time reducing the incoming photosynthetic active radiation.

Our results show that the NEE reduction by daytime rain events is likely driven by reduced light availability and that drought length prior to the rain event was of minor importance. These results seemingly contradict results of previous studies under controlled environment that stress the importance of rewetting by rain for peatmoss photosynthesis (Robroek *et al.*, 2009; Schipperges & Rydin, 1998; Strack & Price, 2009) and drought tolerance (Nijp *et al.*, 2014). This contradiction between the current field study and the controlled experiments likely arises from the differences in light conditions. As shown in this study, light conditions co-vary with rain occurrence in field conditions, while they were maintained at constant levels in controlled experiments. Thus, the exclusion of reduced light conditions associated with rain events in mesocosm experiments probably prevented detection of the stronger shading effect.

On an annual basis, the reduction of net CO_2 uptake, reaching up to 0.54 g CO_2-C m^{-2} per daytime rain event, is comparable to a 10% reduction of the growing season GPP (Peichl *et al.*, 2014). Although the reduction in growing season GPP due to rain events is relatively small, it is equivalent to about 58% of the mean annual net CO_2-C uptake of the study site (Peichl *et al.*, 2014). Extrapolating these quantitative estimates to other hydro-climatic settings and temporal scales must be treated with some caution as the presented results are inferred from a single hydro-climatic setting, for a selected set of discrete rain events. The studied peatland, Degerö Stormyr, a *Sphagnum* and short sedge dominated peatland with a water table relatively close to the peat surface, is though representative for vast peatland areas at high latitudes (see e.g. Nilsson *et al.*, 2001; Riley, 2011). Repeating this analysis for peatlands in different hydro-climatic settings is essential for further upscaling of our results.

For our analysis we selected discrete rain events, needed to obtain independent responses of NEE to rain events. The selection criteria constituted a strong filter on all rain events, for example leaving out long periods of attenuated rain. Consequently, our estimate of 58% annual NEE reduction is an estimate for a climate in which rain mainly occurs in isolated events, while the reduction of 24% (calculated after removing all selection criteria except the daytime rain) is based on the climate at Degerö Stormyr. The sensitivity of the results to these general temporal rainfall characteristics highlights that future shifts in rainfall regime may substantially impact the ecosystem carbon balance in ways current ecosystem models are poorly equipped to predict. To correctly capture rain effects on carbon exchange in northern peatlands, a fine temporal discretization or a parameterization quantifying the effect of intra-annual rain characteristics on NEE is required.

Furthermore, the annual net CO_2 uptake of boreal peatlands, and consequently the future sink strength of those ecosystems, may be highly sensitive to future changes in cloud cover. Multi-model future projections consistently show increased total cloud amount at high latitudes, although exact changes in cloud characteristics and temporal distribution are ambiguous (IPCC, 2013). As changes in cloudiness and rainfall regimes are major constituents of "climate change projections" (IPCC, 2013; Soden & Held, 2006), our findings will be crucial in understanding and predicting carbon exchange at high latitude peatlands under a future climate.

3.5 Acknowledgements

This study was co-funded by the Schure-Beijerinck-Popping fund (KNAW), the Dutch Foundation for the Conservation of Irish Bogs and by WIMEK/SENSE (The Wageningen Institute for Environment & Climate Research, and the Socio-Economic & Natural Sciences of the Environment), the Swedish Research Council for Environment, Agricultural Sciences and Spatial Planning (Grant No. 2007-666) to MN. We also acknowledge the Kempe Foundation for the grants (MN) supporting the micrometeorological instrumentation. Support from the Integrated Carbon Observation System (ICOS) Sweden research infrastructure (Swedish Research Council) is also acknowledged. Furthermore we thank Jörgen Sagerfors, Pernilla Löfvenius, and Mikaell Ottosson Löfvenius for their support in maintaining instrumentation and data collection at the Degerö study site. Finally, we acknowledge Nigel Roulet and Tim Moore for their valuable comments on an earlier version of this manuscript.

Appendix 3.1 Setting the minimum inter-event time

To set the minimum inter-event time (MIT), we estimated the scale of temporal autocorrelation of the rainfall time series (Dunkerley, 2008; Morris, 1984). The temporal autocorrelation (r) between rainfall amount at time t_i and rainfall at time h hours later, t_{i+h}, was calculated for all separation times h using the *acf* function in R (R Core Team, 2014). The temporal autocorrelation decreases with larger separation times h. At the separation time where the autocorrelation drops below a threshold, here set at $r = 0.05$, rain events were assumed to be independent. This threshold separation time was used as a measure of the MIT.

Several common and frequently applied theoretical autocorrelation functions in geostatistics (e.g. Webster & Oliver, 2007) were fitted through the empirical autocorrelation function. A double exponential model (Eq. A3.1) fitted the rainfall time series most parsimoniously and better than a single exponential model or a (double) spherical model, indicating that multiple scales of temporal autocorrelation need be distinguished. Hence multiple MIT criteria were employed in further analyses.

$$r = 1 - \left(\sigma_1\left[1 - e^{-\frac{h}{\alpha_1}}\right] + \sigma_2\left[1 - e^{-\frac{h}{\alpha_2}}\right] + c_0\right) \qquad \text{(Eq. A3.1)}$$

In Eq. A3.1, the α and σ parameters represent the ranges and partial sills of the two exponential models. The intercept c_0 ('nugget') was not significant and was therefore excluded from the model (Table A3.1). The effective ranges, i.e. the MIT values, were set to the range where 95% of the sill was reached and was calculated as $3 \cdot \alpha$ following Webster & Oliver (2007). As a result, mean MIT values ± 95% confidence intervals were 1.45 ± 0.06 hours and 10.01 ± 0.34 hours. In order to match the half hourly measurement frequency, we set the MIT to 1.5 and 10 hours.

Table A3.1. *Fitting parameters for the double exponential model and associated statistics. The root mean square error (RMSE) and normalized root mean square error (RMSE / data range) of the fit were respectively 0.008 (-) and 0.8%.*

Variable	Estimate	Std. Error	t value	P
α_1	3.22	0.18	18.3	< 0.001
α_2	0.47	0.03	14.2	< 0.001
c_0	0.003	0.009	0.299	0.77
c_1	0.40	0.02	17.6	< 0.001
c_2	0.58	0.02	23.9	< 0.001

Appendix 3.2 Frequency distributions of rain characteristics

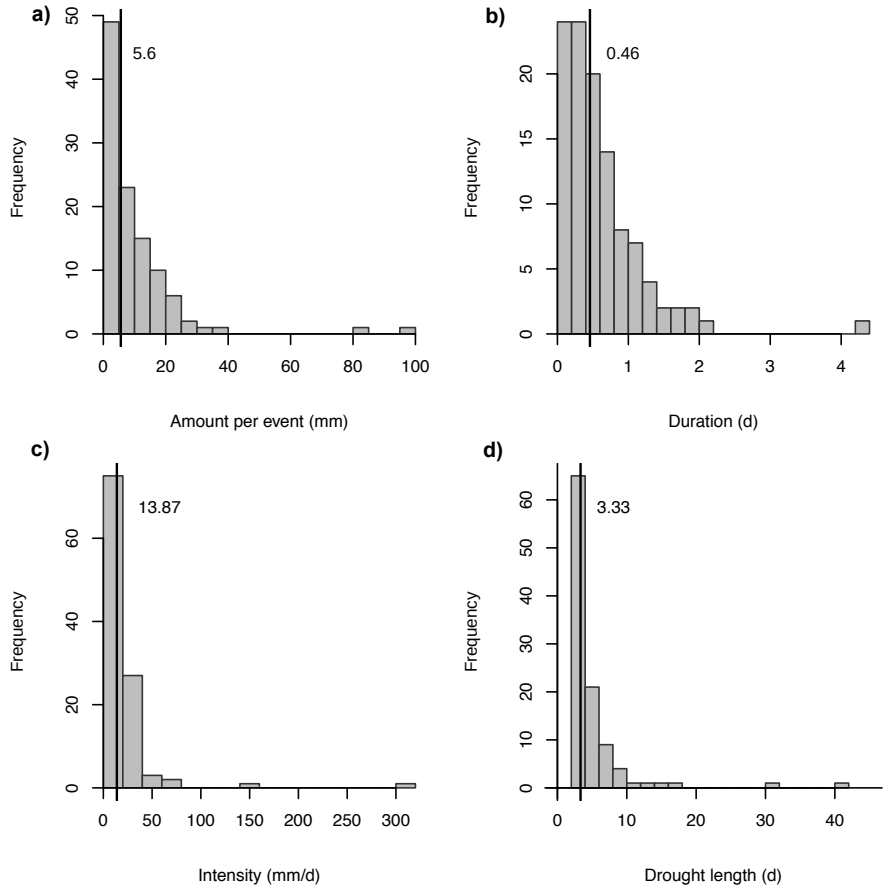

Figure A3.1. *Frequency distributions of rain amount per event (a), rain event duration (b), mean rain event intensity (c) and pre-rain drought length (d). The number and vertical black line represent the median value. Event characteristics are calculated for an MIT of 10 hours and response timeframe of one day.*

Appendix 3.3 Estimating physical CO_2 displacement by rain

The contribution of physical displacement of air in the peat matrix by an average 6.1 mm rain event to the observed decrease in ecosystem net CO_2 uptake can be estimated using the ideal gas law (Eq. A3.2). Here, a mean growing season temperature (T) of 281.5 K, a volume displacement of an average 5.6 mm rain event (V) of 0.0061m^3 m^{-2} and the gas constant R (8.3145 J mol^{-1} K^{-1}) were used to estimate the CO_2 displacement C_D (gC m^{-2}) for a given area A of 1 m^2. M and n are the molar mass (gram mol^{-1}) and moles of C (mol), respectively. Henry's law was applied to estimate the partial CO_2 pressure (P) of air in the peat matrix, assuming the CO_2 concentration in the air filled pores is in equilibrium with a measured pore water CO_2 concentration of about 0.002 M (Nilsson & Bohlin, 1993). A van 't Hoff temperature correction following Washington (1996) was applied to obtain a CO_2 Henry coefficient of 18.3 atm M^{-1} for the given temperature (Eq. A3.2).

$$C_D = \frac{PV}{ART} = \frac{nM}{A} \qquad \text{(A3.2)}$$

An average rain event of 5.6 mm could result in an emission of 0.11 gCO_2-C m^{-2}, which corresponds to 22% of the mean rain induced decreased ecosystem net CO_2 uptake of 0.54 gCO_2-C m^{-2} per rain event (fulfilling the selection criteria). It thus seems very unlikely that physical displacement of CO_2 is the dominant process responsible for the increased net atmospheric uptake.

Appendix 3.4 Potential reduction in GPP by decreased light availability

It is estimated that over an growing season, daytime rain events may result in a reduction of net ecosystem C uptake that corresponds with about 10% of gross primary production (GPP) at the mixed mire complex studied. Reduced light availability associated with rain events is likely the main reason for reduced net ecosystem carbon uptake due to rain events (Table 3.3, Figure 3.4). The aim of this supplementary material is to determine whether the decreased light availability due to rain is large enough to reduce GPP with 10%. GPP was estimated from half-hourly NEE measurements by the procedure described by Barr *et al.* (2004) and Peichl *et al.* (2014). Next, the median GPP during median pre-rain and post-rain light conditions (± 10 μmol m^{-2} s^{-1}) was estimated. The pre-rain and post-rain light conditions were extracted from the rain event analysis (Table 3.3). The reduction in GPP due to decreased light availability (R; %) was calculated as

$$R = 100\ \frac{GPP_{PRE} - GPP_{POST}}{GPP_{PRE}} \qquad \text{(A3.3)}$$

Another way to estimate of the reduction of GPP due to light availability was obtained by fitting the frequently employed rectangular hyperbolic model through the light – production relationship to obtain a light response curve

$$GPP = \frac{\alpha \cdot PPFD \cdot GPP_{max}}{\alpha \cdot PPFD + GPP_{max}} \qquad \text{(A3.4)}$$

Here, α is the initial slope of the curve and GPP_{max} the maximum (light saturated) GPP. Both parameters were significant ($P < 0.05$) and the goodness of fit (R^2) is 0.49. The results of the calculations (Table A3.1) indicate that, when purely based on reduced light, rain would decrease GPP with at least 31%. This is well beyond the estimated effect of rain on net C uptake, and supports the view that positive effects of rewetting may be offset by the more dominant effect of light on GPP.

Table A3.1. *Light availability (PPFD) and calculated gross primary production (GPP) during pre- and post-rain conditions for two response timeframes (0.5 and 1 days). PPFD and GPP are represented with mean values, n is the number of GPP and PPFD observations and R the reduction in GPP. Subscripts 1 and 2 indicate whether GPP is estimated with the median (1) or light response curve (2) based method.*

	Unit	Timeframe = 0.5 day		Timeframe = 1 day	
		Pre-rain	Post-rain	Pre-rain	Post-rain
PPFD	μmol m^{-2} s^{-1}	320	157	381	205
GPP_1	μmol C m^{-2} s^{-1}	2.53	1.70	2.82	1.95
GPP_2	μmol C m^{-2} s^{-1}	2.85	1.79	3.14	2.16
n	count	894	1397	900	1214
R_1	%		33		31
R_2	%		37		31

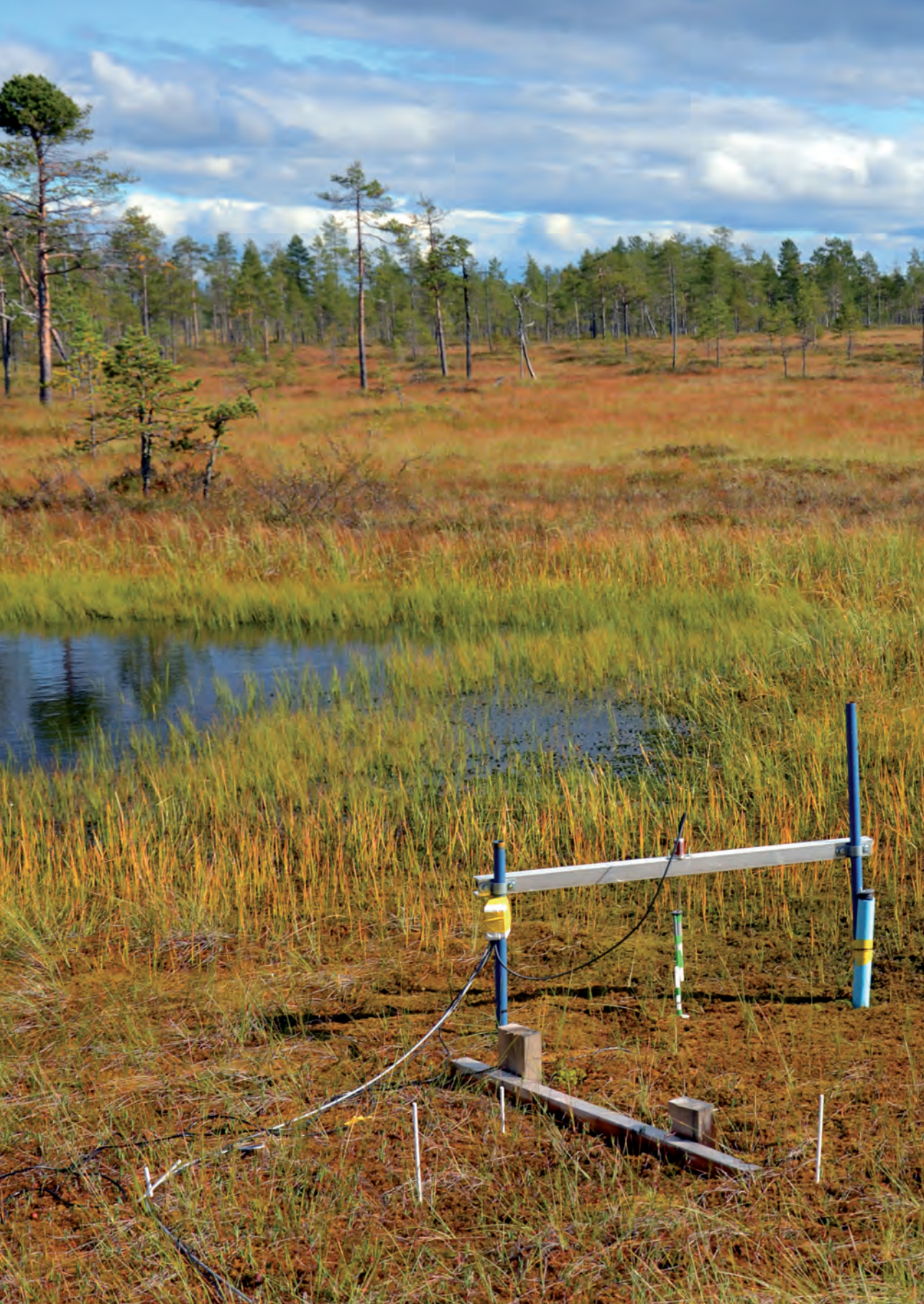

4 Fine scale spatiotemporal variability of surface elevation change in a northern peatland: Interactions with hydrology and vegetation

Jelmer J. Nijp, Klaas Metselaar, Juul Limpens, Harm Bartholomeus, Mats B. Nilsson, Frank Berendse, Sjoerd E.A.T.M. van der Zee

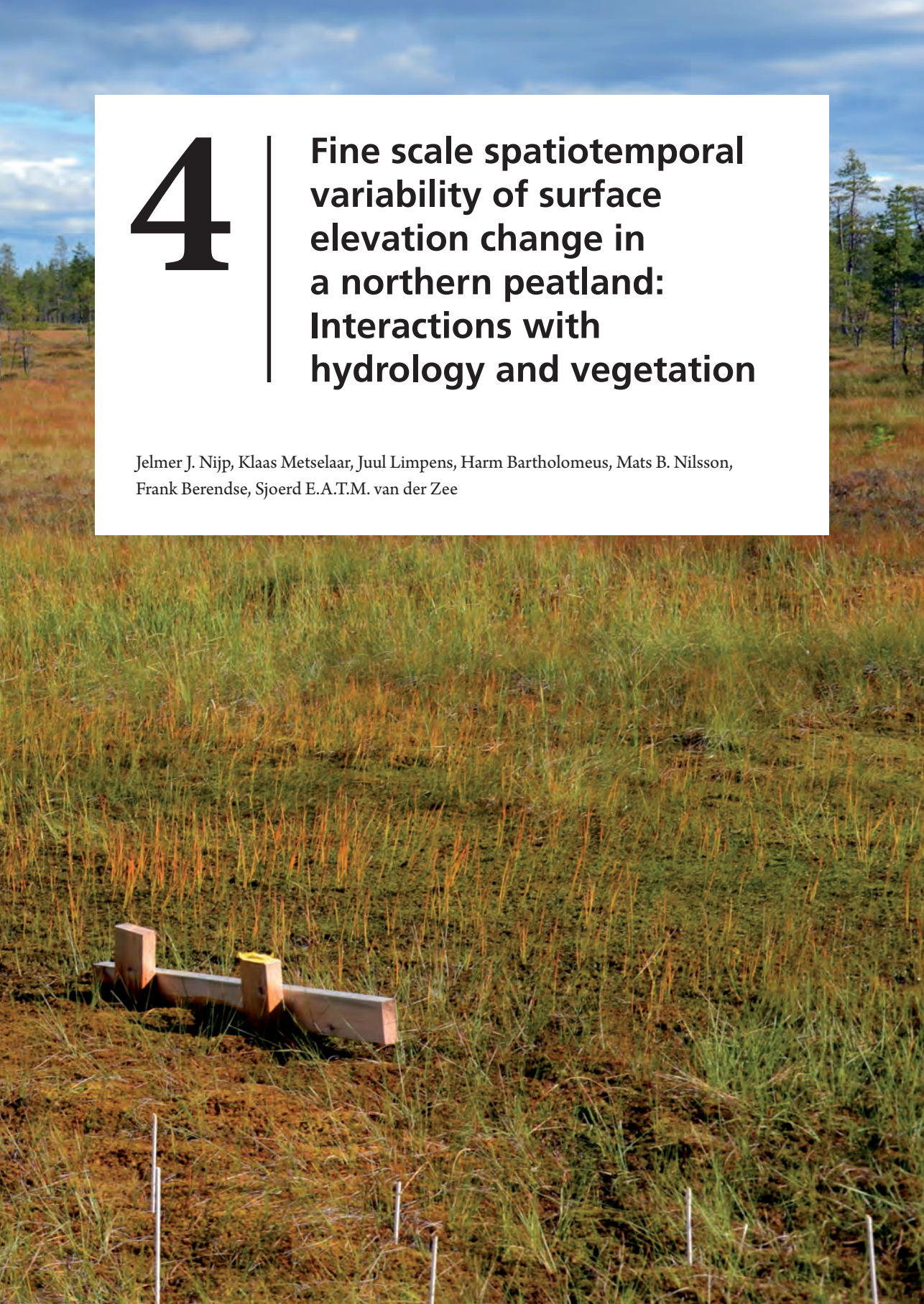

Abstract

The depth of the groundwater table below the surface and its temporal variation are major controls on biogeochemical processes in northern peatlands. In these wetlands, the temporal fluctuations in groundwater table are buffered by peat volume change. Northern peatlands are self-organizing systems, resulting in distinct spatial structures of vegetation and physical properties. While vegetation patterns are well-studied in northern peatlands, the spatial structure of peat volume change and factors controlling it are less clear.

We explored the fine scale (0.5 m resolution) spatial patterning of peat volume change and its relationship to vegetation and hydrology using spatially continuous data of surface elevation and point measurements on plant species composition, geohydrological, and positional factors along a transect throughout a growing season in an oligotrophic minerogenic northern peatland in northern Sweden.

We found that peat volume change was substantial and highly variable through space, ranging from -6.2 cm to +1.2 cm over the growing season. Spatial patterns of peat volume change over the growing season were best described at a spatial scale of 40.8 ± 0.6 m (± SE). Over the growing season, with progressively lower absolute groundwater tables, peat volume change reduced the patch size of peat surface elevation and increased its vertical range. We hypothesize that this seasonal change in topography may result in a more local lateral redistribution of groundwater and augment differences between wet and dry microsites. Spatial variation in peat volume change was mainly related to changes in aquifer thickness, and to a lesser extent also to larger vegetation units (microsites), with magnitude of peat volume change increasing from lawn < hollow < flark.

As a consequence of the high spatial variability, the spatial representativeness of point scale simulation models including peat volume change is restricted to a range up to about 40 m. This study provides empirical evidence of a link between large scale vegetation units and peat volume change, one of the mechanisms hypothesised to play an important role in hydrological self-regulation in northern peatlands.

Keywords: Peat volume change, compression, photogrammetry, northern peatland, Degerö Stormyr, groundwater table, spatial patterns, geostatistics

4.1 Introduction

Northern peatlands are wet ecosystems in which (partially) decomposed organic material (peat) has accumulated over thousands of years, making these ecosystems an important storage component in the global carbon cycle (Kleinen *et al.*, 2012; Turunen *et al.*, 2002; Yu, 2011). In these wetland ecosystems, the depth of the water table is a key factor controlling numerous biogeochemical processes, including greenhouse gas emissions, plant growth and competition, redox state, and water and energy partitioning (Blodau *et al.*, 2004; Kettridge *et al.*, 2015; Lafleur *et al.*, 2005; Limpens *et al.*, 2008; Nijp *et al.*, 2014; Peichl *et al.*, 2013; Waddington *et al.*, 2015).

The distance between the groundwater table and peat surface (relative groundwater table; GWT_R) is controlled by ecohydrological feedbacks, which generally result in a stabilization of GWT_R and surface wetness (Belyea & Baird, 2006; Waddington *et al.*, 2015). One of the feedbacks that stabilizes GWT_R in northern peatlands is peat volume change in response to changes in ground water depth (Ivanov *et al.*, 1981). Peat in northern peatlands generally consists of (partially) decomposed peatmosses (*Sphagnum*) (Rydin & Jeglum, 2013). The open pore structure and high compressibility of this fibrous material (Price *et al.*, 2005; Waddington *et al.*, 2010) enables expansion in wet periods and compression of the saturated peat matrix during dry spells. Dependent on peat type, the stabilizing effect of peat volume on GWT_R can be considerable (~1 – 28 cm), and may e.g. reduce moisture stress for peatmosses and enhance methane emissions (Almendinger *et al.*, 1986; Baden & Eggelsmann, 1964; Fritz *et al.*, 2008; Roulet, 1991). Consequently, peat volume change is an essential process in northern peatlands, as it controls the hydrological functioning and associated biogeochemical processes in northern peatlands.

From classical soil mechanics it follows that the peat volume change potential increases with larger peat compressibility and peat thickness (Almendinger *et al.*, 1986; Schlotzhauer & Price, 1999), and that actual peat volume change is controlled by changes in mechanical effective stress (Terzaghi, 1943). In natural northern peatlands, changes of peat volume can be attributed mainly to compression of the saturated peat matrix (peat aquifer) (Kennedy & Price, 2005).

The overall development of northern peatlands is controlled by mutually dependent processes operating at various spatiotemporal scales (Ivanov *et al.*, 1981; Waddington *et al.*, 2015). As a consequence, alterations in local processes (e.g. plant community) induced by changes in external factors may affect larger scale (e.g. whole peatland) processes and vice versa (Belyea & Baird, 2006). Moreover, cross-scale feedbacks likely

result in self-organized spatial structures of vegetation, mechanical and hydrophysical properties, and of peat accumulation rates (Belyea & Baird, 2006; Belyea & Clymo, 2001; Eppinga *et al.*, 2009; Rydin, 1986). As direct controls on peat volume change (compressibility, peat thickness and changes in groundwater table depth) are indirectly affected by feedbacks at various spatiotemporal scales, it seems likely that also peat volume change is spatially structured at multiple spatial scales. Modifications in the spatial arrangement of northern peatlands caused by changes in external drivers can alter the hydrological and biogeochemical functioning of (Baird *et al.*, 2013), which may non-linearly feed back to the global climate (Belyea, 2009; Belyea & Baird, 2006). Especially considering the projected climate change and its global consequences (IPCC, 2013), it is essential to understand the spatial variability and structure of peat volume change.

The vegetation of northern peatlands regularly forms easily recognizable units in vegetation composition and function (microsites), and is commonly classified in elevated dry hummocks, wet hollows, and lawns located in between (Andrus *et al.*, 1983; Rydin & Jeglum, 2013). As peatland microsites may persist for centuries or even millennia (Hughes *et al.*, 2000; Karofeld, 1998; Nungesser, 2003; van der Linden *et al.*, 2008), the quality of the plant litter added to the peat surface will determine the hydrophysical characteristics of the peat matrix later formed (Belyea & Clymo, 2001). Previous studies suggest that the magnitude of peat volume change and peat compressibility is related to microsite and its associated characteristics such as bulk density, and degree of decomposition (Price *et al.*, 2005; Waddington *et al.*, 2010). Positive feedbacks between compressibility and plant species composition seem to occur, so that spatial variation of peat volume change can be related to present microsite distribution (Waddington *et al.*, 2010).

Spatially structured peat volume change patterns may furthermore arise from processes that affect the peat thickness and fluctuations in groundwater table. The local peat thickness is related to the alignment of the peatland in the landscape and peat accumulation and development over larger spatiotemporal scales (Belyea & Baird, 2006). Besides rainfall and evapotranspiration, lateral flow constitutes a major part of the peatland water balance and therefore impacts groundwater table fluctuations and peat volume change (Kellner & Halldin, 2002; Peichl *et al.*, 2013). Lateral water transport is controlled by the hydraulic gradient, hydraulic conductivity and aquifer thickness (Hillel, 2004; Ivanov *et al.*, 1981). In turn, these properties are a function of larger-scale positional variables describing the regional flow and position of the peatland in the landscape (Grootjans *et al.*, 1996; Ivanov *et al.*, 1981; Kemmers, 1986).

In summary, there are many processes operating at various spatiotemporal scales that

may affect the magnitude and spatial arrangement of peat volume change. Yet, little is known about the spatial structure of peat volume change and its spatial scale of patterning. Moreover, studies establishing links between peat volume change in northern peatlands and potential drivers are rare (Waddington *et al.*, 2010).

This study aims to 1) explore the spatial structure of peat volume change patterns 2) determine the effects of spatially variable peat volume change over the growing season on topography 3) determine whether peat volume change is related to a) vegetation composition, b) global position in the peatland and c) local geohydrological site factors. Due to the strong interrelations between microsite development and their hydrophysical characteristics (Belyea & Baird, 2006; Waddington *et al.*, 2010), we hypothesize that vegetation composition and microsite identity are good predictors of peat volume change. Using photogrammetric processing of digital images taken along a transect in a natural peatland at multiple times throughout the growing season, we obtained high-accuracy fine scale digital terrain models (0.5 m resolution). These digital terrain models allowed quantification of the spatial structure of peat surface elevation through time with geostatistical techniques, and relating it to vegetation composition, positional and geohydrological site factors.

4.2 Methods

4.2.1 Site description and climate

This research was performed in Degerö Stormyr, a natural, minerogenic, ombrotrophic mixed peatland complex located in northern Sweden (64N°19E°). The peat is underlain by acidic gneissic bedrock and glacial till material (Malmström, 1923), and ranges in thickness from 3 – 4 m, locally reaching up to 8 m. The climate is boreal (Peel *et al.*, 2007), with mean (1961 – 1990) annual mean temperature of +1.2°C and a total rainfall sum of 523 mm, of which 34% falls as snow (Alexandersson *et al.*, 1991). The rainfall, potential evapotranspiration and temperature during the growing season (defined as the period from 15 May until 15 October) are estimated at 397 mm, 432 mm and 9.9°C (Nijp *et al.*, 2015).

4.2.2 Data collection

4.2.2.1 Fine scale peat volume change

Within the Degerö Stormyr peatland, we selected a 571 m long transect from the South-western peatland margin to the North-eastern margin along an existing boardwalk. Peatland vegetation and surface elevation are highly sensitive to (compaction by)

treading, and the boardwalk provided an essential means to prevent disturbance of the peat surface.

To estimate peat volume change, we created digital terrain models (DTMs) of the boardwalk transect at five points in the time (See Appendix 4.2 for dates and more details), in the period right after the snowmelt until the middle of the growing season (7^{th} May – 12^{th} July 2013). DTMs were constructed from high resolution top-view photographs with digital close-range photogrammetry. A Canon EOS 450D camera (4272 · 2848 pixels) with a Canon EFS 18-55 mm F/3.5-5.6 lens was attached on a 7 m long stereoscopic rod. The ISO was set at 200 and the exposure time at 1/160 seconds. The focal length of the lens was fixed at 23 mm. To adequately capture the peat surface elevation, overlap of images was 90% and about 2700 photographs were taken per date, 6 m above the peat surface in angles varying from approximately -15 – +15°. For further details on the procedure of deriving a DTM from the photographs see Section 4.2.3.1. The maximum amplitude of peat volume change during the period was quantified by subtracting the DTM with highest mean surface elevation from the DTM with lowest mean surface elevation.

4.2.2.2 Ground survey

To georeference the constructed DTMs twenty-two ground control points were established by installing iron tubes into the underlying mineral glacial deposits. The iron tubes were covered with protective paint to prevent toxic effects of iron on peatmoss (Tyler, 1990) and were placed approximately every 35 m along the transect. The coordinates of the ground control points were determined using a combination of a Total Station and dGPS with a vertical accuracy of ± 7 mm. The ground control points were also used to validate peat surface elevation change in the area surrounding the tube, by measuring the distance between the top of the tube and the peat surface.

Table 4.1. *Overview of variables that may explain peat volume change. Variables are defined for factors of which variations throughout the growing season may be considerable, while parameters are variables assumed to be constant throughout the growing season.*

Fine spatiotemporal scale (Variables)	Coarse spatiotemporal scale (Parameters)
Change in absolute groundwater table *	Position in peatland • Altitude • Distances from peatland margin • Initial peat thickness
Hydraulic conductivity	Vegetation composition

* Absolute groundwater table is defined as the distance between the groundwater table and a fixed datum

4.2.2.3 Explanatory variables

We distinguished two categories of explanatory variables, based on their spatiotemporal variability over the study period (Table 4.1). All information on explanatory variables was obtained at the positions of the groundwater wells (Fig. 4.1), at dates that images were collected.

Geohydrology

Twenty-eight groundwater wells were placed equidistantly along the transect to estimate the depth of the groundwater table relative to the peat surface (GWT_R; cm) and to estimate the horizontal saturated hydraulic conductivity (K_S; cm d^{-1}). The wells consisted of cylindrical closed-bottom polyvinylchloride tubes (inner radius = 1.8 cm) with the filter located 20 – 40 cm below the peat surface (Appendix 4.1). The filter of the groundwater well (length 20 cm) was constructed by covering a perforated section (area of perforation 30%; hole diameter of 0.8 cm) with a filter cloth. The filter cloth was used to prevent clogging of the groundwater well with peat. The bottom of the groundwater well extended 10 cm below the filter to improve stability, and was closed with a water-tight cap. Groundwater table with respect to the peatmoss surface (GWT_R; m) was measured with a ruler at dates coinciding with image collection.

The saturated hydraulic conductivity of the 20 – 40 cm deep peat layer was estimated in-situ using slug tests. In slug tests, a volume of water (*slug*) is quickly poured into the groundwater wells, which generates a hydraulic head difference and induces flow from the groundwater well into the peat matrix. By measuring the change in the water level in the groundwater well over time K_s can be estimated (See Section 4.2.3.3). The water level in the groundwater wells was measured using groundwater level loggers (Diver type DI220, Van Essen Instruments, Delft, The Netherlands). As water chemistry affects saturated hydraulic conductivity estimates (Kettridge & Binley, 2010), the slug-water (100 mL) was collected from a pool in the peatland to match bog water quality.

Peat thickness (PT; m), defined as the distance between the peatmoss surface and the peat to mineral interface, was measured in the first week of May 2013 by manually pushing an extendable metal rod (diameter 2 cm) in peat. Generally a distinct grinding sound of sand against metal confirmed the depth of the peat to mineral interface.

The groundwater table relative to a fixed datum (SWEREF 99 coordinate system, zone 20° 15′), referred to as the absolute groundwater table (GWT_A), was measured in the first week of May at all groundwater well locations. Changes in absolute groundwater table drive peat volume change, and were calculated from changes in GWT_R and surface elevation inferred from DTMs.

Positional factors

The positioning of sites within the peatland may be an important factor controlling peat volume change, and may be an overall descriptor of peat thickness and water flow (Ingram, 1982; Ivanov *et al.*, 1981). This position is described with the Euclidian distance to the closest peat-forest border, the Euclidian distance to the southwest peat-forest border, and initial peat surface elevation above sea level, which were all derived from the ground survey data.

Vegetation

The abundance of vascular plant and bryophyte species was observed as percentage cover in 50 · 50 cm vegetation relevés placed around the 28 groundwater wells in the end of May 2013. Liverwort cover was classified in living and dead. Also the cover of dead plant material and bare peat was recorded.

4.2.2.4 Temporal variability of peat volume change

Temporal variation of peat surface elevation was also monitored at the peatland centre to verify overall peat volume change patterns detected with photogrammetry (See Fig. 4.1a for location) with a magnetostrictive linear position sensor (MTS Linear Position Sensor Type CM250AVH2, MTS Sensor Technologie, Lüdenscheid, Germany). The position sensor was mounted on a frame between two iron tubes that were installed into the underlying mineral soil, providing a fixed height reference to which peat surface elevation changes could be referenced (See Appendix 5.2 for details). A light-weight PVC construction with a thin plate resting on the peat surface attached to a PVC stick with a magnet on top was used. With changing peat surface, this stick moved along the position sensor rod, adjusting the distance between the magnet and magnetostrictive element of the position sensor. This distance was recorded with 30 minute intervals and logged with a CR1000 data logger (Campbell Scientific, Logan, UT, US).

4.2.2.5 Meteorology and groundwater table

Rainfall was measured with a tipping bucket rain gauge (ARG 100, Campbell, Scientific, Logan, Utah, USA, 0.2 mm resolution) about 5 m from the peat volume change measurements. The tipping bucket records were corrected for a 10% systematic underestimation of rain amount following Eriksson (1983) in Nilsson *et al.* (2008). Hourly potential evapotranspiration rates were estimated from air temperature, wind speed, net radiation and relative humidity following FAO standards (Allen *et al.*, 2006; Allen *et al.*, 1998). To determine the drought status from a meteorological perspective we calculated the *cumulative potential rainfall surplus* subtracting daily potential evapotranspiration from daily rainfall (*rainfall surplus*), and adding this value to the

rainfall surplus of the previous day. A half-hourly time series of GWT_R was obtained with a float- and counterweight system attached to a potentiometer (Roulet, 1991) in a lawn microsite at about 200 m distance from the centre of the transect.

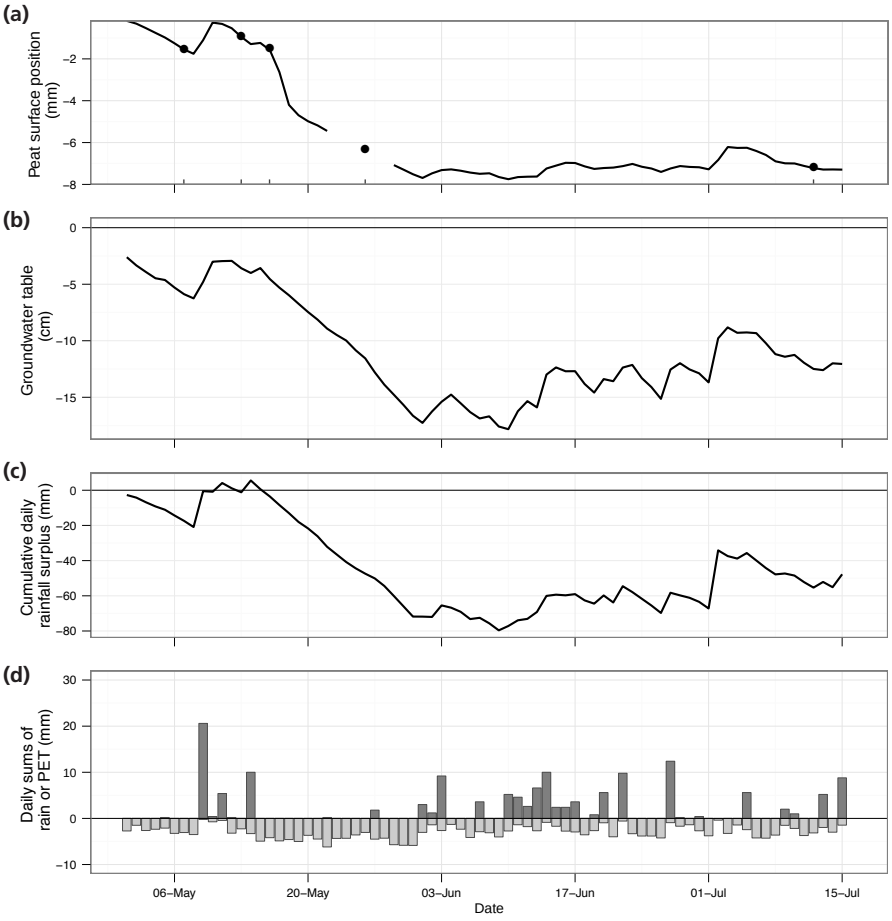

Figure 4.1. *Time series of (a) peat surface position at the peatland centre, (b) groundwater table relative to peat surface, (c) cumulative rainfall surplus, and (d) rainfall and potential evapotranspiration (PET) during the measurement period. Peat surface position is measured with a linear position sensor in the centre of the peatland; the y-axis represents the surface position relative to the first observation. Dates of transect measurements are presented with points in 4.1a. Rainfall, potential evapotranspiration, and cumulative rainfall surplus are daily sums. Potential evapotranspiration is calculated following FAO standards (Allen et al., 1998).*

4.2.3 Data analysis

4.2.3.1 From images to peat volume change

Constructing digital terrain models

Digital terrain models (DTMs) were created for all measurement dates using a Structure-from-Motion algorithm (Jebara *et al.*, 1999) implemented in Photoscan v1.1.2 Professional Edition (Agisoft LCC, St. Petersburg, Russia). Using multiple images taken from different viewpoints and having large overlap, the 3D structure of the terrain can be reconstructed. First, a sparse point cloud was constructed by aligning the images with high accuracy, generic point selection, keypoint limit at 40000 and tie point limit at 1000. Misaligned images were manually realigned or removed if realignment was not successful. Next, to georeference the point cloud and remove non-linear distortions in the constructed peat surface, camera calibration parameters and point coordinates were optimized by comparing observed coordinates of the ground control tubes obtained with the ground survey with simulated coordinates. See Appendix 4.2 for detailed information on the constructed sparse point clouds.

The point clouds included points detected on vascular vegetation, which do not represent the peat surface and were removed with the following procedure. First, isolated point clusters consisting of 5 or fewer points were removed if the vertical position was farther than 0.25 m apart from the main point structure using a noise reduction filter within LAS Tools (version 150406, Rapidlasso GmbH, Gilching, Germany). Since a few points were detected on the moving vegetation, we used LAS Tools to extract the peat surface points with a variant of the triangular irregular network refinement algorithm (See Axelsson (2000) for details). As subtle hummocky features were expected, the setting *ultra_fine* was used with a step size of 3 m (*wilderness*) in the *lasground_new tool* to obtain ground points only. A sensitivity analysis indicated that the exact parameter settings of the noise and vegetation removal algorithms had negligible impact on DTM quality (data not shown). Next, to further prevent vascular plants from biasing peat surface estimates, the lowest surface point in a regular 0.5 · 0.5 m grid was extracted from the sparse point cloud and used as peat surface proxy for each grid cell. To eliminate the effect of boardwalks, measurement equipment and edge artefacts introduced during the point cloud generation process, only elevation data farther than 1 m apart from such objects was used in further analyses, resulting in an area of 0.16 ha suitable for analysis. Finally, the amplitude of peat volume change during the measurement period was estimated by subtracting the elevation of the second point in time (*wet*) from the last (fifth) point in time (*dry*) for all intersecting grid cells.

DTM validation

The quality of the generated DTMs was assessed in three ways. A first estimate of the quality was obtained by comparing the difference between the projected and measured coordinates at the ground control points (i.e. top of tubes installed in mineral soil) after the photogrammetric processing. The mean vertical error at the ground control points was 6.5 mm, averaged over the five datasets. Second, manual measurements of the vertical position of the peat surface at the ground control points were compared to the values produced at the closest grid cell value of the final DTM.

The peat surface position was on average underestimated by 2.6 mm, while the mismatch with observations ranged between -24 and +3 mm (25^{th} – 75^{th} percentile; Appendix 4.2). The mean difference (root mean square error) between manual and photogrammetric peat elevation estimates was 22 mm. This difference includes the manual measurement error of the distance between peat surface and top of reference tube. The tendency towards lower numbers is likely due to the treatment of selecting the minimal value per grid cell, of which the location does not necessarily correspond to the manual measurement at the ground control points. Third, to determine how proximity to ground control points impacts the quality of the DTMs, we sequentially removed ground control points closest to a ground control point in the centre of the transect (Appendix 4.2). This test demonstrated that at the mean separation distance from a ground control point along the transect (35 m), the vertical error may be maximally 7 mm. The distance between ground control points was thus appropriately chosen. Visual comparison of point clouds before and after vegetation removal indicated that points detected on vascular vegetation were successfully removed.

4.2.3.2 Spatial analysis of peat volume change patterns

We derived measures of the spatial structure of peat volume change using variograms to quantify the degree of spatial dependence (Journel & Huijbregts, 1978; Webster & Oliver, 2007). The motivation of using variograms is that for spatially structured environmental variables, the spatial autocorrelation of this variable decreases with increasing separation distance, so that the variance increases with separation distance. The separation distance at which the autocorrelation becomes negligible ($r < 0.05$) and the variance stabilizes is referred to as the *correlation range* (CR). The CR marks the distance of spatial dependence and is a measure of *patch size* (Webster & Oliver, 2007). Consistent with geostatistical terminology we refer to *sill* ($C+C_0$) as the asymptotic value of the variance, which provides a measure of *variability* (range of values) encountered along the transect. Due to random noise, measurement error, and variability occurring at distances smaller than the separation distance, an additional constant random component may added to

the variogram, referred to as *nugget variance* (C_0). The spatially structured component is referred to as the *partial sill* (C) (See Appendix 4.3 for details). To identify whether peat volume change was predominantly spatially structured or randomly distributed, we calculated the relative structural variance, expressed as $C/(C+C_0)$ (Cirkel *et al.*, 2014).

A spatial peat volume change dataset was constructed by subtracting the second (wettest; May 13th) gridded peat surface elevation dataset from the fifth dataset (dry; July 12th). Because variogram calculations are particularly sensitive to outliers (Rossi *et al.*, 1992; Webster & Oliver, 2007), we removed surface elevation outliers (defined as values smaller than $Q_{25} - 1.5 \cdot IQR$ or larger than $Q_{75} + 1.5 \cdot IQR$, where Q_{25} and Q_{75} are the 25th and 75th quantile and IQR the inter-quartile range sensu Hoaglin *et al.* (1986)). Next, to meet the requirement of second order stationarity (i.e. mean and variance do not change in space), we removed the systematic trend with a second order polynomial trend surface. Including higher order polynomial terms in the trend surface did not significantly improve the polynomial trend surface model fit. Spherical, Exponential, and Gaussian theoretical variogram models were fitted through the trend-removed residuals using a weighed non-linear least squares algorithm with the *gstat* package (Pebesma, 2004) in R v3.1.0 (R Core Team, 2014). Linear combinations of up to three variograms models were also tested because empirical variograms indicated multiple spatial scales were present (See Appendix 4.3 for details). The Akaike Information Criterion (AIC; Akaike, 1973) was used to select the model describing the spatial structure best with least parameters. In the case of combined variograms, multiple CRs and partial sills were distinguished. Absolute goodness of fit of the variograms was assessed with the Willmott's index of agreement (Willmott *et al.*, 1985).

To determine whether differences in elevation became more pronounced in drier conditions, resulting in smaller patches and larger vertical variability, we also constructed variograms of peat surface elevation for all dates. The practical correlation range was used as a measure for patch size; the sill was used as a measure for elevation variability. Both variables were related to the mean absolute groundwater table at that point in time as proxy for drought status of the peatland system.

4.2.3.3 Hydraulic conductivity

The horizontal saturated hydraulic conductivity (K_s; m d^{-1}) of the peat layer 20 – 40 cm below the peat surface was estimated with the Bouwer-Rice slug test for partially penetrating wells in unconfined aquifer systems (Bouwer & Rice, 1976). The K_s was calculated from the decline of the water level in the groundwater well using a modified Thiem equation and by accounting for the geometry of the flow system (filter length and radius, installation depth and aquifer thickness) using a shape factor. We

employed the closed-form analytical expression for the shape factor by Zlotnik *et al.* (2010) because the empirically derived shape factor provided in Bouwer & Rice (1976) may result in an 30% underestimation of K_s for the groundwater well configuration presented in this study (See Appendix 4.1 for an R implementation of this shape factor). The Bouwer-Rice evaluation of slug tests assumes that elastic water storage due to peat volume change can be neglected. Even though peat is highly elastic (Schlotzhauer & Price, 1999; Waddington *et al.*, 2015), its impact on estimated K_s is only minimal due to the small filter length : radius ratio of the wells used in this study (Hyder & Butler, 1995).

4.2.3.4 Vegetation: Correspondence analysis and clustering

Multivariate correspondence analyses were used to determine whether vegetation composition is related to the magnitude of peat volume change and other environment variables. First, to explore which environmental variables could explain vegetation composition, an indirect ordination was employed. The gradient length was 2.7 standard deviations, suggesting that the vegetation responses are linear along the ordination axes and a principal component analysis (PCA) is most appropriate (ter Braak & Šmilauer, 2012). The effect of peat volume change on vegetation composition was quantified and tested with an unrestricted Monte Carlo Permutation Test (999 permutations). Missing values of aquifer thickness (missing n = 4) were replaced by distance weighed values of the two nearest points in case no ground control point observation was less than 2 m distant. Correspondence analyses were performed with the CANOCO software (v5.0; Biometris, Plant Research International, Wageningen, The Netherlands; ter Braak & Šmilauer (2012)).

To classify the vegetation relevés in coarser-scale microsites we used hierarchical agglomerative clustering with Euclidian distance as distance measure and Ward's minimum variance method as clustering algorithm using the *pvclust* package in R (Suzuki & Shimodaira, 2006). A multi-scale non-parametric bootstrapping resampling procedure (10000 bootstrap replications) was performed to estimate the uncertainty of the hierarchical clustering (Suzuki & Shimodaira, 2006). This test indicated that maximally six clusters are significantly distinct ($P = 0.05$). Four clusters were merged into two because no important differences in vegetation composition were apparent.

In all analyses the raw untransformed vegetation cover (%) was used as in contrast to presence-absence data, abundance information may be of additional value for small spatial extents with low species turnover rates (as indicated by the small gradient length of 2.7 SD) (Wilson, 2012).

4.3 Results

4.3.1 Description of the transect

The peat surface along the transect slightly sloped downward in North-easterly direction with a mean gradient of 0.0012 m m^{-1} (Fig. 4.2b). The interface between peat and mineral soil is highly undulating and results in a heterogeneous peat (and hence aquifer) thickness throughout the peatland, which is not related to the closest distance from a peat-forest margin (linear regression; $R^2 = 0.07$; $P = 0.04$) or the distance from the South-western margin (linear regression; $R^2 = 0.003$; $P = 0.72$).

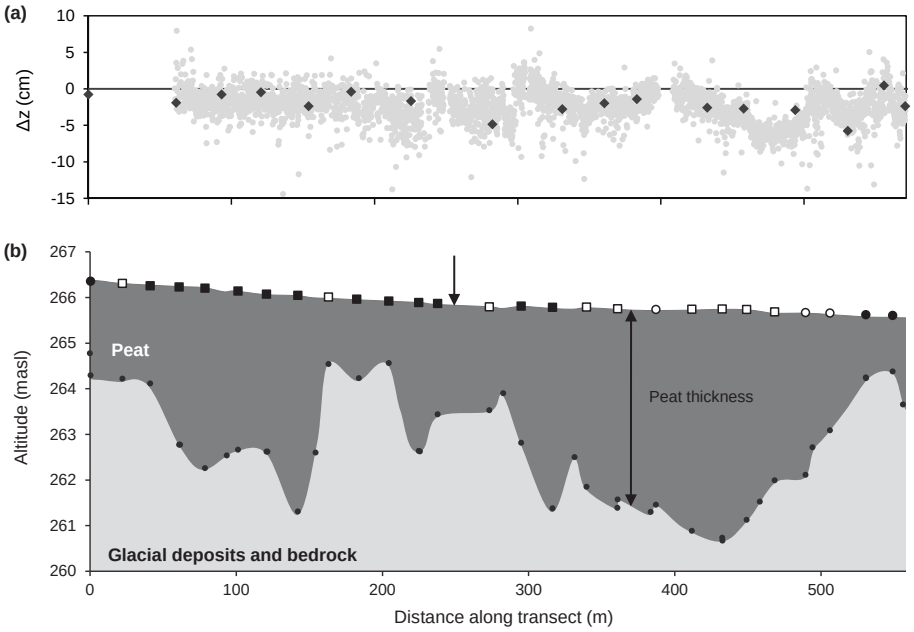

Figure 4.2. *(a) Peat volume change along the transect during the period 16th May – 12th July. Negative values represent compression, positive values expansion. Grey points represent peat volume change obtained by digital photogrammetry in a 2 m wide area along the transect, black diamonds represent ground control tube positions. (b) Cross-section of the transect from Southwest (left) to Northeast (right). Dark grey is peat, pale grey is mineral soil. The groundwater well locations are presented with dots and lines are rough interpolations of peat depth and peat surface; the arrow indicates the position at which the peat volume change time series was obtained (Fig. 4.1a). The symbols on top represent by the four microsites: flarks (●); hollows (○); lawns with high abundance of Vaccinium oxycoccos (■); and lawns (□).*

Four microsites were distinguished on the basis of the hierarchical cluster analysis. The first microsite consisted of flarks (sensu Sjörs, 1948), characterized by dead and living liverworts (mainly *Gymnocolia inflata* and *Cladopodiella fluitans*), *Trichophorum cespitosum* and *Sphagnum papillosum* (Fig. 4.1). The second class represents a hollow vegetation, represented by the species *Sphagnum majus* and *Scheuchzeria palustris*. The two remaining classes were characterized by lawn vegetation with high abundance of *Sphagnum balticum*, *Eriophorum angustifolium* and *Andromeda polifolia*, with a high cover of *Vaccinium oxycoccos* differentiating the two lawn communities.

4.3.2 Temporal patterns of peat volume change

Peat surface elevation decreased over the study period (Fig. 4.1a) and generally followed the changes in the water balance as expressed by the groundwater table relative to the peat surface (Fig. 4.1b) and the cumulative potential rainfall surplus (Fig. 4.1c). The total rainfall amount during the measurement period (224 mm in the period May – July) was representative for the longer term average (Nijp *et al.*, 2015). From 15th of May until June 1st a warm and dry period with mean temperature of 15.5°C (long-term average May temperature is 7.5°C) and only 2 mm of rainfall resulted in high potential evapotranspiration rates and a rapidly increasing cumulative potential rainfall deficit (i.e. rainfall deficit that would have occurred if evapotranspiration is at its potential rate; Fig. 4.1c,d). As a consequence of this dry period, the peat surface at the centre of the peatland dropped with nearly 8 cm.

4.3.3 Spatial patterns of peat volume change

Changes in peat surface elevation along the transect were highly variable in space (Fig. 4.2b). The mean change in peat volume between the wettest (13th May, 2013) and driest (12th July, 2013) point in time was -31 mm (median), with values ranging from +12 to -62 mm (5th and 95th quantiles). The relative structural variance (See Section 4.2.3.2) was 74%, indicating that most of the spatial variation in peat volume change can be attributed to spatially structured processes rather than to random processes. A combined Exponential-Gaussian variogram model described the spatial structure of peat volume change best with least parameters, suggesting two spatial scales of patterning (Appendix 4.3). The two spatial scales of patterning were 3.4 ± 0.8 m (*short-range*; mean correlation range ± standard error) and 40.8 ± 0.6 m (*long-range*). Even though the combined variogram model certainly had the best fit, the short-range model was not significant ($P = 0.16$) and the long-range (Gaussian) model component explained most (78%) of the spatially structured variation in peat volume change. Spatial patterns in peat volume change were thus best described at a spatial scale of 40.8 m.

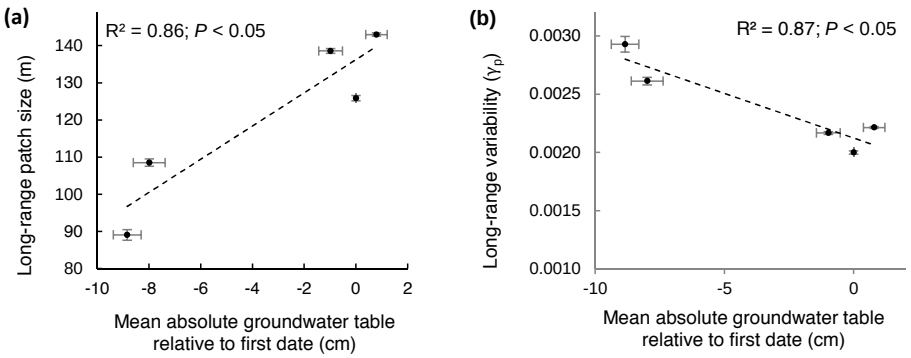

Figure 4.3. *Relation between absolute groundwater table depth (GWT_A) and peat surface position patch size (a), and peat surface position vertical variability (b). The x-axis variable is GWT_A relative to the first observation averaged over the 28 observations, for each point in time. Patch size and variability of surface elevation are represented by the fitted practical correlation range and partial sills, obtained with a combined Exponential-Gaussian variogram model fitted on the digital terrain model data (See Section 4.2.3.2). The goodness of fit and significance of the linear regression models are provided only for the long-range variogram components because patch size and vertical variability did not vary significantly with absolute water tables for the short-range variogram components. Error bars represent one standard error.*

4.3.4 Spatiotemporal changes in topography

Spatial patterns in peat surface elevation at the five points in time emerged at a short-range (3.68 ± 0.22 m (± SD)) and long-range (121 ± 22 m). Surface topography was clearly spatially structured, as the short-range and long-range patterns explained 20% and 73% of the spatial variation in peat surface elevation, leaving only 7% random spatial variation. With deeper (i.e. more negative) space-averaged absolute water tables, the patch size and vertical variability of peat surface elevation decreased and increased significantly for the long-range spatial pattern of surface elevation (Fig. 4.3). This indicates that surface elevation differences became more pronounced with drier conditions (i.e. later in the growing season) and that peat volume change becomes more local with deeper absolute groundwater table. The variogram parameters of the short-range surface elevation pattern do not differ among absolute groundwater tables and was therefore excluded from the analyses.

4.3.5 Variables correlated to peat volume change

4.3.5.1 Positional and geohydrological factors

The spatial patterns in peat volume change were most importantly related to changes of absolute groundwater table (aquifer thickness), with larger change in absolute

groundwater table resulting in larger peat volume change (Table 4.2; Fig. 4.4). Peat thickness, hydraulic conductivity (See Appendix 4.1) and distance to the (closest) peat-forest margin were not related to changes in peat surface elevation. Peat volume change stabilized the distance between the peat surface and GWT_R, buffering on average 26% and maximally 84% of the space averaged GWT_A decline of 9 cm. Spatial variation in decline of GWT_A through time was unrelated to the position in peatland, as expressed by surface elevation and distance from the peat-forest margin (Table 4.2).

Locations in the peatland with large compression corresponded to sites with shallow July GWT_R (Table 4.2). The decline of GWT_R throughout the growing season was largest for sites with deep July GWT_R (Table 4.2), illustrating that dry sites became drier and that spatial heterogeneity in the dominant habitat condition explaining spatial variation in plant species composition increases (Fig. 4.6). This is consistent with the analyses on the spatial structure of topography, which indicated that patchiness and variability of peat surface elevation increased with drier conditions (Fig. 4.3).

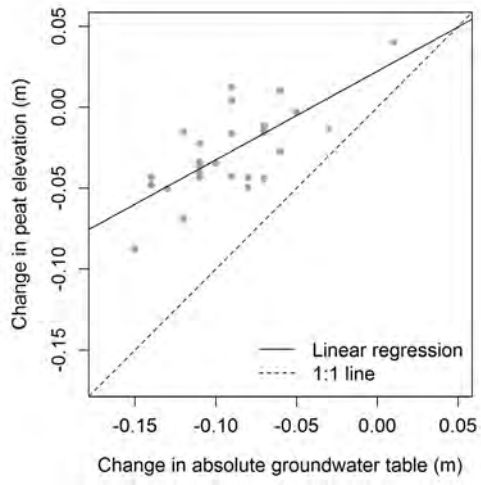

Figure 4.4. *Relation between changes in absolute groundwater table (i.e. aquifer thickness) and peat surface elevation over the period 13 May – 12 July. Negative peat volume change values indicate compression, positive values expansion of the saturated peat matrix. The regression line represents the equation* $\Delta z = -0.55 \cdot \Delta GWT_A - 0.022$. *Fitted parameters were significant (*$P < 0.05$*) and the goodness of fit is 0.51 (*R^2_{adj}*).*

4.3.5.2 Vegetation

Microsite level

The magnitude of peat volume change differed among the four microsites, with flarks having 90% larger shrinkage than the lawn microsites (Fig. 4.5a). Although substantial, these differences were not statistically significant (ANOVA; F = 0.71, $P = 0.55$). The four microsites as established by the cluster analysis were mainly separated along the groundwater table gradient (Fig. 4.6), with hollows and flarks prevailing at sites with shallower GWT_R (ANOVA; F = 6.1, $P < 0.001$) (Fig. 4.5b).

Species level

Peat volume change explained 7.3% (R^2) of the total variation in plant species composition, and its effect was not significant (Monte Carlo Permutation test; F = 2.0, $P = 0.13$). The groundwater table relative to the peat surface (GWT_R) in July explained 30.5% (F = 11.4; $P < 0.01$) of the total variation in plant species composition and was the main explanatory factor for spatial variation in vegetation composition along the transect (Fig. 4.6). Due to the collinearity of GWT_R in July with change in relative groundwater table (ΔGWT_R), peat volume change, distance from the peat-forest border, and surface elevation, the effect can however not be fully separated from these factors (Table 4.2).

Table 4.2. *Spearman Rank-Order correlation coefficients between peat volume change (Δz), positional and geohydrological variables, and its relation to (changes in) groundwater table relative to peat surface (GWT_R). Significant correlations ($P < 0.05$) are indicated in bold.*

	Positional and geohydrological factors						Relative groundwater table		
	Elevation	DB	DB SW	PT	K_S	ΔGWT_A	GWT_R May	GWT_R July	ΔGWT_R
Δz	-0.32	0.13	0.37	0.03	-0.25	**-0.73**	0.01	**0.41**	**0.46**
Elevation		-0.29	**-0.99**	-0.29	-0.13	-0.06	0.03	**-0.44**	**-0.46**
DB			0.15	0.35	0.24	-0.03	-0.20	-0.08	-0.07
DB SW				0.10	-0.08	0.08	0.00	**0.54**	**0.57**
PT					**0.58**	-0.09	-0.37	-0.32	-0.16
K_S						-0.08	-0.07	-0.21	-0.24
ΔGWT_A							-0.12	0.01	0.12
GWT_R May								**0.38**	-0.01
GWT_R July									**0.87**

Δz	Peat volume change (more shrinkage = larger positive value); cm
Elevation	Peat surface elevation with respect to sea level (m.a.s.l)
DB	Euclidian distance to South-western peat-forest border (m)
DB SW	Euclidian distance to closest peat-forest border (m)
PT	Initial peat thickness; distance between peat surface and mineral soil (m)
K_S	Saturated hydraulic conductivity (m d^{-1})
ΔGWT_A	Change in absolute water level between May 13th and July 12th; more negative values indicate larger decline in absolute water level. Equals change in aquifer thickness.
GWT_R May	Groundwater table relative to peat surface on May 13th (cm; negative if below peat surface)
GWT_R July	Groundwater table relative to peat surface on July 12th (cm; negative if below peat surface)
ΔGWT_R	GWT_R May – GWT_R July (cm; more negative values indicate larger water level decline)

Despite the lack of a direct relation between peat volume change and overall vegetation composition, the magnitude of peat volume change was related to abundance of individual species. *Drosera rotundifolia* was indicative for sites with large peat surface position fluctuations (Spearman correlation coefficient $\rho = 0.50$; $P < 0.05$). Plant species indicative for a low magnitude of peat volume change were *Vaccinium uliginosum* ($\rho = 0.44$; $P < 0.05$) and *Eriophorum vaginatum* ($\rho = 0.39$; $P < 0.05$). *Trichophorum cespitosum* ($\rho = 0.33$; $P < 0.1$) and *Sphagnum balticum* ($\rho = 0.33$; $P < 0.1$) were also suggestive of large and small peat volume change magnitude.

4.4 Discussion

4.4.1 Spatial structure of peat volume change patterns

This is, to our knowledge, the first analysis of the fine scale spatial structure of peat volume change patterns within a peatland. In Degerö Stormyr, the northern peatland complex studied, spatial patterns in peat volume change have a spatial scale of 40.8 ± 0.6 m (± SE). The magnitude of peat volume change observed in the studied peatland (up to 6.2 cm, from start – middle growing season) is in the range found for other *Sphagnum* dominated ombrotrophic peatland systems in the boreal and temperate zone, generally ranging between 2 – 11 cm (Almendinger *et al.*, 1986; Baden & Eggelsmann, 1964; Price, 2003; Schlotzhauer & Price, 1999; Schothorst, 1977; Uhden, 1967; Whittington *et al.*, 2007).

The result that spatial peat volume change patterns emerge at a spatial scale of about 40 m indicates that peatland simulation models assuming horizontally uniform peat volume change are representative for a limited area only. Instead, peatland models simulating water flow should include spatially explicit peat volume change. Berne *et al.* (2004) and Schilling (1991) suggest the measurement resolution for autocorrelated data to be 3 – 4 times smaller than the scale of pattern formation to adequately capture the spatial process. Rendering this recommendation in a modelling framework, as rule of thumb a grid resolution of about 12 – 15 m is required in spatially explicit peatland hydrology models to capture the peat volume change (Chapter 5, Kennedy & Price, 2004) for peatland systems comparable to Degerö Stormyr. Given the strong correlation between peat volume change and groundwater dynamics (Table 4.2), this recommendation is also applicable for groundwater flow simulations in general.

Our results demonstrate that digital photogrammetry is an accurate and cost-effective alternative for airborne LiDAR campaigns (Korpela *et al.*, 2009; Lode & Leivits, 2011).

The mean difference between manual and photogrammetrically derived peat surface elevation is 0.02 m. This difference, however, includes both an inaccuracy related to manual peat surface elevation measurements and a position offset due to the selection of the minimum elevation value per grid cell. In a few regions peat expansion occurred, instead of compression (Fig. 4.2). It may be that, despite our efforts to remove all vegetation data points, vegetation was not completely removed from the point clouds, which may have biased peat surface observations with large vegetation cover. This seems unlikely, however, because the vegetation relevés indicate that vascular plant cover is relatively low at locations with peat expansion. An alternative explanation is the accumulation of methane, which may considerably increase peat surface position by enhancing peat buoyancy (Glaser *et al.*, 2004; Smolders *et al.*, 2002; Strack *et al.*, 2006).

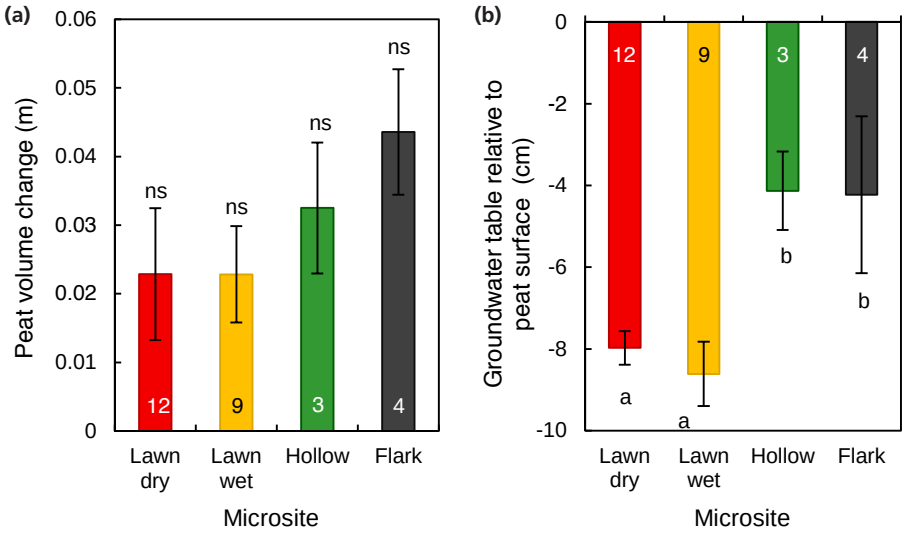

Figure 4.5. *Mean magnitude of peat volume change per microsite between 13th May – 12th July (a) and mean groundwater table relative to peat surface per microsite (b). Significant subgroups groups are presented with letters; ns = not significant (P > 0.05). P values are corrected following Benjamini & Hochberg (1995). Error bars represent standard errors and numbers the number of replicates per microsite.*

4.4.2 Relations between peat volume change and environmental factors

In accordance with studies indicating the importance of groundwater table for temporal surface elevation changes (Fritz *et al.*, 2008; Price, 2003; Roulet, 1991), we found that spatial variation in the change of absolute groundwater table through time was the key

factor related to spatial variability of peat volume change (Fig. 4.4; Table 4.2). This is also supported by the fact that the change in spatial structure of topography was related to changes in absolute groundwater table (Fig. 4.3). Variograms of absolute groundwater table at all points in time seem to confirm that the spatial scale of patterning of absolute groundwater tables (86 ± 40 m [± SD]; not shown) corresponds approximately to that of topography (90 – 140 m; Appendix 4.3). The variograms of absolute groundwater table are, however, based on a too small sample size (Journel & Huijbregts, 1978; Webster & Oliver, 2007) with large distances between groundwater wells, and are therefore only indicative.

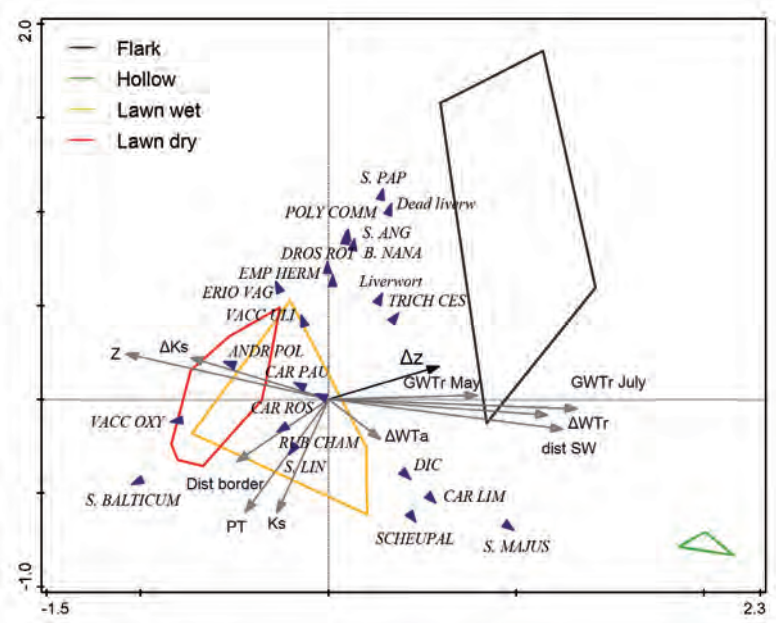

Figure 4.6. *Ordination diagrams (PCA) of the two first ordination axes, showing variation in vegetation composition. Plant species are indicated with triangles, environmental variables with arrows. See Table 4.2 for acronyms. The four identified microsites are shown with the envelopes: flarks (black); hollows (green); lawn with high abundance of Vaccinium oxycoccos (orange); and lawn (red).*

Spatial variability of changes in absolute groundwater table (ΔGWT_A) may arise from spatial differences in local water balance components, which comprises rainfall, evapotranspiration, and lateral groundwater flow. As spatial coverage of rain events is larger than square-kilometres (Ciach & Krajewski, 2006; Rakovec *et al.*, 2012), rainfall can be assumed to be uniform within the peatland. Evapotranspiration rates may vary

with vegetation type (Heijmans *et al.*, 2001; Limpens *et al.*, 2014a), so that spatial variability in ΔGWT_A could potentially result from differential evaporative water losses. However, as ΔGWT_A was not related to vegetation composition (Fig. 4.6) nor to microsite distribution (ANOVA; $F = 0.229$, $df = 3$, $P = 0.87$; $R^2 = 0.035$), it seems unlikely that spatial variability in ΔGWT_A is caused by spatially variable evapotranspiration rates. It thus seems logical that spatial variability in ΔGWT_A is a result of lateral redistribution of groundwater.

The rate and direction of lateral groundwater flow is dependent on the position within the peatland and surrounding landscape (Grootjans *et al.*, 1996; Ivanov *et al.*, 1981; Kemmers, 1986). In contrast, we found no evidence that the position in the peatland, as described by distance to the (closest) peat-forest margin, peat thickness, hydraulic conductivity, or altitude, was related to peat volume change (Table 4.2). As sites with larger peat thickness provide a larger expandable medium, we anticipated that peat volume change was positively correlated with peat thickness as was also hypothesized by Almendinger *et al.* (1986). However, our results indicate that peat thickness was uncorrelated with peat volume change (Table 4.2), which is in accordance with observations by Fritz *et al.* (2008). A probable reason is that, due to the increase of bulk density and degree of decomposition with depth or peat age (Boelter, 1969; Loisel *et al.*, 2014; Päivänen, 1982), most peat volume change is restricted to the upper, less decomposed stratums (~ top 50 cm (Price, 2003; Waddington *et al.*, 2010)). The saturated hydraulic conductivity (K_s) was unrelated to peat volume change, implying that no autogenic peat formation process at coarse spatiotemporal scales relates these two factors.

The lack of a relation between peat volume change and geohydrological and positional factors could be a consequence of the transect being placed perpendicular to the dominant flow direction (unpublished map by Mats B. Nilsson; Malmström (1923)). This positioning may have led to an underestimation of the effect of geohydrological and positional factors. A transect in the dominant flow direction, verified with physically based spatially explicit hydrological models, could produce other results and is recommended for future studies.

4.4.3 Relation between peat volume change and current vegetation composition

Previous studies indicate that the compressibility and magnitude of peat volume change may differ among microsites (Roulet, 1991; Waddington *et al.*, 2010; Whittington & Price, 2006). In Degerö Stormyr, flarks and hollows seemed to be peat volume

change 'hotspots' (Fig. 4.5a) at the microsite level, although differences in peat volume change were not statistically significant among microsites. This suggests that no direct feedback between peat volume change and microsite distribution occurs in the studied peatland. However, the lack of significance may be caused by uncertainty of manual point measurements on peat volume change and by the low number of replicates per microsite. Moreover, an indirect feedback between peat volume change, groundwater table depth, and microsite may still emerge as follows. Despite the larger decline in absolute groundwater level at dry microsites as compared to wet microsites, peat volume change is smaller at dry microsites (Table 4.2; Fig. 4.5b). This indicates that the compressibility of the dry microsites is smaller, which is in accordance with results of Waddington *et al.* (2010). Due to the low compressibility at dry microsites, peat volume change is small and the July groundwater table (relative to peat surface; GWT_R) is deep at these sites (Table 4.2). In turn, the July GWT_R is the dominant factor explaining spatial variation in vegetation composition (Fig. 4.6) (Andersen *et al.*, 2011) and significantly differs between microsites (Fig. 4.5b). Deeper water tables promote the establishment of species adapted to dry sites which (Luken, 1985; Rydin, 1986), due to their low compressibility, may further decrease the local peat compressibility on the long term. Nonetheless, as vegetation and peat soil development occur at different temporal scales (Belyea & Baird, 2006), it is also possible that species turnover is simply faster than turnover of the peat physical traits, so that current microsite distribution is a poor predictor of current physical properties.

The species composition along the transect could explain only 7.3% (R^2) of the spatial variability in peat volume change. In contrast to our hypothesis, plant species abundance is only a weak predictor for peat volume change in the studied peatland. The low explanatory value of current plant species composition may partially originate from the absence of hummock *Sphagna* along the transect, so that variability in vegetation composition was limited (as indicated by the small gradient length of 2.7 SD).

At a species level, *Drosera rotundifolia* and *Trichophorum cespitosum* may be indicative for peat volume change 'hotspots'. Yet, as *D. rotundifolia* and *T. cespitosum* reach low cover only, their contribution to peat hydrophysical characteristics later formed by their litter can only be marginal. The correlation is therefore likely indicative of flark presence rather than suggestive of a direct relation between compressibility and vegetation composition. Abundance of *Vaccinium uliginosum* and *Eriophorum vaginatum* is moderately negatively correlated with peat volume change. In a nearby peatland, vegetation composition remained practically unchanged during the last 70 years, so that the peat material of the top 30 cm is composed of the same plant species (van der Linden *et al.*, 2008). Given that

both peatlands remained undisturbed during this period, it seems likely also in Degerö Stormyr the vegetation remained unchanged. With this assumption, the correlation suggests that plant litter or roots of these plant species increased the rigidity of the peat matrix and thereby reduce its compressibility. The low sample size makes these results speculative, and using these species as indicators for peat volume change 'hot spots' or 'cool spots' requires confirmation with other peatland sites before application.

4.4.4 Effects of peat volume change on topography

The surface topography of the studied peatland was spatially structured, with 73% of the surface patterns originating at a spatial scale of 90 – 140 m and 20% at about 4 m. Microtopographical hummock-hollow patterns in another patterned northern peatland emerged at a spatial scale of 1 – 4 m (Anderson *et al.*, 2010), which corresponds to the short-range pattern found in our study. It thus seems likely that the short-range pattern is related to microsite identity. The long-range topographical pattern is, as argued in Section 4.4.2, likely related to spatial patterns in absolute groundwater table.

Our results indicate that the long-range patch size and vertical variability of peat surface elevation decreased and increased with deeper groundwater tables (Fig. 4.3), while the short range patch size and variability remained constant over time. As spatial variation in peat volume change was mainly related to changes in absolute groundwater table (Table 4.2), this suggests that progressively more sites may become compressed with deeper groundwater tables, while for some other sites the topography may remain more stable (Fig. 4.7). As a result, topographical differences could become more pronounced and more patchy, and also the variance of groundwater table depth relative the peat surface (GWT_R) will increase (Fig. 4.7). The larger habitat variety may increase species richness and thereby enhance ecosystem resilience to environmental extremes, such as droughts (Loreau *et al.*, 2001; Peterson *et al.*, 1998; Scherrer & Körner, 2011).

The increased topographical variability with increased peatland drought status may furthermore affect lateral groundwater flow direction and rate. In unconfined aquifers the groundwater table is frequently assumed to be a subdued replica of topography (Desbarats *et al.*, 2002; Hoeksema *et al.*, 1989; Sonnentag *et al.*, 2008). Theoretically, increased horizontal patchiness and vertical variability of surface elevation may therefore increase the patchiness of GWT_R and result in steeper hydraulic gradients. All things being equal, this would lead to finer-scale drainage from elevated sites to low sites, enhancing the hydrological differentiation between wet and dry sites. The drier conditions may stimulate performance of hummock species (Nijp *et al.*, 2014; Robroek *et al.*, 2007a; Rydin, 1993), of which the (partially) decomposed material has a low compressibility (Waddington *et al.*, 2010).

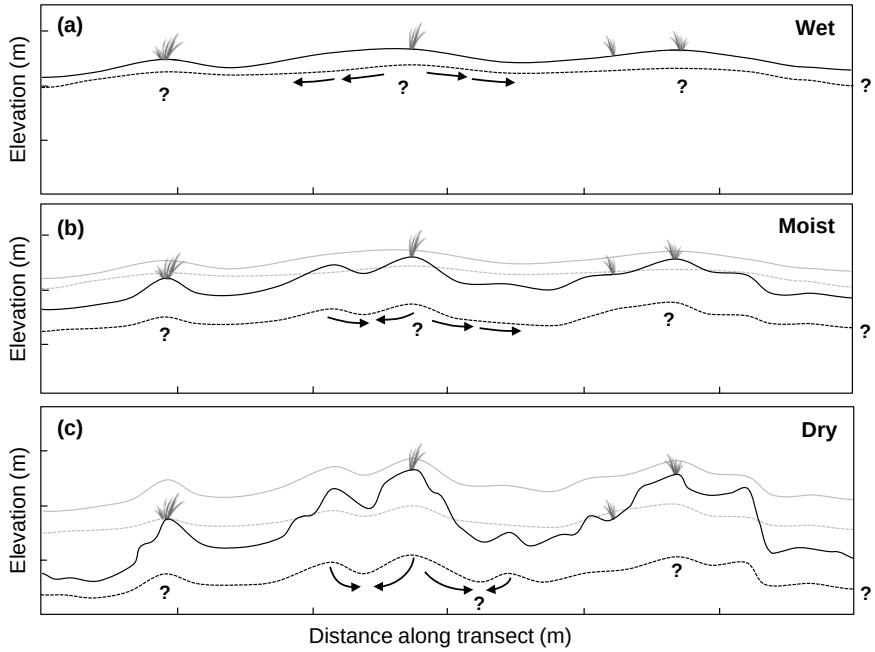

Figure 4.7. *Hypothetical conceptual model of peat volume change impact on topography and hydrology during progressive drying (a-c). The horizontal axis represents a horizontal transect through a peatland, the vertical axis the (exaggerated) position of peat surface elevation (solid black lines) and groundwater table (dashed black lines). Groundwater flow paths are indicated with arrows and peat surface and groundwater positions in previous conditions in grey. Considering compression during the growing season, the peat elevation decreases at all positions through space upon drying (b,c). Due to spatial variability in lateral groundwater inflow and compressibility along the transect, some places start to compress earlier and more than others, enhancing the vertical and horizontal topographical heterogeneity. As a result of the increased vertical range of topography, hydraulic gradients may hypothetically become steeper and groundwater flow more local, as is illustrated with the flow lines.*

The increased lateral discharge from elevated sites to lower depressions may thus amplify a positive feedback between microsite compressibility and species composition and enhance self-organized vegetation patterns. As locations with deeper July GWT_R have a larger decline in GWT_R during the growing season (Table 4.2), our data seem to support this hypothesis. However, the suggested impact of peat volume change on redistribution of groundwater flow needs to be tested in future studies using a denser groundwater well network. Moreover, although the assumption that the groundwater table follows peatland topography at a spatial scale from 90 – 140 m seems reasonable (Fraser *et al.*, 2001), it should be verified whether this assumption holds in given climatic and geohydrological conditions (Haitjema & Mitchell-Bruker, 2005).

4.5 Conclusion and implications

This study shows that peat volume change is spatially structured, and that most of peat volume change occurred at a spatial scale of 40.8 ± 0.6 m (± SE). In contrast to previous research (Almendinger *et al.*, 1986; Waddington *et al.*, 2010; Whittington & Price, 2006), we found only a weak relation between microsite or position in the peatland and peat volume change. Instead, peat volume change was mainly related to changes in absolute groundwater table, which may likely be attributed to lateral groundwater redistribution. Surface topography had a patch size of about 140 m at the start of the growing season, but decreased to 90 m in the middle of the growing season, when deeper groundwater tables occurred. In addition, the vertical variability increased with deeper water tables. We hypothesize that the increased topographical heterogeneity with deeper groundwater tables may result in a more local redistribution of groundwater from elevated sites to depressions, which further enhances the contrast between wet and dry sites during droughts. This hypothesis needs to be tested in other peatlands and various hydro-climatological settings. The Structure-from-Motion technique can be successfully applied to capture temporal changes in peat topography with a vertical accuracy of 2 cm.

From the perspective of self-regulation and ecosystem stability it is relevant to improve the scientific understanding of peat volume change patterns and the mechanism responsible for these patterns. Like other self-regulating ecosystems, northern peatlands may respond non-linearly to external perturbations and rapidly shift to a virtually irreversible, undesired state (Rietkerk *et al.*, 2004; Scheffer *et al.*, 2001). This implies that peatlands may quickly shift from a net carbon sink to source, feeding back to the global climate by altering radiative forcing (Bridgham *et al.*, 2008; Frolking *et al.*, 2006; Frolking & Roulet, 2007). Additionally, the spatial scale of peat volume change identified in this study has direct implications for the spatial representativeness of spatially implicit simulation models (Chapter 5) (Kennedy & Price, 2004) including peat volume change.

4.6 Acknowledgements

We are thankful to Gijs van Dijk, Lena Jonsson and Pernilla Löfvenius for assistance in the field and taking top-view images, Mattias Eklund for surveying ground control points, and Mikaell Ottosson-Löfvenius for kindly providing hydro- and meteorological data. Juha Suomalainen is acknowledged for his involvement in photogrammetric analyses. This study was co-funded by the Schure-Beijerinck-Popping fund (KNAW), the Dutch Foundation for the Conservation of Irish Bogs and WIMEK/SENSE (The Wageningen Institute for Environment & Climate Research, and the Socio-Economic & Natural Sciences of the Environment).

Appendix 4.1. Estimating in-situ hydraulic conductivity

A4.1.1 Slug test description

The horizontal saturated hydraulic conductivity (K_s) of the acrotelm was estimated with slug tests, which provide a relatively simple and cheap tool to estimate the hydraulic conductivity. In a slug test, a volume of water (*slug*) is instantaneously added (or removed) from a groundwater well, which generates a hydraulic head difference and hence flow from the groundwater well into the soil. By measuring the evolvement of the hydraulic head in the groundwater well through time an estimate of K_s can be derived.

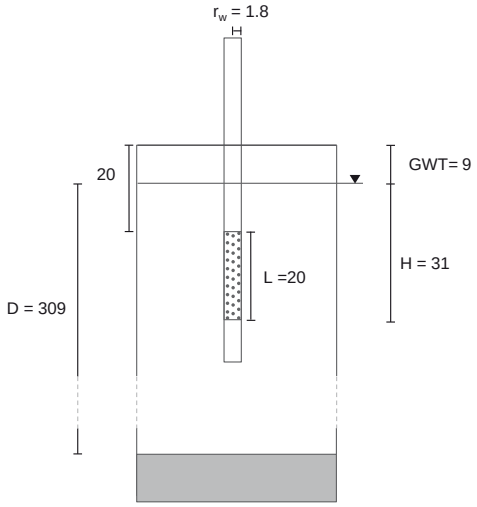

Figure A4.1. *Schematic overview of groundwater well installation. L = filter length, r_w = groundwater well inner radius, D = average aquifer thickness, GWT = mean distance of groundwater table below peat surface, H = distance from bottom of groundwater well filter to mean groundwater table. All lengths are in centimetres.*

For partially penetrating wells in unconfined aquifers the Bouwer-Rice method is frequently applied to analyse slug tests (Bouwer & Rice, 1976). In this method, the theoretical basis is a modified version of the Thiem equation (Thiem, 1906), where the hydraulic conductivity is related to the decline in water table after slug insertion in a radial flow system

$$Q(t) = 2\pi K_s L \frac{h(t)}{F_{BR}} \qquad \text{(A4.1)}$$

where Q is the discharge from the groundwater well ($cm^3\ d^{-1}$), L = filter length (Fig. A4.1),

i.e. the perforated section of the groundwater well (cm), h the difference in water height between the equilibrium aquifer water level and the water level in the groundwater well and F_{BR} a shape factor that accounts for the geometry of the flow system. The Bouwer-Rice shape factor was derived empirically from a steady state electric analog resistance model.

Assumptions in the Bouwer-Rice evaluation of slug tests are 1) a constant groundwater table position during the slug test 2) flow in the unsaturated zone is negligible 3) the aquifer is homogeneous and isotropic 4) elastic storage can be neglected 5) aquifer has infinite extent and 6) groundwater flow is horizontal and 7) the aquifer is underlain by an aquitard.

A recently frequently employed technique in the peatland community is the time-lag theory of Hvorslev (Baird *et al.*, 2004; Hvorslev; Price, 2003; Surridge *et al.*, 2005). This theory, however, is originally intended for confined aquifers. The Bouwer-Rice and Hvorslev model are different only in the evaluation of the shape factor (Brown *et al.*, 1995). While the Bouwer-Rice method assumes a constant head at the top boundary to account for unconfined aquifers, the Hvorslev method assumes a no-flow boundary conditions at the top of the aquifer. In case the well screen is located far from the centre of the aquifer, the Hvorslev method may resulted in an overestimated K_s (Hyder *et al.*, 1994).

However, especially for short screens located near the aquifer boundaries, also the Bouwer-Rice method may result in an underestimation of K_s up to 30% (Brown *et al.*, 1995; Hyder & Butler, 1995; Hyder *et al.*, 1994; Zlotnik *et al.*, 2010). To avoid problems inherent to the traditional Bouwer-Rice shape factor, we use the closed-form analytical form of a shape factor provided by Zlotnik *et al.* (2010), which can be applied at any filter length, installation depth, aquifer thickness and anisotropy in hydraulic conductivity

$$F_{ZGD} = \left(\sum_{i=1}^{\infty} \left\{ \left(\cos\left(\beta_i \frac{H}{D}\right) - \cos\left(\beta_i \frac{H-L}{D}\right) \right)^2 \times \frac{K_0\left(\frac{\beta_i r_w^*}{D}\right)}{\beta_i^3 K_1\left(\frac{\beta_i r_w^*}{D}\right)} \right\} \right) \Big/ \frac{L\, r_w^*}{2\, D^2} \qquad \text{(A4.2)}$$

where K_0 and K_1 are the modified Bessel functions of third kind and 0th or 1st order; r_w^* is the well radius scaled by the anisotropy coefficient

$$r_w^* = \frac{r_w}{\sqrt{K_h/K_v}} \qquad \text{(A4.3)}$$

In Eq. A4.3, $\beta_i = \pi\,(i - 0.5)$. See Zlotnik *et al.* (2010) for details on the derivation. An R script to calculate this general shape factor is provided in Appendix A4.1.5.

A4.1.2 Spatial variability of saturated hydraulic conductivity

The saturated hydraulic conductivity (21 May 2013) was correlated with peat thickness, where K_s was larger with larger peat thickness (Spearman correlation coefficient = 0.58, $P < 0.05$). In accordance with Baird *et al.* (2008), K_s is lower at the peat borders (Fig. A4.2), which may maintain the wetness of peatlands and play an important role in the self regulation of peatland ecosystems (Belyea & Baird, 2006).

A4.1.3 Effect of compression on saturated hydraulic conductivity

Compression of the peat matrix associated with a decline in absolute groundwater table of 7.9 cm between 16th and 21st of May resulted in a significant reduction of the hydraulic conductivity (linear regression, $K_{s,t3} - K_{s,t2}/K_{s,t2} = 0.069 + 0.122\ (z_{t3} - z_{t2})$; $P = 0.02$). Nonetheless, the goodness of fit was poor ($R^2 = 0.20$). Zones with higher saturated hydraulic conductivity were spatially related to regions with larger peat thickness (Table 4.2 in main text).

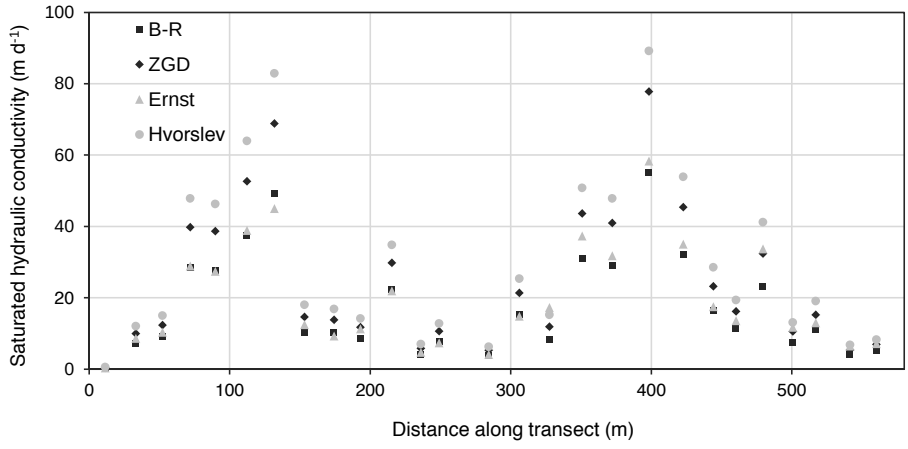

Figure A4.2. *Estimated saturated hydraulic conductivity (K_s) along the transect (left is southwest, right is northeast) with four different slug test analysis methods: Bouwer-Rice (B-R), Zlotnik et al (ZGD), Ernst, and Hvorslev.*

A4.1.4 Comparison among slug test analyses and measurement error

Repeated slug tests (n = 3) for the same groundwater well indicate that slug tests were accurate; minimum and maximum K_s deviated less than 5% from the mean K_s estimate. With the Bouwer-Rice method employing the Zlotnik *et al.* shape factor as reference, the Hvorslev method generally overestimates K_s (15 – 40% higher K_s) while the Bouwer-

Rice method with the empirical shape factor provided in Bouwer & Rice (1976) underestimates K_s (25 – 29% lower) (Figure A4.2). Using the shape factor by Zlotnik *et al.* (2010) yields results consistently between these two extremes. Also the frequently employed augerhole method (Ernst, 1950) as presented in van Beers (1983) is mostly in between the two extremes. The Ernst (1950) variant with an impermeable layer at the bottom approaches the Zlotnik *et al.* solution very well.

A4.1.5 An R implementation for the Zlotnik *et. al.* (2010) shape Factor

```
##=====================================================================
## Shape factor sensu Zlotnik et. al. (2010)
##---------------------------------------------------------------------
##
## Author       : Jelmer J. Nijp (Wageningen University)
## Date         : May 2015
## An R implementation om the theory by Zlotnik et al. (2010) to
## facilitate the applicability of the Zlotnik et al shape factor.
##=====================================================================

## Input (all in same units)
XL     <- 1      # filter length
D      <- 100    # aquifer thickness
H      <- 1      # distance from top aquifer to bottom filter screen
rws    <- 0.01   # well radius, scaled by anisotropy ratio


##---------------------------------------------------------------------
## Calculate shape factor
##---------------------------------------------------------------------

n      <- 10000
betan  <- pi * ( 1 : n - 0.5 )

s2     <- sum( ( cos( betan * H / D) - cos( betan * (H - XL) / D ) )^2 *
               ( besselK( betan * rws / D, nu= 0 ) / ( betan^3 *
                 besselK( betan * rws / D, nu= 1 ) ) ) )

ZGD    <- ( (XL * rws)/(2 * D^2) ) / s2 # inverse shape factor
F.ZGD  <- 1 / ZGD                       # shape factor

##=====================================================================
```

Appendix 4.2: Details photogrammetric analyses

A4.2.1 Accuracy and characteristics of image datasets

To estimate the quality of the photogrammetric analysis, the data generated with the Photoscan software were compared with measurements at ground control tube positions. The mean difference between manual measurements of peat surface elevation and photogrammetrically derived estimates was 2 cm (RMSE; see Fig. A4.3). Table A4.1 provides an overview of most important characteristics of the image datasets.

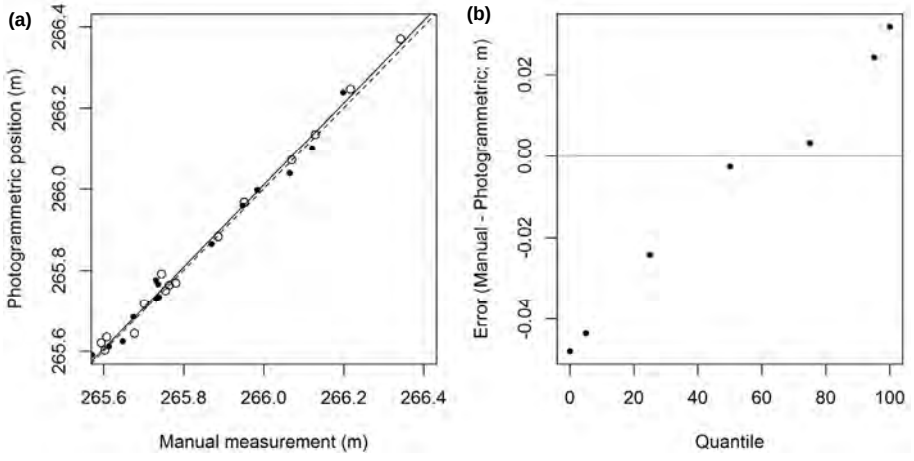

Figure A4.3. *(a) Comparison of position estimated by manual position measurements with position estimated with Structure-from-Motion technique, for two points in time (● = May 13th; ○ =July 12th) and (b) distribution of errors as indicated by the 0th, 5th, 25th, 50th, 75th, 95th and 100th quantile. In the left figure, the solid and dashed line represent the linear regression fit and the 1:1 line.*

Table A4.1. *Overview of characteristics of optimized sparse point clouds obtained with the Structure-from-Motion algorithm applied in the Agisoft Photoscan software.*

Date	07 May	13 May	16 May	26 May	12 July	Avg	St. dev
Number of aligned cameras	1849	3410	2906	2725	2562	2690	568
Detected point count	195032	198176	225463	257936	458889	267099	110165
Effective overlap (%)	9.4	19.0	14.2	12.0	5.2	12.0	5.1
Estimated mean point density (n m^{-2})	122	124	141	161	287	178	74
Mean reprojection error (pixels)	1.24	1.06	1.08	1.16	1.05	1.12	0.08
Mean vertical error (mm)	4.8	8.5	3.3	13.5	2.5	6.5	4.6
Flying altitude (m)	6.66	7.16	7.27	6.72	5.86	6.75	0.64
Ground resolution (mm $pixel^{-1}$)	1.87	2.22	1.87	1.77	1.20	1.79	0.37
Peat volume change rate (mm d^{-1})	-	0.17	-2.17	-0.72	-0.28	-0.75	1.01

A4.2.2 Effect of distance from ground control point on accuracy

To determine how the distance to ground control tubes influenced the accuracy of the generated point clouds, we sequentially removed the nearest ground control tube and checked how this affected the vertical error at a given ground control point. The error increased exponentially with increasing distance to ground control tubes (Fig. A4.4). At the mean separation distance of ground control tubes (35 m), the absolute vertical error is estimated at 4.8 mm with the presented regression equation. This suggests that the employed distance between ground control tubes is appropriate and yields sufficient accuracy.

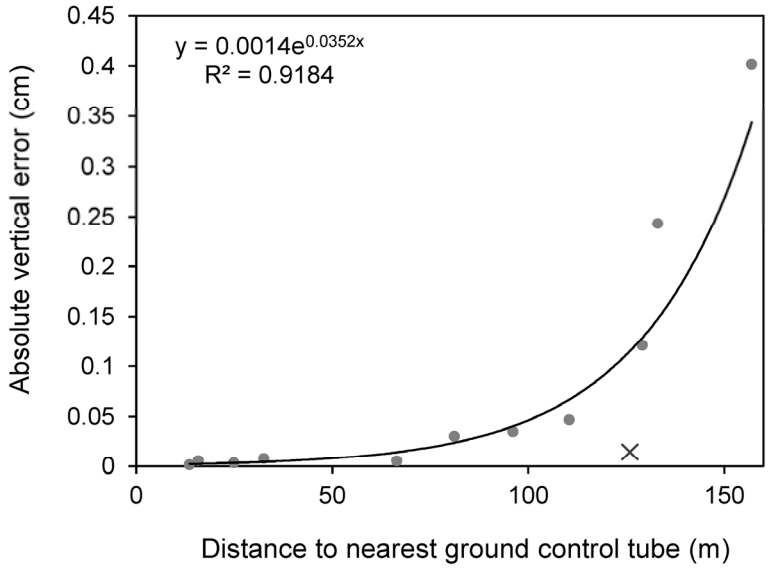

Figure A4.4. *Increase of vertical error as function of distance to nearest ground control tube. Ground control points were sequentially excluded in the point cloud optimization procedure in the Agisoft Photoscan software. The point with the cross was regarded as outlier and excluded from the fit.*

Appendix 4.3. Variogram analysis

Empirical variograms were constructed with a separation (lag) distance equal to the minimum grid spacing (0.5 m). Each lag contained at least 30 data pairs cf (Webster & Oliver, 2007). The maximum lag distance (i.e. separation distance between two points in space) was set at 175 m. Combinations of up to three theoretical variogram model combinations (Table A5.3) were fitted. All models included a nugget effect to account for random measurement variation or variation in peat volume change occurring within the measurement range. Because the Exponential and Gaussian model approach the sill asymptotically, their practical correlation range (CR) is calculated as the separation distance at which 95% of the partial sill is reached. In case combinations of variograms were fitted, multiple partial sills and correlation range parameters were present, describing multiple spatial structures.

Table A5.3. *Theoretical variogram model components employed in this study. The correlation range (CR) is the lag distance at which negligible correlation occurs. For the Exponential and Gaussian model the CR is calculated as the separation distance at 95% of the asymptotic partial sill value.*

Model	Equation	CR
Spherical	$\gamma(h) = \begin{cases} c_p \left(\frac{3h}{2r} - \frac{1}{2}\left(\frac{h}{r}\right)^3\right) & if \quad h < r \\ c_p & if \quad h \geq r \end{cases}$	r
Exponential	$\gamma(h) = c_p \left(1 - exp\left(-\frac{h}{r}\right)\right)$	$3{\cdot}r$
Gaussian	$\gamma(h) = c_p \left(1 - exp\left(-\frac{h^2}{r^2}\right)\right)$	$\sqrt{3}{\cdot}r$
Pure nugget	$\gamma(h) = c_0$	
c_p	Partial sill (γ)	
r	Range parameter (m)	
c_0	Nugget (γ)	
h	Lag distance (m)	

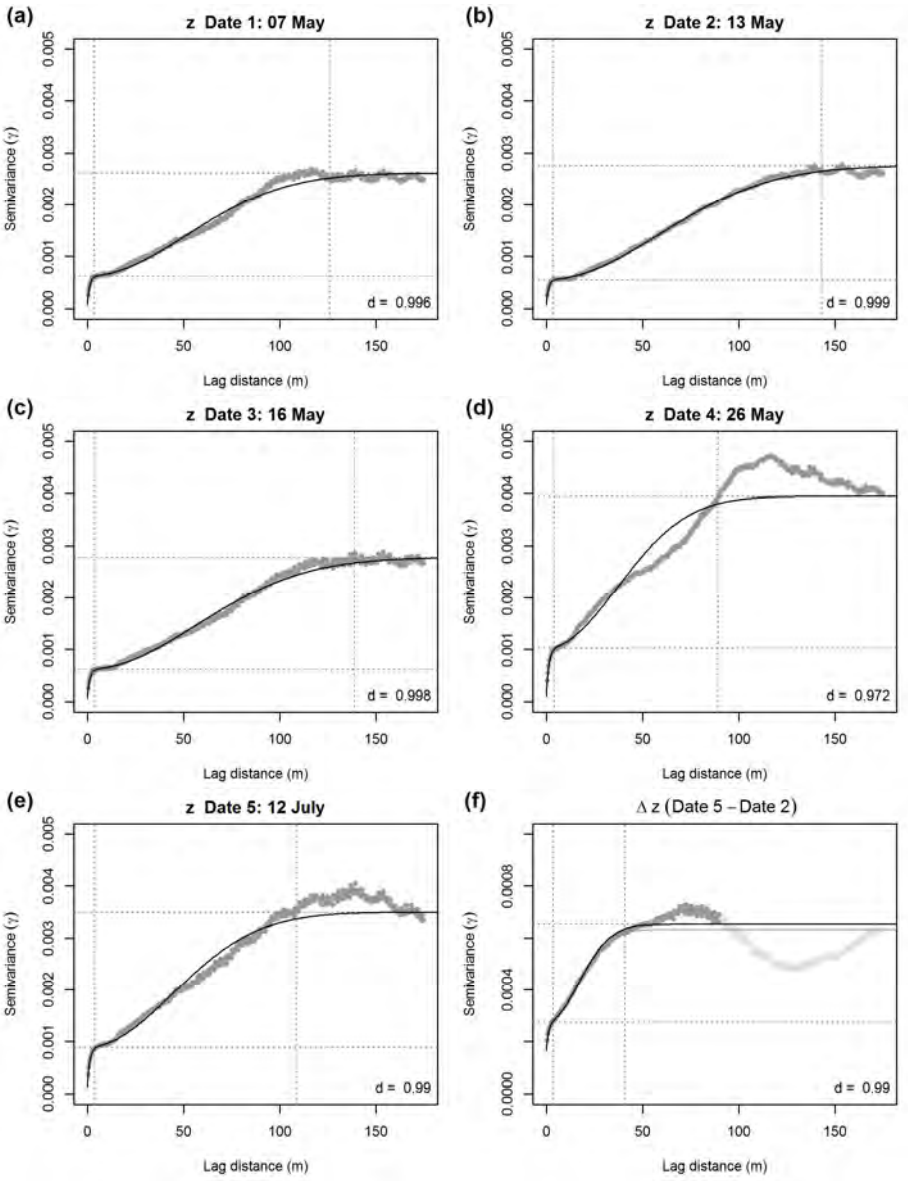

Figure A4.5. *Empirical (points) and fitted (lines) combined exponential-Gaussian variograms for five points in time for peat surface elevation (a-e) and peat volume change (f). For peat volume change two fits are presented, which either include (pale grey) or exclude (dark grey) the cyclic part. Vertical and horizontal dashed lines show the practical correlation ranges and partial sills. The goodness of fit is presented with the Willmotts index of agreement d (1 = perfect match, 0 = no agreement at all) (Willmotts, 1985).*

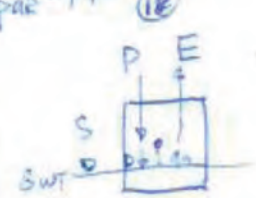

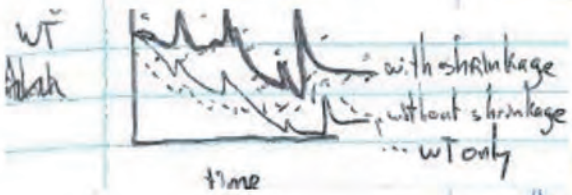

$\frac{dS}{dt} = P - E - D - q_n$

$\frac{dS}{dt} = 0$

$\frac{dS}{dt} = 0$

$\frac{dGWT}{dt} = \frac{D - q_n}{\mu}$

$\frac{dGWT}{dt} = \frac{D_1 - q_n}{\mu}$

$\frac{dGWT}{dt} = \frac{P}{\mu} D$

$\frac{dGWT}{dt} = P$

$D_1 = (P + q_n - E)$

$D_{2,1} = 0 \quad \frac{P - E + Q_1}{\mu + Q_1}$

$D_3 = 0$

$\frac{dDS}{dt} = P - E$

if water supplies !!

then else (GWT < ... ,

if then else (... ≤ what fits,

..., what fits

what does not fit =

what fits = $(S_{max} - S)$

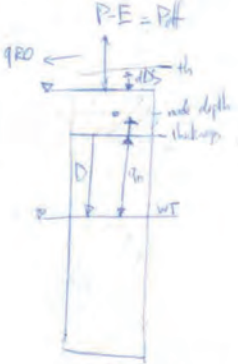

if then else (GWT + TIMESTEP

$+ Q_1$

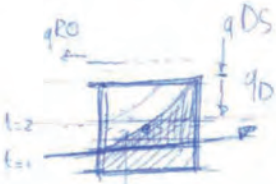

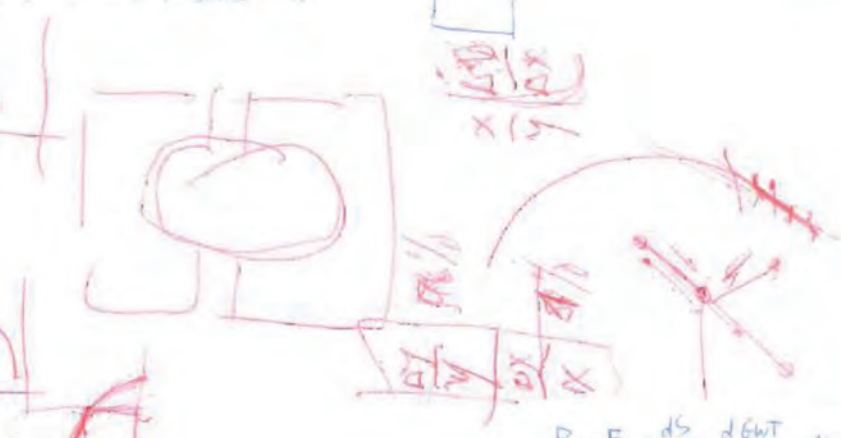

$\frac{dS}{dt}$

$dGWT_D = \frac{\mu}{\mu + \beta_w g \phi \rho^2}$

$P_{in} - E_a - \frac{dS}{dt} - \frac{dGWT}{dt} - q_{RO} = 0$

$dGWT_D = \frac{1}{1 + \frac{\beta_w g \phi \rho^2}{\mu}}$

$\Delta PVC = f\left(\frac{PV}{PV_1}, PARS\right) \Delta S$

5 Predicting peatmoss drought stress: The impact of hydrological complexity

Jelmer J. Nijp, Klaas Metselaar, Juul Limpens, Claudia Teutschbein, Mats B. Nilsson, Matthias Peichl, Frank Berendse, Sjoerd E.A.T.M. van der Zee

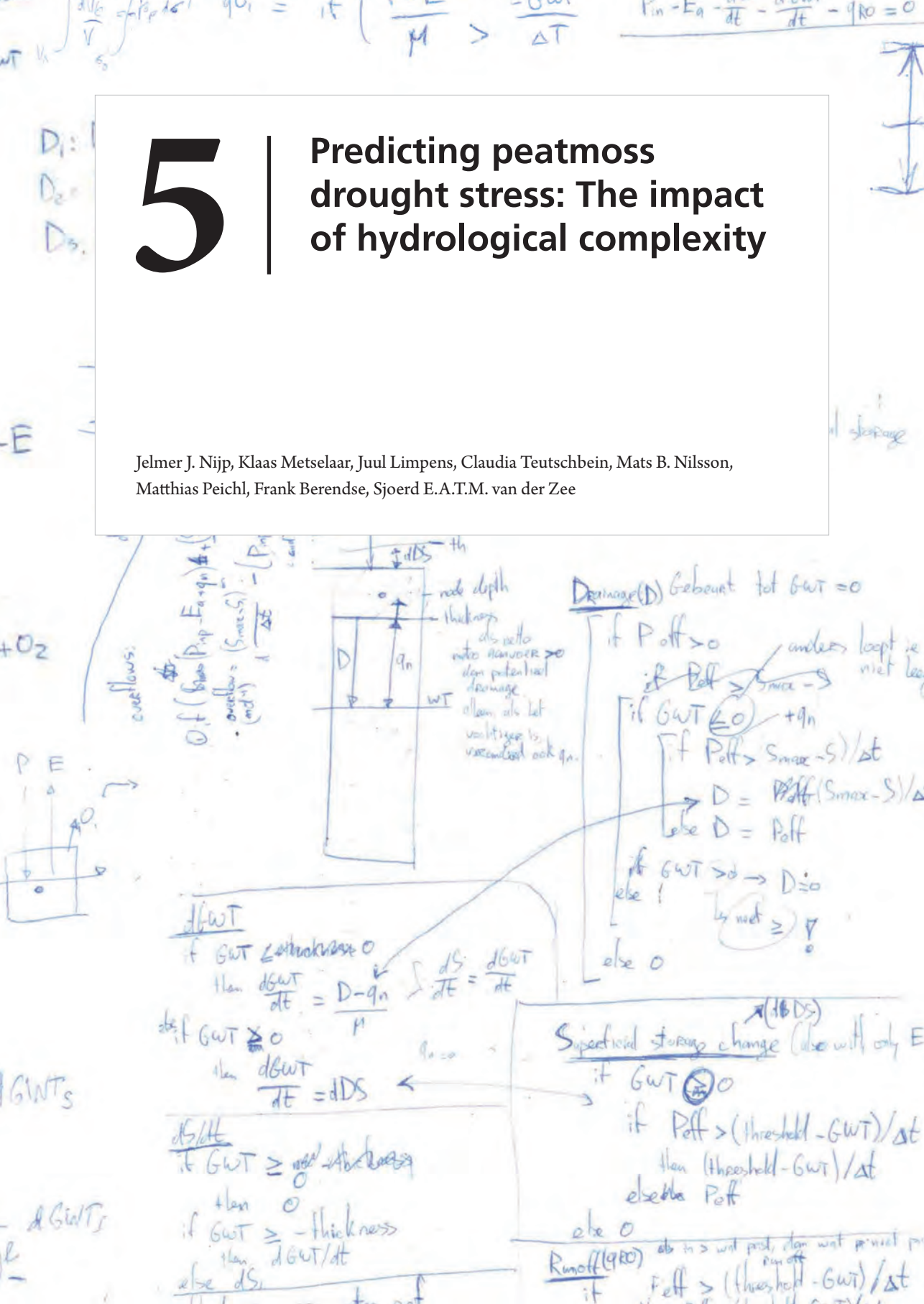

Abstract

Water content in the topsoil is one of the key factors controlling biogeochemical processes, greenhouse gas emissions and land-surface – atmosphere interactions in many ecosystems, particularly in northern peatlands. In these wetland ecosystems, the water content of the top 5 cm of the moss layer is crucial for ecosystem functioning and is sensitive to future shifts in precipitation and drought characteristics. Current peatland models vary in the degree of hydrological detail included, with unknown consequences for peatmoss drought predictions.

In this study we systematically tested if the degree of hydrological complexity could bias future predictions of water content and drought stress for peatmoss in northern peatlands using downscaled future scenarios for rainfall and potential evapotranspiration. We compared peatmoss drought projections among four model concepts including or excluding peat volume change and moss water storage, two processes that are central to self-regulation in northern peatlands. Model performance was validated using field data of a northern peatland in northern Sweden.

We found that including peat volume change as well as moss water storage improved model performance, with the best performance found for the most complex model. Moreover, including these processes, resulted in consistently higher predicted water content, and thus lower frequency and intensity of peatmoss drought stress. Our results demonstrate that ignoring processes important in hydrological self-regulation may lead to overestimation of future climate change impacts on peatlands. The systematic hypotheses testing framework employed in this study proved a useful tool to explore the consequences of alternative model representations and guide model development.

Keywords: Ecohydrology, numerical modelling, soil moisture, northern peatlands, peatmoss, climate change, model complexity and development

5.1 Introduction

Climate change projections indicate that the water cycle will intensify, thereby increasing the frequency of extreme events such as droughts and high intensity rain events (IPCC, 2013), which in turn will modify the amount of water stored in the topsoil (Knapp *et al.*, 2008; Vervoort & van der Zee, 2008). Water content in the topsoil is a major control on biological interactions and therefore plays a crucial role in climate change and land-surface atmosphere interactions (le Roux *et al.*, 2013; Legates *et al.*, 2011; Seneviratne *et al.*, 2006; Teuling *et al.*, 2009).

An example of ecosystems where topsoil water content plays a central role are northern peatlands. These wetland ecosystems are a crucial component of the global carbon and greenhouse gas (GHG) cycle as they store large amounts of the greenhouse gas carbon dioxide (CO_2) (Nilsson *et al.*, 2008; Olefeldt *et al.*, 2012; Roulet *et al.*, 2007; Yu, 2011) and emit large amounts of methane to the atmosphere (Nilsson *et al.*, 2001; Turetsky *et al.*, 2014). Peatland biogeochemistry in general and net ecosystem production in particular are strongly dependent on surface wetness (Fenner & Freeman, 2011; Larmola *et al.*, 2010; Robroek *et al.*, 2007b). Thus, the ability to model the topsoil water content has become a scientific high priority challenge in northern peatlands (Waddington *et al.*, 2015). In oligotrophic (i.e. nutrient poor) northern peatlands, the fixation of atmospheric CO_2 is largely mediated by bryophytes of the genus *Sphagnum* (peatmoss) (Moore *et al.*, 2002). The photosynthetic CO_2 uptake of peatmoss, and therefore carbon storage of peatlands as a whole, is tightly coupled to the water content of the living moss layer (McNeil & Waddington, 2003; Murray *et al.*, 1989; Rydin & McDonald, 1985a; Schipperges & Rydin, 1998). As these bryophyte plants have neither roots nor stomata, their water content is directly affected by water supply to and water losses from the living moss layer, making them extremely vulnerable to future changes in drought frequency and temporal rainfall patterns (Nijp *et al.*, 2015).

To make informed assessments and decisions on climate change impact on peatland functioning and moss water content, dynamic simulation models provide an useful tool. Many peatland models are available, that vary in their objectives and in the ecohydrological feedbacks included (e.g. Baird *et al.*, 2012; Frolking *et al.*, 2010; Granberg *et al.*, 1999; Heijmans *et al.*, 2008; Moore & Waddington, 2015; Price & Whittington, 2010; Schouwenaars & Gosen, 2007; St-Hilaire *et al.*, 2010; Stocker *et al.*, 2014; Wu & Blodau, 2013; Yurova *et al.*, 2007). So far, it has remained unclear which degree of hydrological complexity is required to adequately predict impact of climate change on peatmoss water content and its biogeochemical functioning. Although one may choose to include all processes believed to be relevant for predicting water content

in the living moss layer, this approach is generally not efficient. Any additional process requires instrumental and labour costs for independent parameter measurements, which do not necessarily represent 'effective' parameters for field conditions and increase prediction uncertainty (Beven, 2012; Oreskes *et al.*, 1994). It is therefore essential to test whether increasing hydrological complexity significantly improves model performance (i.e. reduces prediction error).

In peatland ecosystem models, the water content in the living moss layer is frequently modelled as a function of groundwater table depth, assuming the moss water content is in hydrostatic equilibrium with the groundwater table (e.g. Granberg *et al.* (1999) and Yurova *et al.* (2007), but see e.g. Moore & Waddington (2015)), thus ignoring rewetting of the living moss layer by rainwater. Especially at deep water tables, when capillary moisture supply to the living moss layer is limited, the direct supply of rainwater may be crucial for peatmoss growth (Nijp *et al.*, 2014; Robroek *et al.*, 2009). A second assumption made in many models is that the peat moss surface remains at the same vertical position throughout the growing season. Previous work has shown that vertical movement of the peat surface with the groundwater table may be an additional feedback mechanism that reduces summer drought stress in undisturbed peatlands (Fritz *et al.*, 2008; Kennedy & Price, 2005; Roulet, 1991; Waddington *et al.*, 2010).

The aim of this modelling study was to determine the impact of including hydrological complexity on predictions of peatmoss drought in northern peatlands for current and future climate. Using field data from a northern peatland for model calibration and validation, we systematically tested whether sequentially increasing hydrological complexity by including peat volume change or moss water storage significantly improved model performance. To further test the effect of hydrological complexity on the impact of climate change projections, we compared simulated drought impact among four models, varying in degree of hydrological complexity using an ensemble of downscaled climate change projections.

5.2 Model description

5.2.1 General approach

We developed four variants of a model to evaluate the importance of hydrological model complexity in predicting water availability for peatmosses throughout a growing season in ombrotrophic peatland ecosystems. A reference model (M^0V^0) was expanded by including peat volume change (M^0V^1), moss water storage (M^1V^0), or the combination of both (M^1V^1). With the aim to restrict calculation time, the flow system is in all

model variants represented by three interacting water storage reservoirs: a groundwater reservoir, the living moss layer, and a ponding reservoir (Fig. 5.1). In the M^0 variants, the water content in the living moss layer is merely a function of the groundwater table, while in the M^1 variants the moss water storage was included explicitly as an additional state variable, allowing for retention of rainwater by peatmoss (Fig. 5.1, Section 5.2.2).

The flow domain was defined by a vertical column of homogeneous peat at a single point in space in a natural ombrotrophic peatland (i.e. roughly 1 – 10 m^2) in all model variants. As peat deposits are frequently underlain by an impermeable layer (Rydin & Jeglum, 2013), no water could enter the peat profile from beneath (no flow bottom boundary condition). The lateral hydraulic gradient can be assumed to be uniform at the spatial scale we consider (1 – 10 m^2). Hence, lateral water flow was not included in the model structure. Below we provide an overview of model formulations, considerations and assumptions.

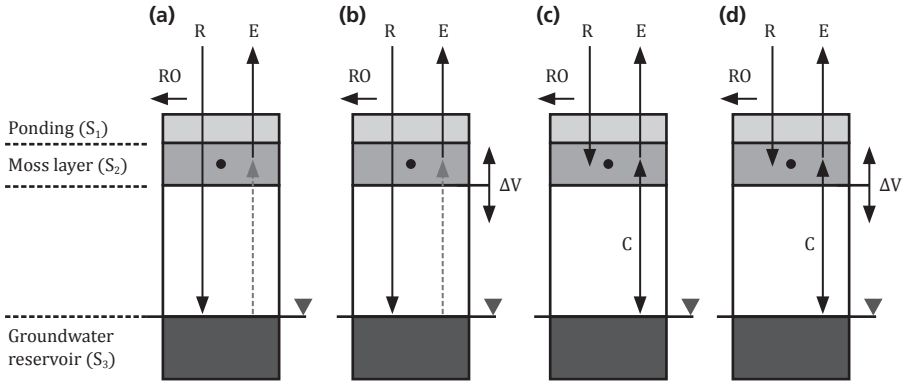

Figure 5.1. *Conceptual overview of the four model variants differing in complexity: (a) Reference model excluding moss water storage and peat volume change (M^0V^0); (b) only peat volume change is included (M^0V^1);v (c) only moss water storage are included (M^1V^0); (d) both peat volume change and moss water storage are included. R = rainfall, E = moss evaporation, RO = runoff, C = capillary flux, ΔV is peat volume change.*

5.2.2 Reference model & additions

5.2.2.1 Reference model

In ombrotrophic peatlands, changes in the groundwater table (GWT (cm); negative if beneath the peat surface) mainly originate from rainfall (R; cm d^{-1}) and actual moss evaporation (E_a; cm d^{-1}) (Fig. 5.1). As peatlands are wet ecosystems it is not uncommon for the groundwater table to be located above the peat surface. Up to a threshold ponding

depth, this water is stored in a ponding reservoir, where it may evaporate. If the threshold is exceeded, the water is assumed to laterally run off (Q_{RO}) (Appels *et al.*, 2011). The changes in water table of this groundwater system can be written as

$$\frac{dGWT}{dt} = \frac{R(t) - E_a(t) - Q_{RO}(t)}{S_y} \tag{5.1}$$

Here, the specific yield (S_y) is a coefficient controlling the storage capacity of the groundwater reservoir and resembles the drainable porosity. In all model variants, actual evaporation (E_a) was calculated from potential evapotranspiration from a reference crop (ET_o; see Section 5.2.5.3) in two steps. First, ET_o was linearly transformed to potential evapotranspiration from the peat surface (ET_p) by multiplying ET_o with a static crop coefficient (K_c). Next, actual evaporation was calculated by multiplying ET_p with an empirical moisture reduction function (f_{VWC}) to account for reduction of ET_p due to limited water availability

$$f_{VWC} = \frac{\alpha_E \left(\frac{\theta - \theta_r}{\theta_s - \theta_r}\right)^2 + \beta_E \left(\frac{\theta - \theta_r}{\theta_s - \theta_r}\right)}{E_{max}} \tag{5.2}$$

where α_E and β_E are regression coefficients (cm d^{-1}) and were obtained experimentally (See Appendix 5.1 for details). E_{max} is a scaling (cm d^{-1}) parameter to guarantee the moisture reduction function scales between zero and one. Taking all factors into account, actual moss evaporation was calculated as

$$E_a = f_{VWC}\, K_c\, ET_o \tag{5.3}$$

In the reference model the moss water content was in hydrostatic equilibrium with the groundwater table. The moss water content could then be estimated as a function of the groundwater table, which was the only state variable in the reference model (Table 5.1). Here, we used the frequently applied water retention curve formulation by Brooks & Corey (1964) (Eq. 5.4) as it yields an efficient closed-form solution for the matric flux potential (See Eq. 5.10).

$$\theta(h) = \begin{cases} (\theta_s - \theta_r)\left(\frac{h}{h_b}\right)^{-\lambda} - \theta_r & if \quad h \le h_b \\ \theta_s & if \quad h > h_b \end{cases} \tag{5.4}$$

where h is the suction pressure in the living moss layer (cm), $\theta(h)$ is the volumetric water content (VWC) in the living moss layer ($cm^3\ cm^{-3}$), θ_s is the saturated VWC, θ_r is the residual VWC, λ is a dimensionless shape parameter, and h_b the air entry value (cm), the suction pressure that must be exceeded before air enters the pores. In all model variants the living moss layer was represented by a single storage reservoir and its water

content was calculated at the centre of the moss layer. Furthermore, all model variants required groundwater storage as state variable.

Table 5.1. *Overview of main differences between model variants, originating from model formulations of change in groundwater table and of moss water content. The model code represents model variant: M^0 and M^1 indicate whether moss water content is excluded or included as state variable while V^0 and V^1 show if peat volume change is excluded or included.*

Model complexity	Code	Groundwater table change	Moss water content change
Reference model	M^0V^0	$\frac{R(t) - E_a(t) - Q_{RO}}{S_y}$	Function of water table (Eq. 5.4)
Reference + peat volume change	M^0V^1	$\frac{R(t) - E_a(t) - Q_{RO}}{S_y + S_s\, b(t)}$	Function of water table (Eq. 5.4)
Reference + moss water storage	M^1V^0	$\frac{q}{S_y}$	$q + I - E_a$
Reference + peat volume change + moss water storage	M^1V^1	$\frac{q}{S_y + S_s\, b(t)}$	$q + I - E_a$

R: Rain (cm d^{-1}), E_a: Actual moss evaporation (cm d^{-1}), Q_{RO} : Runoff (cm d^{-1}), S_y: Specific yield (-), S_s: Specific storage (cm^{-1}), b: Aquifer thickness (cm), q: Capillary flux (cm d^{-1}).

5.2.2.2 Adding peat volume change

The reference model described above was extended with peat volume change by including peat thickness as additional dynamic system state (in the models M^0V^1, M^1V^1). Changes in peat volume may originate from oxidation, primary consolidation, secondary compression, and shrinkage (Kennedy & Price, 2005; Schothorst, 1977). Furthermore, seasonally produced methane may become entrapped in a confining layer, providing buoyancy and resulting in floatation of the peat material above (Strack *et al.*, 2006). Observations in a natural undrained northern peatland suggest, however, that primary consolidation explained about 90% of total peat volume change over the growing season (Kennedy & Price, 2005). In this study, peat volume change was therefore represented by primary consolidation. Primary consolidation of the peat matrix originates from changes in effective stress in the saturated zone, which is modified by pore-water pressure fluctuations during the growing season (Kennedy & Price, 2004; Terzaghi, 1943). Upon drying, overlying weight of material above the surface of a peat cross-section exerts pressure on the contact points between the separate peat fibers in the peat matrix (skeleton). As a consequence the effective stress increases, causing the peat matrix to compress. Primary consolidation occurs in the saturated zone and

in vertical direction only, and was assumed to be fully reversible in the pressure range prevailing in typical field conditions in northern peatlands.

In compressible soils, such as peat soils, the total aquifer storativity (S_t) consists in addition to water storage due to water level change (S_y), of an elastic storativity component (S_e), which is the vertically specific storage (S_s; cm^{-1}) integrated over the aquifer thickness (b; cm). Total aquifer storativity then becomes

$$S_t = S_y + S_e = \ S_y + S_s\, b(t) \tag{5.5}$$

Within the range of hydraulic pressure changes found in peatlands the specific storage is a function of the compressibility (change in thickness due to change in effective stress) of the peat matrix only (Schlotzhauer & Price, 1999). Including the elastic storage component in Eq. 5.1 results in

$$\frac{dGWT}{dt} = \frac{R(t) - E_a(t) - Q_{RO}}{S_y + \ S_s\, b(t)} \tag{5.6}$$

From Equation 5.6 it follows that larger compressibility S_s, or larger peat thickness b, increases peat surface fluctuations, thereby stabilizing the groundwater table relative to the peat surface. Peat volume change is included in the model structure by replacing Equation 5.1 with Equation 5.6, which requires one more parameter and an additional state variable.

5.2.2.3 Adding moss water storage

In the model variants in which moss water storage was explicitly included as state variable (i.e. M^1V^0 and M^1V^1; Fig. 5.1b,d), rainwater first infiltrated into the moss layer, and dependent on water content and depth of the water table was partially transported to the groundwater reservoir. Only the amount of water that saturated the moss layer infiltrated

$$I = \begin{cases} R - E_a & if \quad \Delta t\ (R - E_a) < S_{max} - S \\ \dfrac{S_{max} - S}{\Delta t} & if \quad \Delta t\ (R - E_a) \geq S_{max} - S \end{cases} \tag{5.7}$$

Here, I is the infiltration rate ($cm\ d^{-1}$), S and S_{max} are current and maximum water storage in the moss layer (cm; water content θ · moss layer thickness D) and Δt the time interval (d). Water exceeding the maximum moss storage capacity was stored aboveground in the ponding reservoir, similar to the reference model. Because of the high saturated hydraulic conductivity of the living peatmoss layer (Table 5.2), infiltration excess ponding (i.e. ponding due to limited infiltration capacity) was ignored. Dependent on water retention, infiltrated rainwater was partially retained in the living moss layer, and

partially drained to the groundwater. Water transport between the groundwater reservoir and the living moss layer was controlled by gravitational and capillary forces. The sum of these forces controlled the direction and rate of water flow, which was described with the one-dimensional vertical form of the Darcy Buckingham equation for unsaturated flow

$$q = -K(h)\left(\frac{dh}{dz} + 1\right) \tag{5.8}$$

Here, q is the capillary flux between the moss layer and groundwater reservoir ($cm^3\ cm^{-2}\ d^{-1}$; negative if outflow from moss layer). As with drying less pores contribute to water flow, the hydraulic conductivity is strongly dependent on suction pressure in the moss layer. We employed the relative conductivity function, K(h), introduced by Brooks & Corey (1964)

$$K(h) = \begin{cases} K_s\left(\frac{h_b}{h}\right)^{K_a + K_b\,\lambda} & if \quad h \le h_b \\ K_s & if \quad h > h_b \end{cases} \tag{5.9}$$

Here, K_s ($cm\ d^{-1}$) is the saturated hydraulic conductivity and K_a and K_b are dimensionless shape parameters. The relative hydraulic conductivity function is coupled to the Brooks-Corey water retention function (Eq. 5.4) via the λ and h_b parameters. The value of $K(h)$ represents the average hydraulic conductivity of the unsaturated zone between the groundwater table and the node in the living moss layer. Due to the high non-linearity of the relative hydraulic conductivity function $K(h)$, averaging of $K(h)$ may produce large errors in flux estimates (An & Noh, 2014; Haverkamp & Vauclin, 1979; Warrick, 1991). A numerically convenient form of the transport equation (Eq. 5.8), circumventing averaging complications, is the integral of the hydraulic conductivity over the full pressure potential range

$$M = \int_{-\infty}^{h_{GWT}=0} K(h)\,dh \tag{5.10}$$

where M is referred to as the matric flux potential ($cm^2\ d^{-1}$) (Raats, 1972). By adopting the matric flux potential approach, Eq. 5.8 can be rewritten as

$$q = -\left(\frac{dM}{dz} + \frac{dM}{dh}\right) \tag{5.11}$$

where the first term on the right hand side represent the capillary component and the second term the gravitational component. Fluxes in Eq. 5.11 were positive if the flow direction was towards the living moss layer. Moss water storage (S_{moss}; cm) changes were calculated as the sum of the capillary flux, infiltration and actual evaporation (Eq. 5.12).

$$\frac{dS_{moss}}{dt} = q + I - E_a \quad (5.12)$$

Groundwater storage change over time was calculated with Eq. 5.13 in case peat volume change is excluded (M^1V^0).

$$\frac{dGWT}{dt} = \frac{-q}{S_y} \quad (5.13)$$

In the model structures that included both moss water storage and peat volume change (M^1V^1), the denominator also contained the elastic storage term (S_e ; Table 5.1).

5.2.3 Model implementation

5.2.3.1 Numerical integration scheme

The differential equations of water table and moss water content were solved numerically using an explicit Euler forward numerical integration scheme in the Ventana Simulation Environment (Vensim DSS double precision 5.01c, Ventana Systems Inc., Harvard, USA). The optimal integration time step was identified by decreasing its value until no effect on simulated water content could be distinguished and no numerical instability occurred as checked with the Courant number ($Cr = q\ \Delta t/\Delta z$). All model simulations were performed with an integration time step of 2^{-13} days ($\approx$ 11 seconds). Closure of the water balance, individual water balance terms and simple test cases were used to verify numerical code implementation.

5.2.3.2 Initial and boundary conditions

All state variables required initialization. The measured groundwater table at the start of the simulation was used as initial condition, while the initial moss water content was estimated from the groundwater table using the water retention function assuming hydrostatic equilibrium. For the model variants including peat volume change, an initial peat thickness is provided using measured peat thickness (See Section 5.2.5.2). All model variants require only rainfall and potential evapotranspiration from a reference crop (ET_o) as input variables, defining model boundary conditions.

5.2.4 Model parameterization

Model parameters were derived from a combination of field experiments and laboratory experiments using samples from Degerö Stormyr (Table 5.2; See Appendix 5.1 for a detailed description of the experiments and calibration procedure used to parameterize the model). The parameters of the water retention curve (Eq. 5.4) were derived from a laboratory experiment using the sandbox method (Klute, 1986). An evaporation experiment with *Sphagnum* cores was used to determine the moisture reduction function

(Eq. 5.2; See Appendix 5.1 for more details). The specific storage, the only parameter describing peat volume change, was quantified using field data on peat volume and water table (See Section 5.2.5.2). The elastic storage coefficient was estimated as the slope of the peat thickness versus groundwater head relation (Nuttle *et al.*, 1990) for all data points

$$S_e = b\,S_s = \frac{dV}{db} \tag{5.14}$$

The specific storage was obtained by division of the elastic storage coefficient by aquifer thickness b. No parameter values were available for the crop coefficient (K_c), specific yield (S_y) and the K_a and K_b shape parameters in the hydraulic conductivity function (Eq. 5.9). These parameters were calibrated for the most complex model variant (M^1V^1) using the time series of water content, water table and peat thickness.

5.2.5 Model evaluation

5.2.5.1 Site description

The four models were validated and calibrated using observations from a field setup in Degerö Stormyr (64°11'N, 19°33'E), a 6.5 km^2 minerogenic, oligotrophic mixed peatland complex in northern Sweden, approximately 70 km inland from the Gulf of Botnia. The peatland type studied here is common in large parts of the northern hemisphere (Nilsson *et al.*, 2001; Riley, 2011). The peat deposit has a thickness up to 8 m but generally ranges between 3 – 4 m. The deepest peat layers correspond to a basal age of about 8000 years (Nilsson *et al.*, 2008). The peat is underlain by a heterogeneous pattern of relatively impermeable mineral glacial till and acidic gneissic bedrock (Malmström, 1923).

Two homogeneous ombrotrophic lawn sites (> 5 · 5 m), 360 m apart from each other, were selected with > 60% *Sphagnum balticum* cover and < 10% vascular plant cover (Table 5.3). We focussed on lawns because this is the dominant vegetation type in this particular peatland. Moreover, as the lawn represents the ecotone between drier hummocks and wetter hollows, shifts in habitat quality of this specific habitat indicate possible future shifts in species dominance. The remaining cover consisted of other *Sphagnum* species (mainly *S. lindbergii*, *S. majus*, *S. papillosum*, *S. tenellum*). Vascular plant cover consisted predominantly of *Eriophorum vaginatum*, *Vaccinium oxycoccos*, *Andromeda polifolia* and *Rubus chamaemorus*.

5.2.5.2 Hydrological measurements

At both sites the groundwater table, peatmoss water content and peat surface position were measured from 2 July 2012 – 3 September 2012. A fixed reference height was established by anchoring the equipment into the underlying mineral soil. Between two

Table 5.2. *Parameters employed in the four models. The columns M^1 and V^1 indicate parameters unique for models variants that include moss water storage (M^1) or peat volume change (V^1).*

Symbol	Value	Unit	Description	Source	M^1	V^1
Brooks-Corey water retention function						
θ_{sat}	0.975	$m^3\ m^{-3}$	Saturated water content	Sand box experiment		
θ_{res}	0	$m^3\ m^{-3}$	Residual water content	Sand box experiment		
λ	0.28	-	Shape factor	Sand box experiment		
h_b	-0.005	m	Air entry value; suction pressure air at which air enters the peat matrix	Sand box experiment		
Brooks-Corey relative conductivity function						
K_s	$1.5{\cdot}10^{-3}$	$m\ s^{-1}$	Saturated hydraulic conductivity	Modified permeameter	x	
K_a	1.0031	-	Shape factor in conductivity function (Eq. 5.9)	Calibrated	x	
K_b	0.0001	-	Shape factor in conductivity function (Eq. 5.9)	Calibrated	x	
Evaporation						
K_c	1.50	-	Crop factor; transforms potential evapotranspiration from reference crop to potential moss evaporation	Calibrated		
α_E	-0.171	-	Shape factor in moisture reduction function	Evaporation experiment		
β_E	0.416	-	Shape factor in moisture reduction function	Evaporation experiment		
E_{max}	0.245	$mm\ d^{-1}$	Normalization constant to scale moisture reduction function in the [0,1] domain.	Evaporation experiment		
Groundwater storativity						
S_y	0.38	-	Specific yield	Calibrated		
S_s	$2.0{\cdot}10^{-6}$	m^{-1}	Specific storage	Field data		x
Model parameters						
D_1	0.10	m	Moss layer thickness			
Δt	10.55	s	Time step in numerical integration			
rnd	0.50	-	Relative node depth			

iron tubes, a 1 m wide aluminium bar was installed, in which a magnetostrictive position sensor (MTS Linear Position Sensor Type CM250AVH2, MTS Sensor Technologie, Lüdenscheid, Germany) was mounted (See Appendix 5.2). On top of a light-weight PVC construction with a thin PVC plate resting on the peat surface, a magnet was

attached which moved along the rod of the linear position sensor. A change in peat surface position adjusted the distance between the magnet and the magnetostrictive sensor element, which was recorded and logged on a Campbell CR1000 data logger.

Depth of the absolute groundwater table (relative to the underlying mineral soil) was measured with groundwater level loggers (Diver type DI220, Van Essen Instruments, Delft, The Netherlands), placed in perforated groundwater monitoring tubes. A nylon filter cloth was wrapped around the perforated section (20 – 70 cm below peat surface) to prevent clogging and smearing of the perforated holes. As the water pressure logger signal consisted of variations in both groundwater table and air pressure, air pressure variations were removed to obtain a groundwater level time series.

Table 5.3. *General information of the two validation sites in Degerö Stormyr. Distance to stream is the Euclidian distance between the site location and the Vargstugbäcken stream, which drains about 69% of the mire (Nilsson et al., 2008).*

Site	1	2
Initial peat thickness (m)	4.89	6.01
Distance to stream (m)	1100	1400
VWC range (cm^3 cm^{-3})	0.63 – 0.97	0.82 – 0.97
GWT range (cm)	-10.5 – +1.5	-7.8 – -0.32
PT range (cm)	481.8 – 483.7	612.0 – 616.6
Period 1 usage	Calibration	Temporal validation
Period 2 usage	-	Spatial validation

The volumetric water content of the living *Sphagnum balticum* moss layer was measured with EC5-H_2O moisture sensors (Decagon Devices, Pullman, USA) installed at a depth of 5 cm, representative for the top 3 – 7 cm (Cobos, 2008) of the peat profile. The sensor voltage output was transformed to a volumetric water content using a species-specific calibration curve (Nijp *et al.*, 2014). A considerable range in moisture conditions was obtained during the validation period (See Appendix 5.3; Table 5.3).

5.2.5.3 Meteorological measurements

The model forcing data consisted of rainfall and reference evapotranspiration in all model variants. Meteorological data were obtained from the meteorological station in the centre of Degerö Stormyr. Rainfall was measured during April – October with a tipping-bucket rain gauge (ARG 100, Campbell, Scientific, Logan, Utah, US, 0.2 mm resolution) at 10 min frequency, 4 m away from the eddy-covariance tower. Rain measurements were corrected for a 10% systematic underestimation of tipping bucket measurements following Eriksson (1983).

Reference potential evapotranspiration of 0.12 m high grass (ET_o) was estimated with the Penman-Monteith formulation as proposed by Penman (1948) and Monteith (1965). Calculation of ET_o requires input of net radiation (R_n, MJ m^{-2}), wind speed (ws, m s^{-1}), mean daily temperature (T, °C) and vapour pressure deficit ($e_s - e_a$, kPa). The latter was derived from relative humidity measurements. Mean daily ET_o (mm d^{-1}) is calculated following FAO standards (Allen *et al.*, 1998) as

$$ET_o = \frac{0.408\,\Delta(R_n - G) + \gamma \cdot ws \cdot \frac{c_n}{T + 273} \cdot (e_s - e_a)}{\Delta + \gamma(1 + c_d \cdot ws)} \qquad (5.15)$$

where Δ is the slope of the saturation vapour pressure versus temperature curve (kPa K^{-1}), G the sensible ground heat flux between soil and atmosphere (MJ m^{-2}), e_s the saturation vapour pressure (kPa), e_a the actual vapour pressure (kPa), and γ the psychrometric constant (kPa K^{-1}). The value of the coefficient c_n depends on time step (hourly or daily) and aerodynamic roughness, while the value of c_d depends on time step, bulk surface resistance and aerodynamic roughness (ASCE-EWRI, 2005). G was set to zero for calculating daily ET_o rates (Climate scenarios, Section 5.2.6). To calculate half-hourly ET_o rates (Model validation and calibration), the daytime (defined as $R_n > 0$) and night-time ground heat flux were estimated as $0.1 \cdot R_n$ and $0.5 \cdot R_n$ following the recommendation by Allen *et al.* (2006).

Net radiation was measured using an NR-Lite sensor (Kipp & Zonen, Delft, the Netherlands) mounted at the top of a 4 m tower. Air temperature and relative humidity were measured with an MP100 moisture sensor (Rotronic AG, Bassersdorf, Switzerland) inside a self-ventilated radiation shield. Wind speed was measured 1.8 m above the peat surface with a three-dimensional sonic anemometer (model 1012R2 Solent, Gill Instruments, UK). All environmental variables were averaged to 30 minute average values.

5.2.5.4 Validation

The model structures were validated by comparing simulations with time series of volumetric water content of the moss layer, groundwater table and peat volume from two ombrotrophic sites in a peatland complex in northern Sweden. The time series of the first site (Site 1) was divided in two continuous periods (Table 5.3), where the first half was used for model calibration (See Appendix 5.1 for more details) and the second period to validate the temporal transposability of the model. To test the spatial transposability of the four model variants, the parameters obtained from Site 1 (See Table 5.2) were used to simulate volumetric water content, groundwater table and peat thickness at Site 2, using boundary conditions during period 2.

In both validation experiments, measured half-hourly rainfall and actual evapotranspiration estimated from meteorological variables (See Section 5.2.5.3) were used as forcing data. Values of coefficients c_n and c_d in Eq. 5.12 were adapted for hourly ET_o cf Allen *et al.* (2006). The first measured values of water content, water table and peat thickness within the time series were used as initial conditions for the simulations per site. The root mean square error of prediction (RMSEP) was used as measure for (absolute) model performance with respect to each individual state variable

$$RMSEP = \sqrt{\frac{1}{n}\sum_{i=1}^{n}(O_i - S_i)^2} \tag{5.16}$$

where O_i and S_i are observations and simulations at times i from $1 \ldots n$. To quantify overall model performance, the *RMSEP's* of the three state variables were normalized by the range and subsequently averaged

$$NRMSEP_{OVERALL} = \frac{1}{3}\sum_{j=1}^{3}\frac{RMSEP}{O_{max,j} - O_{min,j}} \tag{5.17}$$

where $O_{max,j}$ and $O_{min,j}$ are the maximum and minimum observed values for state variable j.

5.2.5.5 Comparing model performance

Model performance was quantified with the *NRMSEP* (Eq. 5.17), where an *NRMSEP* of zero indicates a perfect match between simulations and observations and larger *NRMSEP* values indicate that the mean prediction error is more similar to the observed measurement range. To test whether additional hydrological processes significantly improved model performance, we tested the formal null-hypotheses that extra parameters in more complex model structures significantly reduced the prediction error of a simpler model using likelihood ratio tests (Lewis *et al.*, 2011).

To further facilitate model selection we calculated an overall Akaike Information Criterion (AIC; Akaike, 1973) for each model to check if additional hydrological processes reduced prediction error, while penalizing for additional parameters. For a single variable, the AIC can be calculated from the sum of squared differences between simulations (S_i)and observations (O_i) as

$$AIC = n\, ln\left(\frac{1}{n}\sum_{i=1}^{n_i}(O_i - S_i)^2\right) + 2\,K \tag{5.18}$$

where n is the number of observations and K the number of parameters (Burnham & Anderson, 2001). Next, the overall AIC was calculated by summing the range-

standardized squared differences for all three variables j and correcting for the total number of observations

$$AIC_{OVERALL} = 3\,n\,ln\left(\sum_{j=1}^{3}\frac{1}{3\,n}\sum_{i=1}^{n}\left(\frac{O_{ij}-S_{ij}}{O_{ij,max}-O_{ij,min}}\right)^2\right)+2\,K \qquad (5.19)$$

The model with lowest AIC is the optimal model given the empirical data, although simpler models deviating ≤ 2 AIC may perform equally well (Burnham & Anderson, 2001).

5.2.6 Climate change impact assessment

5.2.6.1 Regional climate projections

After assessing the performance of the different model variants, it was checked to what extent hydrological complexity affects drought impact projections in a future climate. Climate simulations were downloaded from the ENSEMBLES project database (Van der Linden & Mitchell, 2009). An ensemble of 15 different regional climate model (RCM) projections for daily rainfall and potential evaporation was created for current (1991 – 2020) and future climate (2061 – 2090). All RCM projections were based on the A1B scenario in the IPCC Special Report on Emissions Scenarios (Nakicenovic *et al.*, 2000). Rainfall time series were used directly as provided in the database. Potential evaporation on the other hand was calculated with the Penman-Monteith formulation (Eq. 5.15) based on net radiation, wind speed, daily mean air temperature, relative humidity and air pressure, which were all provided by the ENSEMBLES data archive (Van der Linden & Mitchell, 2009).

For all variables, values were obtained from the RCM grid cell with centre coordinates closest to the study site. However, the employed RCMs had a grid resolution of 25 km and, thus, the area of a single grid cell clearly exceeded the size of the study catchment. This spatial mismatch in combination with systematic model errors (Teutschbein & Seibert, 2012) provided biased representations of observations during a 12 year period from Degerö Stormyr (2001 – 2012) (Fig. 5.2). Therefore, we applied a bias correction procedure (Ehret *et al.*, 2012; Teutschbein & Seibert, 2013) using the distribution scaling method (Block *et al.*, 2009; Piani *et al.*, 2010), which is based on the idea to adjust the fitted theoretical cumulative distribution functions (cdfs) of RCM-simulated climate values to match the observed cdfs. We assumed the Gamma distribution to be suitable for precipitation events (Watterson, 2003). For potential evaporation, the best fitting theoretical cdf depended on the season and was therefore determined with χ^2 tests separately for summer (May – Aug), winter (Dec –Jan) and shoulder seasons

(March, April, September, October). Gaps in the observed time series were filled using a seasonal regression relationship or with data from a nearby (1 km) meteorological station (rainfall) (Peichl *et al.*, 2014). We further assumed that the median of all ensemble projections corresponds to the most likely climate change scenario.

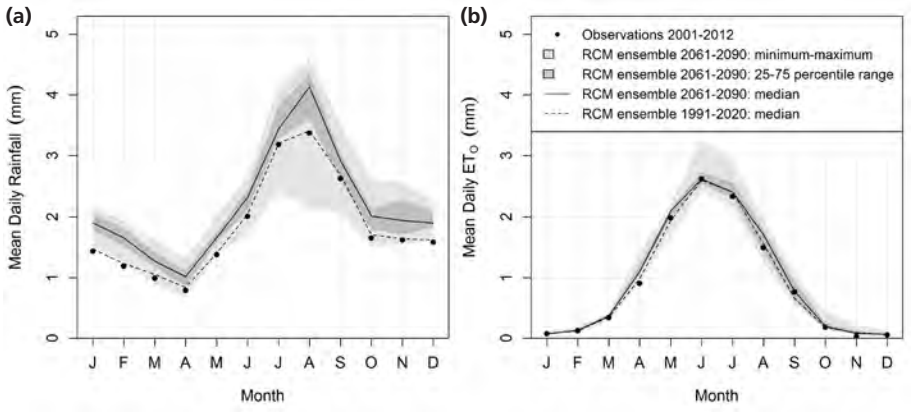

Figure 5.2. *Downscaled, bias-corrected mean daily rainfall (a) and mean daily potential reference evapotranspiration (ET_o; b) based on 15 different regional climate models (RCMs). ET_o was calculated with the Penman-Monteith equation based on climate variables from the RCMs. The black circles are observed values for the period 2001 – 2012, the dashed line the bias corrected RCM median for current climate (1991 – 2020). For the future climate (2061 – 2090), the continuous line represents the bias-corrected RCM median, the light shaded area the minimum-maximum range of all 15 RCMs, the dark shaded area the 25th – 75th percentile range.*

The resulting downscaled, bias-corrected climate projections indicated that mean growing season length is projected to increase with about one month and mean temperature increased with 1.3 °C (Table 5.4). Total rainfall during the growing season was projected to increase more than potential evapotranspiration, resulting in a larger rain surplus (Table 5.4; Fig. 5.2).

The bias-corrected climate projections were used as forcing variables to simulate mean daily water content throughout the growing season for all *model variant (4) · year (60) · climate ensemble member (15)* combinations. The growing season start and end were defined as the first day of a 5 day period of which the mean temperature is > 5 °C or < 5 °C. Assuming the growing season started at the time all melting water was discharged, the initial groundwater level of all simulations was at the peat surface and the water content at saturation. For these simulations we used an initial peat thickness of 5 meter, representative for the calibration site.

5.2.6.2 Defining peatmoss drought stress

In this study a drought was defined as the time period during which the volumetric water content (VWC) drops below a threshold of 0.49 cm^3 cm^{-3}. This threshold corresponds to the VWC at which photosynthetic efficiency of *Sphagnum balticum* decreases sharply and photosynthesis practically ceases (Nijp *et al.*, 2014).

We used drought frequency, mean drought length and mean drought severity to characterize drought for each growing season, to check for differences between model variants and climate periods. Drought frequency was calculated as the number of drought events per simulated growing season; mean drought length by summing the duration of all drought periods and dividing by the number of droughts; mean drought severity (D_s) was quantified as the time averaged moisture deviation from the drought threshold (during drought), averaged over all drought events m

$$D_s = \frac{1}{m}\sum_{j=1}^{m}\left(0.49 - \frac{1}{t_{tot}}\sum_{i=1}^{n}\theta_i\,\Delta t_i\right) \qquad (5.20)$$

where t_{tot} is the drought length of the event, θ_i the water content at time i, and Δt the time period. To test whether differences between model variants and climates were significantly different, we set up an analysis of variance (ANOVA) with model variant and climat period as fixed factors and three drought indicators as dependent variables. We checked for normality and homoscedasticity to validate ANOVA assumptions.

Table 5.4. *Overview of mean growing season characteristics (± 95% confidence intervals) for current and future climate projections.*

Variable	Unit	Current climate (1991 – 2020)	Future climate (2061 – 2090)
Growing season length	days	141 ± 2	174 ± 2
Temperature	°C	11.5 ± 0.09	12.8 ± 0.1
Sum rainfall	mm	366 ± 9	461 ± 11
Sum potential evapotranspiration	mm	263 ± 3	306 ± 4
Sum potential rainfall surplus	mm	103 ± 10	155 ± 13

5.2.7 Sensitivity analysis

We set up a univariate sensitivity analysis to test how the predicted number of drought days (n_d) changes as function of model parameter values p. The parameter range was chosen as plus and minus 50% of the calibrated parameter, except for saturated and residual water content (See Appendix 5.4 for parameter sensitivity ranges). We selected the 10 years of current climate for which the time averaged VWC during the drought

sensitive period (DOY = 165 and 205) was closest to the defined drought threshold of 0.49 cm^3 cm^{-3}. For these years the sensitivity to drought is most relevant. First, a response curve of number of drought days n_d as function of parameter values p was obtained. Next, the elasticity at parameter value i was calculated as the first-order numerical derivative of the response curves at $i = 1 \ldots 30$ equidistant parameter values in the specified range. To compare the effect of parameter changes on n_d, this numerical derivative was standardized by multiplying with the factor p/n (Janssen, 1994)

$$E(p)|_i = \frac{p_i}{n_{d,i}} \frac{\Delta n_{d,i}}{\Delta p_i} = \frac{p}{n_d} \frac{n_{d,i+1} - n_{d,i-1}}{p_{i+1} - p_{i-1}} \tag{5.21}$$

The elasticity at the parameter value used in the model is hereafter referred to as local sensitivity. The inter-quartile range (75% percentile – 25% percentile) of calculated elasticities provides an estimate of elasticity in regions of the parameter space beyond the parameter value used in the model, and is referred to as global sensitivity.

5.3 Results

5.3.1 Effect of hydrological complexity on model performance

Model performance was assessed in terms of temporal transposability by comparing simulated volumetric water content (VWC), groundwater table (GWT) and peat thickness (PT) with observations for Site 1 during period 2, while period 1 had been used to calibrate parameter values. Sequentially increasing hydrological complexity improved overall model performance, as indicated by the decreased overall normalized root mean square error of prediction (NRMSEP) (Table 5.5) and significant differences between model variants (Table 5.6). Accordingly, the model structure including both moss water storage and peat volume change (M^1V^1) has highest model performance and was able to capture the dynamics in volumetric water content, groundwater table and peat thickness throughout the growing season (Appendix 5.3). The largest reduction of prediction error was achieved by including moss water storage in the model structure (Table 5.5).

Although overall model performance was considerably lower at validation Site 2, indicating low spatial transposability, the ranking of the model performance of the four models was identical to that for calibration Site 1. Overall model performance was highest for the most complex model (NRMSEP = 0.26, indicating that the mean prediction error equals 26% of the measurement range).

Table 5.5. *Model performance of the four models for volumetric water content (VWC), groundwater table (GWT) and peat thickness (PT) for Site 1. The absolute model performance is presented by the root mean square error of prediction (RMSEP), the relative overall model performance with range-normalized RMSEP (NRMSEP = RMSEP/observed range), and overall AIC. For each variable the model complexity with largest performance is shown in bold. The overall model performance is provided with the overall NRMSEP, the average of all NRMSEP values per model complexity.*

Model complexity		Overall NRMSEP	Overall AIC	RMSEP		
				VWC ($cm^3\ cm^{-3}$)	GWT (cm)	PT(cm)
1	M^0V^0	0.27	-3571	0.15	2.5	0.4
2	M^0V^1	0.21	-4034	0.12	**1.8**	0.3
3	M^1V^0	0.16	-4810	**0.04**	2.2	0.4
4	M^1V^1	0.13	-5107	0.05	2.0	**0.2**

Table 5.6. *Likelihood ratio test results per state variable, to test the null hypotheses that the additional hydrological process and associated parameters in the more complex model significantly enhance model performance as compared to the simpler model. These tests are based on the parameterization site for the validation period. The column df shows the difference in number of parameters between the two models being compared, χ^2 is the likelihood ratio and P is the level of significance. For peat thickness, the likelihood ratio test for the comparison of M^0V^0 with M^1V^0 was not performed because peat thickness is not modelled but constant through time.*

Simpler model	Complex model	df	VWC		GWT		PT	
			χ^2	P	χ^2	P	χ^2	P
M^0V^0	M^0V^1	1	227	< 0.001	55	< 0.001	562	< 0.001
M^0V^0	M^1V^0	3	1283	< 0.001	68	< 0.001	-	-
M^0V^1	M^1V^1	3	942	< 0.001	86	< 0.001	151	< 0.001
M^1V^0	M^1V^1	1	-114	1	72	< 0.001	713	< 0.001

5.3.2 Effect of model complexity on drought projections

Increasing model complexity significantly decreased simulated drought length, drought severity, and number of droughts in the current as well as the future climate (Table 5.7; Fig. 5.3). Especially including moss water storage in the model structure resulted in a large reduction of simulated mean number of droughts per growing season (-42%), drought length (-45%) and drought severity (-48%). Including peat volume change did not reduce mean drought length but significantly decreased the number of droughts per growing season and drought severity (Fig. 5.3).

Projected climate change did not affect the simulated mean number of droughts per growing season and mean drought length, as was indicated by no significant difference

between the current and future climate (Table 5.7). Climate significantly modified drought severity, but the magnitude of the simulated future increase in mean drought severity of 0.003 m^3 m^{-3} is almost negligible. This suggests that, based on the employed climate projections, the future impact of drought on peatmoss growth will be similar to the impact in current climate.

Table 5.7. *Analysis of variance for projected drought length, drought severity and number of droughts with Model complexity and Climate as fixed factors. The Model variant × Climate interaction was excluded for drought length and number of droughts because the main effect of climate was not significant; the number of replicates was 30. Significant effects (P < 0.05) are indicated in bold; see Fig. 5.3 for pairwise comparisons.*

Variable	Factor	F	df	P
Number of droughts	Model variant	103.287	3	< **0.001**
	Climate	0.338	1	0.56
Drought length	Model variant	43.866	3	< **0.001**
	Climate	1.908	1	0.17
Drought severity	Model variant	131.607	3	< **0.001**
	Climate	4.765	1	**0.03**
	Model variant × Climate	1.085	3	0.35

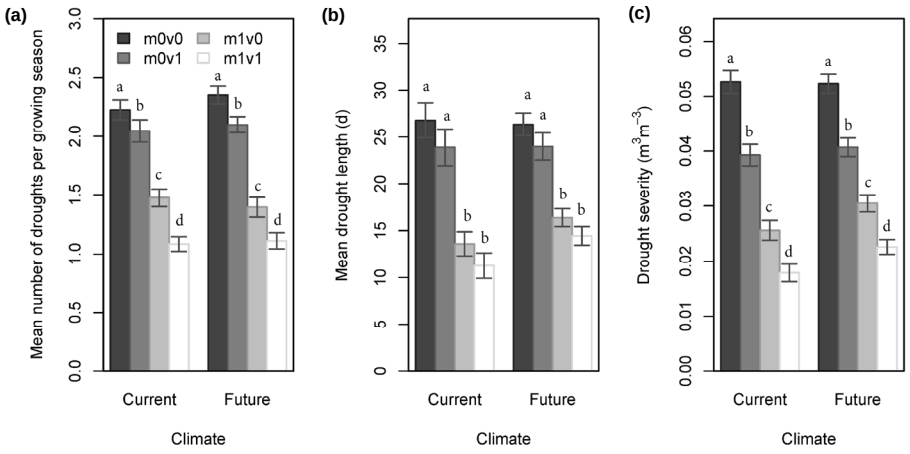

Figure 5.3. *Effect of climate (groups) and model variant (bar colours) on number of droughts (a), drought length (b) and drought severity (c). Characteristics represent mean values of the 30 simulated growing seasons per climate period. The effect of the factor regional climate model is eliminated by averaging the characteristics over all climate ensemble realizations for each year. Error bars represent one standard error and letters represent homogeneous subgroups of model variants (Benjamini-Hochberg corrected multiple comparisons); see Table 5.7 for significance of main and interaction effects.*

5.3.3 Sensitivity of drought projections to model parameters

The simulated number of drought days was influenced most by the saturated water content, the crop factor, and the λ shape parameter in the water retention function (Fig. 5.4, local sensitivity). The simulated number of drought days decreased with larger saturated water contents and increased with larger crop factors and larger λ (i.e. lower retention capacity). The processes related to these most influential parameters were moss evaporation and water retention.

In contrast, parameters associated with peat volume change (i.e. specific storage and peat thickness) had a small effect on the number of drought days. The parameters of the hydraulic conductivity function also have little impact on the simulated number of drought days. The λ shape parameter, which is also included in the water retention function, theoretically affects drought impact through altering unsaturated hydraulic conductivity. Within the employed parameter range, however, λ maximally increased K(h) with 0.0067%, demonstrating that the sensitivity to λ was mainly mediated by water retention characteristics.

The relatively low local sensitivity accompanied with large global sensitivity of θ_r and λ indicates that the sensitivity to those parameters will change if the values of these parameters change. For proper estimation of these parameters experiments are required to observe the range of values field conditions.

5.4 Discussion

5.4.1 Model performance increases with complexity

We showed that including peat volume change or moss water storage significantly improved model performance, and that model performance was best if both processes were included (Table 5.5). These results illustrate the importance of including peat volume change, moss water storage, and potentially also other ecohydrological feedbacks that may help to maintain high water content in the living moss layer during droughts. Peatlands as a whole are often regarded as self-regulating, complex adaptive systems (Belyea & Baird, 2006). It is likely that including more ecohydrological feedbacks results in an even larger stabilization of the water content and in a further enhancement of model performance. For example, at low water content the albedo may increase and reduce evaporative water losses (Waddington *et al.*, 2015) and vertical heterogeneity of soil physical properties may affect groundwater table dynamics through affecting e.g. lateral groundwater flow (Morris *et al.*, 2011; Waddington *et al.*, 2015).

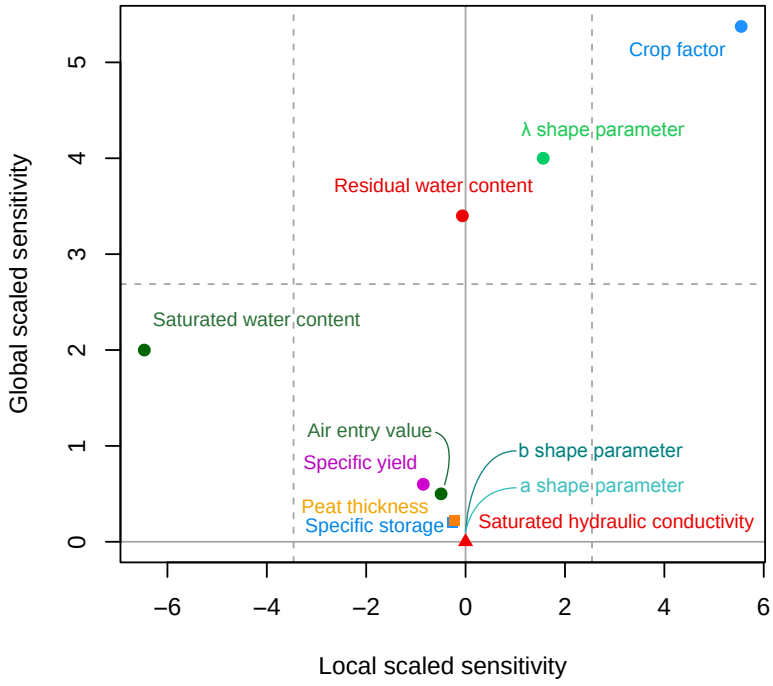

Figure 5.4. *Local and global scaled sensitivity of number of drought (VWC < 0.49 cm^3 cm^{-3}) days to relevant model parameters for the model variant with highest performance (M^1V^1). The local sensitivity (x-axis) represents the sensitivity of number of drought days to a change in parameter at the parameter value used in the model, where larger deviations from 0 indicate larger sensitivity of drought to this parameter. The global sensitivity (y-axis) indicates whether the sensitivity to a parameter varies within the pre-specified range of parameter values (Appendix 5.4), and is expressed as the interquartile range of sensitivity to a specific parameter (IQR; 75^{th} – 25^{th} percentile). A large global sensitivity indicates that parameter sensitivity depends on the parameter value itself. Sensitivity was calculated by dividing the change of number of drought days (Δn) by the change in parameter value (Δp) and multiplied by p/n to allow comparison among different parameters. Symbols represent different model variants and their included hydrological processes: ● = all models; ▲ = moss water storage variants only (M^1); ■ = peat volume change only (V^1). Only current climate projections (1991 – 2020) were used.*

Testing model performance for a second site within the studied peatland resulted in the same ranking of model performance. Here, the most complex model including peat volume change and moss water storage significantly outperformed models excluding peat volume change or moss water storage. Although the ranking remained the same, overall performance of all models decreased, suggesting limited spatial transposability of the predictions. The low model performance for the second site may originate from

1) differences in site characteristics as expressed by parameter values or 2) differences in hydrological processes between sites.

As demonstrated by the sensitivity analysis, the occurrence of droughts is most sensitive to the parameterization of moss evaporation and the water retention function (Fig. 5.4). It can therefore be anticipated that especially differences in peatmoss morphological traits (Luken, 1985; Rydin, 1993) and species identity are sources for spatial variation. While the species composition of the two validation sites was similar, the specific growth form and water retention capacity of peatmoss are highly variable and depend on local hydrological conditions (Luken, 1985; Rydin, 1995). The sensitivity analysis indicates that, with all other parameters being equal, a shift from lawn to hummock peatmoss species, which have higher water retention (Hayward & Clymo, 1982) (i.e. smaller λ shape parameter), likely reduces drought occurrence while a shift to hollow species would increase drought frequency. This finding is coherent with previously reported higher drought tolerance of hummock species relative to hollow species (Hájek & Beckett, 2008; Nijp *et al.*, 2014; Robroek *et al.*, 2007b).

The limited spatial transposability may also result from differences in leading hydrological processes among the two sites. Some of such processes are not included in our model structure and it remains to be tested whether including other ecohydrological processes further improves model performance. Especially processes that impact groundwater table depth may enhance model performance, considering the relatively poor fit of groundwater table as compared to the other variables (Appendix 5.3). Prospective processes that may improve the spatial transposability include for example lateral (sub) surface transport and spatial discretization (Endrizzi *et al.*, 2014; Spieksma *et al.*, 1996), or vertical heterogeneity of hydrophysical characteristics (Frolking *et al.*, 2010; Morris *et al.*, 2011).

5.4.2 Implications for future modelling

In this paper we provide a start in systematically testing the effect of model complexity in peatland hydrology models. By employing a working hypothesis testing procedure as outlined in this paper, other ecohydrological processes, such as those provided above and in an overview by e.g. Waddington *et al.* (2015), can be systematically evaluated for their impact on model performance and relevance for assessing climate change impact. In addition to testing whether additional processes enhance model performance, also the formulation (i.e. constitutive relations) of the various processes requires further systematic testing.

By doing so an integrated computationally efficient hydrological module applicable for peatlands in different ecohydrological settings can be developed. Comparing climate change impact among sites with different simulation models is obstructed by the impossibility to disentangle model effects from site effects. We therefore recommend to systematically test alternative representations of the hydrological component as working hypotheses on multiple peatland sites to define a computationally efficient and spatiotemporal transposable model before doing such impact assessments. Easily accessible long-term time series of volumetric water content from multiple peatland sites are of fundamental importance in these model comparisons, but are currently very scarce. The availability of such data can be improved by creating a citable, quality-controlled, open-access online database.

5.4.3 Increasing hydrological complexity reduces drought occurrence

In this study we demonstrate that drought occurrence is systematically overestimated if moss water storage and peat volume change are excluded from the model structure. Including peat volume change, and especially moss water storage, significantly decreased the number of drought days for the projected future climate (2061 – 2090) (Fig. 5.3). The frequency of droughts and consequently the number of wetting cycles are lower in the most complex model variant that includes both processes. This is likely advantageous for lawn peatmoss species, of which photosynthesis responds only slowly to rewetting (McNeil & Waddington, 2003; Nijp *et al.*, 2014; Proctor & Tuba, 2002).

The reduction in drought days was largest for the models that included moss water storage, illustrating the impact of these processes for moisture supply to the living moss layer. To explore the relative importance of these two mechanisms, we compared the response of moss moisture content to a rain event between the two model variants including (M^1V^1) and excluding (M^0V^1) moss water storage. Both models showed the same increase in moisture content after rain, suggesting differences between the models results from capillary water supply. The importance of including moss water storage is supported by the high sensitivity of the number of drought days to water retention function parameters (Fig. 5.4). Sensitivity analyses for the Holocene Peat Model indicated that peat physical characteristics play an important role in peat accumulation support this finding (Quillet *et al.*, 2013).

Including peat volume change in the model structure also significantly reduced the number of drought days as compared to the reference model. The elastic storage component increased total aquifer storativity with about 25%, buffering changes in

water table and therefore considerably boosting water content during droughts. The number of droughts turned out to be relatively insensitive to either specific storage or peat thickness (Fig. 5.4). Including peat volume change therefore seems more important than estimating accurate parameter values of specific storage or peat thickness.

The earth surface is rapidly warming, which is generally projected to have large impact on the hydrological cycle through less frequent but more intense rainfall, although the exact effect depends on the climate scenario and global circulation model considered (Allen & Ingram, 2002; Chen *et al.*, 2015; IPCC, 2013; Tebaldi *et al.*, 2006). We found no significant increase of the number of peatmoss droughts and drought length due to climate change for the used peatmoss species, climate scenario, regional climate model ensemble, and peatland in northern Sweden (Fig. 5.3; Table 5.7).

5.4.4 Implications of neglecting hydrological processes for ecosystem processes

Water content in the topsoil is one of the key controls on biogeochemical processes, greenhouse gas exchange and interactions between the land-surface and atmosphere. In this study we show that if moss water storage and peat volume change are neglected in climate change impact assessments for northern peatlands, drought occurrence is overestimated. This implies that the climate change impact on northern peatland ecosystem processes may be less severe than predicted in cases where these processes are omitted. Moreover, our results suggest that peatmoss drought occurrence will remain unmodified in similar climatic regions (classified as boreal climate cf the Köppen-Geiger classification system (Peel *et al.*, 2007)) with comparable climate change projections (IPCC, 2013). In these regions, where precipitation is expected to increase, other factors related to environmental change, such as decreased light availability (Letts *et al.*, 2005; Nijp *et al.*, 2015; Wild *et al.*, 2009), may be more important.

In conclusion, our results highlight the need for including moss water storage and peat volume change in peatland models to adequately assess climate change impacts on peatland hydrology and carbon sink strength of northern peatlands.

5.5 Acknowledgements

We thank Harm Gooren, Pieter Hazenberg, Henny Gertsen, and Pernilla Löfvenius for their help with data loggers, preparing samples and for field assistance. This research was supported by the Dutch Foundation for the Conservation of Irish Bogs, the Schure-Beijerinck-Popping fund (KNAW), WIMEK/SENSE (The Wageningen Institute for Environment &Climate Research, and the Socio-Economic & Natural Sciences of the Environment), the Swedish Research Council for Environment, Agricultural Sciences and Spatial Planning (Grant No. 2007-666) to MN. We also acknowledge the Kempe Foundation for the grants (MN) supporting the micrometeorological instrumentation. Support from the Integrated Carbon Observation System (ICOS) Sweden research infrastructure (Swedish Research Council) is also acknowledged.

Appendix 5.1. Model parameterization

A5.1.1 Water retention

We used the sandbox method (Klute, 1986) to parameterize the Brooks-Corey water retention function (Eq. 5.4). Eight samples of homogeneous *Sphagnum balticum* material (top 10 cm, diameter 20 cm) were carefully sawn from four representative lawns in Degerö Stormyr with a serrated knife. To remain the pore structure intact the samples were frozen and transported with a cooling van (T < 0°C) to Wageningen (NL), where a subsample (top 5 cm, diameter 5 cm) of the frozen peat sample was taken. On the sandbox, the water retention was determined in the suction pressures range from 0 to 100 cm, the most relevant part for peatmosses. Repeated weighing ensured that water content was in equilibrium with the applied suction pressure.

The Brooks-Corey function was fitted through empirical data using the *nls* function in R (R Core Team, 2014). The saturated water content was set at maximum measured field water content because fitting parameters were not significant and visually incorrect. Furthermore, as the measured (oven dry) residual water content was < 0.01 cm^3 cm^{-3} we used this value as residual water content. Due to the large correlation between shape parameter λ and air entry pressure h_b, we fixed h_b at -0.5 cm based on the shape of the empirical water retention curve. Consequently only λ was calibrated.

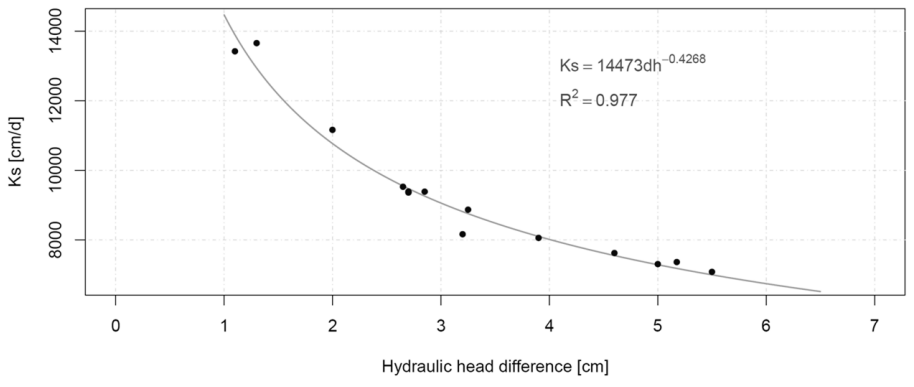

Figure A5.1. *Example illustrating the dependence of hydraulic conductivity on the hydraulic head difference.*

A5.1.2 Saturated hydraulic conductivity

Values of the saturated hydraulic conductivity (K_s) are often experimentally obtained using the constant-head, falling-head, and constant-flux method (Klute, 1986). For the

highly porous living top layer of *Sphagnum* peat, we encountered some issues. In the conventional K_s instrumentation, tubing systems under a sample are used to collect and transport water to an outlet. These tubes have only a restricted capability to transport water. At higher flow rates, resistance with the tube wall non-linearly decreases the velocity at which water is reaching the outlet, resulting in biased estimates of K_s. The flow resistance to tube walls is in a non-linear manner dependent on flow rate and thereby on the employed hydraulic head difference (See Fig. A5.1).

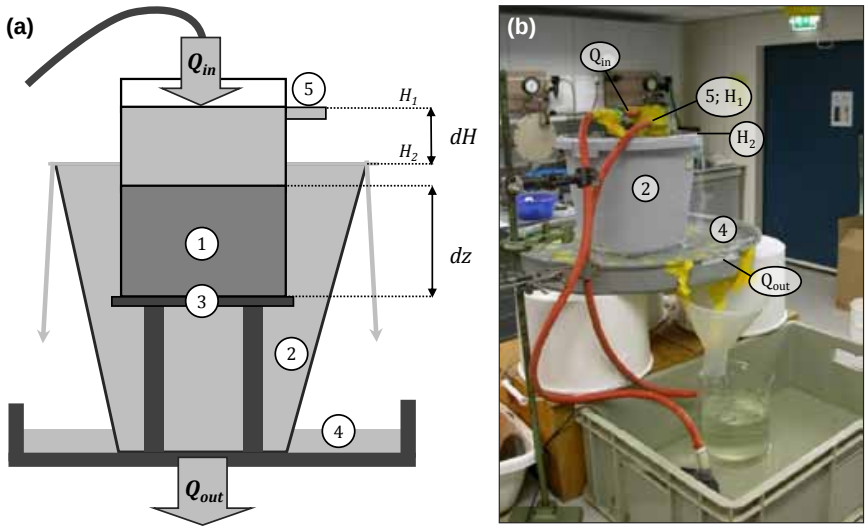

Figure A5.2. *Schematic (a) and representational (b) overview of the modified measurement setup to experimentally determine the saturated hydraulic conductivity (K_s). 1: peatmoss sample, 2: bucket, 3: mesh upon which the sample is placed, 4: overflow reservoir, 5: overflow tube to maintain the hydraulic head difference fixed.*

For this reason we modified the standard method by discarding all tubing systems and using an open outflow, with a low resistance to water flow. A peatmoss sample (diameter = 10 cm, height = 10 cm) in a PVC ring was placed on top of a mesh in a bucked filled with water (Figure A5.2). Another PVC ring was placed (water-tight) onto the sample ring. A pump transported water to the top of the peatmoss sample to create a hydraulic head difference, which induced water flow. The hydraulic head (H_1) was remained fixed with an overflow tube. The water flowed through the sample, over the rim of the bucket (H_2) in the overflow reservoir, and the outflow rate was measured. The hydraulic conductivity was calculated using Darcy's law

$$Q = -K_s\, A \frac{dH}{dz} \qquad \text{(A5.1)}$$

where Q is the outflow rate ($m^3\ d^{-1}$), A the area of the peatmoss sample (m^2), dz the height of the sample (0.1 m), and dH the hydraulic head difference. K_s was calculated from the measured outflow Q and known parameters in Eq. A5.1. The geometric mean of 10 K_s estimates of intact *Sphagnum balticum* cores (collected as described in A5.1.1) was used to parameterize the model.

A5.1.3 Evaporation moisture reduction function

An evaporation experiment was used to obtain parameters in the moisture reduction function of evaporation (Eq. 5.2). An intact *Sphagnum balticum* core (height 10 cm, diameter 15 cm) was placed on a balance. The weight change through time provided both the evaporation rate and the weight of the *Sphagnum* core, which was transformed in a volumetric water content using the bulk density.

A5.1.4 Calibrated parameters

For the crop factor (K_c), specific yield (S_y), the shape parameter λ in the water retention function, and the K_a and K_b shape parameters in the hydraulic conductivity function no parameter values were available. These parameters were calibrated using the time series of water content, water table and peat thickness of Site 1. The first half of the Site 1 time series is used for calibration, the second half for validation. Optimal parameter estimates $\boldsymbol{P}$ were obtained by minimizing a multi-objective function $\varphi(\boldsymbol{P})$ in which residuals between observed (O) and simulated (S) values at time t for variable i were weighed (w_i), squared and summed (Eq. A5.2).

$$\varphi(\boldsymbol{P}) = \sum_{i=1}^{3}\sum_{t=1}^{n}\left(\frac{O_{i,t} - S_{i,t}(\boldsymbol{P})}{w_i}\right)^2 \qquad \text{(A5.2)}$$

The weights w_i represent estimated mean measurement error for water content, water table, and peat thickness, and are used to give them equal weight in the calibration. The multi-objective has the advantage that optimal parameter estimates are not merely based on a best fit between observed and simulated water content. Instead, the criterion also includes how well the processes beyond are simulated, which is essential. The multi-objective function was evaluated with the Powell conjugate direction method, in which a local minimum of a continuous but complex function is determined without knowledge of the derivative (Powell, 1964). To increase the chance of finding a global minimum, ten restarts with random initial parameter settings within the pre-specified range were employed (See Appendix 5.4).

Appendix 5.2. Field measurements peat volume change

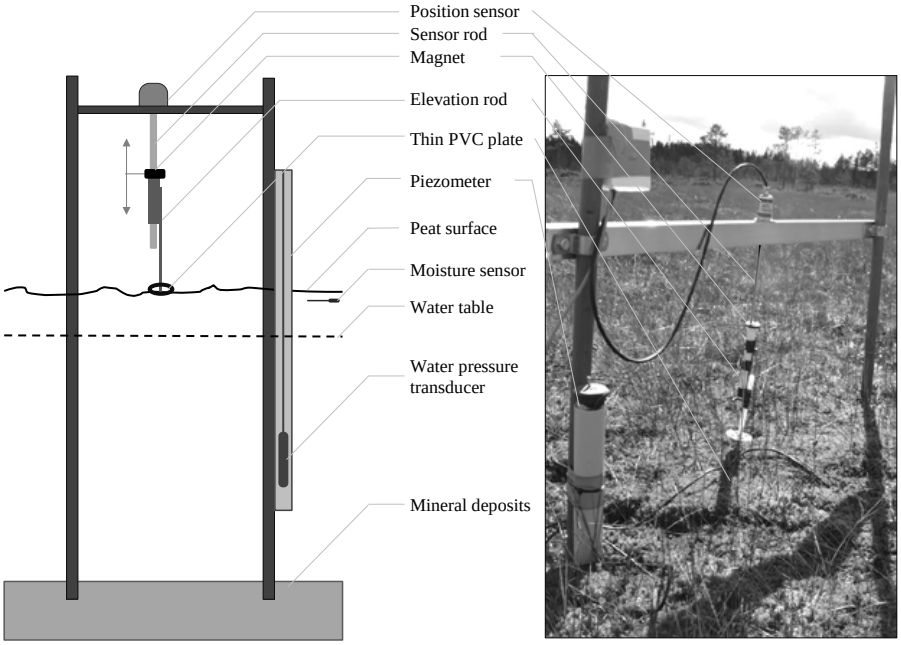

Figure A5.3. *Schematic and representational overview of field measurement setup. The linear position sensor was installed in a frame, which was anchored into the mineral deposit underlying the peat. Changes in peat surface elevation (hence peat volume) were detected by the position sensor as a change in voltage, induced by altered position of the magnet (connected to the elevation rod; dark grey) along the sensor rod (light grey). See main text for information on measurements of water table and volumetric water content.*

Appendix 5.3. Model validation of parameterization site

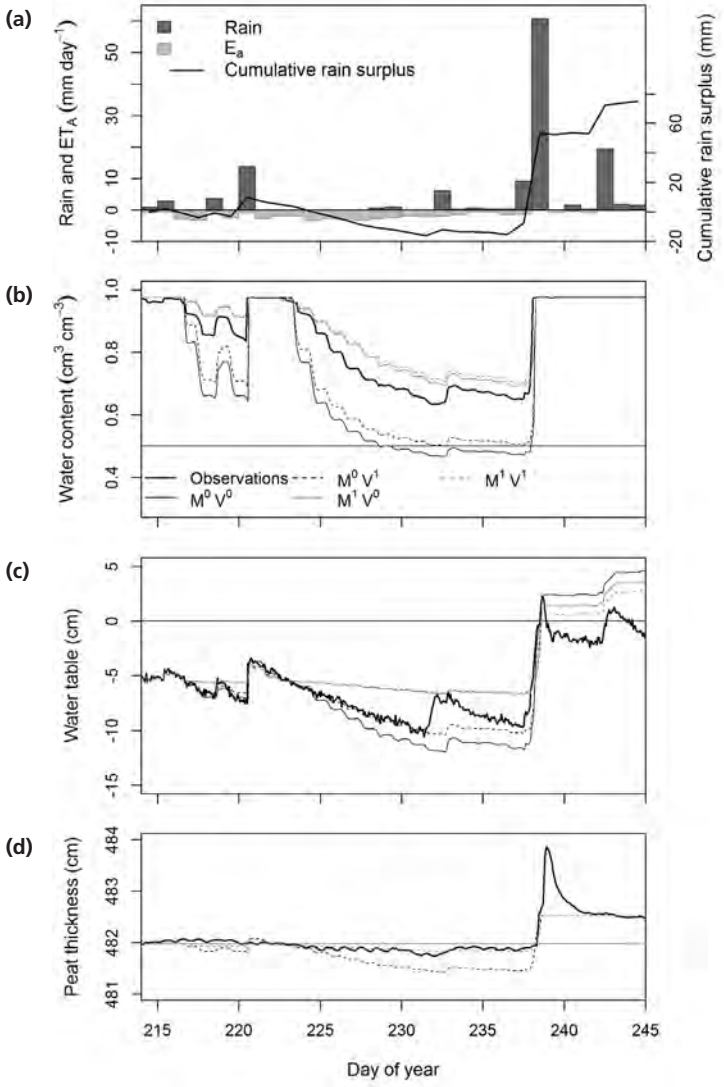

Figure A5.4. *Time series of weather, observations and simulations during the validation time period (2 August – 3 September, 2012). Fig. A5.4a shows daily sums of rainfall and simulated actual evaporation, and the cumulative rainfall surplus (line). Figs. A5.4b-d show observed and simulated volumetric water content (b), groundwater table (c) and peat thickness (d) with the four model variants including (^{1}) or excluding (^{0}) moss rain water retention (M) and/or peat volume change (V). The horizontal line in Fig. A5.4b at 0.5 cm^3 cm^{-3} represents the critical moisture threshold. See Table 5.5 in main text for model performance.*

Appendix 5.4. Range of parameter values in sensitivity analysis

Table A5.4. *Range of parameter values used in the univariate sensitivity analysis.*

Parameter	Meaning	Value in model	Min	Max	Unit
θ_{sat}	Saturated water content	0.975	0.7	1	$m^3\ m^{-3}$
θ_{res}	Residual water content	0	0	0.3	$m^3\ m^{-3}$
h_b	Air entry value	-0.005	-0.0075	-0.0025	m
λ	Shape parameter θ-h	0.28	0.14	0.42	-
K_s	Saturated hydraulic conductivity	$1.5 \cdot 10^{-3}$	$7.5 \cdot 10^{-4}$	$2.26 \cdot 10^{-3}$	$m\ s^{-1}$
K_a	Shape parameter K(h)	1.0031	0.5	1.5	-
K_b	Shape parameter K(h)	0.0001	$5.0 \cdot 10^{-5}$	$1.5 \cdot 10^{-4}$	-
S_s	Specific storage	$2.0 \cdot 10^{-6}$	$8.0 \cdot 10^{-7}$	$3.0 \cdot 10^{-6}$	m^{-1}
S_y	Specific yield	0.38	0.19	0.57	-
K_C	Crop factor	1.5	0.75	2.25	-
PT_{INI}	Peat thickness	5.0	2.5	7.5	m

6 Synthesis

6.1 The relevance of fine scale ecohydrological processes for the carbon cycle of northern peatlands

Northern peatlands accumulated an equivalent of 20% of total terrestrial soil carbon throughout the Holocene (Kleinen *et al.*, 2012; Turunen *et al.*, 2002; Yu, 2011). As such, these northern wetlands represent a significant long-term sink for atmospheric CO_2, resulting in a cooling of the earth and its atmosphere (Frolking & Roulet, 2007). The long-term net carbon uptake of northern peatlands depends on the balance between carbon losses through decomposition and carbon uptake through photosynthesis, mainly of peatmosses (*Sphagnum* spp.). Climate change may alter both decomposition and photosynthesis rates and result in a net release of CO_2 from peatlands into the atmosphere, which could accelerate climate change (Dise, 2009; Limpens *et al.*, 2008).

This thesis presents results of experiments under controlled lab conditions, field monitoring and mathematical modelling aimed to understand how fine scale ecohydrological processes in northern peatlands may be affected by climate change, and how such changes may feed back to the global climate by altering photosynthetic carbon uptake. The *fine scale ecohydrological processes* addressed in this thesis are *rainwater retention* by peatmosses and *peat volume change* for three peatmoss species (*Sphagnum fuscum*, *S. balticum* and *S. majus*) from hydrologically distinct microhabitats (hummock, lawn, hollow).

Our results show that ecohydrological processes operating at fine spatial or temporal scales modify the carbon uptake by photosynthesis of peatmosses in northern peatlands. These processes are to our knowledge not yet all implemented in models simulating feedbacks between peatlands and climate and their impact on feedback strength between peatland and atmosphere is unknown. Current model projections on climate change therefore include additional uncertainty. This additional uncertainty can be reduced by incorporating the ecohydrological processes presented in this thesis. Below we synthesize the results of this thesis and provide an overview of future research needs.

6.2 Rain: carbon loss or carbon gain?

One of the main aims in this thesis was to determine how a shift in temporal distribution of rain impacts photosynthesis of three peatmoss species characteristic for three contrasting microsites (*Sphagnum fuscum*, *S. balticum* and *S. majus*). To assess the effect of rain at different groundwater tables, we developed water retention cylinders, a device to simulate a summer groundwater table draw down extending well below the

peat samples (Chapter 2). Using water balance measurements we quantitatively showed that rainwater becomes an important source of water supply for *Sphagnum* at deep groundwater tables where, dependent on species, 66 to 92% of the evaporated water originated from rainwater.

In accordance with our hypothesis (Chapter 1), the temporal distribution of rainfall did not significantly affect peatmoss carbon uptake in moist conditions. The timing of rain events controlled photosynthetic activity, but its effect was species-specific. The hummock species quickly switched to a photosynthetic active state during a post-drought rain event, and thus was able to take advantage of temporary rewetting by rain after drought. In contrast, hollow and lawn species seem to be adapted to consistently wet conditions. These 'high inertia species' (cf Proctor & Tuba, 2002) were not able to take advantage of the temporary rewetting by rain. We conclude that lawn and hollow peatmosses can only maintain a positive carbon balance with frequent rain or long periods of rewetting, allowing for complete drought recovery, and minimizing leaching of valuable cell constituents of damaged cells (Dilks & Proctor, 1976; Gupta, 1977; Proctor *et al.*, 2007b). Frequent occurrence of drying-wetting cycles can thus be detrimental for survival and competitive strength of lawn and hollow peatmosses. This implies that hollow and lawn peatmosses only thrive in conditions with either continuously shallow water tables or very frequent rain. These observations support the view that hummock species are more drought tolerant than lawn or hollow species (Hájek & Beckett, 2008; Rydin, 1985; Wagner & Titus, 1984). A theoretical modelling framework to further improve simulation and prediction of peatmoss photosynthesis to climate induced alterations in water balance dynamics is provided in Section 6.6.2.

Peatmoss morphological traits in relation to water retention

In addition to species-specific differences in the ecophysiological response to rain, *Sphagnum* morphological traits are also species-specific and may affect peatland resilience to rain regime shifts in a future climate (Turetsky *et al.*, 2012). Accordingly, accounting for species-specific differences in morphological traits can further improve predictions of peatmoss response to episodic rewetting by rain (Elumeeva *et al.*, 2011). The morphological traits characterize the capillary network (Luken, 1985; Rydin, 1985, 1993), which define capillary rise from the groundwater table (hydraulic conductivity), and the moisture retention characteristics. Hummock species, occurring at sites with deep groundwater tables, have smaller shoots, grow in higher densities, and have lower metabolic rates than lawn and hollow species (Hayward & Clymo, 1982; Laing *et al.*, 2014; Luken, 1985; Rydin, 1995). The dense packing of hummock peatmosses results in smaller capillary spaces and is frequently asserted to increase water retention, and

increase capillary rise of groundwater (Rydin, 1986).

A predictive relationship between morphological traits and *Sphagnum* water retention capacity is not yet available. We assessed (Gerard, 2011; Thill, 2011) morphological traits of intact cores of three peatmoss species (*Sphagnum fuscum, S. balticum* and *S. majus*). Next, these traits were related to *Sphagnum* water retention at a range of suction pressures (i.e. groundwater tables) (e.g. Bouma, 1989; Schaap *et al.*, 2001; Wösten *et al.*, 2001). These analyses suggest that morphological traits can be used as predictors of water retention capacity (Fig. 6.1). Macroscopic traits, such as bulk density and shoot density, are mainly correlated to water retention at low suction pressures (i.e. shallow water tables). At larger suction pressures, where only smaller pores retain water, the length of branches, distance between fascicles (branching points) and number of stem leaves were related to water retention. At even larger suction pressures, submicroscopic characteristics, such as the size of hyaline cell pores, likely play an important role in water retention capacity (Hayward & Clymo, 1982).

TAKE HOME MESSAGE

Whereas frequent rain at deep water tables boosts photosynthesis of all peatmosses, no rain at all is more beneficial for lawn and hollow peatmosses than infrequent rain.

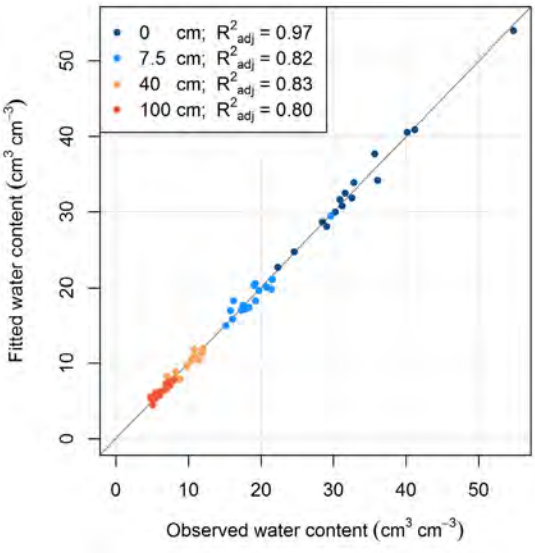

Fig. 6.1. *Observed and fitted water content at various suction pressures (colours) using stepwise multiple regression. Explanatory variables were bulk density, shoot density, shoot overlap, shoot diameter, distance between fascicles (branching points), length of spreading and hanging branches, overlap of hanging branches and stem leaf density. Trait information was based on samples of the top 5 cm (diameter 5 cm), collected from mono-specific patches of S. fuscum (n=9), S. balticum (n=7) and S. majus (n=9).*

6.3 Effect of rain at field scale

The experiment in controlled conditions illustrated the prominent role of rain and its temporal distribution for peatmoss carbon uptake (Chapter 2). To determine whether this conclusion also holds for field conditions we assessed the response of net carbon uptake of a northern peatland to individual rain events using 11 years of eddy-covariance and meteorological data. In contrast to our hypothesis (Chapter 1) and the results of the experiment (Chapter 2), our analysis of long-term eddy-covariance data (Chapter 3) showed that rain characteristics and preceding moisture conditions had a minor effect on peatland carbon uptake. In contrast to the experiment, the reduction in light availability due to increased cloud cover associated with rain reduced net CO_2 uptake with 0.2 – 0.5 gC m^{-2} per individual rain event. On an annual basis, this reduction corresponds to about 24% of annual net CO_2 uptake. As light availability was kept constant in the controlled experiment, these effects associated to rain showers were not observed.

TAKE HOME MESSAGE

Daytime rain events decrease northern peatland net CO_2 uptake by reducing light availability, rather than increasing it by rewetting.

Does peat volume change diminish the rain effect?

The rewetting effect of rain observed in the growth chamber experiment was only weakly supported by the analysis under field conditions, which raises the question which factor could explain this difference. In addition to the difference in light conditions, another major difference between the chamber experiment and the field is the presence of a thick peat deposit beneath the living moss layer in field conditions. The open pore structure and high compressibility of fibrous material (Price *et al.*, 2005; Waddington *et al.*, 2010) allows peat to expand in wet periods and to compress during dry spells. As a result, variability in the depth of the groundwater table is reduced and the capillary water supply to the living moss layer may be stabilized, reducing peatmoss water stress (Kennedy & Price, 2005). At the eddy-covariance footprint in Degerö Stormyr, peat volume change reduced the decline in groundwater table throughout the growing season with 7.8 cm (Chapter 4). Especially for hollow and lawn peatmosses, abundantly present in the footprint (> 95% cover) and growing at habitats with shallow groundwater tables (Andrus *et al.*, 1983; Nilsson *et al.*, 2008), such stabilization effects may maintain peatmoss photosynthesis during drought. This buffering of extremes due to peat volume change may also have prevented rain events to have a direct rewetting effect on peatmoss photosynthesis (Chapter 3). The groundwater table was, however, frequently well below

the optimal range of groundwater tables for the species in the eddy-covariance footprint (Andrus *et al.*, 1983; Rydin & McDonald, 1985b), making it likely that drought stress occurred and that the direct rewetting effect should have been present. This suggests that the light reduction effect of rain over the footprint is indeed more important than the rewetting effect, and stresses the importance of separating cloudiness and rainfall in analysing effects of climate change on carbon exchange.

The stabilization effect of expansion and compression is expected to be spatially heterogeneous given that peat depth and peat material are spatially variable. In the simplest explanation, expansion and compression are related to current local vegetation composition. To better understand the response of net carbon uptake to wetting and drying events, spatial variability of expansion and compression, and vegetation composition were analysed along a 571 m transect comprising the eddy-covariance footprint area in Degerö Stormyr (Chapter 4).

We used a Structure-from-Motion algorithm (Jebara *et al.*, 1999) to create high-resolution height maps from multiple images with different viewpoints taken. The magnitude of peat volume change throughout the growing season varied considerably through space. Geostatistical analysis showed furthermore that peat volume change was highly spatially structured, and spatial correlations became negligible at a characteristic spatial scale of about 40 m. The spatial variability of peat volume change was mainly related (R^2 = 51%) to changes in absolute groundwater tables, which controls the mechanical stress on the peat matrix (Terzaghi, 1943). Vegetation composition only marginally explained (R^2 = 7.3%) the spatial variability of peat volume change. However, point measurements at other locations in the Degerö Stormyr peatland indicate that peat volume change magnitude increases clearly in the sequence hummock < lawn < hollow (Fig. 6.2).

Both the transect analysis and the point-measurement time series provide further evidence that vegetation cannot be the sole predictor for peat volume change magnitude, as the response of peat elevation to rain events varies considerably within microsites (Fig. 6.2). Moreover, considerable overlap in seasonal range of peat surface position among microsites occurs. As indicated by the transect study, spatial variability in peat volume change is likely driven by spatial variability in absolute groundwater level fluctuations. Especially for the hollow site located near the main discharge (Site 2), where upstream infiltrated water may accumulate, considerable volume change was observed (Fig. 6.2). This suggests that lateral groundwater redistribution may be an important control of changes in absolute groundwater table, peat volume change, and net carbon response.

TAKE HOME MESSAGE

Peat volume change is highly spatially structured, and spatial patterns are (in the studied peatland) mainly related to spatial variation in absolute groundwater table change through time and to a lesser extent also to microsite, with magnitude of peat volume change increasing from hummock < lawn < hollow < flark.

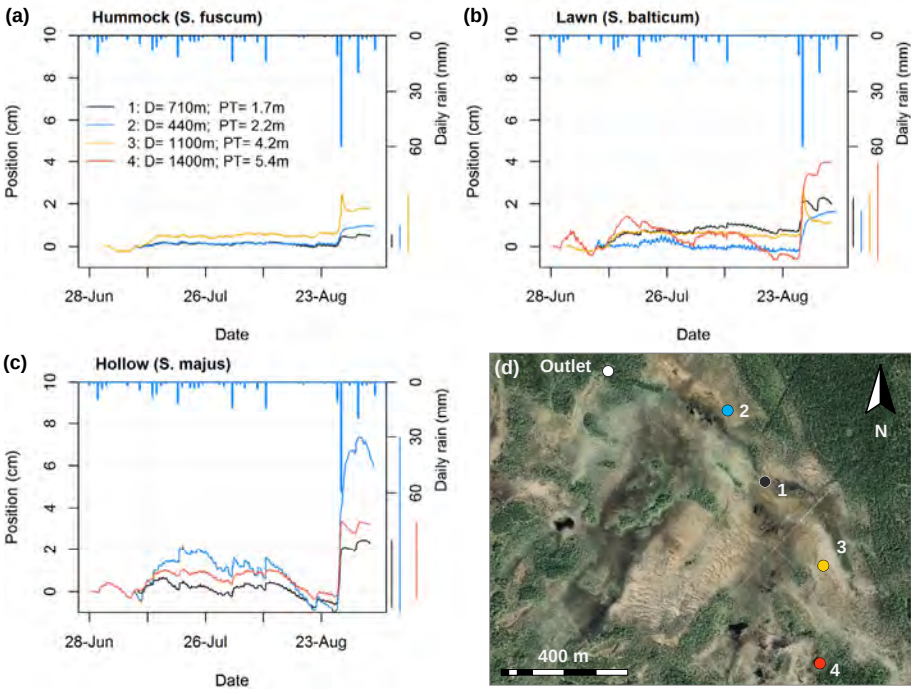

Figure. 6.2. *Time series of peat surface elevation (DOY 179 – 247 in 2012) obtained with linear position sensors for different microsites (a-c) and locations (lines) within the Degerö Stormyr peatland. Daily rainfall sums are presented with vertical bars (secondary y-axis). The mean distance (D) from the main discharge outlet and mean peat thickness (PT) are given in Fig. 6.2a. Coloured line segments in the right plot margin show the range of the minimum and maximum peat volume. The four locations are shown on the map in (d). Map source: 64°10'N 19°33'E, © Google Earth, 31 December 2009. Last accessed in August 2015.*

6.4 Importance of moss water storage and peat volume change for peatmoss water availability

We concluded that both rainwater retention and peat volume change are important processes regulating water availability in the living moss layer. The importance of these fine scale ecohydrological processes for peatmoss photosynthesis was quantified in a modelling study (Chapter 5). We built a simulation model and extended it with peatmoss rainwater retention, peat volume change, or the combination of both. These model extensions significantly reduced the number of droughts experienced by peatmoss with 33%, 11% and 51%. Moreover, model performance was best if both processes were incorporated. So, the numerical model simulations in Chapter 5 further support our laboratory and field observations, and stress the importance of including peat volume change and a moss water storage reservoir to accurately simulate water availability for peatmoss.

Using an ensemble of climate projections (bias-corrected and downscaled) for current and future climate, we showed that including peat volume change and moss water storage reduced the projected number of droughts. In this modelling study, climate change did not affect the number of peatmoss droughts. Furthermore, increasing model complexity by including ecohydrological feedback mechanisms improved model predictions, illustrating the resistance of peatlands to drought.

TAKE HOME MESSAGE

Including rainwater retention and peat volume change improves simulations of water content in the living moss layer and results in lower projected droughts in both current and future climate, suggesting that including more ecohydrological feedbacks in peatland models buffers the impacts of climate change.

6.5 Implications

6.5.1 Ecosystem functioning

It is generally accepted among peatland ecologists that hummock species are better able to cope with dry conditions than lawn and hollow species simply because their capillary network and the resulting hydraulic properties stabilize their moisture content (Hayward & Clymo, 1982; Luken, 1985; Robroek *et al.*, 2007a; Rydin & McDonald, 1985b). Current climate projections for the boreal zone indicate that summer rainfall amount will increase (IPCC, 2013). Although these wetter conditions may seem to be

in favour of hollow and lawn species, this may not be correct if we neglect the ability of species to deal with the projected less frequent but more intense rainfall (Allen & Ingram, 2002; IPCC, 2013). The results of Chapter 2 suggest that in a scenario with less frequent but more intense rain events, hummock species will have a competitive advantage over lawn species. On the longer term, hummock species may thus intrude the lawn microsite and outcompete lawn peatmosses. Assuming hollow species are also less capable to deal with intermittent rainwater supply than lawn species, hollow species would be replaced by lawn species.

When rain becomes even less frequent, also hummock *Sphagna* may lose the competitive advantage at the hummock site. As trees and vascular plants are more resilient to droughts and intermittent water supply due to their roots and xylem tissue than peatmosses, they are able to exploit these brief rewetting events. Hence, this extreme future rain regime could further increase the abundance of trees and other vascular plants on hummock sites (Heijmans *et al.*, 2013; Limpens *et al.*, 2014b).

A species-specific ability to deal with intermittent rainwater supply has to our knowledge not been included in any dynamic vegetation model (Heijmans *et al.*, 2008; Krinner *et al.*, 2005). The absence of an ecophysiological component describing the ability of plants to deal with transient rewetting limits current evaluation of drought impact on species competition. In Section 6.6.2 we provide a conceptual model to include such transient rewetting effects.

The model study in Chapter 5 demonstrates that peat volume change significantly reduced the frequency of droughts by 11 – 26% for lawn microsites during the growing season. Peat volume change therefore is an indispensable mechanism stabilizing surface wetness and peatmoss photosynthesis, and hence increases peatland resistance to climatic perturbations.

6.5.2 Hydrological functioning

Simulating peatmoss water availability

The model study (Chapter 5) clearly demonstrates that including both peat volume change and rainwater retention improved predictions of water content in the living moss layer with 50%. Moreover, the number of simulated droughts is significantly reduced by including these processes (from 2.25 to 1.1 droughts per average growing season, with drought being defined as a volumetric water content below 0.49 cm^3 cm^{-3}, Chapter 2 and 5), and the water content in the moss layer is stabilized. This suggests that including more hydrological processes controlling moss water availability may result in

even larger stabilization of moss water availability and reduction of drought occurrence (Waddington *et al.*, 2015).

The results of Chapter 5 suggest that lateral groundwater flow may be one of these hydrological processes currently missing in models. The spatial variability of peat volume change was mainly related to spatial variation in absolute groundwater table fluctuations, which in turn was ascribed to lateral groundwater redistribution. Increased awareness of the importance of lateral groundwater flow and the functioning of peatlands as self-regulating, spatially structured complex adaptive systems (Belyea & Baird, 2006; Eppinga *et al.*, 2008) triggered recent development of spatially explicit peatland models including lateral groundwater flow (Baird *et al.*, 2012; Eppinga *et al.*, 2009; Sonnentag *et al.*, 2008; Tang *et al.*, 2015). Using the Structure-from-motion technique (Chapter 4), we found that a grid size of maximally 40 m would be required to adequately represent spatial patterns in peat volume change over the growing season in such models. Spatially explicit models are important to understand the functioning of individual peatlands, but are computationally demanding at such fine grid sizes. This makes spatially explicit models difficult to couple to atmospheric circulation models working with grids at the km scale. In Section 6.6.3 we describe a way to couple peatland ecohydrology to atmospheric processes.

Consequences for land-surface – atmosphere feedbacks

In addition to controlling peatmoss photosynthesis, the water content in the living moss layer regulates the evaporative water flux and partitioning of the energy balance (Seneviratne *et al.*, 2010). The inclusion of peat volume change and moss water retention in the model structure reduced simulated drought frequency which, in turn, could cause moss evaporation to be less frequently limited by water, and more frequently by net radiative energy. Current land-surface – atmosphere models do not (yet) include fine scale ecohydrological processes (species response, peat volume change, and groundwater dynamics), and may therefore underestimate the latent heat flux at high latitudes areas with large peatland cover. Especially in the boreal zone, where peatlands cover is substantial (15 – 30% of the land surface cf Joosten & Clarke, 2002), including fine scale ecohydrology in land-surface schemes will have a yet unknown impact on regional atmospheric circulation. An increased surface wetness could for example amplify a local positive soil moisture – rainfall feedback, where larger surface wetness enhances cloud formation and increases precipitation, which in turn increases surface wetness (Ek & Holtslag, 2004; Eltahir, 1998; Eltahir & Bras, 1996). The impact and strength of feedbacks between ecohydrological processes and regional climate can be tested by incorporating the peatmoss processes as described in Chapter 5 in land-surface

models (e.g. HTESSEL, Balsamo *et al.* (2011) or SURFEX, Masson *et al.* (2013)). In a next step, such land-surface models can be coupled to a one-dimensional (e.g. Chang *et al.*, 1999) or spatially explicit mesoscale (10^4 – 10^6 km^2) weather prediction model with fine spatial resolution (≤ 2.5 km; e.g. HARMONIE, Seity *et al.* (2010) or HIRLAM, Undén *et al.* (2002)).

Currently, climate projections frequently focus on shifts at coarse temporal scales, such as the total rain amount per winter and summer season, or per month. However, fine scaled projections on shifts in temporal distribution, intensity and duration of rain events will be required to adequately model feedbacks between the land surface and atmosphere. This thesis provides insight as to why such fine scale projections are required for the specific case of northern peatlands.

6.5.3 Carbon budget functioning

Consequences of less frequent but more intense rain

The results of the growth chamber experiment demonstrate that the temporal distribution of rainfall has an important effect on atmospheric carbon uptake. In peatlands with large cover of lawn and hollow microsites, a future climate with less frequent but more intense rainfall may significantly reduce net peatland carbon uptake. As described in Section 6.5.1, shifts in the rain regime will also likely modify species composition in the longer term. Such shifts may, due to species-specific carbon assimilation rates, be accompanied with shifts in net carbon uptake rates (Granath *et al.*, 2010; Hájek & Beckett, 2008; Laing *et al.*, 2014). Due to complex interactions with other environmental variables, no clear relationship seems to exist between microsites and net carbon accumulation rates (Alm *et al.*, 1997; Belyea & Clymo, 2001; Bubier *et al.*, 1998; Leppälä *et al.*, 2011; Waddington & Roulet, 2000). If – as expected – encroachment of vascular plants and trees occurs at the hummocks (Section 6.5.1), this likely reduces net carbon uptake due to the larger decomposability of vascular plants compared to peatmosses (Aerts *et al.*, 1999; Verhoeven & Toth, 1995). A model coupling the biogeochemical, hydrological, and dynamic vegetation components would be required to assess how the feedbacks between different facets of northern peatlands affect the carbon budget given climate change scenarios. Our results (Chapter 2) indicate that such models should include the non-linear complex relation between water availability and peatmoss growth to produce realistic predictions of drought impacts on peatmosses (See Section 6.6.2).

Rain events reduce carbon uptake at field scale

The results presented in Chapter 3 indicate that rain events, rather than increasing the net carbon uptake of Degerö Stormyr, decrease peatland net carbon uptake through

reducing light intensities. This finding highlights that the ecosystem carbon balance of peatlands is sensitive to future shifts in the rainfall regime or changes in cloud cover. Several studies pointed to 'global dimming' from 1960s to late 1980s (Dutton *et al.*, 1991; Stanhill & Cohen, 2001), caused by an increased concentration of atmospheric aerosols from anthropogenic pollution. After that period, the global dimming has stopped and seemed to turned into, on average, a global brightening (Wild *et al.*, 2005; Wild *et al.*, 2009). Although multimodel future projections consistently show increased total cloud amount, detailed projections on future shifts in cloud cover are ambiguous (IPCC, 2013). Given the results in Chapter 3, the ambiguity in this information seriously hampers projections of peatmoss carbon sequestration rates as affected by global change. With a projected rain regime with less frequent but more intense rainfall, light availability will be reduced less frequently by rain showers, and may therefore increase carbon uptake of northern peatlands. Of course, care should be taken when extrapolating these results to other locations, and to different peatland types. The studied peatland can nonetheless be regarded as representative for vast peatland areas at high latitudes (Nilsson *et al.*, 2001; Riley, 2011).

The large sensitivity of peatland carbon uptake to rain events at field scale (Chapter 3) strongly suggests that peatland models should take the decreased light availability during rain events into account. To correctly capture rain effects on carbon exchange in northern peatlands, a fine temporal discretization (e.g. hourly time step) is required. Neglecting these suggestions may result in biased climate change impact assessments on northern peatland carbon uptake. Although multimodel climate projections consistently predict increased cloud cover, it is not clear yet how cloud cover, type, and variability will change (IPCC, 2013). We conclude that including cloud cover and type in scenarios for future climate change is essential to predict peatland – atmosphere feedbacks, as cloud cover directly affects light availability and peatland CO_2 uptake. This is closely related to aerosol emission projections, as aerosols influence cloud formation and incoming radiation (Bréon, 2006; Charlson *et al.*, 1992; Ramanathan *et al.*, 2001).

Hydrological model complexity and carbon exchange simulations

The modelling study indicates that including peat volume change and moss rainwater retention in a point-scale hydrological model decreases peatmoss drought frequency. This suggests that models excluding such hydrological complexity will overestimate the (negative) impact of drought on peatmoss CO_2 uptake. The increased complexity will, considering the importance of surface moisture, not only affect peatmoss photosynthesis but also other biogeochemical processes related to greenhouse gas emissions. For example, simulated methane emissions are likely larger with increased hydrological

complexity due to higher water contents (Larmola *et al.*, 2010).

6.6 Outlook

In this thesis we showed how climatic changes may affect peatland water and carbon budgets. We identified two areas in which scientific knowledge is currently missing, but which are of fundamental importance to fully assess climate change impacts on ecohydrological functioning of northern peatlands. These two research topics are the ecophysiological ability of poikilohydric plants, such as bryophytes, to deal with intermittent rainwater supply and the quantification of lateral groundwater flow impact on local groundwater table dynamics (Fig. 6.3). We start with an overview of recommendations for future empirical research.

6.6.1 Directions future empirical research

We consider it very likely that the net carbon uptake response of peatmoss to rain in our empirical studies mainly originates from photosynthesis or autotrophic respiration (Chapter 2, 3). However, our studies provide no empirical evidence that this is not a result of heterotrophic respiration, which may also be affected by rain and drought (Huxman *et al.*, 2004; Lee *et al.*, 2004; Meisner *et al.*, 2013). Observational field and growth chamber experiments separating heterotrophic respiration, autotrophic respiration, and photosynthesis at fine temporal resolution are required to determine how the different carbon flux components respond to rain events. This separation is impossible with eddy-covariance data only, stressing the necessity for controlled (field) experiments.

In Section 6.2 we quantified the relation between peatmoss morphological traits and their capacity to retain water. The applicability of these results is, however, limited to one study area and mono-specific patches of three peatmoss species. Given the high potential of peatmoss traits to describe water retention, it seems productive to extend the established relationship to other peatmoss species and other peatlands. More analyses are required to not only predict specific points of interest of the water retention characteristic, but also to predict parameters that describe the water retention – suction pressure – hydraulic conductivity relationship (Gupta & Larson, 1979; Wösten *et al.*, 2001).

While field experiments with rain shelters may be useful to identify how ecosystems respond to extreme drought events, more subtle changes in the temporal distribution of rain may be as important, as we show in this thesis (Chapter 2). By definition, extreme events do not occur frequently, which limits the relevance of experiments comparing

rain – no rain treatments. Future experiments should therefore be set up testing different rain and drought regimes instead of establishing rain shelters. Moreover, the light reduction effect of rain should be included in controlled lab experiments, as it is a dominant control on net CO_2 uptake and co-varies with rain occurrence (Chapter 3).

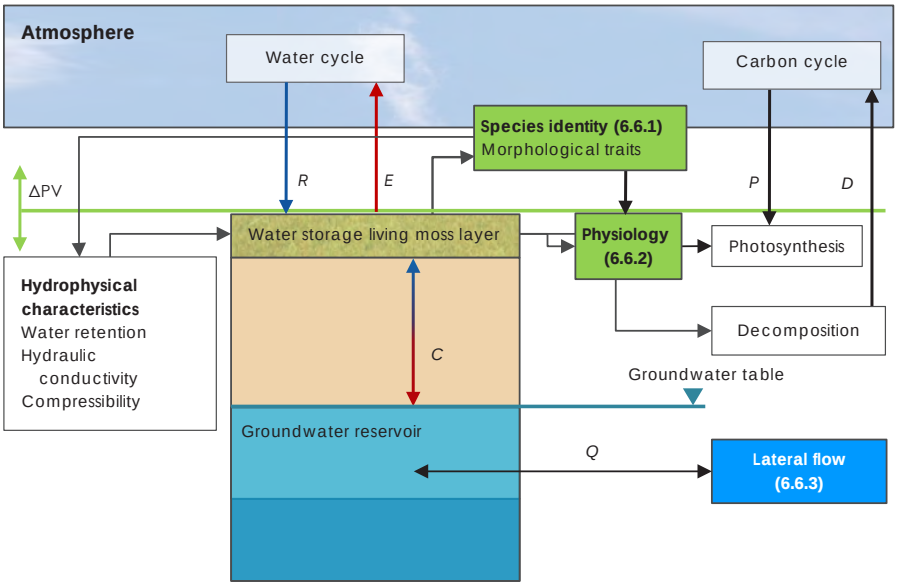

Figure 6.3. *Conceptual overview of ecohydrological processes in the living peatmoss layer as in the introduction, extended with a peatmoss identity component (Section 6.6.1), an eco-physiological component (Section 6.6.2), and a lateral groundwater flow component (Section 6.6.3). R = rainfall, E = evaporation, C = capillary flow, Q = lateral groundwater flow, ΔPV = peat volume change, P = photosynthesis, D = decomposition.*

The finding that light is more important than water for photosynthesis is currently based on one northern peatland only. We strongly recommend repeating the analysis for multiple peatlands using long-term eddy-covariance data. Moreover, cloud cover is shown to profoundly affect global terrestrial gross primary production (Nemani *et al.*, 2003) and clouds associated with the rainy season limit tropical rainforest production (Graham *et al.*, 2003). Using eddy-covariance time series from e.g. Fluxnet (Baldocchi *et al.*, 2001), we may apply a standardized version of our analysis for multiple ecosystems around the world. This way, general patterns of ecosystem response to individual events could be distinguished. Our study indicates that CO_2 uptake is very sensitive to individual rain events. Averaging over rain events may consequently bias the relationship between net ecosystem CO_2 exchange and rainfall.

6.6.2 Modelling the water-photosynthesis relation for poikilihydric plants

A key finding of the growth chamber experiment is that, for rain to have a positive effect on carbon uptake, peatmosses must be ecophysiologically adapted to take advantage of temporary increases in water content in the living moss layer. Hence, even though the water content increases due to rain, photosynthetic carbon uptake may be negligible. This implies that there is not a direct relation between photosynthetic activity and water availability (Chapter 2). Current peatland models, dynamic global vegetation models and land-surface schemes including carbon cycling assume a direct link between moisture availability and net carbon uptake (e.g. Bonan *et al.*, 2003; Boussetta *et al.*, 2013; Frolking *et al.*, 2010; Krinner *et al.*, 2005; St-Hilaire *et al.*, 2010). Especially when we attempt to predict drought impacts on ecosystem carbon fluxes and peatmoss competition, including the ability of peatmoss to deal with intermittent moisture supply becomes an important component.

For semi-arid environments, concepts linking the physiological plant response to rain events are relatively well-developed compared to peatlands. This is due to the clear rainy seasons, where distinct rain pulses markedly trigger observable plant growth (Huxman *et al.*, 2004; Reynolds *et al.*, 2004; Schwinning & Ehleringer, 2001; Schwinning & Sala, 2004). The threshold-delay model, developed for semi-arid ecosystems by Ogle & Reynolds (2004) provides a valuable basis to establish a more mechanistic representation of drought impacts on peatmoss in northern peatlands. An adapted version of this conceptual model is described below (Fig. 6.4).

The following processes may be relevant for simulating the peatmoss response to rainfall, and could result in a non-linear and complex relation between peatmoss water content and photosynthesis:

1) After drought, drought damage needs to be repaired before photosynthesis can start. This may introduce a lagged photosynthetic response to rewetting (Williams *et al.*, 2009).
2) The duration of this lag is hypothetically a function of the cumulative drought damage, which in turn is be determined by preceding moisture conditions (Cable *et al.*, 2013). In other words, peatmosses may have a 'hydrological memory'.
3) A minimum amount of rain may be required to trigger photosynthesis or repair. In the original model proposed by Ogle & Reynolds (2004) this amount is species-specific but fixed through time. However, this amount likely equals the amount required to replenish the water content above the minimum water content at which photosynthetic activity takes place, and therefore needs to be included dynamically.

4) After the beginning of a drought period, photosynthetic activity ceases. As indicated in Chapter 2, the ability to switch between the photosynthetically active/inactive states seems to be species dependent. A species-specific decay rate of photosynthetic activity after drought commences thus needs to be included.

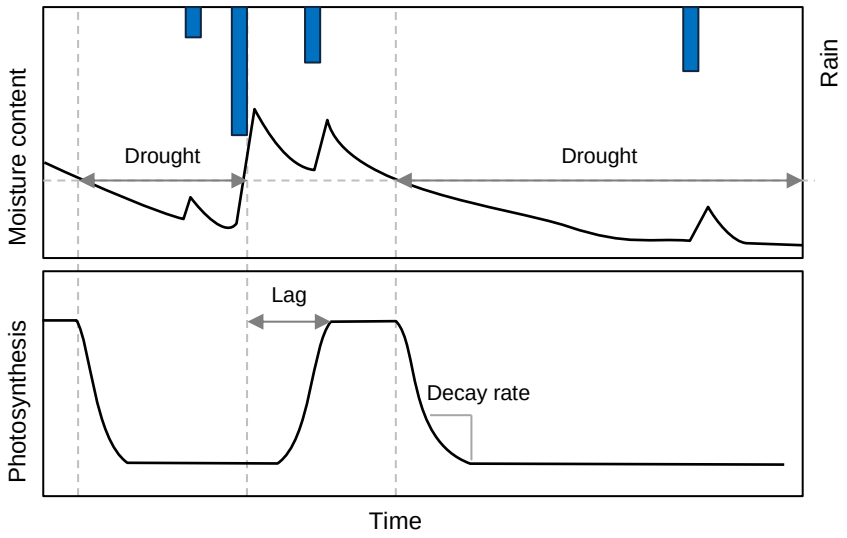

Figure 6.4. *Hypothetical response of photosynthesis to rewetting based on experimental findings in Chapter 2. The horizontal dashed line in the top figure represents the moisture level at which photosynthesis switches on/off. Based on Ogle & Reynolds (2004).*

The non-linearity and differential response of photosynthesis in a drying and wetting trajectory may cause hysteresis in the moss water content – photosynthetic activity relation. Hysteresis is a recognized mechanism introducing catastrophic shifts between alternative stable states (Scheffer *et al.*, 2001), represented by the shift between a photosynthetically active and inactive state. Although the occurrence of hysteresis is hypothetical and needs to be validated, Fig. 2.5b in Chapter 2 suggests that hysteresis in the water content – photosynthesis relation may occur (See Fig. 6.5). Both at low and high volumetric water contents, the variability in photosynthetic efficiency is small, representing the photosynthetically inactive and active state. In the water content range of 0.40 – 0.65 m^3 m^{-3}, large variability occurs, representing hysteresis loops. Additional laboratory experiments are required to test this hypothesis and parameterize the ecophysiological component for different functional species groups with different ecophysiological drought-response traits.

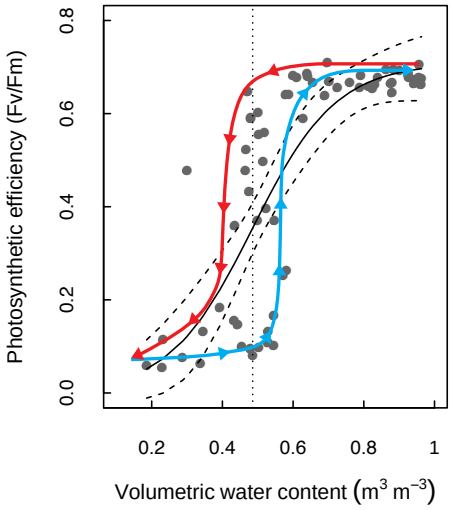

Figure 6.5. *Relation between volumetric water content and photosynthetic efficiency for Sphagnum balticum. Points represent observations of multiple mesocosms exposed to various drought conditions, the black lines represent a logistic fit (and 95% confidence intervals; Chapter 2). A hypothetical hysteresis effect arising from a non-linear and complex response of photosynthesis to rewetting is presented with the blue and red lines. The blue and red lines represent the wetting and drying curve.*

Integration of the ecophysiological non-linear complex processes in peatland models or land-surface schemes will improve climate change impact assessments in an important part of the world, where abundance of poikilohydric plants, such as bryophytes, is high (Daniels & Eddy, 1985; Proctor & Tuba, 2002; Turetsky *et al.*, 2012).

6.6.3 Towards an improved peatland ecohydrological model

In many scientific disciplines the comparison of models varying in complexity to verify which processes are relevant is relatively common (Ajami *et al.*, 2004; Eitzinger *et al.*, 2004; Henderson-Sellers *et al.*, 1993; Taylor *et al.*, 2012). Though model comparison is a crucial component in model development, to our knowledge no comparisons of models varying in complexity and focussing on the (eco)hydrology of northern peatlands are currently available. As a result, many models are available (e.g. Baird *et al.*, 2012; Frolking *et al.*, 2010; Granberg *et al.*, 1999; Heijmans *et al.*, 2008; Kennedy & Price, 2004; St-Hilaire *et al.*, 2010; Wu & Blodau, 2013; Yurova *et al.*, 2007), which are often employed at different peatland sites. This seriously impedes differentiating model effects from site effects and obstructs establishing general concepts for peatlands in different hydro-climatic settings. It is therefore essential to develop a unified peatland model by systematically comparing various complexities. Comparison of the output of models with various complexities with field data from multiple peatlands plays a vital role in this context. A central and accessible database, such as the peat properties database established by Loisel *et al.* (2014), would be valuable in stimulating the peatland community performing such model comparisons.

In this thesis we provided a start in unifying model concepts by systematically testing the importance of peat volume change and rainwater retention for water content in the living moss layer (Chapter 5). Our results stress the importance of also including lateral groundwater flow in predicting groundwater table fluctuations and its consequent effects on peatmoss water availability (Chapter 5) and peat volume change (Chapters 4 and 5). Several model approaches exist to simulate lateral groundwater flow at multiple spatial scales smaller than grid cells used in atmospheric circulation models. These approaches are either based on explicit flow routing procedures (Chen *et al.*, 2005b; Tang *et al.*, 2014; Wigmosta *et al.*, 1994), implicit statistical procedures (Beven *et al.*, 1984; Quinn *et al.*, 1995; Tague & Band, 2001), or physically based lateral groundwater flow in point-models (van Dam *et al.*, 2008; Yurova *et al.*, 2007). Although spatially explicit simulations where water is routed from cell-to-cell would be beneficial from peatland hydrological perspective, it is currently computationally unrealistic to simulate mesoscale climate with e.g. a 40 · 40 m grid resolution. Moreover, data requirements are very large and the geohydrological parameters are difficult to obtain, especially for remote northern peatlands. Conversely, the absence of a process-based description in implicit statistical procedures and point models may bias lateral groundwater flow estimates.

We advocate adopting an approach in which several simplifying modelling concepts are compared with a complex spatially explicit model (using Chapter 5 as a guideline). The performance of these lateral groundwater flow concepts can be assessed using observational data of a set of representative, data-rich peatlands differing in hydrological setting. To simulate lateral flows, measurements of saturated hydraulic conductivities, groundwater tables and discharge are required. Given the strong relationship between peat volume change and change in absolute groundwater table (Chapter 4), spatially explicit changes in groundwater table may be potentially derived from changes in surface elevation using Structure-from-Motion and airborne or terrestrial laser scanning techniques (Andersen *et al.*, 2011; Anderson *et al.*, 2010; Jebara *et al.*, 1999; Lode & Leivits, 2011). Applying Structure-from-Motion on digital images collected with unmanned aerial vehicles (UAVs) is a cost-effective and accurate method to determine fine scale topographic differences over time (Chapter 4). Especially combining photogrammetry with ground observations makes it possible to take peatland hydrology models one step further by adopting a 3D approach. This allows determining how peat volume change affects groundwater dynamics and local flow paths during a growing season in a peatland.

6.7 Conclusion

In this thesis we show that rainwater retention and peat volume change, operating at fine spatiotemporal resolution (square meters; hourly), play an essential role in carbon and water exchange between peatland and atmosphere. Hence, taking these fine scale ecohydrological processes in account is essential to predict whether northern peatlands, carbon pools of global importance, may shift from carbon sink to carbon source in a future climate.

7 References

Adkinson AC, Humphreys ER (2011) The response of carbon dioxide exchange to manipulations of *Sphagnum* water content in an ombrotrophic bog. *Ecohydrology*, **4**, 733-743.

Aerts R, Verhoeven JTA, Whigham DF (1999) Plant-mediated controls on nutrient cycling in temperate fens and bogs. *Ecology*, **80**, 2170-2181.

Ajami NK, Gupta H, Wagener T, Sorooshian S (2004) Calibration of a semi-distributed hydrologic model for streamflow estimation along a river system. *Journal of Hydrology*, **298**, 112-135.

Akaike H (1973) Information theory as an extension of the maximum likelihood principle. In: *Second International Symposium on Information Theory*. (eds Petrov BN, Csaki F), pp 267-281, Akademiai Kiado, Budapest, Hungary.

Alexandersson H, Karlström C, Larsson-Mccann S (1991) *Temperature and precipitation in Sweden 1961–1990. Reference normals (In Swedish)*, Swedish Meteorological and Hydrological Institute (SMHI), Norrköping, Sweden.

Allen MR, Ingram WJ (2002) Constraints on future changes in climate and the hydrologic cycle. *Nature*, **419**, 224-232.

Allen RG, Pruitt WO, Wright JL *et al.* (2006) A recommendation on standardized surface resistance for hourly calculation of reference ETo by the FAO56 Penman-Monteith method. *Agricultural Water Management*, **81**, 1-22.

Allen RG, Raes D, Pereira LS, Smith M (1998) *Crop evapotranspiration - Guidelines for computing crop water requirements - FAO Irrigation and drainage paper 56*, FAO - Food and Agriculture Organization of the United Nations, Rome, Italy.

Alm J, Schulman L, Walden J, Nyknen H, Martikainen PJ, Silvola J (1999) Carbon balance of a boreal bog during a year with an exceptionally dry summer. *Ecology*, **80**, 161-174.

Alm J, Talanov A, Saarnio S *et al.* (1997) Reconstruction of the carbon balance for microsites in a boreal oligotrophic pine fen, Finland. *Oecologia*, **110**, 423-431.

Almendinger JC, Almendinger JE, Glaser PH (1986) Topographic Fluctuations Across a Spring Fen and Raised Bog in the Lost River Peatland, Northern Minnesota. *Journal of Ecology*, **74**, 393-401.

An H, Noh SJ (2014) High-order averaging method of hydraulic conductivity for accurate soil moisture modeling. *Journal of Hydrology*, **516**, 119-130.

Andersen R, Poulin M, Borcard D, Laiho R, Laine J, Vasander H, Tuittila ET (2011) Environmental control and spatial structures in peatland vegetation. *Journal of Vegetation Science*, **22**, 878-890.

Anderson K, Bennie J, Wetherelt A (2010) Laser scanning of fine scale pattern along a hydrological gradient in a peatland ecosystem. *Landscape Ecology*, **25**, 477-492.

Andrus RE, Wagner DJ, Titus JE (1983) Vertical zonation of *Sphagnum* mosses along hummock-hollow gradients. *Canadian Journal Of Botany*, **61**, 3128-3139.

Appels WM, Bogaart PW, van der Zee SEATM (2011) Influence of spatial variations of microtopography and infiltration on surface runoff and field scale hydrological connectivity. *Advances in Water Resources*, **34**, 303-313.

ASCE-EWRI (2005) *The ASCE Standardized Reference Evapotranspiration Equation*, Technical Committee report to the Environmental and Water Resources Institute of the American Society of Civil Engineers from the Task Committee on Standardization of Reference Evapotranspiration. ASCE-EWRI, 1801, Reston, US.

Aubinet M, Grelle A, Ibrom A *et al.* (2000) Estimates of the annual net carbon and water exchange of forests: The EUROFLUX methodology. *Advances in Ecological Research*, Vol 30, **30**, 113-175.

Aurela M, Riutta T, Laurila T *et al.* (2007) CO_2 exchange of a sedge fen in southern Finland - the impact of a drought period. *Tellus B*, **59**, 826-837.

Axelsson P (2000) DEM generation from laser scanner data using adaptive tin models. *International Archives of Photogrammetry and Remote Sensing, XXXIII, Part B3*, 85-92.

Baden W, Eggelsmann R (1964) *Der wasserkreislauf eines Nordwestdeutschen hochmoores - Eine hydrologische studie über den Einfluß von Entwässerung und Kultivierung auf den Wasserhaushalt des Königsmoores. Tostedt/Han [GERMAN] The water cycle of a Northwest German bog - A hydrological study on the influence of drainage and cultivation on the water balance of the Königsmoor,* Verlag Wasser und Boden, Hamburg, Germany.

Baird AJ, Belyea LR, Morris PJ (2013) Upscaling of Peatland-Atmosphere Fluxes of Methane: Small-Scale Heterogeneity in Process Rates and the Pitfalls of "Bucket-and-Slab" Models. In: *Carbon Cycling in Northern Peatlands*, pp 37-53, American Geophysical Union.

Baird AJ, Eades PA, Surridge BWJ (2008) The hydraulic structure of a raised bog and its implications for ecohydrological modelling of bog development. *Ecohydrology*, **1**, 289-298.

Baird AJ, Morris PJ, Belyea LR (2012) The DigiBog peatland development model 1: rationale, conceptual model, and hydrological basis. *Ecohydrology*, **5**, 242-255.

Baird AJ, Surridge BWJ, Money RP (2004) An assessment of the piezometer method for measuring the hydraulic conductivity of a Cladium mariscus - Phragmites australis root mat in a Norfolk (UK) fen. *Hydrological Processes*, **18**, 275-291.

Baldocchi D, Falge E, Gu LH *et al.* (2001) FLUXNET: A new tool to study the temporal and spatial variability of ecosystem-scale carbon dioxide, water vapor, and energy flux densities. *Bulletin of the American Meteorological Society*, **82**, 2415-2434.

Balsamo G, Pappenberger F, Dutra E, Viterbo P, van den Hurk B (2011) A revised land hydrology in the ECMWF model: a step towards daily water flux prediction in a fully-closed water cycle. *Hydrological Processes*, **25**, 1046-1054.

Barr AG, Black TA, Hogg EH, Kljun N, Morgenstern K, Nesic Z (2004) Inter-annual variability in the leaf area index of a boreal aspen-hazelnut forest in relation to net ecosystem production. *Agricultural and Forest Meteorology*, **126**, 237-255.

Belyea LR (1996) Separating the Effects of Litter Quality and Microenvironment on Decomposition Rates in a Patterned Peatland. *Oikos*, **77**, 529-539.

Belyea LR (2009) Nonlinear dynamics of peatlands and potential feedbacks on the climate system. In: *Northern Peatlands and Carbon Cycling*. (eds Baird A, Belyea L, Comas X, Reeve A, Slater L), pp 5-18, Geophysical Monograph Series, American Geophysical Union, Washington DC, United States.

Belyea LR, Baird AJ (2006) Beyond "The limits to peat bog growth": Cross-scale feedback in peatland development. *Ecological Monographs*, **76**, 299-322.

Belyea LR, Clymo RS (2001) Feedback control of the rate of peat formation. *Proceedings of the Royal Society of London Series B-Biological Sciences*, **268**, 1315-1321.

Benjamini Y, Hochberg Y (1995) Controlling the False Discovery Rate: A Practical and Powerful Approach to Multiple Testing. *Journal of the Royal Statistical Society Series B (Methodological)*, **57**, 289-300.

Berne A, Delrieu G, Creutin J-D, Obled C (2004) Temporal and spatial resolution of rainfall measurements required for urban hydrology. *Journal of Hydrology*, **299**, 166-179.

Beven K (2012) Causal models as multiple working hypotheses about environmental processes. *Comptes Rendus Geoscience*, **344**, 77-88.

Beven KJ, Kirkby MJ, Schofield N, Tagg AF (1984) Testing a physically-based flood forecasting-model (TOPMODEL) for 3 UK catchments. *Journal of Hydrology*, **69**, 119-143.

Block PJ, Souza Filho FA, Sun L, Kwon HH (2009) A Streamflow Forecasting Framework using Multiple Climate and Hydrological Models. *Journal of the American Water Resources Association*, **45**, 828-843.

Blodau C, Basiliko N, Moore TR (2004) Carbon turnover in peatland mesocosms exposed to different water table levels. *Biogeochemistry*, **67**, 331-351.

Boelter DH (1969) Physical Properties of Peat as Related to Degree of Decomposition. Soil Science Society of America, 33, 606-609.

Bonan GB, Levis S, Sitch S, Vertenstein M, Oleson KW (2003) A dynamic global vegetation model for use with climate models: concepts and description of simulated vegetation dynamics. *Global Change Biology*, **9**, 1543-1566.

Bouma J (1989) Using soil survey data for quantitative land evaluation. *Advances in Soil Science*, **9**, 177-213.

Boussetta S, Balsamo G, Beljaars A *et al.* (2013) Natural land carbon dioxide exchanges in the ECMWF integrated forecasting system: Implementation and offline validation. *Journal of Geophysical Research: Atmospheres*, **118**, 5923-5946.

Bouwer H, Rice RC (1976) Slug test for determining hydraulic conductivity of unconfined aquifers with completely or partially penetrating wells. *Water Resources Research*, **12**, 423-428.

Bragazza L (2008) A climatic threshold triggers the die-off of peat mosses during an extreme heat wave. *Global Change Biology*, **14**, 2688-2695.

Bréon F-M (2006) How Do Aerosols Affect Cloudiness and Climate? *Science*, **313**, 623-624.

Bridgham SD, Pastor J, Dewey B, Weltzin JF, Updegraff K (2008) Rapid carbon response of peatlands to climate change. *Ecology*, **89**, 3041-3048.

Brock TD (1981) Calculating Solar-radiation for ecological studies. *Ecological Modelling*, **14**, 1-19.

Brooks RH, Corey AT (1964) *Hydraulic properties of porous media*, Colorado State University, Fort Collins, US.

Brown DL, Narasimhan TN, Demir Z (1995) An evaluation of the Bouwer and Rice method of slug test analysis. *Water Resources Research*, **31**, 1239-1246.

Bubier JL, Crill PM, Moore TR, Savage K, Varner RK (1998) Seasonal patterns and controls on net ecosystem CO_2 exchange in a boreal peatland complex. *Global Biogeochemical Cycles*, **12**, 703-714.

Bunce JA (1998) Effects of environment during growth on the sensitivity of leaf conductance to changes in humidity. *Global Change Biology*, **4**, 269-274.

Burnham KP, Anderson DR (2001) Kullback-Leibler information as a basis for strong inference in ecological studies. *Wildlife Research*, **28**, 111-119.

Cable J, Ogle K, Barron-Gafford G *et al.* (2013) Antecedent conditions influence soil respiration differences in shrub and grass patches. *Ecosystems*, **16**, 1230-1247.

Cagampan JP, Waddington JM (2008) Moisture dynamics and hydrophysical properties of a transplanted acrotelm on a cutover peatland. *Hydrological Processes*, **22**, 1776-1787.

Campbell BD, Grime JP (1989) A comparative study of plant responsiveness to the duration of episodes of mineral nutrient enrichment. *New Phytologist*, **112**, 261-267.

Cannavo P, Michel JC (2013) Peat particle size effects on spatial root distribution, and changes on hydraulic and aeration properties. *Scientia Horticulturae*, **151**, 11-21.

Chang S, Hahn D, Yang CH, Norquist D, Ek M (1999) Validation Study of the CAPS Model Land Surface Scheme Using the 1987 Cabauw/PILPS Dataset. *Journal of Applied Meteorology*, **38**, 405-422.

Chapin III FS, Woodwell GM, Randerson JT *et al.* (2006) Reconciling carbon-cycle concepts, terminology, and methods. *Ecosystems*, **9**, 1041-1050.

Chapman LTEH (1916) The relation between atmospheric pressure and rainfall at Kew and Valencia observatories. *Quarterly Journal of the Royal Meteorological Society*, **42**, 289-299.

Charlson RJ, Schwartz SE, Hales JM, Cess RD, Coakley JA, Jr., Hansen JE, Hofmann DJ (1992) Climate Forcing by Anthropogenic Aerosols. *Science*, **255**, 423-430.

Chen D, Achberger C, Ou T, Postgård U, Walther A, Liao Y (2015) Projecting Future Local Precipitation and Its Extremes for Sweden. *Geografiska Annaler: Series A, Physical Geography*, **97**, 25-39.

Chen D, Molina JAE, Clapp CE, Venterea RT, Palazzo AJ (2005a) Corn root influence on automated measurement of soil carbon dioxide concentrations. *Soil Science*, **170**, 779-787.

Chen JM, Chen X, Ju W, Geng X (2005b) Distributed hydrological model for mapping evapotranspiration using remote sensing inputs. *Journal of Hydrology*, **305**, 15-39.

Che Sudaka (2009). Será posible [Recorded by Kasba Music]. On *Tudo é possible* [CD]. Location: Cavernicola Records.

Ciach GJ, Krajewski WF (2006) Analysis and modeling of spatial correlation structure in small-scale rainfall in Central Oklahoma. *Advances in Water Resources*, **29**, 1450-1463.

Ciais P, Reichstein M, Viovy N *et al.* (2005) Europe-wide reduction in primary productivity caused by the heat and drought in 2003. *Nature*, **437**, 529-533.

Cirkel DG, Witte J-PM, van Bodegom PM, Nijp JJ, van der Zee SEATM (2014) The influence of spatiotemporal variability and adaptations to hypoxia on empirical relationships between soil acidity and vegetation. *Ecohydrology*, **7**, 21–32.

Cobos D (2008) *Measurement Volume of Decagon Volumetric Water Content Sensors - Application Note.*

Dahlström B (2006) *Regnintensitet i Sverige - en klimatologisk analys [Rain intensity in Sweden - a climatological analysis]*, Svensk Vatten AB, V. A. Forsk, Stockholm, Sweden.

Daniels RE, Eddy A (1985) *Handbook Of European Sphagna*, Institute of Terrestrial Ecology.

Davidson EA, Janssens IA (2006) Temperature sensitivity of soil carbon decomposition and feedbacks to climate change. *Nature*, **440**, 165-173.

de Zeeuw JW (1978) *Peat and the Dutch Golden Age: The historical meaning of energy-attainability*, Afdeling Agrarische Geschiedenis Landbouwhogeschool Wageningen, The Netherlands.

Desbarats AJ, Logan CE, Hinton MJ, Sharpe DR (2002) On the kriging of water table elevations using collateral information from a digital elevation model. *Journal of Hydrology*, **255**, 25-38.

Dilks TJK, Proctor MCF (1976) Effects of intermittent desiccation on bryophytes. *Journal of Bryology*, **9**, 249-264.

Dinsmore KJ, Billett MF, Skiba UM, Rees RM, Drewer J, Helfter C (2010) Role of the aquatic pathway in the carbon and greenhouse gas budgets of a peatland catchment. *Global Change Biology*, **16**, 2750-2762.

Dise NB (2009) Peatland Response to Global Change. *Science*, **326**, 810-811.

Dorrepaal E, Cornelissen JHC, Aerts R, Wallén BO, Van Logtestijn RSP (2005) Are growth forms consistent predictors of leaf litter quality and decomposability across peatlands along a latitudinal gradient? *Journal of Ecology*, **93**, 817-828.

Dunkerley D (2008) Identifying individual rain events from pluviograph records: a review with analysis of data from an Australian dryland site. *Hydrological Processes*, **22**, 5024-5036.

Dutton EG, Stone RS, Nelson DW, Mendonca BG (1991) Recent Interannual Variations in Solar Radiation, Cloudiness, and Surface Temperature at the South Pole. *Journal of Climate*, **4**, 848-858.

Ehret U, Zehe E, Wulfmeyer V, Warrach-Sagi K, Liebert J (2012) HESS Opinions "Should we apply bias correction to global and regional climate model data?". *Hydrology and Earth System Sciences*, **16**, 3391–3404.

Eitzinger J, Trnka M, Hosch J, Zalud Z, Dubrovsky M (2004) Comparison of CERES, WOFOST and SWAP models in simulating soil water content during growing season under different soil conditions. *Ecological Modelling*, **171**, 223-246.

Ek MB, Holtslag AAM (2004) Influence of Soil Moisture on Boundary Layer Cloud Development. *Journal of Hydrometeorology*, **5**, 86-99.

Eltahir EAB (1998) A soil moisture rainfall feedback mechanism 1. Theory and observations. *Water Resources Research*, **34**, 765-776.

Eltahir EAB, Bras RL (1996) Precipitation recycling. *Reviews of Geophysics*, **34**, 367-378.

Elumeeva TG, Soudzilovskaia NA, During HJ, Cornelissen JHC (2011) The importance of colony structure versus shoot morphology for the water balance of 22 subarctic bryophyte species. *Journal of Vegetation Science*, **22**, 152-164.

Endrizzi S, Gruber S, Dall'Amico M, Rigon R (2014) GEOtop 2.0: simulating the combined energy and water balance at and below the land surface accounting for soil freezing, snow cover and terrain effects. *Geoscientific Model Development*, **7**, 2831-2857.

Englund G, Cooper SD (2003) Scale effects and extrapolation in ecological experiments. In: *Advances in Ecological Research*, pp 161-213, Academic Press.

Eppinga MB, de Ruiter PC, Wassen MJ, Rietkerk M (2009) Nutrients and Hydrology Indicate the Driving Mechanisms of Peatland Surface Patterning. *American Naturalist*, **173**, 803-818.

Eppinga MB, Rietkerk M, Borren W, Lapshina ED, Bleuten W, Wassen MJ (2008) Regular surface patterning of peatlands: Confronting theory with field data. *Ecosystems*, **11**, 520-536.

Eriksson B (1983) *Data Concerning the Precipitation Climate of Sweden, Mean Values for the Period 1951–80*, Swedish Meteorological and Hydrological Institute (SMHI), Norrköping, Sweden.

Ernst LF (1950) *A new formula for the calculation of the permeability factor with the auger hole method. Translated from the Dutch by H. Bouwer, Cornell University, Ithaca, US, 1955.*, T.N.O. , Groningen, The Netherlands.

Feddes RA, Hoff H, Bruen M *et al.* (2001) Modeling root water uptake in hydrological and climate models. *Bulletin of the American Meteorological Society*, **82**, 2797-2809.

Fenner N, Freeman C (2011) Drought-induced carbon loss in peatlands. *Nature Geoscience*, **4**, 895-900.

Fraser CJD, Roulet NT, Lafleur M (2001) Groundwater flow patterns in a large peatland. *Journal of Hydrology*, **246**, 142-154.

Fritz C, Campbell DI, Schipper LA (2008) Oscillating peat surface levels in a restiad peatland, New Zealand - magnitude and spatiotemporal variability. *Hydrological Processes*, **22**, 3264-3274.

Frolking S, Roulet N, Fuglestvedt J (2006) How northern peatlands influence the Earth's radiative budget: Sustained methane emission versus sustained carbon sequestration. *Journal of Geophysical Research: Biogeosciences*, **111**, G01008, doi:01010.01029/02005JG000091.

Frolking S, Roulet N, Lawrence D (2013) Issues Related to Incorporating Northern Peatlands into Global Climate Models. In: *Carbon Cycling in Northern Peatlands.* (eds Baird A, Belyea L, Comas X, Reeve A, Slater L), pp 19-35, American Geophysical Union, Washington DC, United States.

Frolking S, Roulet NT (2007) Holocene radiative forcing impact of northern peatland carbon accumulation and methane emissions. *Global Change Biology*, **13**, 1079-1088.

Frolking S, Roulet NT, Moore TR, Lafleur PM, Bubier JL, Crill PM (2002) Modeling seasonal to annual carbon balance of Mer Bleue Bog, Ontario, Canada. *Global Biogeochemical Cycles*, **16**, doi:10.1029/2001GB001457.

Frolking S, Roulet NT, Tuittila E, Bubier JL, Quillet A, Talbot J, Richard PJH (2010) A new model of Holocene peatland net primary production, decomposition, water balance, and peat accumulation. *Earth Syst Dynam*, **1**, 1-21.

Gadonneix P, Nadeau M-J, Kim YD *et al.* (2013) *World Energy Resources. 2013 Survey*, World Energy Council, London, UK.

Garrels, Christ (1965) *Solutions, Minerals, and Equilibria*, Harper, Row, New York U. S. A.

Garbage (1995) I'm only happy when it rains [Recorded by Smart Studios]. On *Garbage* [CD]. Location: Mushroom Records UK.

Gerard M (2011) *Morphological characterisation of Sphagnum fuscum, Sphagnum balticum and Sphagnum majus in order to explain their hydrological properties, BSc Thesis*, Wageningen University, Wageningen.

Gerdol R, Bonora A, Gualandri R, Pancaldi S (1996) CO_2 exchange, photosynthetic pigment composition, and cell ultrastructure of *Sphagnum* mosses during dehydration and subsequent rehydration. *Canadian Journal Of Botany*, **74**, 726-734.

Gignac LD, Vitt DH, Zoltai SC, Bayley SE (1991) Bryophyte response surfaces along climatic, chemical, and physical gradients in peatlands of western Canada. *Nova Hedwigia*, **53**, 27-71.

Glaser PH, Chanton JP, Morin P *et al.* (2004) Surface deformations as indicators of deep ebullition fluxes in a large northern peatland. *Global Biogeochemical Cycles*, **18**, GB1003, doi:1010.1029/2003GB002069.

Gorham E (1991) Northern Peatlands - Role In The Carbon Cycle And Probable Responses To Climatic Warming. *Ecological Applications*, **1**, 182-195.

Graham EA, Mulkey SS, Kitajima K, Phillips NG, Wright SJ (2003) Cloud cover limits net CO_2 uptake and growth of a rainforest tree during tropical rainy seasons. *Proceedings of the National Academy of Sciences*, **100**, 572-576.

Granath G, Strengbom J, Breeuwer A, Heijmans MMPD, Berendse F, Rydin H (2009) Photosynthetic performance in *Sphagnum* transplanted along a latitudinal nitrogen deposition gradient. *Oecologia*, **159**, 705-715.

Granath G, Strengbom J, Rydin H (2010) Rapid ecosystem shifts in peatlands: linking plant physiology and succession. *Ecology*, **91**, 3047-3056.

Granberg G, Grip H, Lofvenius MO, Sundh I, Svensson BH, Nilsson M (1999) A simple model for simulation of water content, soil frost, and soil temperatures in boreal mixed mires. *Water Resources Research*, **35**, 3771-3782.

Grootjans AP, van Wirdum G, Kemmers R, van Diggelen R (1996) Ecohydrology in The Netherlands: principles of an application-driven interdiscipline. *Acta Botanica Neerlandica*, **45**, 491-516.

Gupta RK (1977) A study of photosynthesis and leakage of solutes in relation to the desiccation effects in bryophytes. *Canadian Journal Of Botany*, **55**, 1186-1194.

Gupta SC, Larson WE (1979) Estimating soil water retention characteristics from particle size distribution, organic matter percent, and bulk density. *Water Resources Research*, **15**, 1633-1635.

Haitjema HM, Mitchell-Bruker S (2005) Are Water Tables a Subdued Replica of the Topography? *Ground Water*, **43**, 781-786.

Hájek T, Beckett RP (2008) Effect of water content components on desiccation and recovery in *Sphagnum* mosses. *Annals of Botany*, **101**, 165-173.

Hansen MC, Potapov PV, Moore R *et al.* (2013) High-Resolution Global Maps of 21st-Century Forest Cover Change. *Science*, **342**, 850-853.

Hargreaves GJ, Samani ZA (1985) Reference crop evapotranspiration from temperature. *Applied engineering in agriculture*, **1**, 96-99.

Haverkamp R, Vauclin M (1979) A note on estimating finite difference interblock hydraulic conductivity values for transient unsaturated flow problems. *Water Resources Research*, **15**, 181-187.

Hayward PM, Clymo RS (1982) Profiles of Water-Content and Pore-Size in *Sphagnum* and Peat, and Their Relation to Peat Bog Ecology. *Proceedings of the Royal Society of London Series B-Biological Sciences*, **215**, 299-325.

Heijmans MMPD, Arp WJ, Berendse F (2001) Effects of elevated CO_2 and vascular plants on evapotranspiration in bog vegetation. *Global Change Biology*, **7**, 817-827.

Heijmans MMPD, Mauquoy D, van Geel B, Berendse F (2008) Long-term effects of climate change on vegetation and carbon dynamics in peat bogs. *Journal of Vegetation Science*, **19**, 307-320.

Heijmans MMPD, van der Knaap YAM, Holmgren M, Limpens J (2013) Persistent versus transient tree encroachment of temperate peat bogs: effects of climate warming and drought events. *Global Change Biology*, **19**, 2240-2250.

Heiskanen J (1995) Physical properties of two-component growth media based on *Sphagnum* peat and their implications for plant-available water and aeration. *Plant and Soil*, **172**, 45-54.

Heisler JL, Weltzin JF (2006) Variability matters: towards a perspective on the influence of precipitation on terrestrial ecosystems. *New Phytologist*, **172**, 189-192.

Henderson-Sellers A, Yang ZL, Dickinson RE (1993) The project for intercomparison of land-surface parameterization schemes. *Bulletin of the American Meteorological Society*, **74**, 1335-1349.

Hillel D (2004) *Introduction to environmental soil physics*, Elsevier Academic Press, Amsterdam, NL.

Hoaglin DC, Iglewicz B, Tukey JW (1986) Performance of Some Resistant Rules for Outlier Labeling. *Journal of the American Statistical Association*, **81**, 991-999.

Hoeksema RJ, Clapp RB, Thomas AL, Hunley AE, Farrow ND, Dearstone KC (1989) Cokriging model for estimation of water table elevation. *Water Resources Research*, **25**, 429-438.

Hoffmann R (2014) *An Environmental History of Medieval Europe*, Cambridge University Press, Cambridge, UK.

Holmes PR, Fowles AP, Boyce DC, Reed DK (1993) The ground beetle (coleoptera: Carabidae) fauna of welsh peatland biotopes—species assemblages in relation to peatland habitats and management. *Biological Conservation*, **65**, 61-67.

Hovenden MJ, Newton PCD, Wills KE (2014) Seasonal not annual rainfall determines grassland biomass response to carbon dioxide. *Nature*, **511**, 583-586.

Hughes PDM, Mauquoy D, Barber KE, Langdon PG (2000) Mire-development pathways and palaeoclimatic records from a full Holocene peat archive at Walton Moss, Cumbria, England. *The Holocene*, **10**, 465-479.

Huxman TE, Snyder KA, Tissue D *et al.* (2004) Precipitation pulses and carbon fluxes in semiarid and arid ecosystems. *Oecologia*, **141**, 254-268.

Hvorslev J (1951) *Time Lag and Soil Permeability in Groundwater Observations, Waterways Experimental Station Bulletin 36.*

Hyder Z, Butler JJ (1995) Slug tests in unconfined formations - an assessment of the Bouwer and Rice technique. *Ground Water*, **33**, 16-22.

Hyder Z, Butler JJ, McElwee CD, Liu WZ (1994) Slug tests in partially penetrating wells. *Water Resources Research*, **30**, 2945-2957.

Ingram HAP (1978) Soil layers in mires: Function and terminology. *Journal of Soil Science*, **29**, 224-227.

Ingram HAP (1982) Size and shape in raised mire ecosystems: a geophysical model. *Nature*, **297**, 300-303.

IPCC (2007) *Climate Change 2007: The Physical Science Basis. Contribution of Working Group I to the Fourth Assessment Report of the Intergovernmental Panel on Climate Change*, Cambridge University Press, Cambridge, UK & New York, NY, USA.

IPCC (2013) Long-term climate change: projections, commitments and irreversability. In: *Climate Change 2013: The Physical Science Basis Contribution of Working Group I to the Fifth Assessment Report of the Intergovernmental Panel on Climate Change.* (eds Stocker TF, Qin D, Plattner G-K, Tignor M, Allen SK, Boschung J, Nauels A, Xia Y, Bex V, Midgley PM), pp 1535, Cambridge University Press, Cambridge, United Kingdom and New York, USA.

Ise T, Dunn AL, Wofsy SC, Moorcroft PR (2008) High sensitivity of peat decomposition to climate change through water-table feedback. *Nature*, **1**, 763-766.

Ivanov KE, Thomson A, Ingram HAP (1981) *Water movement in Mirelands*, Academic Press, London, UK.

Janssen PHM (1994) Assessing sensitivities and uncertainties in models: A critical evaluation. In: *Predictability and non-linear modelling in natural sciences and economics.* (eds Grasman J, van Straten G), pp 344-361, Kluwer, Dordrecht, The Netherlands.

Jebara T, Azarbayejani A, Pentland A (1999) 3D structure from 2D motion. *Signal Processing Magazine, IEEE*, **16**, 66-84.

Jobbágy EG, Jackson RB (2000) The vertical distribution of soil organic carbon and its relation to climate and vegetation. *Ecological Applications*, **10**, 423-436.

Joosten H, Clarke D (2002) *Wise use of mires and peatlands*, International Mire Conservation Group and International Peat Society, Jyskä, Finland.

Journel AG, Huijbregts CJ (1978) *Mining Geostatistics*, Academic press inc, Londen, UK.

Karofeld E (1998) The dynamics of the formation and development of hollows in raised bogs in Estonia. *The Holocene*, **8**, 697-704.

Kellner E (2001) Surface Energy Exchange and Hydrology of a Poor *Sphagnum* Mire. PhD Thesis. Uppsala.

Kellner E, Halldin S (2002) Water budget and surface-layer water storage in a *Sphagnum* bog in central Sweden. *Hydrological Processes*, **16**, 87-103.

Kemmers RH (1986) *Perspectives in modelling of root zone of spontaneous vegetation at wet and damp sites in relation to regional water management*, Proc. Inf., CHO-TNO, The Hague, Netherlands.

Kennedy GW, Price JS (2004) Simulating soil water dynamics in a cutover bog. *Water Resources Research*, **40**.

Kennedy GW, Price JS (2005) A conceptual model of volume-change controls on the hydrology of cutover peats. *Journal of Hydrology*, **302**, 13-27.

Ketcheson SJ, Price JS (2013) Characterization of the fluxes and stores of water within newly formed *Sphagnum* moss cushions and their environment. *Ecohydrology*, **7**, 771–782.

Kettridge N, Binley A (2010) Evaluating the effect of using artificial pore water on the quality of laboratory hydraulic conductivity measurements of peat. *Hydrological Processes*, **24**, 2629-2640.

Kettridge N, Turetsky MR, Sherwood JH *et al.* (2015) Moderate drop in water table increases peatland vulnerability to post-fire regime shift. *Nature*, **5**, doi:10.1038/srep08063.

Keuper F, Parmentier F-J, Blok D *et al.* (2012) Tundra in the rain: differential vegetation responses to three years of experimentally doubled summer precipitation in Siberian shrub and Swedish bog tundra. *Ambio*, **41**, 269-280.

Kleinen T, Brovkin V, Schuldt RJ (2012) A dynamic model of wetland extent and peat accumulation: results for the Holocene. *Biogeosciences*, **9**, 235-248.

Klute A (1986) *Methods of Soil Analysis. Part 1. Physical and Mineralogical Methods*, Soil Science Society of America, Madison, Wisconsin, USA.

Knapp AK, Beier C, Briske DD *et al.* (2008) Consequences of more extreme precipitation regimes for terrestrial ecosystems. *BioScience*, **58**, 811-821.

Knapp AK, Fay PA, Blair JM *et al.* (2002) Rainfall Variability, Carbon Cycling, and Plant Species Diversity in a Mesic Grassland. *Science*, **298**, 2202-2205.

Knorr W, Prentice IC, House JI, Holland EA (2005) Long-term sensitivity of soil carbon turnover to warming. *Nature*, **433**, 298-301.

Koehler A-K, Sottocornola M, Kiely G (2011) How strong is the current carbon sequestration of an Atlantic blanket bog? *Global Change Biology*, **17**, 309-319.

Korpela I, Koskinen M, Vasander H, Holopainen M, Minkkinen K (2009) Airborne small-footprint discrete-return LiDAR data in the assessment of boreal mire surface patterns, vegetation, and habitats. *Forest Ecology and Management*, **258**, 1549-1566.

Krinner G, Viovy N, de Noblet-Ducoudré N *et al.* (2005) A dynamic global vegetation model for studies of the coupled atmosphere-biosphere system. *Global Biogeochemical Cycles*, **19**, GB1015, doi:1010.1029/2003GB002199.

Kuiper JJ, Mooij WM, Bragazza L, Robroek BJM (2013) Plant functional types define magnitude of drought response in peatland CO_2 exchange. *Ecology*, **95**, 123-131.

Kujala K, Seppälä M, Holappa T (2008) Physical properties of peat and palsa formation. *Cold Regions Science and Technology*, **52**, 408-414.

Lafleur PM, Hember RA, Admiral SW, Roulet NT (2005) Annual and seasonal variability in evapotranspiration and water table at a shrub-covered bog in southern Ontario, Canada. *Hydrological Processes*, **19**, 3533-3550.

Laine AM, Bubier J, Riutta T, Nilsson MB, Moore TR, Vasander H, Tuittila E-S (2011) Abundance and composition of plant biomass as potential controls for mire net ecosytem CO_2 exchange. *Botany*, **90**, 63-74.

Laing CG, Granath G, Belyea LR, Allton KE, Rydin H (2014) Tradeoffs and scaling of functional traits in *Sphagnum* as drivers of carbon cycling in peatlands. *Oikos*, **123**, 817-828.

Lappalainen E (1996) *Global peat resources*, International Peat Society, Jyskä, Finland.

Larmola T, Tuittila E-S, Tiirola M *et al.* (2010) The role of *Sphagnum* mosses in the methane cycling of a boreal mire. *Ecology*, **8**, 2356–2365.

le Roux PC, Aalto J, Luoto M (2013) Soil moisture's underestimated role in climate change impact modelling in low-energy systems. *Global Change Biology*, **19**, 2965-2975.

Lee X, Wu HJ, Sigler J, Oishi C, Siccama T (2004) Rapid and transient response of soil respiration to rain. *Global Change Biology*, **10**, 1017-1026.

Leenders KAHW (1989) *Een onderzoek naar de ligging en exploitatie van thans verdwenen venen in het gebied tussen Antwerpen, Turnhout, Geertruidenberg en Willemstad (1250 - 1750) [IN DUTCH]*, Gemeentekrediet van België. Wageningen Pudoc, Brussels, Belgium.

Legates DR, Mahmood R, Levia DF, DeLiberty TL, Quiring SM, Houser C, Nelson FE (2011) Soil moisture: A central and unifying theme in physical geography. *Progress in Physical Geography*, **35**, 65-86.

Leppälä M, Laine AM, Seväkivi M-L, Tuittila E-S (2011) Differences in CO_2 dynamics between successional mire plant communities during wet and dry summers. *Journal of Vegetation Science*, **22**, 357-366.

Letts MG, Lafleur PM, Roulet NT (2005) On the relationship between cloudiness and net ecosystem carbon dioxide exchange in a peatland ecosystem. *Ecoscience*, **12**, 53-59.

Lewis F, Butler A, Gilbert L (2011) A unified approach to model selection using the likelihood ratio test. *Methods in Ecology and Evolution*, **2**, 155-162.

Lichtenthaler HK (1987) Chlorophylls and carotenoids: Pigments of photosynthetic biomembranes. *Methods Enzymology*, **148**, 350-382.

Limpens J, Berendse F, Blodau C *et al.* (2008) Peatlands and the carbon cycle: from local processes to global implications - a synthesis. *Biogeosciences*, **5**, 1475-1491.

Limpens J, Granath G, Aerts R *et al.* (2012) Glasshouse vs field experiments: do they yield ecologically similar results for assessing N impacts on peat mosses? *New Phytologist*, **195**, 408-418.

Limpens J, Holmgren M, Jacobs CMJ, Van der Zee SEATM, Karofeld E, Berendse F (2014a) How Does Tree Density Affect Water Loss of Peatlands? A Mesocosm Experiment. *PLoS ONE*, **9**, e91748.

Limpens J, van Egmond E, Li B, Holmgren M (2014b) Do plant traits explain tree seedling survival in bogs? *Functional Ecology*, **28**, 283-290.

Lode E, Leivits M (2011) The LiDAR-based topo-hydrological modelling of the Nigula mire, SW Estonia. *Estonian Journal of Earth Sciences*, **60**, 232-248.

Loisel J, Gallego-Sala AV, Yu Z (2012) Global-scale pattern of peatland *Sphagnum* growth driven by photosynthetically active radiation and growing season length. *Biogeosciences*, **9**, 2737-2746.

Loisel J, Yu Z, Beilman DW *et al.* (2014) A database and synthesis of northern peatland soil properties and Holocene carbon and nitrogen accumulation. *The Holocene*, 1-15, 10.1177/0959683614538073.

Loreau M, Naeem S, Inchausti P *et al.* (2001) Biodiversity and Ecosystem Functioning: Current Knowledge and Future Challenges. *Science*, **294**, 804-808.

Luken JO (1985) Zonation of *Sphagnum* Mosses: Interactions among Shoot Growth, Growth Form, and Water Balance. *The Bryologist*, **88**, 374-379.

Lund M, Christensen TR, Lindroth A, Schubert P (2012) Effects of drought conditions on the carbon dioxide dynamics in a temperate peatland. *Environmental Research Letters*, **7**, 045704, doi:045710.041088/041748-049326/045707/045704/045704.

Mac Nally R (2000) Regression and model-building in conservation biology, biogeography and ecology: The distinction between and reconciliation of 'predictive' and 'explanatory' models. *Biodiversity and Conservation*, **9**, 655-671.

Malmström C (1923) Degerö Stormyr - En botanisk, hydrologisk och utvecklingshistorisk undersökning över ett nordsvenskt myrkomplex [IN SWEDISH]. PhD Thesis. Uppsala, Stockholm.

Marschall M, Proctor MCF (2004) Are bryophytes shade plants? Photosynthetic light responses and proportions of chlorophyll a, chlorophyll b and total carotenoids. *Annals of Botany*, **94**, 593-603.

Masson V, Le Moigne P, Martin E *et al.* (2013) The SURFEXv7.2 land and ocean surface platform for coupled or offline simulation of earth surface variables and fluxes. *Geoscientific Model Development*, **6**, 929-960.

McCarter CPR, Price JS (2014) Ecohydrology of *Sphagnum* moss hummocks: mechanisms of capitula water supply and simulated effects of evaporation. *Ecohydrology*, **7**, 33-44.

McNeil P, Waddington JM (2003) Moisture Controls on *Sphagnum* Growth and CO_2 Exchange on a Cutover Bog. *Journal of Applied Ecology*, **40**, 354-367.

Meisner A, Bååth E, Rousk J (2013) Microbial growth responses upon rewetting soil dried for four days or one year. *Soil Biology and Biochemistry*, **66**, 188-192.

Mellegård H, Stalheim T, Hormazabal V, Granum PE, Hardy SP (2009) Antibacterial activity of sphagnum acid and other phenolic compounds found in *Sphagnum* papillosum against food-borne bacteria. *Letters in Applied Microbiology*, **49**, 85-90.

Metselaar K (1999) Auditing predictive models: a case study in crop growth. PhD Thesis. Wageningen University, Wageningen, The Netherlands.

Metselaar K, de Jong van Lier Q (2007) The Shape of the Transpiration Reduction Function under Plant Water Stress. *Vadose Zone Journal*, **6**, 124-139.

Monteith JL (1965) Evaporation and environment. *Symposia of the Society for Experimental Biology*, **19**, 205-234.

Moore PA, Waddington JM (2015) Modelling *Sphagnum* moisture stress in response to projected 21st-century climate change. *Hydrological Processes*, doi: 10.1002/hyp.10484.

Moore TR, Bubier JL, Frolking SE, Lafleur PM, Roulet NT (2002) Plant biomass and production and CO2 exchange in an ombrotrophic bog. *Journal of Ecology*, **90**, 25-36.

Moore TR, Dalva M (1993) The influence of temperature and water-table position on carbon-dioxide and methane emissions from laboratory columns of peatland soils. *Journal of Soil Science*, **44**, 651-664.

Morris CD (1984) A stochastic model for a small-time-interval-intermittent hydrologic process. *Journal of Hydrology*, **68**, 247-272.

Morris PJ, Belyea LR, Baird AJ (2011) Ecohydrological feedbacks in peatland development: a theoretical modelling study. *Journal of Ecology*, **99**, 1190-1201.

Murray KJ, Harley PC, Beyers J, Walz H, Tenhunen JD (1989) Water-content effects on photosynthetic response of *Sphagnum* mosses from the foothills of the Philip Smith mountains, Alaska. *Oecologia*, **79**, 244-250.

Nakicenovic N, Alcamo J, Davis G *et al.* (2000) *Special report on emissions scenarios: a special report of Working Group III of the Intergovernmental Panel on Climate Change*, Pacific Northwest National Laboratory, Richland, WA (US), Environmental Molecular Sciences Laboratory (US), Cambridge, UK.

Nemani RR, Keeling CD, Hashimoto H *et al.* (2003) Climate-Driven Increases in Global Terrestrial Net Primary Production from 1982 to 1999. *Science*, **300**, 1560-1563.

Nijp JJ, Limpens J, Metselaar K, Peichl M, Nilsson MB, van der Zee SEATM, Berendse F (2015) Rain events decrease boreal peatland net CO_2 uptake through reduced light availability. *Global Change Biology*, **21**, 2309-2320.

Nijp JJ, Limpens J, Metselaar K, van der Zee S, Berendse F, Robroek BJM (2014) Can frequent precipitation moderate the impact of drought on peatmoss carbon uptake in northern peatlands? *New Phytologist*, **203**, 70-80.

Nilsson M, Bohlin E (1993) Methane and Carbon Dioxide Concentrations in Bogs and Fens--with Special Reference to the Effects of the Botanical Composition of the Peat. *Journal of Ecology*, **81**, 615-625.

Nilsson M, Mikkela C, Sundh I, Granberg G, Svensson BH, Ranneby B (2001) Methane emission from Swedish mires: National and regional budgets and dependence on mire vegetation. *Journal of Geophysical Research-Atmospheres*, **106**, 20847-20860.

Nilsson M, Sagerfors J, Buffam I *et al.* (2008) Contemporary carbon accumulation in a boreal oligotrophic minerogenic mire - a significant sink after accounting for all C-fluxes. *Global Change Biology*, **14**, 2317-2332.

NOAA (2015) www.esrl.noaa.gov/gmd/ccgg/trends/. 2015-07-06.

Nungesser MK (2003) Modelling microtopography in boreal peatlands: hummocks and hollows. *Ecological Modelling*, **165**, 175-207.

Nuttle WK, Hemond HF, Stolzenbach KD (1990) Mechanisms of water storage in salt marsh sediments: The importance of dilation. *Hydrological Processes*, **4**, 1-13.

O'Gorman PA, Schneider T (2009) The physical basis for increases in precipitation extremes in simulations of 21st-century climate change. *Proceedings of the National Academy of Sciences*, **106**, 14773-14777.

Ogle K, Reynolds JF (2004) Plant responses to precipitation in desert ecosystems: integrating functional types, pulses, thresholds, and delays. *Oecologia*, **141**, 282-294.

Olefeldt D, Roulet NT, Bergeron O, Crill P, Backstrand K, Christensen TR (2012) Net carbon accumulation of a high-latitude permafrost palsa mire similar to permafrost-free peatlands. *Geophysical Research Letters*, **39**, L03501, doi: 03510.01029/02011GL050355.

Oreskes N, Shraderfrechette K, Belitz K (1994) Verification, validation, and confirmation of numerical models in in the earth sciences. *Science*, **263**, 641-646.

Päivänen J (1973) Hydraulic conductivity and water retention in peat soils. *Acta Forestalia Fennica*, **129**.

Päivänen J (1982) Physical properties of peat samples in relation to shrinkage upon drying. *Silva Fennica*, **16**, 247-265.

Pebesma EJ (2004) Multivariable geostatistics in S: the gstat package. *Computers & Geosciences*, **30**, 683-691.

Peel MC, Finlayson BL, McMahon TA (2007) Updated world map of the Koppen-Geiger climate classification. *Hydrology and Earth System Sciences*, **11**, 1633-1644.

Peichl M, Öquist M, Löfvenius MO *et al.* (2014) A 12-year record reveals pre-growing season temperature and water table level threshold effects on the net carbon dioxide exchange in a boreal fen. *Environmental Research Letters*, **9**, 055006, doi:055010.051088/051748-059326/055009/055005/055006.

Peichl M, Sagerfors J, Lindroth A *et al.* (2013) Energy exchange and water budget partitioning in a boreal minerogenic mire. Journal of Geophysical Research - Biogeosciences, 118, 1-13.

Penman HL (1948) Natural evaporation from open water, bare soil and grass. *Proceedings of the Royal Society of London*, **193**, 120-146.

Peterson G, Allen CR, Holling CS (1998) Ecological Resilience, Biodiversity, and Scale. *Ecosystems*, **1**, 6-18.

Piani C, Haerter JO, Coppola E (2010) Statistical bias correction for daily precipitation in regional climate models over Europe. *Theoretical and Applied Climatology*, **99**, 187-192.

Porporato A, Daly E, Rodriguez-Iturbe I (2004) Soil water balance and ecosystem response to climate change. *American Naturalist*, **164**, 625-632.

Potts DL, Huxman TE, Cable JM *et al.* (2006) Antecedent moisture and seasonal precipitation influence the response of canopy-scale carbon and water exchange to rainfall pulses in a semi-arid grassland. *New Phytologist*, **170**, 849-860.

Powell MJD (1964) An efficient method for finding the minimum of a function of several variables without calculating derivatives. *The Computer Journal*, **7**, 155-162.

Price JS (2003) Role and character of seasonal peat soil deformation on the hydrology of undisturbed and cutover peatlands. *Water Resources Research*, **39**, 1241-1251.

Price JS, Cagampan J, Kellner E (2005) Assessment of peat compressibility: is there an easy way? *Hydrological Processes*, **19**, 3469-3475.

Price JS, Elrick DE, Strack M, Brunet N, Faux E (2008) A method to determine unsaturated hydraulic conductivity in living and undecomposed *Sphagnum* moss. *Soil Science Society Of America Journal*, **72**, 487-491.

Price JS, Schlotzhauer SM (1999) Importance of shrinkage and compression in determining water storage changes in peat: the case of a mined peatland. *Hydrological Processes*, **13**, 2591-2601.

Price JS, Whittington PN (2010) Water flow in *Sphagnum* hummocks: Mesocosm measurements and modelling. *Journal of Hydrology*, **381**, 333-340.

Proctor (2000) Mosses and Alternative Adaptation to Life on Land. *New Phytologist*, **148**, 1-3.

Proctor MCF, Ligrone R, Duckett JG (2007a) Desiccation Tolerance in the Moss Polytrichum formosum: Physiological and Fine-structural Changes during Desiccation and Recovery. *Annals of Botany*, **99**, 1243-1243.

Proctor MCF, Oliver MJ, Wood AJ, Alpert P, Stark LR, Cleavitt NL, Mishler BD (2007b) Desiccation-tolerance in bryophytes: a review. *The Bryologist*, **110**, 595-621.

Proctor MCF, Tuba Z (2002) Tansley Review No. 141. Poikilohydry and Homoihydry: Antithesis or Spectrum of Possibilities? *New Phytologist*, **156**, 327-349.

Quillet A, Garneau M, Frolking S (2013) Sobol' sensitivity analysis of the Holocene Peat Model: What drives carbon accumulation in peatlands? *Journal of Geophysical Research - Biogeosciences*, **118**, 203-214.

Quinn P, Beven K, Culf A (1995) The introduction of macroscale hydrological complexity into land surface-atmosphere transfer models and the effect on planetary boundary layer development. *Journal of Hydrology*, **166**, 421-444.

R Core Team (2014) R: A language and environment for statistical computing, R Foundation for Statistical Computing, Vienna, Austria. URL http://www.R-project.org/.

Raats PAC (1972) Steady Infiltration From Sources At Arbitrary Depth. *Soil Science Society of America Proceedings*, **36**, 399-401.

Rackham H, Jones WHS, Eichholz DE (1949) *Naturalis Historia. Pliny's Natural History*, Harvard University Press, Massachusetts, US.

Rakovec O, Hazenberg P, Torfs PJJF, Weerts AH, Uijlenhoet R (2012) Generating spatial precipitation ensembles: impact of temporal correlation structure. *Hydrology and Earth System Sciences*, **16**, 3419-3434.

Ramanathan V, Crutzen PJ, Kiehl JT, Rosenfeld D (2001) Aerosols, Climate, and the Hydrological Cycle. *Science*, **294**, 2119-2124.

Reynolds JF, Kemp PR, Ogle K, Fernandez RJ (2004) Modifying the 'pulse-reserve' paradigm for deserts of North America: precipitation pulses, soil water, and plant responses. *Oecologia*, **141**, 194-210.

Rietkerk M, Dekker SC, de Ruiter PC, van de Koppel J (2004) Self-organized patchiness and catastrophic shifts in ecosystems. *Science*, **305**, 1926-1929.

Riley JL (2011) *Wetlands of the Ontario Hudson Bay Lowland: A Regional Overview*, Nature Conservancy of Canada, Toronto, Canada.

Riutta T, Laine J, Tuittila ES (2007) Sensitivity of CO_2 Exchange of Fen Ecosystem Components to Water Level Variation. *Ecosystems*, **10**, 718-733.

Robroek BJM, Limpens J, Breeuwer A, Crushell PH, Schouten MGC (2007a) Interspecific competition between *Sphagnum* mosses at different water tables. *Functional Ecology*, **21**, 805-812.

Robroek BJM, Limpens J, Breeuwer A, Schouten MGC (2007b) Effects of water level and temperature on performance of four *Sphagnum* mosses. *Plant Ecology*, **190**, 97-107.

Robroek BJM, Schouten MGC, Limpens J, Berendse F, Poorter H (2009) Interactive effects of water table and precipitation on net CO_2 assimilation of three co-occurring *Sphagnum* mosses differing in distribution above the water table. *Global Change Biology*, **15**, 680-691.

Rossi RE, Mulla DJ, Journel AG, Franz EH (1992) Geostatistical tools for modeling and interpreting ecological spatial dependence. *Ecological Monographs*, **62**, 277-314.

Roulet NT (1991) Surface level and water table fluctuations in a subarctic fen. *Arctic and Alpine Research*, **23**, 303-310.

Roulet NT, Lafleur PM, Richard PJH, Moore TR, Humphreys ER, Bubier J (2007) Contemporary carbon balance and late Holocene carbon accumulation in a northern peatland. *Global Change Biology*, **13**, 397-411.

Roulet NT, Moore T, Bubier J, Lafleur P (1992) Northern fens - Methane flux and climatic-change. *Tellus Series B-Chemical and Physical Meteorology*, **44**, 100-105.

Rudolph H, Samland J (1985) Occurrence and metabolism of sphagnum acid in the cell walls of bryophytes. *Phytochemistry*, **24**, 745-749.

Rydin H (1985) Effect of Water Level on Dessication of *Sphagnum* in Relation to Surrounding Sphagna. *Oikos*, **45**, 374-379.

Rydin H (1986) Competition and niche separation in *Sphagnum*. *Canadian Journal Of Botany*, **64**, 1817-1824.

Rydin H (1993) Interspecific competition between *Sphagnum* Mosses On A Raised Bog. *Oikos*, **66**, 413-423.

Rydin H (1995) Effects of density and water level on recruitment, mortality and shoot size in *Sphagnum* populations. *Journal of Bryology*, **18**, 439-453.

Rydin H, Jeglum JR (2013) The biology of peatlands. Oxford University Press, Oxford, United Kingdom.

Rydin H, McDonald AJS (1985a) Photosynthesis in *Sphagnum* at different water contents. *Journal of Bryology*, **13**, 579-584.

Rydin H, McDonald AJS (1985b) Tolerance of *Sphagnum* to water level. *Journal of Bryology*, **13**, 571-578.

Sagerfors J, Lindroth A, Grelle A, Klemedtsson L, Weslien P, Nilsson M (2008) Annual CO_2 exchange between a nutrient-poor, minerotrophic, boreal mire and the atmosphere. *Journal of Geophysical Research-Biogeosciences*, **113**, G01001.

Scanlon D, Moore T (2000) Carbon dioxide production from peatland soil profiles: The influence of temperature, oxic/anoxic conditions and substrate. *Soil Science*, **165**, 153-160.

Schaap MG, Leij FJ, van Genuchten MT (2001) Rosetta: a computer program for estimating soil hydraulic parameters with hierarchical pedotransfer functions. *Journal of Hydrology*, **251**, 163-176.

Scheffer F, Schachtschabel P (1989) *Lehrbuck der bodenkunde, 12th edition*, Stuttgart, Germany.

Scheffer M, Carpenter S, Foley JA, Folke C, Walker B (2001) Catastrophic shifts in ecosystems. *Nature*, **413**, 591-596.

Scherrer D, Körner C (2011) Topographically controlled thermal-habitat differentiation buffers alpine plant diversity against climate warming. *Journal of Biogeography*, **38**, 406-416.

Schilling W (1991) Rainfall data for urban hydrology: what do we need? *Atmospheric Research*, **27**, 5-21.

Schipperges B, Rydin H (1998) Response of photosynthesis of *Sphagnum* species from contrasting microhabitats to tissue water content and repeated desiccation. *New Phytologist*, **140**, 677-684.

Schlotzhauer SM, Price JS (1999) Soil water flow dynamics in a managed cutover peat field, Quebec: Field and laboratory investigations. *Water Resources Research*, **35**, 3675-3683.

Schothorst CJ (1977) Subsidence of low moor peat soils in the western Netherlands. *Geoderma*, **17**, 265-291.

Schouwenaars JM, Gosen AM (2007) The sensitivity of *Sphagnum* to surface layer conditions in a re-wetted bog: a simulation study of water stress. *Mires and peat*, **2**, 1-19.

Schwinning S, Ehleringer JR (2001) Water Use Trade-Offs and Optimal Adaptations to Pulse-Driven Arid Ecosystems. *Journal of Ecology*, **89**, 464-480.

Schwinning S, Sala OE (2004) Hierarchy of responses to resource pulses in and and semi-arid ecosystems. *Oecologia*, **141**, 211-220.

Seity Y, Brousseau P, Malardel S *et al.* (2010) The AROME-France Convective-Scale Operational Model. *Monthly Weather Review*, **139**, 976-991.

Seneviratne SI, Corti T, Davin EL *et al.* (2010) Investigating soil moisture–climate interactions in a changing climate: A review. *Earth-Science Reviews*, **99**, 125-161.

Seneviratne SI, Luthi D, Litschi M, Schar C (2006) Land-atmosphere coupling and climate change in Europe. *Nature*, **443**, 205-209.

Sjörs H (1948) Myrvegetation i Bergslagen. [Mire vegetation in Bergslagen, Sweden.]. *Acta Phytogeographica Suecica*, **21**, 1-299.

Skre O, Oechel WC, Miller PM (1983) Moss leaf water content and solar radiation at the moss surface in a mature black spruce forest in central Alaska. *Canadian Journal of Forest Research*, **13**, 860-868.

SMHI, Swedish Meteorological and Hydrological Institute, (2014) Open Data. November 2014. http://opendata-catalog.smhi.se/explore/.

Smith AC, Koper N, Francis CM, Fahrig L (2009) Confronting collinearity: comparing methods for disentangling the effects of habitat loss and fragmentation. *Landscape Ecology*, **24**, 1271-1285.

Smith DC, Molesworth S (1973) Lichen Physiology. XIII. Effects of Rewetting Dry Lichens. New Phytologist, 72, 525-533.

Smolders AJP, Tomassen HBM, Leon PML, Lomans BP, Roelofs JGM (2002) Peat Bog Restoration by Floating Raft Formation: The Effects of Groundwater and Peat Quality. *Journal of Applied Ecology*, **39**, 391-401.

Soden BJ, Held IM (2006) An assessment of climate feedbacks in coupled ocean-atmosphere models. *Journal of Climate*, **19**, 3354-3360.

Sonesson M, Carlsson BÅ, Callaghan TV, Halling S, Björn LO, Bertgren M, Johanson U (2002) Growth of Two Peat-Forming Mosses in Subarctic Mires: Species Interactions and Effects of Simulated Climate Change. *Oikos*, **99**, 151-160.

Sonnentag O, Chen JM, Roulet NT, Ju W, Govind A (2008) Spatially explicit simulation of peatland hydrology and carbon dioxide exchange: Influence of mesoscale topography. *Journal of Geophysical Research: Biogeosciences*, **113**, G02005, doi:02010.01029/02007JG000605.

Spieksma JFm, Schouwenaars JM, Blankenburg J (1996) Combined Modelling of Groundwater Table and Open Water Level in Raised Mires. *Nordic Hydrology*, **27**, 231-246.

Spitzer K, Danks HV (2005) Insect biodiversity of boreal peat bogs. *Annual Review of Entomology*, **51**, 137-161.

St-Hilaire F, Wu J, Roulet NT, Frolking S, Lafleur PM, Humphreys ER, Arora V (2010) McGill wetland model: evaluation of a peatland carbon simulator developed for global assessments. *Biogeosciences*, **7**, 3517-3530.

Stanhill G, Cohen S (2001) Global dimming: a review of the evidence for a widespread and significant reduction in global radiation with discussion of its probable causes and possible agricultural consequences. *Agricultural and Forest Meteorology*, **107**, 255-278.

Stocker BD, Spahni R, Joos F (2014) DYPTOP: a cost-efficient TOPMODEL implementation to simulate sub-grid spatio-temporal dynamics of global wetlands and peatlands. *Geoscientific Model Development*, **7**, 3089-3110.

Strack M, Kellner E, Waddington JM (2006) Effect of entrapped gas on peatland surface level fluctuations. *Hydrological Processes*, **20**, 3611-3622.

Strack M, Price JS (2009) Moisture controls on carbon dioxide dynamics of peat-*Sphagnum* monoliths. *Ecohydrology*, **2**, 34-41.

Strack M, Waddington JM, Lucchese MC, Cagampan JP (2009) Moisture controls on CO_2 exchange in a *Sphagnum*-dominated peatland: results from an extreme drought field experiment. *Ecohydrology*, **2**, 454-461.

Street LE, Subke J-A, Sommerkorn M, Sloan V, Ducrotoy H, Phoenix GK, Williams M (2013) The role of mosses in carbon uptake and partitioning in arctic vegetation. *New Phytologist*, **199**, 163-175.

Surridge BWJ, Baird AJ, Heathwaite AL (2005) Evaluating the quality of hydraulic conductivity estimates from piezometer slug tests in peat. *Hydrological Processes*, **19**, 1227-1244.

Suzuki R, Shimodaira H (2006) Pvclust: an R package for assessing the uncertainty in hierarchical clustering. *Bioinformatics*, **22**, 1540-1542.

Tague CL, Band LE (2001) Evaluating explicit and implicit routing for watershed hydro-ecological models of forest hydrology at the small catchment scale. *Hydrological Processes*, **15**, 1415-1439.

Tang J, Miller PA, Crill PM, Olin S, Pilesjö P (2015) Investigating the influence of two different flow routing algorithms on soil–water–vegetation interactions using the dynamic ecosystem model LPJ-GUESS. *Ecohydrology*, **8**, 570-583.

Tang J, Pilesjö P, Miller PA, Persson A, Yang Z, Hanna E, Callaghan TV (2014) Incorporating topographic indices into dynamic ecosystem modelling using LPJ-GUESS. *Ecohydrology*, **7**, 1147-1162.

Taylor KE, Stouffer RJ, Meehl GA (2012) An overview of CMIP5 and the experiment design. *Bulletin of the American Meteorological Society*, **93**, 485-498.

Tebaldi C, Hayhoe K, Arblaster J, Meehl G (2006) Going to the Extremes. *Climatic Change*, **79**, 185-211.

ter Braak CJF, Šmilauer P (2012) *Canoco Reference Manual and User's Guide: Software for Ordination (version 5.0)*, Microcomputer Power, Ithaca, NY, USA.

Terzaghi K (1943) *Theoretical Soil Mechanics*, John Wiley & Sons, New York, US.

Teuling AJ, Hirschi M, Ohmura A *et al.* (2009) A regional perspective on trends in continental evaporation. *Geophysical Research Letters*, **36**, L02404, doi:02410.01029/02008GL036584.

Teutschbein C, Seibert J (2012) Bias correction of regional climate model simulations for hydrological climate-change impact studies: Review and evaluation of different methods. *Journal of Hydrology*, **456–457**, 12-29.

Teutschbein C, Seibert J (2013) Is bias correction of regional climate model (RCM) simulations possible for non-stationary conditions? *Hydrology and Earth System Sciences*, **17**, 5061-5077.

Thiem G (1906) *Hydrologische Methoden*, Gebhardt, Leipzig, Germany.

Thill L (2011) *Relating morphological characteristics to hydrological properties of Sphagnum carpets, MSc Thesis*, Wageningen University, Wageningen.

Thormann M, Szumigalski A, Bayley S (1999) Aboveground peat and carbon accumulation potentials along a bog-fen-marsh wetland gradient in southern boreal Alberta, Canada. *Wetlands*, **19**, 305-317.

Titus JE, Wagner DJ (1984) Carbon balance for two *Sphagnum* mosses: water balance resolves a physiological paradox. *Ecology*, **65**, 1765-1774.

Tokida T, Miyazaki T, Mizoguchi M, Nagata O, Takakai F, Kagemoto A, Hatano R (2007) Falling atmospheric pressure as a trigger for methane ebullition from peatland. *Global Biogeochemical Cycles*, **21**, GB2003, doi:2010.1029/2006GB002790.

Turetsky MR, Bond-Lamberty B, Euskirchen E, Talbot J, Frolking S, McGuire AD, Tuittila ES (2012) The resilience and functional role of moss in boreal and arctic ecosystems. *New Phytologist*, **196**, 49-67.

Turetsky MR, Kotowska A, Bubier J *et al.* (2014) A synthesis of methane emissions from 71 northern, temperate, and subtropical wetlands. *Global Change Biology*, **20**, 2183-2197.

Turunen J, Tomppo E, Tolonen K, Reinikainen A (2002) Estimating carbon accumulation rates of undrained mires in Finland-application to boreal and subarctic regions. *The Holocene*, **12**, 69-80.

Tyler G (1990) Bryophytes and heavy metals: a literature review. *Botanical Journal of the Linnean Society*, **104**, 231-253.

Uhden EHO (1967) *Niederschlags- und Abflußbeobachtungen auf unberührten, vorentwässerten und kultivierten Teilen eines nordwestdeuttschen Hochmoores der Esterweger Dose am Küstkanal bei Papenburg [GERMAN] Rainfall- and discharge observations on pristine, drained and cultivated parts of a Northwestern German bog in the Esterweger Dose at the Küsten Canal near Papenburg*, Verlag Wasser und Boden, Hamburg, Germany.

Undén P, Rontu L, Järvinen H *et al.* (2002) *HIRLAM-5 Project: HIRLAM-5 Scientic Documentation*, Swedish Meteorological Institute, Norrköping, Sweden.

Unger S, Maguas C, Pereira JS, David TS, Werner C (2010) The influence of precipitation pulses on soil respiration - Assessing the "Birch effect" by stable carbon isotopes. *Soil Biology & Biochemistry*, **42**, 1800-1810.

van Beers WFJ (1983) *The auger hole method. A field measurement of the hydraulic conductivity of soil below the water table*, International Institute for Land Reclamation and Improvement, Wageningen, The Netherlands.

van Breemen N (1995) How *Sphagnum* bogs down other plants. *Trends In Ecology And Evolution*, **10**, 270-275.

van Dam JC, Groenendijk P, Hendriks RFA, Kroes JG (2008) Advances of modeling water flow in variably saturated soils with SWAP. *Vadose Zone Journal*, **7**, 640-653.

van der Linden M, Barke J, Vickery E, Charman DJ, van Geel B (2008) Late Holocene human impact and climate change recorded in a North Swedish peat deposit. *Palaeogeography, Palaeoclimatology, Palaeoecology*, **258**, 1-27.

Van der Linden P, Mitchell JFB (2009) *ENSEMBLES: Climate Change and its Impacts: Summary of research and results from the ENSEMBLES project*, Met Office Hadley Centre, Exeter, UK, available at: http://ensembles-eu.metoffice.com/docs/Ensembles_final_report_Nov09.pdf (last access: 07 July 2015).

Verhoeven JTA, Toth E (1995) Decomposition of Carex and *Sphagnum* litter in fens. Effect of litter quality and inhibition by living tissue homogenates. *Soil Biology and Biochemistry*, **27**, 271-275.

Vervoort RW, van der Zee SEATM (2008) Simulating the effect of capillary flux on the soil water balance in a stochastic ecohydrological framework. *Water Resources Research*, **44**, W08425, doi:08410.01029/02008WR006889.

Waddington JM, Kellner E, Strack M, Price JS (2010) Differential peat deformation, compressibility, and water storage between peatland microforms: Implications for ecosystem function and development. *Water Resources Research*, **46**, W07538, doi:07510.01029/02009WR008802.

Waddington JM, Morris PJ, Kettridge N, Granath G, Thompson DK, Moore PA (2015) Hydrological feedbacks in northern peatlands. *Ecohydrology*, **8**, 113-127.

Waddington JM, Roulet NT (2000) Carbon balance of a boreal patterned peatland. *Global Change Biology*, **6**, 87-97.

Wagner DJ, Titus JE (1984) Comparative Desiccation Tolerance Of 2 *Sphagnum* Mosses. *Oecologia*, **62**, 182-187.

Waite TA, Campbell LG (2006) Controlling the false discovery rate and increasing statistical power in ecological studies. *Écoscience*, **13**, 439-442.

Warrick AW (1991) Numerical approximations of darcian flow through unsaturated soil. *Water Resources Research*, **27**, 1215-1222.

Washington JW (1996) Gas Partitioning of Dissolved Volatile Organic Compounds in the Vadose Zone: Principles, Temperature Effects and Literature Review. *Ground Water*, **34**, 709-718.

Watterson IG (2003) Simulated changes due to global warming in daily precipitation means and extremes and their interpretation using the gamma distribution. *Journal of Geophysical Research*, **108**, 4379.

Webster R, Oliver MA (2007) *Geostatistics for Environmental Scientists*, John Wiley & Sons, Chichester, England.

Weking S, Hermann G, Fartmann T (2013) Effects of mire type, land use and climate on a strongly declining wetland butterfly. *Journal of Insect Conservation*, **17**, 1081-1091.

Whittingham MJ, Stephens PA, Bradbury RB, Freckleton RP (2006) Why do we still use stepwise modelling in ecology and behaviour? *Journal of Animal Ecology*, **75**, 1182-1189.

Whittington P, Strack M, van Haarlem R *et al.* (2007) The influence of peat volume change and vegetation on the hydrology of a kettle-hole wetland in Southern Ontario, Canada. *Mires and peat*, **2**, 1-14.

Whittington PN, Price JS (2006) The effects of water table draw-down (as a surrogate for climate change) on the hydrology of a fen peatland, Canada. *Hydrological Processes*, **20**, 3589-3600.

Wieder RK, Vitt DH, Benscoter B (2006) Peatlands and the boreal forest. In: *Boreal peatland ecosystems.* (eds Wieder RK, Vitt DH), Springer Science & Business Media, Heidelberg, Germany.

Wigmosta MS, Vail LW, Lettenmaier DP (1994) A distributed hydrology-vegetation model for complex terrain. *Water Resources Research*, **30**, 1665-1679.

Wild M, Gilgen H, Roesch A *et al.* (2005) From Dimming to Brightening: Decadal Changes in Solar Radiation at Earth's Surface. *Science*, **308**, 847-850.

Wild M, Truessel B, Ohmura A, Long CN, Konig-Langlo G, Dutton EG, Tsvetkov A (2009) Global dimming and brightening: An update beyond 2000. *Journal of Geophysical Research-Atmospheres*, **114**, D00D13, doi:10.1029/2008JD011382.

Williams C, Hanan N, Scholes R, Kutsch W (2009) Complexity in water and carbon dioxide fluxes following rain pulses in an African savanna. *Oecologia*, **161**, 469-480.

Williams TG, Flanagan LB (1996) Effect of changes in water content on photosynthesis, transpiration and discrimination against $^{13}CO_2$ and $C^{18}O^{16}O$ in *Pleurozium and Sphagnum*. *Oecologia*, **108**, 38-46.

Willmott CJ, Ackleson SG, Davis RE *et al.* (1985) Statistics for the evaluation and comparison of models. *Journal of Geophysical Research-Oceans*, **90**, 8995-9005.

Wilson JB (2012) Species presence/absence sometimes represents a plant community as well as species abundances do, or better. *Journal of Vegetation Science*, **23**, 1013-1023.

Wood SN (2004) Stable and efficient multiple smoothing parameter estimation for generalized additive models. *Journal of the American Statistical Association*, **99**, 673-686.

Wösten JHM, Pachepsky YA, W.J R (2001) Pedotransfer functions. Bridging the gap between available soil data and missing soil hydraulic characteristics. *Journal of Hydrology*, **251**, 123-150.

Wu Y, Blodau C (2013) PEATBOG: a biogeochemical model for analyzing coupled carbon and nitrogen dynamics in northern peatlands. *Geoscientific Model Development*, **6**, 1173-1207.

Xu CG, McDowell NG, Sevanto S, Fisher RA (2013) Our limited ability to predict vegetation dynamics under water stress. *New Phytologist*, **200**, 298-300.

Yoshikawa K, Overduin PP, Harden JW (2004) Moisture content measurements of moss (*Sphagnum* spp.) using commercial sensors. *Permafrost Periglac Process*, **15**, 309-318.

Yu Z (2011) Holocene carbon flux histories of the world's peatlands: Global carbon-cycle implications. *Holocene*, **21**, 761-774.

Yurova A, Wolf A, Sagerfors J, Nilsson M (2007) Variations in net ecosystem exchange of carbon dioxide in a boreal mire: Modeling mechanisms linked to water table position. *Journal of Geophysical Research-Biogeosciences*, **112**, G02025, doi:02010.01029/02006JG000342.

Zlotnik VA, Goss D, Duffield GM (2010) General Steady-State Shape Factor for a Partially Penetrating Well. *Ground Water*, **48**, 111-116.

Summary

Northern peatlands, wetland ecosystems occurring in the boreal and arctic zones of our planet, store large amounts of carbon, corresponding to 34 – 46% currently stored in the atmosphere as carbon dioxide (CO_2). Northern peatlands are therefore an essential component in the global carbon cycle. The carbon in northern peatlands mainly originates from peatmosses (*Sphagnum*) that fix atmospheric CO_2 through photosynthesis, and of which the (partially) decomposed material accumulates as peat. Peatmoss photosynthesis, i.e. CO_2 uptake from the atmosphere, strongly depends on the water availability in the living moss layer. The water availability to peatmosses will likely change in the future as a consequence of climate change, which is projected to result in increased evapotranspiration and changed rainfall regimes. However, the magnitude of change in peatmoss water availability and the effect of such changes on the living moss layer are uncertain and unknown. Therefore, it remains highly uncertain whether peatlands will continue to sequester carbon in future. By combining climate chamber-, field-, and modelling studies, we show that rainwater retention and peat volume change play a crucial self-regulating and stabilizing role in the interactions between climate and exchange of water and carbon between peatland and atmosphere. Through these processes, northern peatlands seem to be more resilient to changes in evapotranspiration and rain regimes than generally assumed.

In a growth chamber experiment we assessed the sensitivity of peatmoss photosynthesis to temporal rainfall patterns during a stepwise decrease in groundwater table, resembling progressively drier conditions. CO_2 exchange was measured for intact moss cores of three peatmoss species (*Sphagnum majus*, *S. fuscum* and *S. balticum*) from contrasting peatland habitats (wet hollows, dry hummocks, and lawns in between). Carbon uptake of the hummock species increased linearly with precipitation frequency in dry conditions, whereas carbon uptake by the lawn and hollow species was reduced at intermediate rainfall frequencies. The experiment highlights that the ability to deal with transient water supply differs among species and that the temporal distribution of rainfall controls peatmoss carbon uptake during droughts.

To determine whether the findings of the growth chamber experiment are also valid in field conditions, we analysed an 11 year eddy-covariance and meteorological time series of a northern peatland to explore the response of net carbon uptake to individual rain events. Daytime rain events systematically decreased the sink strength of peatlands for atmospheric CO_2. This reduction corresponds to 24% of the annual net CO_2 uptake of the studied peatland, and was caused by reduced light availability due to increased

cloud cover during rain events. Reduced light availability was a more important factor in explaining the net carbon uptake response to rain events than changes in water availability and timing of rain. Our results show that peatland CO_2 uptake is highly sensitive to changes in cloud cover and to altered rainfall regimes. The results of the growth chamber experiment and field study may seem contradictory, which very likely originated from differences in light conditions. While light was maintained at constant level in the growth chamber experiment, it co-varied with rain events under field conditions.

Additionally, the presence of a compressible peat layer beneath the living moss layer in field conditions may have reduced drought impact on peatmoss photosynthesis by stabilizing the distance between the groundwater table and the moss surface. How the magnitude of this peat volume change varies through space, and which processes controlled its magnitude is, however, unknown. We therefore explored the fine scale spatial structure of peat volume change in a northern peatland, and its relationship with vegetation and hydrology using spatially continuous data of surface elevation change and point measurements of vegetation and geohydrology. The magnitude of peat volume change over the growing season varied spatially from -6 cm (compression) to +1.2 cm (expansion). Peat volume change over the growing season emerged at a spatial scale of about 40 m. It was mainly related to changes in aquifer thickness, and to a lesser extent to larger scale vegetation units such as flarks and hollows. This suggests that the spatial representativeness of simulation models including peat volume change is restricted, and that peat volume change cannot be derived merely from vegetation units.

Both peat volume change and retention of rainwater seem to be key factors controlling the water content in the moss layer. Current peatland models vary in the degree of hydrological detail included, and do not necessarily include these processes. At present, the consequences of excluding these processes for peatmoss drought predictions are unknown. In a modelling study we therefore systematically tested whether including these fine scale ecohydrological processes biases future predictions of peatmoss drought stress. Peatmoss drought projections were compared among four model concepts including or excluding peat volume change or moss water storage. Our results demonstrated that including peat volume change as well as moss water storage significantly increased model performance and reduced frequency of peatmoss drought stress (from 2.25 to 1.1 droughts per average growing season). Ignoring these processes, which are important in hydrological self-regulation, may thus lead to overestimation of future climate change impacts on peatlands.

In this thesis we show that, although rainwater retention and peat volume change occur at a fine spatiotemporal scale (< 1 m^2; hourly), these processes play a self-regulating

and stabilizing role in the exchange of water and carbon between peatland and atmosphere. Through these feedbacks, peatlands seem to be more resilient to changes in evapotranspiration and precipitation than generally assumed. Hence, accounting for these processes is essential in predicting whether northern peatlands, carbon pools of global importance, may shift from carbon sinks to carbon sources in a future climate.

Samenvatting

De noordelijke veengebieden, moerassige ecosystemen in de boreale en arctische klimaatzones, zijn gezamenlijk een enorme koolstofopslag die overeenkomt met 34 – 46% van het in de atmosfeer opgeslagen koolstof (als koolstofdioxide; CO_2). Noordelijke venen vormen daarmee een essentiële component van de mondiale koolstofkringloop. De in deze venen vastgelegde koolstof is voornamelijk afkomstig van veenmossen (*Sphagnum*), die CO_2 uit de atmosfeer opnemen middels fotosynthese, en waarvan het (gedeeltelijk) afgebroken plantenmateriaal ophoopt als veen. De fotosynthese van veenmos, en daarmee de opname van CO_2 uit de atmosfeer, is sterk afhankelijk van de vochtbeschikbaarheid in de levende moslaag. De vochtbeschikbaarheid voor veenmos zal als gevolg van klimaatverandering door verhoogde evapotranspiratie en gewijzigde neerslagpatronen waarschijnlijk veranderen. De mate van de verandering in vochtbeschikbaarheid en het effect van deze verandering op de levende moslaag is echter onzeker en onbekend. Daardoor blijft het erg onzeker of venen zullen blijven functioneren als belangrijke koolstofopslag in de toekomst. Door klimaatkamer-, veld- en modelstudies te combineren laten we zien dat regenretentie en veenvolumeverandering een cruciale zelfregulerende en stabiliserende rol spelen in de interacties tussen klimaat en de uitwisseling van water en koolstof tussen veen en atmosfeer. Noordelijke veengebieden blijken daardoor beter bestand te zijn voor wijzigingen in evapotranspiratie en neerslagpatronen dan algemeen werd aangenomen.

In een klimaatkamer experiment hebben we onderzocht hoe gevoelig de fotosynthese van veenmos is voor temporele variatie in neerslag bij verschillende grondwaterstanden. We hebben het experiment uitgevoerd met drie veenmossoorten (*Sphagnum majus*, *S. fuscum* en *S. balticum*) van hydrologisch contrasterende veenhabitats (natte slenken, droge bulten, en tapijten ertussenin). De respons verschilde per waterstand en per soort. Bij een ondiepe grondwaterstand speelde regenfrequentie geen rol voor de koolstofopname van veenmos, terwijl bij een diepe grondwaterstand de regenfrequentie belangrijk werd. Bij diepe grondwaterstanden nam de koolstofopname van *S. fuscum* lineair toe met regenfrequentie, terwijl koolstofopname van *S. balticum* en *S. majus* afnam bij gemiddelde regenfrequenties. Dit experiment laat zien dat het vermogen van veenmossen om met wisselende vochtbeschikbaarheid om te gaan soortafhankelijk is, en dat de temporele verdeling van regen een belangrijk niet-lineair effect heeft op de koolstofvastlegging bij diepe grondwaterstanden.

Om te bepalen of de bevindingen in het klimaatkamer experiment ook geldig zijn in veldcondities, hebben we een 11-jarige tijdreeks van CO_2 uitwisseling van een Zweeds

veen gekoppeld aan meteorologische waarnemingen. Onze resultaten laten zien dat buien (overdag) de opname van CO_2 uit de atmosfeer systematisch verlaagden. Deze reductie komt op jaarbasis overeen met 24% van de netto koolstofopname van het bestudeerde veengebied. Dit onverwacht negatieve effect van regenbuien op koolstofopname werd waarschijnlijk veroorzaakt door de lagere lichtbeschikbaarheid tijdens regenbuien en niet door regenfrequentie of waterstand, zoals we vonden in het klimaatkamer experiment. De contrasterende resultaten van de klimaatkamer- en veldstudie kunnen waarschijnlijk verklaard worden door de verschillende lichtregimes. Terwijl de lichthoeveelheid in de klimaatkamerstudie gehandhaafd werd op een constant niveau, varieerde deze met de aanwezigheid van regenbuien in veldcondities. Onze resultaten geven aan dat de opname van CO_2 door venen erg gevoelig is voor toekomstige veranderingen in wolkvorming en neerslagregimes.

Een andere mogelijke oorzaak voor het verschil in resultaten tussen de klimaatkamer- en veldstudie is dat in veldcondities krimp van het veenpakket de invloed van droogte op veenmosfotosynthese beperkt heeft door het stabiliseren van de afstand tussen de het grondwater en het veenoppervlak. Hoe deze veenvolumeverandering varieert in de ruimte en of het samenhangt met is echter grotendeels onbekend. Daarom verkenden we de fijnschalige ruimtelijke structuur van veenvolumeverandering en haar relatie met vegetatie en hydrologie. Hiertoe combineerden we ruimtelijk continue data van veranderingen in het veenoppervlak en puntmetingen van vegetatiesamenstelling en geohydrologie. De mate van veenvolumeverandering over het groeiseizoen varieerde ruimtelijk van -6 cm (krimp) tot +1.2 cm (zwel). Ruimtelijke patronen van veenvolumeverandering over het gehele groeiseizoen manifesteren zich op een ruimtelijke schaal van ongeveer 40 m, en waren met name gerelateerd aan veranderingen in de dikte van het watervoerende pakket, en in mindere mate aan grotere vegetatie-eenheden, zoals bulten en slenken. Dit betekent dat de ruimtelijke representativiteit van simulatiemodellen van veenvolumeverandering slechts zeer beperkt is en veenvolumeverandering niet alleen op basis van vegetatietypering bepaald kan worden.

Onze experimenten en veldmetingen lieten zien dat fijnschalige processen voor een belangrijke mate de vochthuishouding en koolstofopname van veenmossen bepalen. De retentie van regenwater of veenvolumeverandering worden echter niet tot nauwelijks meegenomen in huidige simulatiemodellen van veenhydrologie. De consequenties van het opnemen of weglaten van deze processen voor verwachtingen van droogtestress, en daarmee de potentiele koolstofopname, van veenmos is onbekend. Met vier modellen hebben we daarom getest hoe het al dan niet in begrip nemen van regenretentie en veenvolumeverandering droogtestress beïnvloedt, door gesimuleerd vochtgehalte te

vergelijken met veldwaarnemingen uit een Zweeds veen. De vier modellen verschilden in hydrologische complexiteit, waarbij veenvolumeverandering en opslag van water in de veenmoslaag al dan niet opgenomen waren in de modelstructuur. Het meenemen van zowel veenvolumeverandering als opslag van water in de veenmoslaag bleek de modelkwaliteit significant te verbeteren. Verder geven simulaties met klimaatprojecties aan dat het aantal voorspelde momenten van droogtestress voor veenmos significant lager wordt (van 2.3 droogtes per gemiddeld groeiseizoen in 1991 – 2020 naar 1.1 droogtes in 2061 – 2090). Het negeren van ecohydrologische zelfregulatie door veenvolumeverandering en opslag van water in de veenmoslaag zou dus tot een overschatting van het effect van klimaatverandering op noordelijke venen kunnen leiden.

In dit proefschrift laten we zien dat, alhoewel regenretentie en veenvolumeverandering plaatsvinden op een fijne spatiotemporele schaal (< 1 m^2; uurlijks), deze een cruciale zelfregulerende en stabiliserende rol spelen in uitwisseling van water en koolstof tussen veen en atmosfeer. Door deze terugkoppelingen lijken venen beter bestand te zijn tegen wijzigingen in evapotranspiratie en neerslagpatronen dan algemeen werd aangenomen. Het meenemen van deze fijnschalige ecohydrologische processen is dus essentieel om te voorspellen of de koolstofbalans van noordelijke venen, koolstofbronnen van mondiaal belang, zal verschuiven van opslag naar emissie in een toekomstig klimaat.

Dankwoord / Acknowledgements

Ecohydrologie is een prachtig vakgebied. Niet alleen omdat ecohydrologie het snijvlak van vele boeiende vakdisciplines is, maar bovenal omdat de aard van werkzaamheden varieert van praktisch (de kunst om met laarzen door het veen zompend en handenvol meetapparatuur tillend de Zweedse muggen op je handen te negeren) tot theoretisch (simulatiemodellen ontwikkelen achter de computer). Dit brede scala aan werkzaamheden bracht mij in contact met een grote verscheidenheid aan mensen waar ik mee heb samengewerkt, veel van geleerd heb, en die ik ontzettend dankbaar ben. Zonder de hulp van hen was dit proefschrift er namelijk niet geweest.

Als eerste wil ik graag mijn co-promotoren Juul Limpens en Klaas Metselaar bedanken. Jullie hebben er door de ontspannen samenwerking voor gezorgd dat ik mijn promotie met veel plezier heb afgerond, ik vond jullie geweldige co-promotoren! Ik zal onze gezellige veenlunches missen. Juul, ik heb ontzettend veel van je geleerd over wetenschappelijk schrijven, zinnen goed te formuleren, veenecologie en het opzetten van experimenten. Klaas, jouw kennis van modelbouw en hydrologische processen was essentieel in dit proefschrift, ik heb veel van je opgestoken. Ook heb ik het erg gewaardeerd dat je, zeker aan het eind, vaak binnenwipte om me over de eindstreep heen te sleuren. Onze avontuurlijke 'koelbus-roadtrip' van Wageningen naar noord Zweden en weer terug, met allerlei avonturen onderweg, zal me altijd bij blijven (enorme stukken eland in een vriezer waar we onze veenkernen bewaarden, met veel moeite stroom op de veerboot regelen die het toch niet zo goed bleek te doen, etc).

Verder wil ik graag mijn promotoren Frank Berendse en Sjoerd van der Zee bedanken. Ik waardeer dat jullie me de wetenschappelijke vrijheid gegeven hebben om het proefschrift de huidige vorm te geven. Frank, dank voor het becommentariëren van de manuscripten, je vertrouwen in me, en het toelaten van een wellicht iets hydrologischere en minder ecologische model component dan je aanvankelijk voor ogen had. Sjoerd, ondanks dat ik de laatste tijd van mijn promotie bij de Natuurbeheer en Plantenecologie vakgroep heb doorgebracht, ben je erg betrokken gebleven bij mijn promotie en stond je altijd klaar voor overleg. Dank voor het voorzien van manuscripten met degelijk commentaar met een luchtige, positieve noot. Coen Ritsema, ook jou wil ik graag bedanken voor de vrijheid, en de probleemloze organisatorische overgang van SEG naar SLM.

Much of the data used in this thesis is collected in the peatland complex Degerö Stormyr, a beautiful peatland complex in the north of Sweden near the small, scenic village Vindeln. The field campaigns were definitely among the highlights of the activities performed during my PhD, not least due to the pleasant cooperation with Mats Nilsson

and Matthias Peichl of Sveriges Lantbruksuniversitet (SLU) in Umeå. Thanks both for your welcoming and friendly attitude, insights on functioning of boreal mire ecosystems and eddy covariance matters, and rapid commenting on manuscripts. Matthias, days when you were out on the mire were much better, not just because you appeared in the peatland strictly with sunshine only :-).

The field campaigns to Degerö Stormyr required quite some a priori organization, and would have been impossible without the infrastructure and help of people at the 'Svartbergets fältstation' near Vindeln. Great I could rely on your help to transport heavy field equipment into the Degerö Stormyr peatland with snowmobiles in wintertime (Lena Jonsson), measuring groundwater tables, reading data loggers, sending materials, looking up to a camera on top of a telescopic rod (Pernilla Löfvenius - "My neck was a bit loose") and arranging the first contacts (Charlotta Erefur). Tack så mycket! Many thanks also to Mikaell Ottenson-Löfvenius and Jörgen Sagerförs for providing the time series data from Degerö Stormyr. Jalle, tack så mycket för att du lånade ut din lastbil för transport av 6 m långa järnrör och din hjälp till att designa mätinstrument utifrån vardagliga saker, till ett mycket förmånligt pris.

Henny Gertsen, zonder je hulp met het kiezen van de juiste PVC materialen en het vakkundig uitzagen van bevroren veenmonsters (gelukkig heb je al je vingers nog...) waren de experimenten nooit zo goed geslaagd. Dank daarvoor! Harm Gooren, bedankt voor het meedenken over de meetmethoden en onderzoeksopzet tijdens de veenlunches in de experimentele fase van het onderzoek en hulp met het programmeren van de dataloggers. Jan van Walsem & Frans Moller, bedankt voor de helpende hand bij het verzamelen en in elkaar zetten van onderzoeksmateriaal, en het "Koffieee!!!" roepen als jullie langs mijn kamer liepen voor een pauze. Dankzij de hulp van Pieter Hazenberg heeft de zwel-krimp meetopzet in het veld, uitgerust met positiesensoren, erg fraaie data opgeleverd. Bedankt allemaal!

Also students contributed to new insights on peatmoss ecohydrology. Marianne Gerard and Lisa Thill, many thanks for your perseverance and watching patiently through the microscope to analyse morphological *Sphagnum* traits, and Lisa also thanks for the help in the field. Natalie, thanks for the measurements in the field. Dirk-Jan Pasma, thanks for helping a hand in the climate chamber experiment and for performing field spectrometer and thermal camera measurements. Carla Gomez, I'd like to thank you for your thorough analysis on fine scale peatmosses competition using GIS tools and for your perseverance in the field. Although not too much of the hard work of you all ended up in this thesis, you documented your work perfectly in your own theses. Your enthusiasm and fresh brainpower made working together with all of you very pleasant. Many thanks all!

Fia Bengtsson and Bingxi Li are thanked for the exciting peat sampling campaign in the magnificent peatlands Kulflyten and Skinnskatteberg, Southern Sweden. Håkan Rydin, I'd like to thank you for your help to select coring sites and the species identification at Rygmossen. Fia, thanks for help with peatmoss identification and arranging such a beautiful Swedish stuga. Bingxi, you're a very energetic, positive and active field companion, thanks for your nice attitude! Bjorn Robroek, thanks for your help with the peatmoss photosynthesis experiment in the climate chamber at Utrecht University. I know you secretly enjoyed spending your time helping to build the constructions in the climate chamber, but also that the experiment took a lot of it. Thanks a lot! I also like to thank the employees of the Ecology & Biodiversity Group of Utrecht University for helping me find my way.

Inhoudelijk hebben veel mensen meegedacht. George Bier, Paul Torfs en Toon Leijnse wil ik bedanken voor het delen van hun kennis met betrekking tot het ontwikkelen van modelconcepten en de numerieke implementatie daarvan. Harm Bartholomeus, bedankt voor het lenen van de veldspectrometer en thermal camera, en het meedenken over het toepassen van onconventionele Remote Sensing technieken. Juha Suomalainen and Niels Anders, thanks for help concerning photogrammetry and the Photoscan software. Quirijn de Jong van Lier and Angelica Durigon are thanked for sharing their insights in obtaining soil physical characteristics from evaporation experiments. Claudia Teutschbein, without your techniques for bias-correction and downscaling of climate projections, Chapter 5 of this dissertation would have been much less valuable, thanks!

Ook heb ik het erg leuk gevonden bij te dragen aan het onderwijs van zowel de Natuurbeheer & Plantenecologie als van de Bodemfysica & Landbeheer groep. Ik kijk met veel plezier terug naar onder andere het vak Ecological Methods II en het geven van de Ecologie excursies. Daarnaast heb ik me erg goed vermaakt met het begeleiden van de Hydrogeologie modelpractica.

Gijs van Dijk en Ake Nauta, ik vind het erg leuk dat jullie mijn paranimfen willen zijn, bedankt daarvoor! Gijs, tof dat we als vrienden zo over veen kunnen praten en nu samen lachend doch serieus onderzoek kunnen doen. Dank ook voor de hulp in Zweden. Ake, je was een vrolijke kamergenote; ik heb veel aan je gehad, zowel op inhoudelijk als op persoonlijk vlak.

Furthermore I want to thank my Nature Conservation & Plant Ecology and Soil Physics & Land Management colleagues for the relaxed atmosphere at work, organizing Sinterklaas parties, drinking beers together, etc. Here I also want to thank former colleagues as well as a bunch of other people from the groups Soil Physics, Ecohydrology

& Groundwater Management, Hydrology & Quantitative Water Management, Forest Ecology & Forest Management, and the Resource Ecology Group, who all made the work-life more enjoyable.

Ellen Okken (Ontwerp22), de lay-out en voorkant van dit proefschrift zijn door jou verzorgd. Ik ben er erg tevreden mee, bedankt! Henriette Drenth wil ik hier graag bedanken voor haar hulp om de puntjes op de i zetten voor de leesversie.

Alhoewel dagen(nachten)lang achter de computer simulatiemodellen bouwen en testen, data analyseren, manuscripten uitwerken leuk is/kan zijn, is het ook goed om deze activiteiten af te wisselen met eens per jaar een paar dagen(nachten)lang computerspellen te spelen. Jorik en Sierd, dank voor het behouden van de LAN-spirit, het gitaarspelen tot de oren piepen en de zinvolle dwaasheid. Chris, Conny, Dana, Femke, Frank, Gijs, Hilde, Inge, Janneke, Johnny, Luuk, Nicole, Olda, Thijs: bedankt voor een ontspannen leven naast het proefschrift. Olda & Durk, thanks for the running and talks about the fun and less fun things about science.

Papa en mama, door jullie ben ik geworden wie ik ben en doe ik wat ik doe. Dat deze bijdrage aan de wetenschap er ligt komt doordat jullie me al op jonge leeftijd mee de natuur in hebben genomen en hebben laten inzien dat die er toe doet. De onvoorwaardelijke positieve steun, liefde, interesse, het bewaren van kranten-knipsels, en het meedenken hebben me veel steun geboden en doen doorzetten. Ook mijn schoonouders verdienen in dezelfde context een bedankje voor hun blijvende interesse en vragen.

Hylco, als broers hebben wij vroeger veel hutten gebouwd in het openbare groen (tja, 'natuur' blijft daarvoor een groot woord). Ik wens je nog veel succes met de afronding van jouw proefschrift (en ben toch blij dat je me, ondanks dat je later begonnen bent, net niet ingehaald hebt ;).

Suzanne, ik ben blij dat je me geholpen hebt mijn perfectionisme enigszins in toom te houden tijdens deze intensieve periode: ook zonder jou was dit proefschrift er nooit geweest! Behalve voor je zorgzaamheid, steun en ook het maken van onderzoeksmateriaal, ben ik dankbaar dat je er simpelweg altijd voor me bent. Ik hou van je en kijk er naar uit samen de wereld verder te verkennen en mooie avonturen te beleven. En dan bedoel ik niet alleen in de regen en in hoogvenen!


About the author

Jelmer Jan Nijp was born at 29th of August in Leeuwarden, in a region rich in peat. In his childhood spent his time making huts in the public greenspace. When he was younger, Jelmer wanted to become farmer, construction worker, or forest ranger. After his secondary school (Piter Jelles Montessori, Leeuwarden) he decided to study Environmental Sciences at the Van Hall Instituut in Leeuwarden, where he got acquainted with a large variety of subjects, ranging from waste (water) treatment and soil remediation to terrestrial nature conservation. An internship at Natuurmonumenten, supervised by Frank van Belle and Casper Zoete, provided a background in applied ecohydrology and Dutch nature conservation issues. For half a year, he went for another internship at Metsäntutkimuslaitos (supervised by Ilkka Vanha-Majamaa) to Helsinki in Finland, where he did research to the rehabilitating boreal forest structure with fire and logging, to determine their effects on microhabitat distribution. Jelmer obtained his BSc with the thesis entitled *"Effects of artificial inundation on soil quality and vegetation composition"*, supervised by Ab Grootjans, Ben Helming and Roelof Eleveld. The interest for wet, northern, terrestrial ecosystems and fine scale processes was set.

Jelmer continued his academic career at Wageningen University. Not being able to choose between studying Nature Conservation & Plant Ecology (NCP) or Soil Physics, Ecohydrology & Groundwater Management (SEG), he decided to go for both. He finished his first MSc thesis *"Spatial heterogeneity of microtopography, soil water acidity and vegetation composition in a Cirsio-Molinietum – Caricetum elatae gradient"*, supervised by Karlè Sykora, Gijsbert Cirkel, Klaas Metselaar and Jan-Phillipe Witte. Just about to start his next thesis, the joined SEG-NCP PhD position *"Climate induced critical transitions in peatland carbon sequestration: feedbacks between vegetation and near surface moisture"* passed by and Jelmer got the job! His promotors and co-promotors were Frank Berendse, Sjoerd E.A.T.M. van der Zee, Juul Limpens and Klaas Metselaar. Currently, Jelmer is employed as Post-Doctoral Researcher by the Soil Geography & Landscape department at Wageningen University, where he conducts research on catastrophic shifts in heterogeneous landscapes.

Publications

Cirkel DG, Witte J-PM, van Bodegom PM, **Nijp JJ**, van der Zee SEATM (2014) The influence of spatiotemporal variability and adaptations to hypoxia on empirical relationships between soil acidity and vegetation. *Ecohydrology*, **7**, 21–32.

Kemmers RH, Grootjans AP, Bakker M, Baaijens GJ, **Nijp JJ**, van Dijk G (2007) Leidt bevloeiing van schraallanden tot eutrofiëring? *De Levende Natuur*, **3**, 127-131 [In Dutch].

Kemmers RH, Grootjans AP, **Nijp JJ**, van Delft SPH, van Dijk G (2007) Continuering experimenteel bevloeiingsonderzoek langs de Reest – Eindrapport 2006. Ministerie van Landbouw, Natuur en Voedselkwaliteit, Ede, The Netherlands [In Dutch].

Nijp JJ, Limpens J, Metselaar K, Peichl M, Nilsson MB, van der Zee SEATM, Berendse F (2015) Rain events decrease boreal peatland net CO_2 uptake through reduced light availability. *Global Change Biology*, **21**, 2309-2320.

Nijp JJ, Limpens J, Metselaar K, van der Zee S, Berendse F, Robroek BJM (2014) Can frequent precipitation moderate the impact of drought on peatmoss carbon uptake in northern peatlands? *New Phytologist*, **203**, 70-80.

Nijp JJ, Metselaar K, Limpens J, Teutschbein C, Nilsson MB, Peichl M, Berendse F, van der Zee SEATM (2015) Predicting peatmoss drought stress: The impact of hydrological complexity (**In progress**).

Nijp JJ, Metselaar K, Limpens J, Bartholomeus HM, Nilsson, MB, Berendse F, van der Zee SEATM (2015) Fine scale spatiotemporal variability of surface elevation change in a northern peatland: Interactions with hydrology and vegetation (**In progress**).

van Dijk G, **Nijp JJ**, Smolders AJP, Metselaar K, Lamers LPM (201x) Surface water salinization increases water loss rates in coastal wetlands through downward seepage (**In progress**)

Affiliations of co-authors

Harm M Bartholomeus	Laboratory of Geo-information Science and Remote Sensing, Wageningen University, Wageningen The Netherlands
Frank Berendse	Nature Conservation & Plant Ecology Group Wageningen University, Wageningen The Netherlands
Juul Limpens	Nature Conservation & Plant Ecology Group Wageningen University, Wageningen The Netherlands
Klaas Metselaar	Soil Physics & Land Management Group Wageningen University, Wageningen The Netherlands
Mats B Nilsson	Department of Forest Ecology and Management Sveriges Lantbruksuniversitet, Umeå Sweden
Matthias Peichl	Department of Forest Ecology and Management Sveriges Lantbruksuniversitet, Umeå Sweden
Bjorn JM Robroek	Ecology & Biodiversity Group Utrecht University, Utrecht The Netherlands
Claudia Teutschbein	Department of Earth Sciences Uppsala University, Uppsala Sweden
Sjoerd EATM van der Zee	Soil Physics & Land Management Group Wageningen University, Wageningen The Netherlands

"Tudo é possible"
(Che Sudaka – Será posible, 2015)

Netherlands Research School for the
Socio-Economic and Natural Sciences of the Environment

D I P L O M A

For specialised PhD training

The Netherlands Research School for the
Socio-Economic and Natural Sciences of the Environment
(SENSE) declares that

Jelmer Jan Nijp

born on 29 August 1985 Leeuwarden, The Netherlands

has successfully fulfilled all requirements of the
Educational Programme of SENSE.

Wageningen, 1 December 2015

the Chairman of the SENSE board	the SENSE Director of Education
Prof. dr. Huub Rijnaarts	Dr. Ad van Dommelen

The SENSE Research School has been accredited by the Royal Netherlands Academy of Arts and Sciences (KNAW)

KONINKLIJKE NEDERLANDSE
AKADEMIE VAN WETENSCHAPPEN

The SENSE Research School declares that **Mr Jelmer Nijp** has successfully fulfilled all requirements of the Educational PhD Programme of SENSE with a work load of 47.2 EC, including the following activities:

SENSE PhD Courses

- Environmental Research in Context (2011)
- Research in Context Activity: 'Co-Organisation of WIMEK and SENSE Symposium: Water & energy cycles at multiple scales' (2012)
- Bayesian Statistics (2013)

Other PhD and Advanced MSc Courses

- Afstudeervakken opzetten en begeleiden, Wageningen University (2010)
- Boreal Forest Ecosystems, Swedish University of Agricultural Sciences (SLU) (2011)
- Carbon Dynamics & Exchange in Peatlands, Swedish University of Agricultural Sciences (SLU) (2012)
- Techniques for Writing a Scientific Paper, Wageningen University (2012)

Management and Didactic Skills Training

- Supervising two BSc students with thesis entitled 'Morphological characterisation of *Sphagnum fuscum*, *Sphagnum balticum* and *Sphagnum majus* in order to explain their hydrological properties' (2010) and 'Studying the effects of rain frequency and water table on water content and evaporation of three *Sphagnum* species using remote sensing techniques' (2012)
- Leading excursion of BSc course 'Ecology I' (2010-2013)
- Assisting computer practical of the BSc course 'Hydrogeology' (2010-2014)
- Supervising two MSc students with thesis entitled 'Relating morphological characteristics to hydrological properties of *Sphagnum* carpets' (2011) and 'Scale dependency in the interspecific competition and facilitation dynamics of *Sphagnum* mosses' (2013)
- Supervising of research groups of MSc course 'Ecological Methods II' (2012)
- Leading excursion in BSc course 'Habitat Analysis for Ecologists' (2012)

Oral Presentations

- *Drought in ombrotrophic mires: Can frequent rain sustain carbon uptake of Sphagnum at deep groundwater tables?* Sphagnum Symposium, 1 October 2013, Nijmegen, The Netherlands
- *Vegetation – moisture interaction in peatlands.* SENSE PhD Water Pitch Contest, 30 January 2014, Wageningen, The Netherlands
- *Can frequent precipitation moderate drought impact on peatmoss carbon uptake in northern peatlands?* European Geosciences Union (EGU) - General Assembly 2014 , 27 April-4 May 2014, Vienna, Austria
- *Rain events reduce net CO_2 uptake in a boreal peatland*. Integrated Carbon Observation System (ICOS) Annual workshop, 2-3 September 2014, Umeå, Sweden

SENSE Coordinator PhD Education

Dr. ing. Monique Gulickx

Colofon

Pictures: Jelmer J. Nijp
Cover & Layout: Ellen Okken, Ontwerp22 (www.ontwerp22.nl), Groningen
Printed by: Gildeprint, Enschede, The Netherlands